Proceedings of the

Forty-Fourth
DOE Solar Photochemistry
P.I. Meeting

Hilton Washington DC/Rockville Hotel
and Executive Meeting Center
Rockville, Maryland
May 22-24, 2023

Chemical Sciences, Geosciences, and Biosciences Division
Office of Basic Energy Sciences
Office of Science
U.S. Department of Energy

FOREWORD

The 44th Department of Energy Solar Photochemistry Principal Investigators' Meeting, sponsored by the Chemical Sciences, Geosciences, and Biosciences Division of the Office of Basic Energy Sciences (BES), is being held May 22-24, 2023 at the Hilton Washington DC/Rockville Hotel and Executive Meeting Center in Rockville, Maryland. These proceedings include the meeting agenda, abstracts of the formal presentations and posters, and a list of participants.

The Solar Photochemistry Program supports fundamental, molecular-level research on solar energy capture and conversion in the condensed phase and at interfaces. This conference is the annual meeting of the PIs who conduct research with support from this Program. After holding the meeting in a virtual format in 2021 and 2022, we are excited to resume meeting in person. The objective of the meeting is to facilitate the exchange of scientific ideas and foster collaboration among researchers.

We would like to express our thanks to Teresa Crockett of Basic Energy Sciences, as well as Kimberly Olson, Paul Hudson and their colleagues at the Oak Ridge Institute for Science and Education for their assistance with meeting logistics. Finally, we are grateful to all of the participants in this meeting who have contributed so much to the continued success of the Solar Photochemistry Program.

Chris Fecko and Jennifer Roizen
Chemical Sciences, Geosciences,
and Biosciences Division
Office of Basic Energy Sciences

TABLE OF CONTENTS

SESSION 4 – Triplet Energy Transfer Processes

SESSION 5 – Photochemistry with Quantum-Confined and Nanoscale Semiconductors

SESSION 6 – Charge Transfer Energetics

SESSION 7 – Semiconductor Interfaces

SESSION 8 – Controlling Excited State Dynamics with Structure in Molecular Chromophores

SESSION 9 – Molecular Photochemistry

SESSION 10 – Photochemistry of Electrodes and Heterogeneous Molecular Systems

SESSION 11 – Optical-Vibrational Coupling in Molecular Chromophores

Abstracts of Poster Presentations (by poster number)

44th DOE SOLAR PHOTOCHEMISTRY-
P.I. MEETING

May 22-24, 2023

Hilton Washington DC/Rockville Hotel and Executive Meeting Center
Rockville, MD

Monday, May 22

7:30 a.m. Breakfast

SESSION 1
Opening Session

8:30 a.m. News from DOE-BES Chemical Sciences, Geosciences, and Biosciences Division
Gail McLean, Chris Fecko and Jenny Roizen, DOE Office of Basic Energy Sciences

9:00 a.m. Fundamental Mechanisms for Solar Energy Conversion in Artificial Photosynthetic Assemblies
Karen Mulfort, Argonne National Laboratory

9:30 a.m. Computational Modeling of Artificial Photosynthesis Components
Mehmed Z. Ertem, Brookhaven National Laboratory

10:00 a.m. Break

SESSION 2
Electrocatalysts for Solar Fuels Generation
Charles McCrory, Chair

10:30 a.m. C—H Bond Formation with CO_2: Toward Carbon Neutral Fuel Production
Louise Berben, University of California, Davis

11:00 a.m. Probing Water Oxidation Mechanisms on Atomically Dispersed Catalysts
Dunwei Wang, Boston College

11:30 a.m. Mixed-Metal Oxide Catalysts for the Oxygen Evolution Reaction
Daniel Nocera, Harvard University

12:00 p.m. Working Lunch (*discussion of the scientific presentations throughout the meeting*)

1:30 p.m. Informal Networking

SESSION 3
Charge Transfer in Organic Systems
Matt Sfeir, Chair

3:15 p.m. The Role of Vibronic Coupling in Symmetry-breaking Charge Separation in Chromophore Assemblies
Michael R. Wasielewski, Northwestern University

3:45 p.m. Molecular regulation of charge transfer at organic semiconductor electrodes
Erin Ratcliff, University of Arizona

4:15 p.m. Charge-Transfer States in Organic Solid-State Systems: Friend or Foe?
Garry Rumbles, National Renewable Energy Laboratory

4:45 p.m. Break

SESSION 4
Triplet Energy Transfer Processes
Gary Moore, Chair

5:00 p.m. Towards a Molecular Understanding of the Spin-statistical Factor during Triplet-Triplet Annihilation for Photon Upconversion
Ming Lee Tang, University of Utah

5:30 p.m. Dexter Energy Transfer Pathways
David Beratan, Duke University

6:00 p.m. Working Dinner (*poster preview flash talks*)

7:30 p.m. Posters (Odd numbers)

Tuesday, May 23

7:30 a.m. Breakfast

SESSION 5
Photochemistry with Quantum-Confined and Nanoscale Semiconductors
Justin Sambur, Chair

8:30 a.m. Rational Design of Metal-tipped Semiconductor Quantum Rod Heterostructures for Efficient Light-driven Charge Separation and H_2 Evolution
Tianquan (Tim) Lian, Emory University

9:00 a.m. Multi-Electron and Triplet Energy Transfer at the Interface of Two-Dimensional Semiconductors
Libai Huang, Purdue University

9:30 a.m. Managing Excited-State Interactions in Semiconductor Nanocrystal-Molecular Hybrids. Energy Versus Electron Transfer
Prashant Kamat, University of Notre Dame

10:00 a.m. Break

SESSION 6
Charge Transfer Energetics
Francis Houle, Chair

10:30 a.m. Controlling Charge-Transfer Reactions with First Row Transition Metal Complexes
Thomas W. Hamann, Michigan State University

11:00 a.m. 'Dark' Voltammetry with Semiconductor Electrodes
Stephen Maldonado, University of Michigan

11:30 p.m. The determination of referenced HOMO/LUMO levels with pulse radiolysis
Matthew Bird, Brookhaven National Laboratory

12:00 p.m. Working Lunch (*discussion of the scientific presentations throughout the meeting*)

1:30 p.m. Informal Networking

SESSION 7
Semiconductor Interfaces
Annie Greenaway, Chair

3:15 p.m. *In Situ* Spectroscopy of Electrochemical and Photoelectrochemical Interfaces
Stephen Cronin, University of Southern California

3:45 p.m. Elucidating Design Principles of Semiconductor|Molecule Electronic Coupling for Improved Photoelectrochemical Function
Michael J. Rose, University of Texas at Austin

4:00 p.m. Elucidating the Dynamic Surfaces of Solar Photocatalysts
John Gregoire, California Institute of Technology

4:30 p.m. Break

SESSION 8
Controlling Excited State Dynamics with Structure in Molecular Chromophores
Natia Frank, Chair

4:45 p.m. Photophysics of Co(III) Polypyridyl Complexes: Ligand Field Excited State Dynamics in the Marcus Inverted Region
James McCusker, Michigan State University

5:15 p.m. Toward Conformational Control over Charge Separation

Lisa Olshansky, University of Illinois, Urbana-Champaign

5:30 p.m. Earth Abundant Transition Metal Photosensitizers Based on Cu(I) and Cr(III) Phenanthrolines
Felix N. Castellano, North Carolina State University

6:00 p.m. Working Dinner (*poster preview flash talks*)

7:30 p.m. Posters (Even numbers)

Wednesday, May 24

7:30 a.m. Breakfast

SESSION 9
Molecular Photochemistry
Jier Huang, Chair

8:30 a.m. Photo- and Electrochemical Hydrogen Evolution by Rh2(II,II) Complexes Containing a Benzo[c]cyannoline (bncn) Ligand
Claudia Turro, The Ohio State University

9:00 a.m. Photohydrides: Mechanism-Guided Development of Molecular Photoelectrocatalysts
Alexander J. M. Miller, University of North Carolina at Chapel Hill

9:30 a.m. Photooxidation of Hydroxymethylated Polycyclic Aromatic Dyes: Mechanism and Scope
Dugan Hayes, University of Rhode Island

9:45 a.m. Break

SESSION 10
Photochemistry of Electrodes and Heterogeneous Molecular Systems
Shu Hu, Chair

10:15 a.m. Electrochemical Nitrogen and Proton Reduction using 2D Transition Metal Dichalcogenides
Elisa Miller, National Renewable Energy Laboratory

10:45 a.m. Contactless Measurement of Quasi-Fermi Level Splitting in Solar Fuel Photoelectrodes
Frank Osterloh, University of California, Davis

11:15 a.m. Rational design of light-driven proton pumps using knowledge from photoelectrochemical experiments, transient absorption spectroscopies, and detailed-balance simulations
Shane Ardo, University of California, Irvine

11:45 a.m. Working Lunch (*discussion of the scientific presentations throughout the meeting*)

SESSION 11
Optical-Vibrational Coupling in Molecular Chromophores
Ana Moore, Chair

1:00 p.m. Light Harvesting: From the First Step to the Photosystem II Supercomplex Landscape
Graham Fleming, Lawrence Berkeley National Laboratory

1:30 p.m. Ultrafast Functional Structural Dynamics in Solar Energy Conversion
L. X. Chen and **R. D. Schaller**, Argonne National Laboratory
X. Li, University of Washington

2:15 p.m. Closing Comments
Chris Fecko and Jenny Roizen, DOE Office of Basic Energy Sciences

2:45 p.m. Adjourn

Fundamental Mechanisms for Solar Energy Conversion in Artificial Photosynthetic Assemblies

Karen L. Mulfort,[1] Lin X. Chen,[1,3] Oleg G. Poluektov,[1] Jens Niklas,[1] Alex B. F. Martinson,[2] David M. Tiede[1]

[1]Chemical Sciences and Engineering and [2]Materials Science Divisions, Argonne National Laboratory, Lemont IL 60439

[3]Department of Chemistry, Northwestern University, Evanston IL 60208

A central challenge in the realization of effective systems for artificial photosynthesis lies in the ability to transition from mechanisms that stabilize charge separation from initial transient excited states to those that enable multi-electron, proton-coupled charge accumulation which is needed to drive water-splitting coupled to fuels catalysis. At the heart of this challenge is the timescale mismatch between the ultrafast formation of charge-transfer (CT) and charge-separated (CS) states and typically much slower, rate-determining processes associated with charge transport, accumulation, and bond-making/breaking reactions at catalyst sites. Natural photosynthetic systems provide design principles for efficient conversion of light energy to chemical fuels using molecular cofactors by implementing dynamic interactions between electron donors and acceptors, manipulating the cofactor microenvironment to stabilize multiple possible oxidation states, and using these physical constructs to exert precise control over electronic structure and spin state. The goal of this program is to uncover the fundamental atomic, electronic, and spin chemistry that can be used to effectively link one-electron CT/CS states to the multiple charge accumulations that are essential for solar fuels catalysis. This Argonne team addresses this goal by bringing together targeted molecular, supramolecular, and thin film synthesis strategies with advanced optical and EPR spectroscopies and synchrotron X-ray characterization methods to provide unprecedented insight to our unique molecular and molecularly-defined architectures (Figure 1). This talk will focus on our group's progress in the design and discovery of modular, molecular architectures for artificial photosynthesis, specifically recent work using heteroleptic Cu(I)bis(phenanthroline) complexes (CuHETPHEN) to map directional, intramolecular metal-to-ligand charge transfer (MLCT) and understand dynamic assembly mechanisms for long-lived photoinduced charge separation.

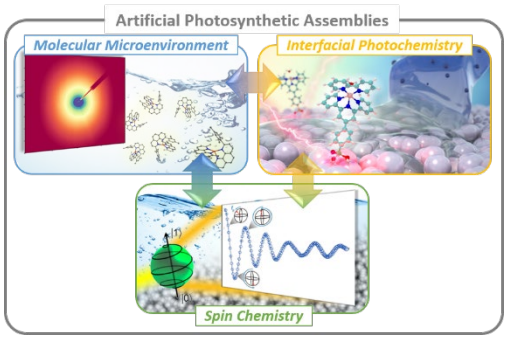

Figure 1. Scope of and connection between program activities.

Understanding where photogenerated electronic excited states localize and how long they persist is of fundamental, critical importance for effective solar energy conversion. The asymmetric and stable coordination environment of CuHETPHEN complexes presents a special opportunity to understand how to promote efficient directional photoinduced charge transfer, particularly for earth-abundant first row transition metal coordination complexes which typically suffer from relatively short excited-state lifetimes. We have synthesized a series of CuHETPHEN complexes functionalized with electron-donating or -withdrawing substituents with Hammett parameters ranging from $-0.37 < \sigma_p < 0.60$, which have allowed us to investigate the directionality of intramolecular photoinduced MLCT (Figure 2, left). In this series, the Cu(II/I) oxidation potential

is tuned over nearly 500 mV, and DFT and TD-DFT calculations confirm that for complexes with electron-donating groups the major contribution to the MLCT transition comes from charge transfer from the Cu(I) 3d orbital to the mesphen blocking ligand, while electron-withdrawing groups direct the MLCT transition to the secondary phenanthroline ligand. The ^{3}MLCT lifetime for each complex is substantially shorter in coordinating solvent than that found in non-coordinating solvent, which generally agrees with previous photophysical studies of Cu(I)diimine complexes. However, functionalization of the secondary ligand with electron-donating or –withdrawing substituents reveals unexpected, non-linear trends in the ^{3}MLCT lifetime with σ_p which is different in coordinating and non-coordinating solvents (Figure 2, right). We interpret this activity as a direct outcome of the directionality of MLCT and localization of the CS state on just one of the ligands, suggesting a complicated interplay of MLCT localization and solvent interaction with the Cu(II) center of the MLCT state.

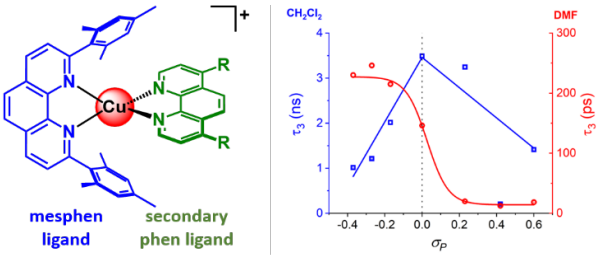

Figure 2. Left: chemical structure of CuHETPHEN complexes with electron-donating and –withdrawing substituents. Right: comparison of ^{3}MLCT lifetime in CH_2Cl_2 (blue) and DMF (red) as a function of σ_p of secondary ligand R substituent.

Facilitating intermolecular photoinduced electron transfer (PET) from CuHETPHEN complexes while minimizing rapid charge recombination processes to produce a long-lived CS state is challenging because of their typically short excited state lifetimes. To overcome this limitation, we hypothesized that weak but specific and dynamic interactions between photosensitizers and catalysts would allow for efficient PET, and potentially provide strategies to discourage fast charge recombination. This concept was tested by creating electrostatic interactions between a sulfonate-functionalized CuHETPHEN complex, Cu-SO_3, and the methyl viologen (MV^{2+}) electron acceptor to induce a ground state association (Figure 3). The effect of the sulfonate groups on the ground- and excited-state properties was evaluated by comparison with the unsulfonated analogs in 1:1 acetonitrile:water. For Cu-SO_3 we clearly detected reduced $MV^{+\bullet}$ following MLCT excitation, which was not observed with the unsulfonated analogs, indicating that electrostatically-driven association of Cu-SO_3 with MV^{2+} facilitates the observed PET. The sulfonate groups of Cu-SO_3 enable solubility in pure water, and in water the quantum yield (Φ_{ET}) for PET from Cu-SO_3 to MV^{2+} is a remarkable 98% with a 3 μs charge separation lifetime, suggesting that the ground state association is dynamic and fluctuates with the charge redistribution from the ground to the CS state. This work provides a set of design principles for directional and efficient photoinduced charge transfer using earth-abundant complexes, and will be used to design pathways for connecting Cu(I)-based photosensitizers to catalysts or electrodes, and integration into systems for light-driven catalysis. Additionally, ongoing work in our group will focus on understanding the impact of solvation and microenvironment on molecular photochemistry and photocatalysis driven by CuHETPHEN complexes using pulsed EPR and high-energy X-ray scattering methods.

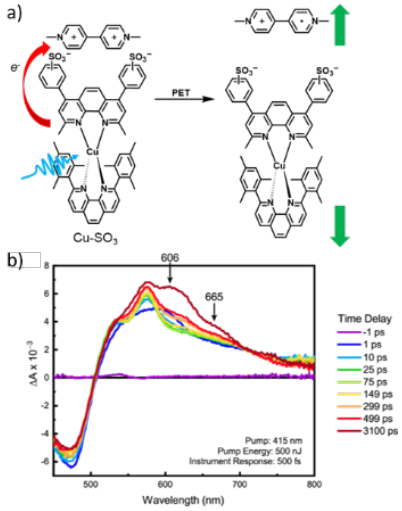

Figure 3. a) Chemical structure of Cu-SO_3 and proposed dynamic assembly with MV^{2+}. b) Ultrafast spectra of Cu-SO_3 with 1 equivalent MV^{2+} in water; spectral signature of $MV^{+\cdot}$ appears within 1 ns.

DOE Solar Photochemistry Sponsored Publications 2020-2023

McCullough, K. E.; Peczak, I. L.; Kennedy, R. M.; Wang, Y.-Y.; Lin, J.; Wu, X.; Paterson, A. L.; Perras, F. A.; Hall, J.; Kropf, A. J.; Hackler, R. A.; Shin, Y.; Niklas, J.; Poluektov, O. G.; Wen, J.; Huang, W.; Sadow, A. D.; Poeppelmeier, K. R.; Delferro, M.; Ferrandon, M. S. Synthesis of Platinum Nanoparticles on Strontium Titanate Nanocuboids Via Surface Organometallic Grafting for the Catalytic Hydrogenolysis of Plastic Waste. *J. Mater. Chem. A* **2023**, *11*, 1216-1231.

Lee, A.; Colleran, T.; Jain, A.; Niklas, J.; Rugg, B. K.; Mani, T.; Poluektov, O. G. Poluektov; Olshansky, J. H. Quantum dot-organic molecule conjugates as host for photogenerated spin qubit pairs. *J. Am. Chem. Soc.* **2023**, *145*, 4372-4377.

Potocny, A. M.; Phelan, B. T.; Sprague-Klein, E. A.; Mara, M. W.; Tiede, D. M.; Chen, L. X.; Mulfort, K. L. Harnessing intermolecular interactions to promote long-lived photoinduced charge separation from copper phenanthroline chromophores. *Inorg. Chem.* **2022**, *61*, 19119–19133.

Sprague-Klein, E. A.; He, X.; Mara, M. W.; Reinhart, B. J.; Lee, S.; Utschig, L. M.; Mulfort, K. L.; Chen, L. X.; Tiede, D. M. Photo-electrochemical effect in the amorphous cobalt oxide water oxidation catalyst cobalt–phosphate (CoPi). *ACS Energy Lett.* **2022**, 3129-3138.

Niklas, J.; Kohler, L.; Potocny, A. M.; Mardis, K. L.; Mulfort, K. L.; Poluektov, O. G. Electronic structure of molecular cobalt catalysts for H_2 production revealed by multifrequency EPR. *J. Phys. Chem. C* **2022**, *126*, 11889-11899.

Gimeno, L.; Phelan, B. T.; Sprague-Klein, E. A.; Roisnel, T.; Blart, E.; Gourlaouen, C.; Chen, L. X.; Pellegrin, Y. Bulky and stable copper(I)-phenanthroline complex: Impact of steric strain and symmetry on the excited-state properties. *Inorg. Chem.* **2022**, *61*, 7296-7307.

Mara, M. W.; Phelan, B. T.; Xie, Z.-L.; Kim, T. W.; Hsu, D. J.; Liu, X.; Valentine, A. J. S.; Kim, P.; Li, X.; Adachi, S.; Katayama, T.; Mulfort, K. L.; Chen, L. X. Unveiling ultrafast dynamics in bridged bimetallic complexes using optical and X-ray transient absorption spectroscopies. *Chem. Sci*. **2022**, *13*, 1715-1724.

Xie, Z.-L.; Liu, X.; Valentine, A. J. S.; Lynch, V.; Tiede, D. T.; Li, X.; Mulfort, K. L. Bimetallic Cu/Ru/Os complexes: Observation of conformational differences between the solution phase and solid state by atomic pair distribution function analysis. *Angew. Chem. Int. Ed.* **2022**, *61*, e202111764.

Lui, X. S.; Xie J. Z.; Niklas, J.; Turner, E. E.; Yuan, D.; Anderson, J. S.; Rack, J. J.; Poluektov, O.G.; Yu, L. Donor-Acceptor Conjugated Copolymers Containing Transition-Metal Complex: Intrachain Magnetic Exchange Interactions and Magneto-Optical Activity. *Chem. Mater.* **2022**, *34*, 5740-5747.

Chapovetsky, A.; Kennedy, R. M.; Witzke, R.; Wegener, E. C.; Dogan, F.; Patel, P.; Ferrandon, M.; Niklas, J.; Poluektov, O. G.; Rui, N.; Senanayake, S. D.; Rodriguez, J.A.; Zaluzec, N. J.; Yu, L.; Wen, J. G.; Johnson, C.; Jenks, C. J.; Kropf, A. J.; Liu, C.; Delferro, M.; Kaphan, D. M. Kaphan. Lithium Ion Battery Materials as Tunable, "Redox Non-Innocent" Catalyst Supports. *ACS Catal.* **2022**, *12*, 7233-7242.

Kwon, G.; Chang, S. H.; Heo, J. E.; Lee, K. J.; Kim, J.-K.; Cho, B.-G.; Koo, T. Y.; Kim, B. J.; Kim, C.; Lee, J. H.; Bak, S.-M.; Beyer, K. A.; Zhong, H.; Koch, R. J.; Hwang, S.; Utschig, L. M.;

Huang, X.; Hu, G.; Brudvig, G. W.; Tiede, D. M.; Kim, J. Experimental verification of Ir 5d orbital states and atomic structures in highly active amorphous iridium oxide catalysts. *ACS Catal.* **2021**, *11*, 10084-10094.

Kohler, L.; Potocny, A. M.; Niklas, J.; Zeller, M.; Poluektov, O. G.; Mulfort, K. L. Replacing pyridine with pyrazine in molecular cobalt catalysts: Effects on electrochemical properties and aqueous H_2 generation. *Catalysts* **2021**, *11*, 75.

Li, N.; Hadt, R. G.; Hayes, D.; Chen, L. X.; Nocera, D. G. Detection of high-valent iron species in alloyed oxidic cobaltates for catalysing the oxygen evolution reaction. *Nat. Commun.* **2021**, *12*, 4218.

Kinigstein, E. D.; Jennings, G.; Kurtz, C. A.; March, A. M.; Zuo, X.; Chen, L. X.; Attenkofer, K.; Zhang, X. X-ray multi-probe data acquisition: A novel technique for laser pump x-ray transient absorption spectroscopy. *Rev. Sci. Instrum.* **2021**, *92*, 085109.

Phelan, B. T.; Mara, M. W.; Chen, L. X. Excited-state structural dynamics of nickel complexes probed by optical and x-ray transient absorption spectroscopies: insights and implications. *Chem. Commun.* **2021**, *57*, 11904-11921.

Ma, T. Z.; Dong, B. X.; Onorato, J. W.; Niklas, J.; Poluektov, O. G.; Luscombe, C. K.; Patel, S. N. Correlating conductivity and Seebeck coefficient to doping within crystalline and amorphous domains in poly(3-(methoxyethoxyethoxy)thiophene). *J. Polymer Sci.* **2021**, *59*, 2797-2808.

Sha, Y.; Lin, X. M.; Niklas, J.; Poluektov, O. G.; Diroll, B. T.; Lin, Y.; Wen, J.; Hood, Z. D.; Lei, A.; Shevchenko, E. V. Insights into the Extraction of Photogenerated Holes from CdSe/CdS Nanorods for Oxidative Organic Catalysis. *J. Mater. Chem. A* **2021**, *9*, 12690-1299.

Dong, B. X.; Nowak, C.; Onorato, J. W.; Ma, T.; Niklas, J.; Poluektov, O. G.; Grocke, G.; DiTusa, M. F.; Escobedo, F. A.; Luscombe, C. K.; Nealey, P. F.; Patel, S. N. Complex Relationship between Side-Chain Polarity, Conductivity, and Thermal Stability in Molecularly Doped Conjugated Polymers. *Chem. Mater.* **2021**, *33*, 741-753.

Kaphan, D. M.; Brereton, K. R.; Klet, R. C.; Witzke, R. J.; Miller, A. J. M.; Mulfort, K. L.; Delferro, M.; Tiede, D. M. Photocatalytic Transfer Hydrogenation in Water: Insight into Mechanism and Catalyst Speciation. *Organometallics* **2021**, *40*, 1482-1491.

Kramar, B. V.; Phelan, B. T.; Sprague-Klein, E. A.; Diroll, B. T.; Lee, S.; Otake, K.-i.; Palmer, R.; Mara, M. W.; Farha, O. K.; Hupp, J. T.; Chen, L. X. Single-Atom Metal Oxide Sites as Traps for Charge Separation in the Zirconium-Based Metal–Organic Framework NDC–NU-1000. *Energy Fuels* **2021**, *35*, 19081-19095.

Lee, C.-H.; Yun, Y. J.; Guo, J.; Chen, L. X.; Mandal, B. K. Synthesis of a new zinc phthalocyanine–benzoquinone rigid dyad. *J. Porphyrins Phthalocyanines* **2021**, *25*, 56-65.

Ji, W.; Hamachi, L. S.; Natraj, A.; Flanders, N. C.; Li, Rebecca L.; Chen, L. X.; Dichtel, W. R. Solvothermal depolymerization and recrystallization of imine-linked two-dimensional covalent organic frameworks. *Chem. Sci.* **2021**, *12*, 16014-16022.

Guda, A.; Windisch, J.; Probst, B.; van Bokhoven, J. A.; Alberto, R.; Nachtegaal, M.; Chen, L. X.; Smolentsev, G. Excited-state structure of copper phenanthroline-based photosensitizers. *Phys. Chem. Chem. Phys.* **2021**, *23*, 26729-26736.

Eberhart, M. S.; Phelan, B. T.; Niklas, J.; Sprague-Klein, E. A.; Kaphan, D. M.; Gosztola, D. J.; Chen, L. X.; Tiede, D. M.; Poluektov, O. G.; Mulfort, K. L. Surface immobilized copper(I) diimine photosensitizers as molecular probes for elucidating the effects of confinement at interfaces for solar energy conversion. *Chem. Commun.* **2020**, *56*, 12130-12333.

Li, N.; Keane, T. P.; Veroneau, S. S.; Hadt, R. G.; Hayes, D.; Chen, L. X.; Nocera, D. G. Template-stabilized oxidic nickel oxygen evolution catalysts. *Proc. Nat. Acad. Sci.* **2020**, *117*, 16187-16192.

Tiede, D. M.; Kwon, G.; He, X.; Mulfort, K. L.; Martinson, A. B. F. Characterizing electronic and atomic structures for amorphous and molecular metal oxide catalysts at functional interfaces by combining soft X-ray spectroscopy and high-energy X-ray scattering. *Nanoscale* **2020**, *12*, 13276-13296. (Invited minireview)

Mardis, K. L.; Niklas, J.; Omodayo, H.; Odella, E.; Moore, T. A.; Moore, A. L.; Poluektov, O. G. One electron multiple proton transfer in model organic donor–acceptor systems: Implications for high-frequency EPR. *Appl. Mag. Res.* **2020**, *51*, 977-991.

Niklas, J.; Zheng, T.; Neshchadin, A.; Mardis, K. L.; Yu, L.; Poluektov, O. G. Polaron and exciton delocalization in oligomers of high-performance polymer PTB7. *J. Am. Chem. Soc.* **2020**, *142*, 1359-1366.

Chen, L. X. From photosynthesis to photocatalysis: Dual catalytic oxidation/reduction in one system. *Proc. Nat. Acad. Sci.* **2020**, *117*, 8672-8673.

Wolfowicz, G.; Anderson, C. P.; Diler, B.; Poluektov, O. G.; Heremans, F. J.; Awschalom, D. D. Vanadium spin qubits as telecom quantum emitters in silicon carbide. *Sci. Adv.* **2020**, *6*, eaaz1192.

Singamaneni, S. R.; Martinez, L. M.; Niklas, J.; Poluektov, O. G.; Yadav, R.; Pizzochero, M.; Yazyev, O. V.; McGuire, M. A. Light induced electron spin resonance properties of van der Waals CrX_3 (X = Cl, I) crystals. *Appl. Phys. Lett.* **2020**, *17*, 082406.

Lee, A.; Voros, M.; Dose, W. M.; Niklas, J.; Poluektov, O. G.; Schaller, R. D.; Iddir, H.; Maroni, V.; Lee, E.; Ingram, B.; Curtiss, L. A.; Johnson, C. Photo-Accelerated Fast Charging of Lithium-Ion Batteries. *Nat. Commun.* **2020**, *143*, 183-192.

Nash, A. G.; Breyer, C. J.; Vincenzini, B. D.; Elliott, G. I.; Niklas, J.; Poluektov, O. G.; Rheingold, A. L.; Smith, D. K.; Musaev, D. G.; Grotjahn, D. B. An Active-Site Sulfonate Group Creates a Fast Water Oxidation Electrocatalyst That Exhibits High Activity in Acid. *Angew. Chem. Int. Ed.* **2020**, *60*, 1540-1545.

Burke, D. W.; Sun, C.; Castano, I.; Flanders, N. C.; Evans, A. M.; Vitaku, E.; McLeod, D. C.; Lambeth, R. H.; Chen, L. X.; Gianneschi, N. C.; Dichtel, W. R. Acid Exfoliation of Imine-linked Covalent Organic Frameworks Enables Solution Processing into Crystalline Thin Films. *Angew. Chem. Int. Ed.* **2020**, *59*, 5165-5171.

Peng, G.; Wu, J.; Wang, M.; Niklas, J.; Zhou, H.; Liu, C. Nitrogen-Defective Polymeric Carbon Nitride Nanolayer Enabled Efficient Electrocatalytic Nitrogen Reduction with High Faradaic Efficiency. *Nano Lett.* **2020**, *20*, 2879-2885.

Computational Modeling of Artificial Photosynthesis Components

Mehmed Z. Ertem, Javier J. Concepcion, Dmitry E. Polyansky, David C. Grills, Gerald F. Manbeck
Chemistry Division, Energy & Photon Sciences Directorate
Brookhaven National Laboratory
Upton, NY 11973-5000

The goal of our research in the Artificial Photosynthesis Program at Brookhaven National Laboratory is to gain a fundamental understanding of processes involved in the chemical conversion of solar energy. We perform coordinated experimental and theoretical studies to address the scientific challenges associated with efficient coupling of light absorption, photo-induced electron-transfer processes, and chemical transformations, together with managing proton movement and charge leveling in catalysts. Among the oxidative chemical transformations, we devote significant attention to water oxidation because of its importance in both natural and artificial photosynthesis as the ideal source of electrons and protons. For the light-driven reductive transformations, we focus on electro- and photocatalytic reduction of CO_2.

The first part of the talk will highlight how our detailed mechanistic studies of water oxidation by transition metal-based complexes enable the development of highly efficient catalysts by carefully controlling the factors that govern the critical O-O bond formation step and new research directions on ligand-based water oxidation catalysis. The second part of the talk will focus on our efforts to decipher the correlation between thermodynamic and kinetic hydricities of transition metal hydrides, which are often key intermediates in CO_2 reduction.

Ligand-Based Water Oxidation

Fundamental understanding of catalytic mechanisms of water oxidation is a prerequisite for the design and development of efficient and rugged water oxidation catalysts. Over the last three decades, inspired by Nature, synthetic water oxidation catalysts (WOCs) based on transition metal complexes have been developed. Among these, Ru-based WOCs have been critical to help understand the reaction mechanisms at a molecular level due to the significant amount of knowledge gained via experiments and computations. In recent years, these advances led to the design and development of seven-coordinate Ru complexes with anionic ligands[1] that exhibit impressive performance, with maximum turnover frequencies (TOF_{MAX}) in basic conditions even exceeding that of Nature's OEC. In our recent work,[2] a detailed mechanistic study of the water oxidation mechanism for $[Ru^{II}(npm)(4\text{-pic})_2(H_2O)]^{2+}$ (npm = 4-t-butyl-2,6-di(1',8'-naphthyrid-2'-yl)-pyridine, pic = 4-picoline), **$[Ru^{II}\text{-}OH_2]^{2+}$**, revealed oxygen atom transfer (OAT) from highly reactive ruthenium oxo intermediates to non-coordinating nitrogen atoms of the ligand as a novel route for oxygen evolution via storage of oxidizing equivalents as N-oxide groups on the ligand framework. Theoretical calculations show that the initial complex, **$[Ru^{II}\text{-}OH_2]^{2+}$**, is transformed

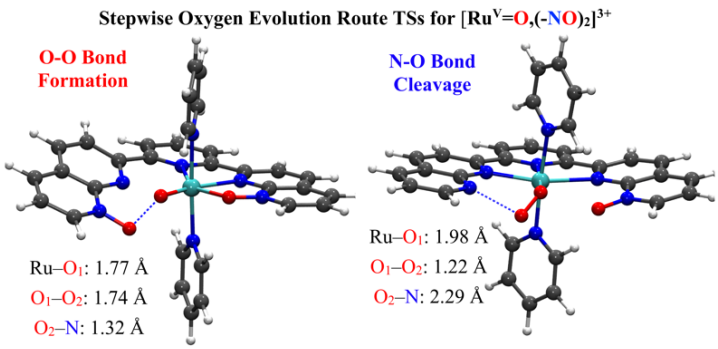

to a di-N-Oxide **[Ru^{II}-OH$_2$,(-NO)$_2$]$^{2+}$** complex upon oxidation via facile OAT steps from the **Ru^{V}=O** species. **[Ru^{V}=O,(-NO)$_2$]$^{3+}$** represents the most likely reactive species for the critical O-O bond formation step. Furthermore, a new stepwise mechanism for oxygen evolution is introduced which proceeds via coupling of **Ru-O** and **N-O** moieties, producing a peroxide intermediate, **[Ru^{V}-OO-N,(-NO)]$^{3+}$**, that can compete with the water nucleophilic attack (WNA) pathway for the oxygen evolution reaction. Inspired by this work, we have developed self-healing ligand-based water oxidation catalysts using Ru molecular complexes and we plan to extend this to earth abundant transition metals in future work.

Thermodynamic vs Kinetic Hydricity

Transition metal hydrides are essential intermediates in a wide range of catalytic reactions including those relevant to energy storage applications such as the reversible hydrogenation and dehydrogenation of CO_2 to formic acid or methanol. In many of these reactions, hydride transfer is the rate limiting step. Thus, an increased fundamental understanding of hydride transfer with transition metals as either the hydride donor or acceptor is critical for the rational design of efficient catalysts. The ability of a transition metal hydride to donate a hydride can be depicted by **(i)** thermodynamic hydricity (Fig. 1a), defined as the free energy required to release a free hydride ion, H^-, from a species in solution ($\Delta G^o_{H^-}$), and by **(ii)** kinetic hydricity (Fig. 1b), which is related to the free energy of activation ($\Delta G^{\ddagger}_{H^-}$) and provides information on the rate of hydride transfer.

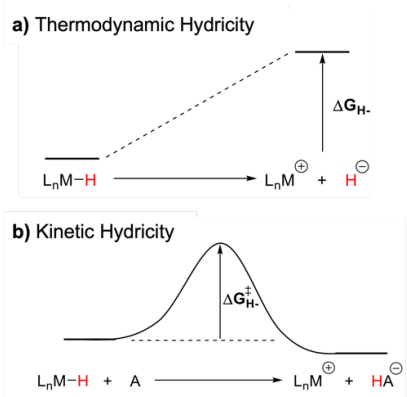

Figure 1. Schematic representations of **(a)** Thermodynamic hydricity and **(b)** Kinetic hydricity.

In this part, I will present our computational modeling studies on the correlation between thermodynamic and kinetic hydricities of **(i)** a series of pentamethylcyclopentadienyl iridium(III) complexes with [Cp*Ir(L)(H)]^q general formula (q = –1, 0, 1 depending on the ligand charge by deprotonation or protonation events) towards CO_2,[9] **(ii)** similar correlations for hydride transfer from Re(^{R}bpy)(CO)$_3$H (bpy = 4,4'-R-2,2'-bipyridine; R = OMe, ^{t}Bu, Me, H, Br, COOMe, CF_3) to CO_2 and different cationic N-heterocycles,[15] and **(iii)** isomers of a series of Ru(^{R}L)$_2$(CO)H type complexes. Our results show that in general, the rate of hydride transfer increases as the thermodynamic driving force for the reaction increases, but even slight perturbations in the steric properties and/or *trans* effects in the case of carbene ligands result in deviations in the predicted rate of hydride transfer based on thermodynamic driving forces. This indicates that thermodynamic considerations alone cannot be used to predict the rate of hydride transfer, which has implications for catalyst design.

Acknowledgments: We thank Prof. Nilay Hazari (Yale University), Prof. Alexander J. M. Miller (University of North Carolina at Chapel Hill), Prof. Yuichiro Himeda (AIST, Japan) and Antoni Llobet (ICIQ, Spain) for insightful discussions and for providing experimental results used in the studies.

DOE Solar Photochemistry Sponsored Publications 2020-2023

1. Second Coordination Sphere Effects in an Evolved Ru Complex Based on Highly Adaptable Ligand Results in Rapid Water Oxidation Catalysis, Vereshchuk, N.; Matheu, R.; Benet-Buchholz, J.; Pipelier, M.; Lebreton, J.; Dubreuil, D.; Tessier, A.; Gimbert-Surinach, C.; Ertem, M. Z.; Llobet, A., *J. Am. Chem. Soc.* **2020**, *142*, 5068-5077.
2. Oxygen Atom Transfer as an Alternative Pathway for Oxygen-Oxygen Bond Formation, Ertem, M. Z.; Concepcion, J. J., *Inorg. Chem.* **2020**, *59*, 5966-5974.
3. CO_2 Hydrogenation and Formic Acid Dehydrogenation Using Ir Catalysts with Amide-Based Ligands, Kanega, R.; Ertem, M. Z.; Onishi, N.; Szalda, D. J.; Fujita, E.; Himeda, Y., *Organometallics* **2020**, *39*, 1519-1531.
4. Synthesis, Characterization, and Water Oxidation Activity of Isomeric Ru Complexes, Hoque, A. M.; Chowdhury, A. D.; Maji, S.; Benet-Buchholz, J.; Ertem, M. Z.; Gimbert-Surinach, C.; Lahiri, G. K.; Llobet, A., *Inorg. Chem.* **2021**, *60*, 5791-5803.
5. Efficient Iridium Catalysts for Formic Acid Dehydrogenation: Investigating the Electronic Effect on the Elementary β-Hydride Elimination and Hydrogen Formation Steps, Liu, H.; Wang, W. H.; Xiong, H.; Nijamudheen, A.; Ertem, M. Z.; Wang, M.; Duan L., *Inorg. Chem.* **2021**, *60*, 3410-3417.
6. Mechanistic Investigation of the Aerobic Oxidation of 2-pyridylacetate Coordinated to a Ru(II) Polypyridyl Complex, Sousa, S. F. Ertem, M. Z.; Faustino, L. A.; Machado, A. E. H.; Concepcion, J. J.; Maia, P. I. S.; Patrocinio, A. O. T., *Dalton Trans.* **2021**, 50, 15248-15259.
7. Methane Generation from CO_2 with a Molecular Rhenium Catalyst, Nganga, J. K.; Wolf, L. M.; Mullick, K.; Reinheimer, E.; Saucedo, C.; Wilson, M. E.; Grice, K. A.; Ertem, M. Z.; Angeles-Boza, A. M., *Inorg. Chem.* **2021**, *60*, 3572–3584.
8. Amide-based Second Coordination Sphere Promotes the Dimer Pathway of Mn-catalyzed CO_2-to-CO Reduction at Low Overpotential, Yang, Y.; Ertem, M. Z.; Duan, L., *Chem. Sci.* **2021**, *12*, 4779-4788.
9. Distinct Mechanisms and Hydricities of Cp*Ir-based CO_2 Hydrogenation Catalysts in Basic Water, Nijamudheen, A.; Kanega, R.; Onishi, N.; Himeda, Y.; Fujita, E.; Ertem, M. Z., *ACS Catal.* **2021**, *11*, 5776–5788.
10. Understanding the Reactivity and Decomposition of a Highly Active Iron Pincer Catalyst for Hydrogenation and Dehydrogenation Reactions, Curley, J. B.; Smith, N. E.; Bernskoetter, W. H.; Ertem, M. Z.; Hazari, N.; Mercado, B. Q.; Townsend, T. M.; Wang, X., *ACS Catal.* **2021**, *11*, 10631–10646.
11. Calcium-ion Binding Mediates the Reversible Interconversion of Cis and Trans Peroxido Dicopper Cores, Vargo N. P.; Harland J. B.; Musselman B. W.; Lehnert N.; Ertem M. Z.; Robinson J. R., *Angew. Chem. Int. Ed.* **2021**, *60*, 19836–19842.
12. Role of Bimetallic Interactions in Enhancement of Catalytic CO_2 Reduction by a Macrocyclic Cobalt Catalyst, Polyansky, D. E.; Grills, D. C.; Ertem, M. Z.; Ngo, T.; Fujita, E., *ACS Catal.* **2022**, *12*, 1706-1717.
13. Reorganization Energy of Electron Transfer in Ionic Liquids, Kodis, G.; Ertem, M. Z.; Newton, M. D., Matyushov, D. V., *J. Phys. Chem. Lett.* **2022**, *13*, 3297–3303.
14. Peroxide-Selective Reduction of O_2 at Redox-Inactive Rare-Earth(III) Triflates Generates an Ambiphilic Peroxide, Lueckheide, J. M.; Ertem, M. Z.; Michon, M. A.; Chmielniak, P.; Robinson J. R., *J. Am. Chem. Soc.* **2022**, *144*, 17295–17306.

15. Correlating Thermodynamic and Kinetic Hydricities of Rhenium Hydrides, Espinosa, M. R.; Ertem, M. Z.; Barakat, M.; Bruch, Q. J.; Deziel, A. P.; Elsby, M. R.; Hasanayn, F.; Hazari, N.; Miller, A. J. M.; Pecoraro, M. V.; Smith, A. M.; Smith, N. E., *J. Am. Chem. Soc.* **2022**, *144*, 17939–17954.

16. Steric and Electronic Influence of the Second Coordination Sphere on Electrocatalytic CO_2 Reduction by Manganese Bipyridyl Complexes, Blasczak, V.; McKinnon, M,; Suntrup, L.; Aminudin, N. A.; Reed, B.; Groysman, S.; Ertem, M. Z.; Grills, D. C.; Rochford, J., *Inorg. Chem.* **2022***, 61*, 15784–15800.

17. Heterogeneous Electrochemical Ammonia Oxidation with a Ru-bda Oligomer Anchored on Graphitic Electrodes via CH−π Interactions, Beiler, A. M.; Denisiuk, A.; Holub, J.; Sánchez-Baygual, F. J.; Gil-Sepulcre, M.; Ertem, M. Z.; Moonshiram, D.; Piccioni, A.; Antoni Llobet, A., *ACS Energy Lett.* **2023**, *8*, 172–178.

18. Predicting Mössbauer Parameters of Nonheme Diiron Complexes with Density Functional Theory, Banerjee, A.; Liu, Q.; Shanklin, J.; Ertem, M. Z., *Inorg. Chem.* **2023**, under review.

C-H Bond Formation with CO_2: Toward Carbon Neutral Fuel Production

Santanu Pattanayak, JongHwa Shon, Kirti Singh, Natalia D. Loewen, and Louise A. Berben*
Department of Chemistry
The University of California
Davis, CA 95616

This project uses nanoscale metal carbonyl clusters (MCC's), which have delocalized bonding and electronic structures, to model nanoparticle and heterogeneous (electro/photo)catalysis. It is the chemical steps in catalytic cycles for solar fuels production which are rate limiting; and thus it is those chemical steps which provide product selectivity and dictate reaction mechanisms in solar fuels chemistry which is photochemically or electrochemically driven. The project is structured around two Specific Objectives. ***Objective 1:*** To study the structure-function relationships for CO_2 reduction by modifying the microenvironment structure. The focus will be on structure-function correlations for the elementary chemical steps of hydride formation and hydride transfer (HT) reactions. Cationic, hydrophobic, and hydrogen-bond-accepting microenvironments will be studied. ***Objective 2:*** To study multi-electron and multi-proton chemistry on the surface of nanoscale metal clusters which are atomically defined. Initial work on this objective has demonstrated the use of a pre-equilibrium mechanism to enhance hydride transfer rates by five orders of magnitude without sacrificing product selectivity.

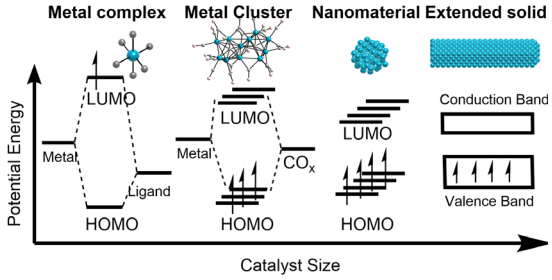

Nanoscale metal clusters enable use of molecular characterization tools to probe the elementary chemical steps in reactions involving electron transfer events.

Progress on Objective 1: Previous grant cycles have laid the groundwork for development of synthetic methods for the installation of *multiple* phosphine ligands surrounding an iron cluster core, and phosphine ligands can have varied electron donating/withdrawing properties, varied sizes, and varied physical properties such as cationic, hydrophobic, and hydrogen-bond-accepting. The controlled placement of phosphine ligands surrounding metal clusters therefore provides access to a wide array of catalyst microenvironments.

Linear Correlation: Reduction Potential vs. ν_{CO}. The impact of cationic and Lewis acidic functional groups installed in the primary or secondary coordination sphere (PCS or SCS) of an (electro)catalyst is thought to vary depending on the precise positioning of those groups but it is difficult to systematically probe the effect of that position. In this report we defined the effect of the functional group position and identity on the observed reduction potentials ($E_{p,c}$) using $[Fe_4N(CO)_{11}R]^n$, where R = NO^+, PPh_2-$CH_2CH_2$9BBN, $(MePTA^+)_2$, $(MePTA^+)_4$, and H+, where n = 0, -1, +1, or +3 (9-BBN is 9-borabicyclo(3.3.1)nonane and MePTA+ is 1-methyl-

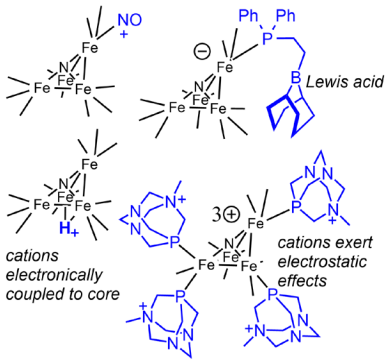

Clusters with cationic PCS & SCS

1 azonia-3,5-diaza-7-phosphaadamantane). The cationic NO^+ and H^+ ligands cause anodic shifts of 700 and 320 mV, respectively, in $E_{p,c}$ relative to unsubstituted $[Fe_4N(CO)_{12}]^-$. Infra-red absorption band data, ν_{CO}, suggests that some of the 700 mV shift by NO^+ results from electronic changes to the cluster core. This contrasts with the effects of cationic $MePTA^+$ and H^+ which cause primarily electrostatic effects on $E_{p,c}$ because they are located further from the catalyst. Lewis acidic 9-BBN in the SCS had almost no effect on $E_{p,c}$.

Microenvironment: H-Bond Acceptors. Here we are studying the role of hydrogen bond (H-bond) accepting functional groups in a microenvironment, and their effect on electrochemically driven catalyst-hydride formation from protons, and on hydride transfer to the substrates H^+ and CO_2. Phosphine substitution of $Na(diglyme)_2[Fe_4N(CO)_{12}]$ was used to access a series of six clusters with various hydrogen bond accepting functional groups that were chosen to span a wide range of H-bond acceptor strength. The rate of formation of [H- $Fe_4N(CO)_{12}$] increases linearly with H-bond acceptor strength (B) of the SCS functional group and is not correlated its pK_a. The rate of hydride transfer to H^+ or to CO_2 also varies with enhanced H-bond acceptor strength but only up to a point. The most strongly H-bond accepting SCS groups lower hydride transfer rates, presumably because they can directly interact with the catalyst-hydride. For future catalyst design these results suggest that enhancement of catalytic rates using a H-bond accepting microenvironment effects must optimize the choice of H-bond acceptor strength according to both the hydride formation and hydride transfer chemical steps in the overall catalytic cycle.

Progress on Objective 2: Pre-equilibrium reaction kinetics enable the overall rate of a catalytic reaction to be orders of magnitude faster than the rate-determining step. Herein, we demonstrate how pre-equilibrium kinetics can be applied to breaking the linear free energy relationship (LFER) for electrocatalysis, leading to rate enhancement five orders of magnitude and lowering of overpotential to approximately thermoneutral. This approach is applied to pre-equilibrium formation of a metal-hydride intermediate to achieve fast formate formation rates from CO_2 reduction without loss of selectivity (ie. H_2 evolution). Fast pre-equilibrium metal-hydride formation, at 108 $M^{-1}s^{-1}$, boosts the CO_2 electroreduction to formate rate up to 296 s^{-1}. Compared with molecular catalysts that have similar overpotential, this rate is enhanced by five orders of magnitude. As an alternative comparison, overpotential is lowered by ~50 mV compared to catalysts with similar rate. The principles elucidated here to obtain pre-equilibrium reaction kinetics via catalyst design are general. Design and development that builds on these principles should be possible in both molecular homogeneous and heterogeneous electrocatalysis.

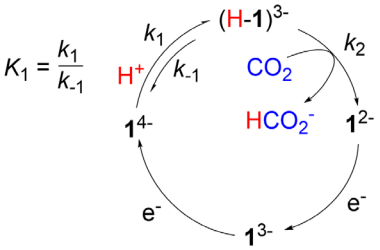

Proposed pre-equilibrium mechanism for formate formation by $[Co_{11}C_2(CO)_{24}]^{3-}$ ($\mathbf{1}^{3-}$). A five-fold enhancement in formate formation rate above the linear free energy relationship s obtained without loss of product selectivity.

Our future efforts are directed toward the two objectives. In objective 1 we continue elucidation of the role of catalyst microenvironment on the mechanism of hydride formation and hydride transfer in HER and CO_2RR, and various properties of those microenvironments are currently under investigation. In objective 2 we are exploring formation of multiple hydride equivalents on the surface of Co clusters, and this will be approached using Pourbaix-style diagrams which map out the relationships between ET and PT events to guide choice of reaction conditions for catalysis.

Publications Sponsored by DOE BES Solar Photochemistry Program 2020 – 2023

9. Pattanayak, S.; Berben, L. A. Pre-equilibrium Reaction Mechanism as a Strategy to Enhance Rate and Lower Overpotential in Electrocatalysis. *J. Am. Chem. Soc.* **2023**, *145*, 3419–3426.
8. Pattanayak, S.; Myers, T. W.; Loewen, N. D.; Berben, L. A. Using Substituted $[Fe_4N(CO)_{12}]^-$ as a Platform To Probe the Effect of Cation and Lewis Acid Location on Redox Potential. *Inorg. Chem.* **2023**, *62*, 1919-1925.

   * *Forum Issue on Discrete Coordination Cages and Metal Clusters*
7. Cesari, C.; Shon, J.-H.; Zacchini, S.; Berben, L. A. Metal Carbonyl Clusters of Groups 8 - 10: Synthesis and Catalysis. *Chem. Soc. Rev.* **2021**, *50*, 9503-9539.

   * *Themed Issue on Multimetallic Clusters: Synthesis, Reactivity, and Properties*
6. Pattanayak, S.; Berben, L. A. Cobalt Carbonyl Clusters Enable Independent Control of Two Proton Transfer Rates in the Mechanism for Hydrogen Evolution. *ChemElectroChem.* **2021**, *8*, 2488-2494.

   * *Special Collection in Memoriam: Prof. JM Savéant*
5. Loewen, N. D.; Pattanayak, S.; Herber, R.; Fettinger, J. C.; Berben, L. A. Quantification of the Electrostatic Effect on Redox Potential of Positive Charges in a Catalyst Microenvironment. *J. Phys. Chem. Lett.* **2021**, *12*, 3066-3073.
4. Loewen, N. D.; Berben, L. A. Group 7 and 8 Catalysts for Electrocatalytic CO_2 Conversion, in *Comprehensive Coordination Chemistry III*. Constable, E. C.; Parkin, G.; Que, L. (Eds.), Elsevier, Amsterdam **2021**, 742-773.
3. Carr, C. R.; Taheri, A.; Berben, L. A. Fast Proton Transfer and Hydrogen Evolution Mediated by $[Co_{13}C_2(CO)_{24}]^{4-}$. *J. Am. Chem. Soc.* **2020**, *142*, 12299–12305.
2. Carr, C. R.; Cluff, D. B.; Berben, L. A. Breaking Scaling Relationships in CO_2 Electroreduction with Isoelectronic Analogs $[Fe_4N(CO)_{12}]^-$ and $[Fe_3MnO(CO)_{12}]^-$. *Organometallics* **2020**, *39*, 1659-1653.

   * *Special Issue on Organometallic Chemistry for Enabling Carbon Dioxide Utilization*
1. Carr, C. R.; Berben, L. A. Homogeneous Electroreduction of CO_2, in *CO_2 Hydrogenation Catalysis* Himeda, Y. (Ed.) Wiley-VCH, Hoboken **2020**, 237-258.

Probing Water Oxidation Mechanisms on Atomically Dispersed Catalysts

Hongna Zhang, Tianying Liu, Nicholas Dulock, Boqiang Chen, David Z. Wang, Haden Wikar, Wei Li, Matthias M. Waegele, Dunwei Wang
Department of Chemistry
Boston College
Chestnut Hill, MA 02467

Our research goal is to understand the mechanisms by which solar water oxidation proceeds on heterogeneous catalysts. Toward this goal, we introduce two key innovations: (1) a model catalyst system whose water oxidation active sites are structurally defined; and (2) time-resolved detection of the reaction mediates by FT-IR spectroscopy. These choices of model catalyst systems and techniques allowed us to not only vary the density of the active sites systematically but also to corroborate the spectroscopic results unambiguously. During the current funding cycle, we have focused on understanding how the water oxidation kinetics are affected by the hole concentration on the surface. As shown in Figure 1, our hypothesis is that the water oxidation kinetics is jointly determined by the concentration of surface holes and the density of catalytically active sites. For substrates that are sluggish in distributing the holes, inefficient hole utilization would be expected; conversely, too fast hole redistribution could compete with water oxidation and lead to poor oxidizing power.

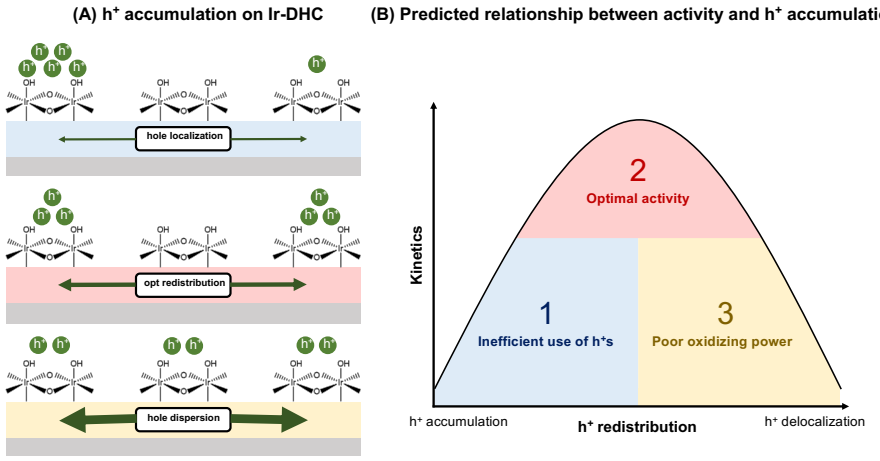

Figure 1. Schematics showing how water oxidation kinetics may be determined by hole redistribution properties of the substrate that supports the catalytic center. Poor hole redistribution could lead to inefficient utilization of holes, and too fast hole redistribution may result in insufficient hole accumulation for the completion of water oxidation, neither of which are desired for optimized water oxidation kinetics.

To test this hypothesis, we performed two sets of different experiments. In the first set, we compared three different types of catalyst support, CeO_2, ITO, and SiO_2. The active centers were all Ir dinuclear heterogeneous catalysts (Ir-DHC) that are derived from dinuclear Ir molecular complexes. Under photochemical conditions at room temperature, these catalysts exhibited comparable kinetics; at elevated temperatures (>35 °C), a bifurcation was observed, where ITO-Ir DHCs were twice as fast in oxidizing water as that by CeO_2-Ir DHC. We rationalized that the

reducible nature of CeO_2 slowed down hole redistribution and led to inefficient utilization of holes. The effect was only observed at elevated temperatures because the overall kinetics were limited by the surface chemical steps at lower temperatures. In the second set of experiments, we systematically and independently varied the density of active sites and the hole concentrations on the surface of a photoelectrode. Two kinetic constants, the forward charge transfer and charge recombination, were monitored. It was found that at low surface hole concentrations (≤0.4 holes/nm^2), lower catalyst density featured faster charge transfer rate. Only the surface hole concentration was sufficiently high (>0.4 holes/nm^2) did we observe the benefits of increased catalyst densities. Moving forward, we plan to corroborate the kinetic studies with time-resolved intermediate detection by FT-IR spectroscopy. A critical challenge for this goal is the low signal intensity of intermediates. To address this issue, we plan to use the lock-in amplification technique to suppress the noises.

DOE Solar Photochemistry Sponsored Publications 2020-2023

1. C.M. Gunathunge, J. Li, X. Li, J.J. Hong, and M.M. Waegele, "Revealing the Predominant Surface Facets of Rough Cu Electrodes During the Electrocatalytic Reduction of CO," *ACS Catal.* **2020**, *10*, 6908–6923
2. Xiaogang Yang, Yuanxing Wang, Chang Ming Li, Dunwei Wang, "Mechanisms of Water Oxidation on Heterogeneous Catalyst Surfaces," *Nano Research* **2021**, *14*, 3446-3457
3. Chaochao Lang, Jingyi Li, Ke R. Yang, Yuanxing Wang, Da He, James E. Thorne, Seth Croslow, Qi Dong, Yanyan Zhao, Gabriela Prostko, Gary W. Brudvig, Victor S. Batista, Matthias Waegele, Dunwei Wang, "Observation of a Potential-Dependent Switch of Water Oxidation Mechanism on Co-Oxide-Based Catalysts," *Chem* **2021,** *7*, 2101-2117
4. Carlota Bozal-Ginesta, Reshma Rao, Camilo A. Mesa, Yuanxing Wang, Yanyan Zhao, Gongfang Hu, Daniel Antón-García, Ifan Stephens, Erwin Reisner, Gary Brudvig, Dunwei Wang, James Durrant, "Spectroelectrochemistry of water oxidation kinetics in molecular versus heterogeneous oxide iridium electrocatalysts," *J. Am. Chem. Soc.* **2022**, *14*, 8454
5. Jingyi Li and Matthias M. Waegele; "Advances in Understanding the Role of Surface Hole Formation in Heterogeneous Water Oxidation." *Curr. Opin. Electrochem.* **2022,** 33, 100932.
6. Ken J. Jenewein, Yuanxing Wang, Tianying Liu, Tara McDonald, Matej Zlatar, Nadiia Kulyk, Attila Kormányos, Dunwei Wang, Serhiy Cherevko, "Electrolyte engineering stabilizes photoanodes decorated with molecular catalysts," *Chem. Sus. Chem.* **2023**, e202202319
7. Hongna Zhang, Tianying Liu, Nicholas Dulock, Benjamin P. Williams, Yuanxing Wang, Boqiang Chen, Haden Wikar, David Z. Wang, Gary W. Brudvig, Dunwei Wang, Matthias M. Waegele, "Atomically Dispersed Ir Catalysts Exhibit Support-Dependent Water Oxidation Kinetics," *Chem. Sci.* **2023**, *under review*
8. Tianying Liu, Wei Li, David Z. Wang, Matthias Waegele, Dunwei Wang, "Low Catalyst Loading Enhances Charge Accumulation for Photoelectrochemical Water Splitting," *J. Am. Chem. Soc.* **2023**, *under review*

Mixed-Metal Oxide Catalysts for the Oxygen Evolution Reaction

Daniel G. Nocera
Department of Chemistry and Chemical Biology
Harvard University
Cambridge, MA and 02138

Heterogeneous metallate oxygen evolution catalysts (M-OECs) comprise molecular clusters and accordingly are linchpins between the heterogeneous and homogeneous worlds of catalysis. The M-OECs are composed of catenated M_4O_4 molecular cubanes, akin to the OEC of Photosystem II, allowing for "molecular" characterization of their OER catalysis. The addition of secondary metals to unary M-OECs to produce mixed-metal alloys, M′M-OECs, can lead to intriguing catalytic properties. Generally, the activity of M′M-OECs increases with alloying, expanding the palette of mechanistic possibilities. Increased activity has been attributed to a variety of mechanisms including: M'^{4+} active sites or higher valent species, near neighbor M′ effects on M resulting from strain on the oxide lattice, active oxygen intermediates at M′M sites, M′-induced partial charge transfer to M sites, and M′ acting as a Lewis acid that promotes charge transfer character and favorable energetics for M–oxyl formation. The effect of Fe loading on Ni-OECs and Co-OECs is an exemplar of the complexity that M′ manifests in the OER mechanism. Whereas Ni-OECs show maximal activity with Fe loadings of ~5 mol% Fe, the maximal activity of Co-OECs is observed for Fe loadings of >40 mol% Fe. These observations suggest different operative mechanisms, none of which have yet been disentangled in M′M-OECs, offering an imperative for a deeper understanding of the OER mechanism in M′M-OECs.

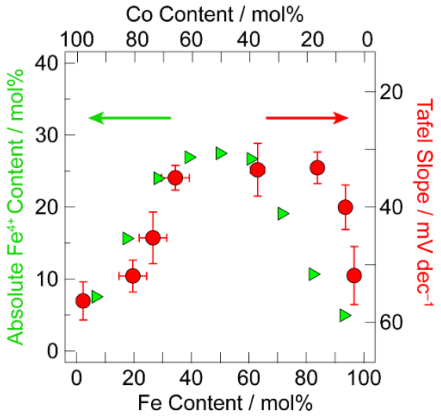

Correlation of Tafel slope with Fe^{4+} composition FeCo-OECs. Overlay of Tafel slope (red circle, ●) with absolute Fe^{4+} population (green triangle, ▶) in with increasing Fe content.

The delineation of the OER mechanism in M′M-OECs presents many interesting scientific challenges worthy of exploration. The incorporation of different metals requires new synthetic strategies, as the commonly used electrodeposition techniques are not always viable owing to different solubility of metal oxide constituents. Additionally, a detailed mechanistic understanding requires that OER be examined under a variety of conditions (pH, concentration, supporting anion/cation speciation), thus demanding the design of catalysts that are stable outside of concentrated base, the condition that most OER catalysis is performed. Importantly, the active catalyst in almost all OER systems is not crystalline, but rather assumes an amorphous phase derived from the crystalline state. Our insights into the mechanism of OER in M′M-OECs will be presented.

The talk will conclude with addressing a new proposal for OER—is there an advantage to developing OER from a substrate other than OH^-/H_2O? We will make the case that there is indeed a good case, especially for CO_2 solar-to-fuels cycles. Such a research direction will also be beneficial to other energy areas of investigation, including the development of metal-air batteries.

DOE Solar Photochemistry Sponsored Publications 2020-2023

1. Role of Electrolyte Composition on the Acid Stability of Mixed-Metal Oxygen Evolution Catalysts. Nancy Li, Thomas P. Keane, Samuel S. Veroneau and Daniel G. Nocera, *Chem. Commun.* **2020**, *56*, 10477–10480.
2. Template-Stabilized Oxidic Nickel Oxygen Evolution Catalysts. Nancy Li, Thomas P. Keane, Samuel S. Veroneau, Ryan G. Hadt, Dugan Hayes, Lin X. Chen and Daniel G. Nocera, *Proc. Natl. Acad. Sci. U.S.A.* **2020**, *117*, 16187–16192.
3. Practical Challenges in the Development of Photoelectrochemical Solar Fuels Production. Mark T. Spitler, Miguel A. Modestino, Todd G. Deutsch, Chengxiang X. Xiang, James R. Durrant, Daniel V. Esposito, Sophia Haussener, Stephen Maldonado, Ian D. Sharp, Bruce A. Parkinson, David S. Ginley, Frances A. Houle, Thomas Hannappel, Nathan R. Neale, Daniel G. Nocera and Paul C. McIntyre, *Sustain. Energy Fuels* **2020**, *4*, 985–995.
4. Synthesis of Hangman Chlorins. Mengran Liu, Dilek K. Dogutan and Daniel G. Nocera, *J. Org. Chem.* **2020**, *85*, 5065–5072.
5. Valorization of CO_2 through Lithoautotrophic Production of Sustainable Chemicals in *Cupriavidus Necator*. Shannon N. Nangle, Marika Ziesack, Sarabeth Buckley, Disha Trivedi, Daniel M. Loh, Daniel G. Nocera and Pamela A. Silver, *Metab. Eng.* **2020**, *62*, 207–220.
6. Hybrid Biological-Inorganic Systems for CO_2 Conversion to Fuels. Rebecca S. Sherbo, Daniel M. Loh and Daniel G. Nocera in *Carbon Dioxide Electrochemistry: Homogeneous and Heterogeneous Catalysis*; Cyrille Costentin, Kim Daasbjerg and Marc Robert, Eds.; Royal Society of Chemistry: London, **2020**; Ch 8.
7. Detection of High-Valent Iron Species in Alloyed Oxidic Cobaltates for Catalysing the Oxygen Evolution Reaction. Nancy Li, Ryan G. Hadt, Dugan Hayes, Lin X. Chen and Daniel G. Nocera, *Nat. Commun*. **2021**, *12*, 4218.
8. Long-Lived Triplet Excited State in a Heterogeneous Modified Carbon Nitride Photocatalyst. Adam J. Rieth, Yangzhong Qin, Benjamin C. M. Martindale and Daniel G. Nocera, *J. Am. Chem. Soc.* **2021**, *143*, 4646–4652.
9. Energy Catalysis Needs Ligands with High Oxidative Stability. Agnes E. Thorarinsdottir and Daniel G. Nocera, *Chem. Catal.* **2021**, *1*, 32–43.
10. Lithium Superoxide Encapsulated in a Benzoquinone Anion Matrix. Matthew Nava, Shiyu Zhang, Katherine S. Pastore, Kyle M. Lancaster, Xiaowen Feng, Daniel G. Nocera and Christopher C. Cummins, *Proc. Natl. Acad. Sci. U.S.A.* **2021**, *118*, e2019392118.
11. Influence of the Proton Relay Spacer on Hydrogen Electrocatalysis by Cobalt Hangman Porphyrins. Manolis M. Roubelakis, D. Kwabena Bediako, Dilek K. Dogutan and Daniel G. Nocera, *J. Porph. Phthalocyanines* **2021**, *25*, 714–723.
12. p-Block Metal Oxide Noninnocence in the Oxygen Evolution Reaction in Acid: The Case of Bismuth Oxide. Agnes E. Thorarinsdottir, Cyrille Costentin, Samuel S. Veroneau and Daniel G. Nocera, *Chem Mater.* **2022**, *34*, 826–835.
13. Self-Healing Oxygen Evolution Catalysts. Agnes E. Thorarinsdottir, Samuel S. Veroneau and Daniel G. Nocera, *Nat. Commun.* **2022**, *13*, 1243.
14. Electronic Thermal Transport Measurement in Low-Dimensional Materials with Graphene Non-local Noise Thermometry. Jonah Waissman, Laurel E. Anderson, Artem V. Talanov, Zhongying Yan, Young J. Shin, Danial H. Najafabadi, Mehdi Rezaee, Xiaowen Feng, Daniel G. Nocera, Takashi Taniguchi, Kenji Watanabe, Brian Skinner, Konstantin A. Matveev and Philip Kim, *Nat. Nanotechnol.* **2022**, *17*, 166–173.
15. Proton-Coupled Electron Transfer: The Engine of Energy Conversion and Storage. Daniel G. Nocera, *J. Am. Chem. Soc.* **2022,** *144***,** 1069–1081.
16. The 2022 Solar Fuels Roadmap: Comparing Artificial and Natural Photosynthesis – Bio Concepts and Hybrid Systems. Jenny Z. Zhang, Leif Hammarström and Daniel G. Nocera, *J. Phys. D: Appl. Phys.* **2022**, *55*, 323003.
17. Proton-Coupled Electron Transfer of Macrocyclic Ring Hydrogenation: The Chlorinphlorin. Rui Sun, Mengran Liu, Shao-Liang Zheng, Dilek K. Dogutan, Cyrille Costentin and Daniel G. Nocera, *Proc. Natl. Acad. Sci. U.S.A.* **2022**, *119*, e2122063119.
18. Synthesis, Characterization, and Hydrogen Evolution Activity of Metallo-*meso*-(4-fluoro-2,6-dimethylphenyl)porphyrin Derivatives. Pallas Chou, Lauren Kim, Sammer M. Marzouk, Rui Sun, Alaina C. Hartnett, Dilek K. Dogutan, Shao-Liang Zheng and Daniel G. Nocera, *ACS Omega* **2022**, *7*, 8988–8994.
19. Electrolyte-Induced Restructuring of Acid-Stable Oxygen Evolution Catalyst. Samuel S. Veroneau, Thomas. P. Keane, Agnes E. Thorarinsdottir, Daniel M. Loh Alaina C. Hartnett, Thomas P. Keane and Daniel G. Nocera, *Chem. Mater.* **2023**, *35*, doi 10.1021/acs.chemmater.3c00032.

The Role of Vibronic Coupling in Symmetry-breaking Charge Separation in Chromophore Assemblies

Taeyeon Kim, Chenjian Lin, Jonathan D. Schultz, Ryan M. Young, and Michael R. Wasielewski
Department of Chemistry and Institute for Sustainability and Energy at Northwestern,
Northwestern University, 2145 Sheridan Road, Evanston, Illinois 60208-3113

Photoinduced symmetry-breaking charge-separation (SB-CS) occurs in photosynthetic reaction center proteins and could significantly boost the open circuit voltage in organic photovoltaics. Therefore, it is important to understand the fundamental mechanism of SB-CS as well as other competing relaxation pathways in chromophore oligomers, such as excimer formation and singlet fission (SF), to design functional molecules for solar energy conversion applications. The "oligomer approach" employs molecular π stacks that mimic these systems using a small number of constituent units and has been successful for understanding structure-property relationships in discrete, well-defined constructs. Among the various chromophores studied with this approach, perylenediimide (PDI) has been one of the most actively investigated due to its robustness, tunable absorption spectrum range, appreciable extinction coefficients, and propensity for strong π-π interactions.

In recent years, the molecular exciton theory developed by Kasha and Davydov has been advanced by Spano and co-workers to emphasize the vital role of short-range charge-transfer (CT) mediated coupling in molecular aggregates. This short-range coupling is very sensitive to the molecular packing geometry such that sub-angstrom displacements along the molecular long- or short-axis can impact the coupling strength. Thus, various photophysical pathways such as excimer formation, SB-CS, or even SF may be promoted or suppressed depending on the molecular packing geometry along with the relative energies of the Frenkel excitons (FEs), CT states, and correlated triplet pair states.

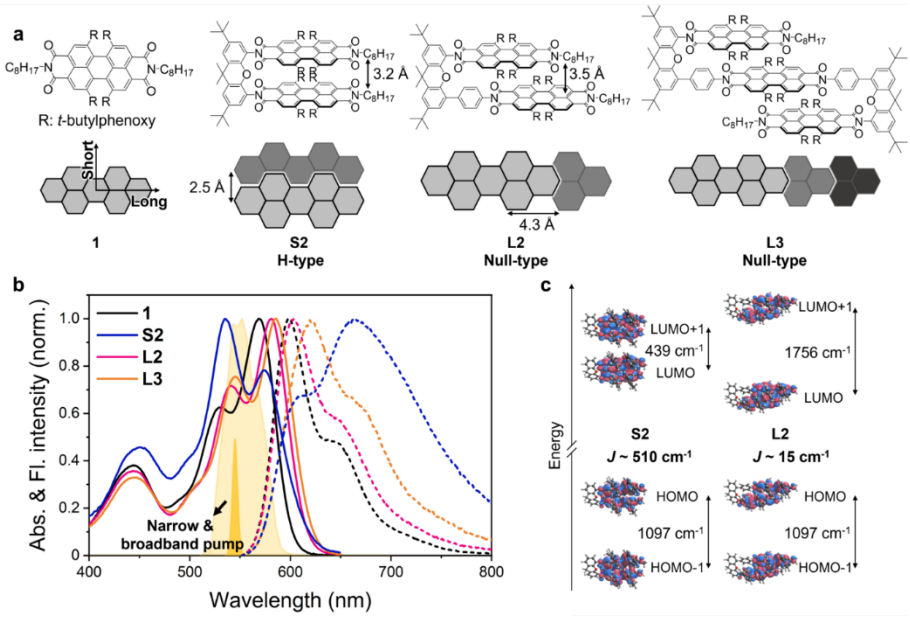

Figure 1. (a) Molecular structures of **1**, **S2**, **L2**, and **L3** based on optimized structures. (b) Steady-state UV-vis absorption and fluorescence spectra of the compounds in tetrahydrofuran (THF) and laser spectra (narrowband and broadband TA) used in this work. (c) Four frontier molecular orbitals of **S2** and **L2** where *J* values (exciton coupling strength) are calculated from the steady state absorption spectra in (b).

We have synthesized a series of geometry constrained PDI oligomers, Figure 1, and employed broad-band transient absorption (BBTA) and two-dimensional electronic spectroscopy (2DES) to investigate the properties and role(s) of vibronic coherence across the entire series of slip-stacked

PDI compounds, including the long-axis slip-stacked dimer (**L2**) and trimer (**L3**). These model systems exhibit unique excited-state dynamics, where **S2** rapidly relaxes to the excimer state, while **L2** and **L3** form a mixture between the FE and CT states. By performing BBTA measurements, we first explored the photophysical properties and vibronic structure of **S2** in comparison with those of the long-axis slip-stacks. We found that a characteristic low-frequency vibration persists for **S2** that can coincide with structural evolution contracting the interchromophoric distance between PDI units, whereas most of the other vibrations were silent during formation of the EX species. By performing 2DES measurements and extracting quantum beatmaps from the data, we reveal characteristic signatures that clarify how vibronic couplings in the slip-stacks are connected to formation of the EX and mixed FE/CT states. Along with a high-frequency vibration that was previously inferred as a key coordinate in forming the mixed state, we leveraged the pump energy resolution afforded by 2DES to identify a pair of low-frequency modes that resonantly bridge the electronic states in conjunction with this higher-frequency mode.

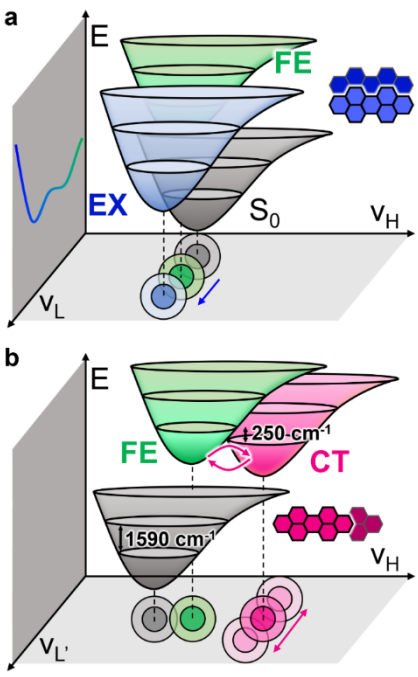

Figure 2. Potential energy surfaces of (a) **S2** and (b) **L2**. V_L (180 cm^{-1}) survives the excimer formation, where a blue arrow indicates the shortening of interchromophoric distance between the PDI units in **S2**. $V_{L'}$ (250 cm^{-1}) is resonant to the energy difference between FE and CT state, vibronically enhancing the electronic state mixing accompanied with the high-frequency FC-active mode (V_H), where red arrows represent the electronic state mixing.

Based on the experimental results, we depicted approximate potential energy surfaces and vibronic couplings of the PDI slip-stacks in Figure 2. For the short slip-stack (**S2**), the FC state does not exhibit vibronic coherences characteristic of the FE state, and the high-frequency mode (1370 cm^{-1}) is 20 cm^{-1} blue-shifted compared to that of the FE state. These results indicate photoexcitation directly populates a state having less FE character than **1**. In addition, the low-frequency 180 cm^{-1} interchromophoric mode, which shows elongated dephasing and different phase compared to those of **1**, **L2**, and **L3**, coincides with structural evolution (shortening interchromophoric distance) during EX formation as shown in Figure 2a. For the long slip-stacked systems, two additional low-frequency modes (**L2**: 250 and 279 cm^{-1}; **L3**: 231 and 259 cm^{-1}) are prominent and exhibit characteristic coherence maps that indicate significant beating in the $PDI^{\bullet+}$ and $PDI^{\bullet-}$ absorption regions. Moreover, both of these vibrational energies approximately coincide with the energy difference between the FE and CT state (242 cm^{-1}). We observed with 2DES that these vibronic couplings are most active upon excitation of a higher vibronic state (1590 cm^{-1}), where the formation of the mixed state is accelerated. In addition, the energy differences between these two low-frequency modes in **L2** and **L3** are 29 and 28 cm^{-1}, respectively, which could be correlated to the energy difference between the C=C stretching modes ca. 1590 (FE) and 1550 cm^{-1} (CT). The energy difference between 250(279) cm^{-1} for **L2** and 231(259) cm^{-1} for **L3** is 19(20) cm^{-1}, which may indicate the energy difference between FE and CT state is ca. 20 cm^{-1} lower in **L3**. Thus, a pair of low-frequency modes around 250 cm^{-1} seems to directly facilitate the electronic state mixing between FE and CT state in the long-axis, slip-stacked PDIs (Figure 2b), followed by the population of SB-CS state in **L3**.

DOE Solar Photochemistry Sponsored Publications 2020-2023

1. Wu, G.; Bae, Y. J.; Olesinska, M.; Anton-Garcia, D.; Szabo, I.; Rosta, E.; Wasielewski, M. R.; Scherman, O. A., Controlling the structure and photophysics of fluorophore dimers using multiple cucurbit[8]uril clampings. *Chem. Sci.* **2020,** *11*, 812-825.
2. Chen, M.; Powers-Riggs, N. E.; Coleman, A. F.; Young, R. M.; Wasielewski, M. R., Singlet fission in quaterrylenediimide thin films. *J. Phys. Chem. C* **2020,** *124*, 2791-2798.
3. Myong, M. S.; Zhou, J.; Young, R. M.; Wasielewski, M. R., Charge-transfer character in excimers of perylenediimides self-assembled on anodic aluminum oxide membrane walls. *J. Phys. Chem. C* **2020,** *124*, 4369-4377.
4. Galstyan, A.; Maurya, Y. K.; Zhylitskaya, H.; Bae, Y. J.; Wu, Y.-L.; Wasielewski, M. R.; Lis, T.; Dobrindt, U.; Stępień, M. π-Extended donor–acceptor porphyrins as low-bandgap agents for antimicrobial photodynamic therapy. *Chem. Eur. J.* **2020**, *26*, 8262-8266.
5. Bae, Y. J.; Zhao, X.; Kryzaniak, M. D.; Nagashima, H.; Strzalka, J.; Zhang, Q.; Wasielewski, M. R., Spin dynamics of quintet and triplet states resulting from singlet fission in oriented terrylenediimide and quaterrylenediimide films. *J. Phys. Chem. C* **2020,** *124*, 9822-9833.
6. Wu, Y.; Frasconi, M.; Liu, W.-G.; Young, R. M.; Goddard, W. A.; Wasielewski, M. R.; Stoddart, J. F., Electrochemical switching of a fluorescent molecular rotor embedded within a bistable rotaxane. *J. Am. Chem. Soc.* **2020,** *142*, 11835-11846.
7. Coleman, A. F.; Chen, M.; Zhou, J.; Shin, J. Y.; Wu, Y.; Young, R. M.; Wasielewski, M. R., Reversible symmetry-breaking charge separation in a series of perylenediimide cyclophanes. *J. Phys. Chem. C* **2020,** *124*, 10408-10419.
8. Chen, M.; Shin, J. Y.; Young, R. M.; Wasielewski, M. R. Tuning the charge transfer character of the multiexciton state in singlet fission. *J. Chem. Phys.* **2020**, *153*, 094302.
9. Young, R. M.; Wasielewski, M. R. Mixed electronic states in molecular dimers: Connecting singlet fission, excimer formation and symmetry-breaking charge transfer. *Acc. Chem. Res.* **2020**, *53*, 1957-1968.
10. Wang, Y.; Wu, H.; Li, P.; Chen, S.; Jones, L. O.; Mosquera, M. A.; Zhang, L.; Cai, K.; Chen, H.; Chen, X.; Stern, C. L.; Wasielewski, M. R.; Ratner, M. A.; Schatz, G. C.; Stoddart, J. F. Two-photon excited near-infrared emissive organic supramolecular co-crystals. *Nat. Commun.* **2020**, *11*, 4633.
11. Roy, I.; Garci, A.; Beldjoudi, Y.; Young, R. M.; Pe, D. J.; Nguyen, M. T.; Das, P. J.; Wasielewski, M. R.; Stoddart, J. F. Supramolecular photon upconversion. *J. Am. Chem. Soc.* **2020**, *142*, 16600-16609.
12. Bae, Y. J.; Shimizu, D.; Schultz, J. D.; Kang, G.; Zhou, J.; Schatz, G. C.; Osuka, A.; Wasielewski, M. R. Balancing charge transfer and Frenkel exciton coupling leads to excimer formation in molecular dimers: Implications for singlet fission. *J. Phys. Chem. A* **2020**, *124*, 8478-8487.
13. Ramirez, C. E.; Chen, S.; Powers-Riggs, N. E.; Schlesinger, I.; Young, R. M.; Wasielewski, M. R. Symmetry-breaking charge separation in the solid state: tetra(phenoxy)-perylenediimide polycrystalline films. *J. Am. Chem. Soc.* **2020**, *142*, 18243-18250.
14. Zhou, J.; Stojanović, l.; Berezin, A. A.; Battisti, T.; Gill, A.; Kariuki, B. M.; Bonifazi, D.; Crespo-Otero, R.; Wasielewski, M. R.; Wu, Y.-L. Organic room-temperature phosphorescence from halogen-bonded organic frameworks: hidden electronic effects in rigidified chromophores. *Chem. Sci.* **2021**, *12*, 767-773.

15. Chen, M.; Coleman, A. F.; Young, R. M. Wasielewski, M. R. Interplay between intramolecular and intermolecular singlet fission in thin films of a covalently linked terrylenediimide dimer. *J. Phys. Chem. C* **2021,** *125*, 6999-7009.
16. Harvey, S. M.; Houck, D. W.; Kirschner, M. S.; Flanders, N. C.; Brumberg, A.; Leonard, A. A.; Watkins, N. E.; Chen, L. X.; Dichtel, W. R.; Zhang, X. Y.; Korgel, B. A.; Wasielewski, M. R.; Schaller, R. D., Transient lattice response upon photoexcitation in $CuInSe_2$ nanocrystals with organic or inorganic surface passivation. *ACS Nano* **2020,** *14*, 13548-13556.
17. Powers-Riggs, N. E.; Schlesinger, I.; Wasielewski, M. R., Correlating structural changes with the photophysics of terrylenediimide films during spontaneous annealing. *J. Mater. Chem. C* **2020,** *8*, 15189-15198.
18. Powers-Riggs, N. E.; Zuo, X. B.; Young, R. M.; Wasielewski, M. R., Solvent independent symmetry-breaking charge separation in terrylenediimide guanine-quadruplex nanoparticles. *J. Chem. Phys.* **2020,** *153*, 204302.
19. Zhang, X.; Li, P.; Krzyaniak, M.; Knapp, J.; Wasielewski, M. R.; Farha, O. K., Stabilization of photocatalytically active uranyl species in a uranyl-organic framework for heterogeneous alkane fluorination driven by visible light. *Inorg. Chem.* **2020,** *59*, 16795-16798.
20. Zhao, X. A.; Bae, Y. J.; Chen, M.; Harvey, S. M.; Lin, C. J.; Zhou, J. W.; Schaller, R. D.; Young, R. M.; Wasielewski, M. R., Singlet fission in core-linked terrylenediimide dimers. *J. Chem. Phys.* **2020,** *153*, 244306.
21. Brumberg, A.; Kirschner, M. S.; Diroll, B. T.; Williams, K. R.; Flanders, N. C.; Harvey, S. M.; Leonard, A. A.; Watkins, N. E.; Liu, C.; Kinigstein, E. D.; Yu, J.; Evans, A. M.; Liu, Y.; Cuthriell, S. A.; Panuganti, S.; Dichtel, W. R.; Kanatzidis, M. G.; Wasielewski, M. R.; Zhang, X.; Chen, L. X.; Schaller, R. D., Anisotropic transient disordering of colloidal, two-dimensional CdSe nanoplatelets upon optical excitation. *Nano Lett.* **2021,** *21*, 1288-1294.
22. Chen, H. L.; Jiang, F.; Hu, C.; Jiao, Y.; Chen, S.; Qiu, Y. Y.; Zhou, P.; Zhang, L.; Cai, K.; Song, B.; Chen, X. Y.; Zhao, X. G.; Wasielewski, M. R.; Guo, H.; Hong, W. J.; Stoddart, J. F., Electron-catalyzed dehydrogenation in a single-molecule junction. *J. Am. Chem. Soc.* **2021,** *143*, 8476-8487.
23. Wang, Y.; Wu, H.; Li, P.; Chen, S.; Jones, L. O.; Mosquera, M. A.; Zhang, L.; Cai, K.; Chen, H.; Chen, X.-Y.; Stern, C. L.; Wasielewski, M. R.; Ratner, M. A.; Schatz, G. C.; Stoddart, J. F., Two-photon excited deep-red and near-infrared emissive organic co-crystals. *Nat. Commun.* **2020,** *11*, 4633.
24. Chen, S.; Zhou, J. W.; Young, R. M.; Wasielewski, M. R., Excited-state dynamics of perylene-based chromophore assemblies on nanoporous anodic aluminum oxide membranes. *J. Phys. Chem. C* **2021,** *125*, 14843-14853.
25. Dannenhoffer, A. J.; Sai, H.; Harutyunyan, B.; Narayanan, A.; Powers-Riggs, N. E.; Edelbrock, A. N.; Passarelli, J. V.; Weigand, S. J.; Wasielewski, M. R.; Bedzyk, M. J.; Palmer, L. C.; Stupp, S. I., Growth of extra-large chromophore supramolecular polymers for enhanced hydrogen production. *Nano Lett.* **2021,** *21*, 3745-3752.
26. Diroll, B. T.; Brumberg, A.; Leonard, A. A.; Panuganti, S.; Watkins, N. E.; Cuthriell, S. A.; Harvey, S. M.; Kinigstein, E. D.; Yu, J.; Zhang, X. Y.; Kanatzidis, M. G.; Wasielewski, M. R.; Chen, L. X.; Schaller, R. D., Photothermal behaviour of titanium nitride nanoparticles evaluated by transient x-ray diffraction. *Nanoscale* **2021,** *13*, 2658-2664.
27. Harvey, S. M.; Houck, D. W.; Liu, W.; Liu, Y.; Gosztola, D. J.; Korgel, B. A.; Wasielewski, M. R.; Schaller, R. D., Synthetic ligand selection affects stoichiometry, carrier dynamics, and trapping in $CuInSe_2$ nanocrystals. *ACS Nano* **2021,** *15*, 19588-19599.

28. Jiao, Y.; Dordevic, L.; Mao, H.; Young, R. M.; Jaynes, T.; Chen, H. L.; Qiu, Y. Y.; Cai, K.; Zhang, L.; Chen, X. Y.; Feng, Y. N.; Wasielewski, M. R.; Stupp, S. I.; Stoddart, J. F., A donor-acceptor [2]catenane for visible light photocatalysis. *J. Am. Chem. Soc.* **2021,** *143*, 8000-8010.
29. Myong, M. S.; Young, R. M.; Wasielewski, M. R., Excimer diffusivity in 9,10-bis(phenylethynyl)anthracene assemblies on anodic aluminum oxide membranes. *J. Phys. Chem. C* **2021,** *125*, 24498-24504.
30. Roy, I.; Goswami, S.; Young, R. M.; Schlesinger, I.; Mian, M. R.; Enciso, A. E.; Zhang, X.; Hornick, J. E.; Farha, O. K.; Wasielewski, M. R.; Hupp, J. T.; Stoddart, J. F., Photon upconversion in a glowing metal-organic framework. *J. Am. Chem. Soc.* **2021,** *143*, 5053-5059.
31. Schlesinger, I.; Zhao, X. G.; Powers-Riggs, N. E.; Wasielewski, M. R., Singlet fission in terrylenediimide single crystals: Competition between biexciton annihilation and free triplet exciton formation. *J. Phys. Chem. C* **2021,** *125*, 13946-13953.
32. Schultz, J. D.; Shin, J. Y.; Chen, M.; O'Connor, J. P.; Young, R. M.; Ratner, M. A.; Wasielewski, M. R., Influence of vibronic coupling on ultrafast singlet fission in a linear terrylenediimide dimer. *J. Am. Chem. Soc.* **2021,** *143*, 2049-2058.
33. Torma, A. J.; Li, W. B.; Zhang, H.; Tu, Q.; Klepov, V. V.; Brennan, M. C.; McCleese, C. L.; Krzyaniak, M. D.; Wasielewski, M. R.; Katan, C.; Even, J.; Holt, M. V.; Grusenmeyer, T. A.; Jiang, J.; Pachter, R.; Kanatzidis, M. G.; Blancon, J. C.; Mohite, A. D., Interstitial nature of Mn^{2+} doping in 2D perovskites. *ACS Nano* **2021,** *15*, 20550-20561.
34. Zhao, X. G.; O'Connor, J. P.; Schultz, J. D.; Bae, Y. J.; Lin, C. J.; Young, R. M.; Wasielewski, M. R., Temperature tuning of coherent mixing between states driving singlet fission in a spiro-fused terrylenediimide dimer. *J. Phys. Chem. B* **2021,** *125*, 6945-6954.
35. Wu, Y. L.; Schneider, S.; Yuan, Y.; Young, R. M.; Francese, T.; Mansoor, I. F.; Dudenas, P. J.; Lei, Y. S.; Gomez, E. D.; DeLongchamp, D. M.; Lipke, M. C.; Galli, G.; Wasielewski, M. R.; Asbury, J. B.; Toney, M. F.; Bao, Z. N., Twisted A-D-A type acceptors with thermally-activated delayed crystallization behavior for efficient nonfullerene organic solar cells. *Adv. Ener. Mater.* **2022,** *12*, 2103957.
36. Williams, M. L.; Schlesinger, I.; Ramirez, C. E.; Jacobberger, R. M.; Brown, P. J.; Young, R. M.; Wasielewski, M. R., Effect of crystallinity on endoergic singlet fission in perylenediimide single crystals and polycrystalline films. *J. Phys. Chem. C* **2022,** *126*, 10287-10297.
37. Wang, X.; Xie, H.; Knapp, J. G.; Wasson, M. C.; Wu, Y.; Ma, K.; Stone, A. E. B. S.; Krzyaniak, M. D.; Chen, Y.; Zhang, X.; Notestein, J. M.; Wasielewski, M. R.; Farha, O. K., Mechanistic investigation of enhanced catalytic selectivity toward alcohol oxidation with Ce oxysulfate clusters. *J. Am. Chem. Soc.* **2022,** *144*, 12092-12101.
38. Wang, X.; Ma, K.; Goh, T.; Mian, M. R.; Xie, H.; Mao, H.; Duan, J.; Kirlikovali, K. O.; Stone, A. E. B. S.; Ray, D.; Wasielewski, M. R.; Gagliardi, L.; Farha, O. K., Photocatalytic biocidal coatings featuring Zr_6Ti_4-based metal-organic frameworks. *J. Am. Chem. Soc.* **2022,** *144*, 12192-12201.
39. Schultz, J. D.; Kim, T.; O'Connor, J. P.; Young, R. M.; Wasielewski, M. R., Coupling between harmonic vibrations influences quantum beating signatures in two-dimensional electronic spectra. *J. Phys. Chem. C* **2022,** *126*, 120-131.
40. Ramirez, C. E.; Jacobberger, R.; Young, R. M.; Wasielewski, M. R., Photophysics of zinc 2,11,20,29-tetra-tert-butyl-2,3-naphthalocyanine: Aggregation-induced S-2 emission and rapid intersystem crossing in the solid state. *J. Phys. Chem. C* **2022,** *126*, 11680-11689.

41. Lin, C. J.; Kim, T.; Schultz, J. D.; Young, R. M.; Wasielewski, M. R., Accelerating symmetry-breaking charge separation in a perylenediimide trimer through a vibronically coherent dimer intermediate. *Nat. Chem.* **2022,** *14*, 786-793.
42. Li, G. P.; Feng, L. W.; Mukherjee, S.; Jones, L. O.; Jacobberger, R. M.; Huang, W.; Young, R. M.; Pankow, R. M.; Zhu, W. G.; Lu, N.; Kohlstedt, K. L.; Sangwan, V. K.; Wasielewski, M. R.; Hersam, M. C.; Schatz, G. C.; DeLongchamp, D. M.; Facchetti, A.; Marks, T. J., Non-fullerene acceptors with direct and indirect hexa-fluorination afford > 17% efficiency in polymer solar cells. *Energy Environ. Sci.* **2022,** *15*, 645-659.
43. Kim, T.; Lin, C.; Schultz, J. D.; Young, R. M.; Wasielewski, M. R., π-Stacking-dependent vibronic couplings drive excited-state dynamics in perylenediimide assemblies. *J. Am. Chem. Soc.* **2022,** *144*, 11386-11396.
44. Jiao, Y.; Qiu, Y. Y.; Zhang, L.; Liu, W. G.; Mao, H. C.; Chen, H. L.; Feng, Y. N.; Cai, K.; Shen, D. K.; Song, B.; Chen, X. Y.; Li, X. S.; Zhao, X. G.; Young, R. M.; Stern, C. L.; Wasielewski, M. R.; Astumian, R. D.; Goddard, W. A.; Stoddart, J. F., Electron-catalysed molecular recognition. *Nature* **2022,** *603*, 265-270.
45. Afraj, S. N.; Zheng, D.; Velusamy, A.; Ke, W. J.; Cuthriell, S.; Zhang, X. H.; Chen, Y.; Lin, C. J.; Ni, J. S.; Wasielewski, M. R.; Huang, W.; Yu, J. S.; Pan, C. H.; Schaller, R. D.; Chen, M. C.; Kanatzidis, M. G.; Facchetti, A.; Marks, T. J., 2,3-diphenylthieno[3,4-b]pyrazines as hole-transporting materials for stable, high-performance perovskite solar cells. *ACS Energy Lett.* **2022,** *7*, 2118-2127.
46. Leonard, A. A.; Diroll, B. T.; Flanders, N. C.; Panuganti, S.; Brumberg, A.; Kirschner, M. S.; Cuthriell, S. A.; Harvey, S. M.; Watkins, N. E.; Yu, J.; Wasielewski, M. R.; Kanatzidis, M. G.; Dichtel, W. R.; Zhang, X.; Chen, L. X.; Schaller, R. D. Light-induced transient lattice dynamics and metastable phase transition in $CH_3NH_3PbI_3$ nanocrystals. *ACS Nano* **2023**, *17*, 5306-5315.
47. Fisher, J. M.; O'Connor, J. P.; Brown, P. J.; Kim, T.; Lorenzo, E. R.; Young, R. M.; Wasielewski, M. R. Two-dimensional electronic spectroscopy reveals vibrational modes coupled to charge transfer in a julolidine-BODIPY dyad. *J. Phys. Chem. A* **2023**, *127*, 2946-2957.
48. Lin, C.; Qi, Y.; Brown, P. J.; Williams, M. L.; Myong, M.; Zhao, X.; Young, R. M.; Wasielewski, M. R. Singlet fission in perylene monoimide single crystals and polycrystalline films. *J. Phys. Chem. Lett.* **2023**, *14*, 2573-2579.
49. Kim, T.; Feng, Y.; O'Connor, J. P.; Stoddart, J. F.; Young, R. M.; Wasielewski, M. R. Coherent vibronic wavepackets show structure-directed charge flow in host-guest donor-acceptor complexes. *J. Am. Chem. Soc.* **2023**, DOI: 10.1021/jacs.2c13576.
50. Trippodo, E.; Campisciano, V.; Feng, L.-W. Chen, Y.; Huang, W.; Alzola, J. M.; Zheng, D.; Sangwan, V. K.; Hersam, M. C.; Wasielewski, M. R.; Pignataro, B.; Giacalone, F.; Marks, T. J.; Facchetti, A. Air-stable ternary organic solar cells achieved by using fullerene additives in non-fullerene acceptor-polymer donor blends. *J. Mater. Chem. C* DOI: 10.1039/D2TC04971F.
51. Chen, H.; Roy, I.; Myong, M. S.; Seale, J. S. W.; Cai, K.; Jiao, Y.; Liu, W.; Song, B.; Zhang, L.; Zhao, X.; Feng, Y.; Liu, F.; Young, R. M.; Wasielewski, M. R.; Stoddart, J. F. Triplet−triplet annihilation upconversion in a porphyrinic molecular container. *J. Am. Chem. Soc.* (submitted).

Molecular regulation of charge transfer at organic semiconductor electrodes

Erin L. Ratcliff
Department of Chemical and Environmental Engineering
University of Arizona
Tucson, AZ 85721

The goal of this work is to seek fundamental new understanding of the mechanisms governing charge transfer and charge transport at organic semiconductor/electrolyte interfaces that underpin the development of new molecular catalysts and generation of fuels from sunlight. This talk will focus on spectroscopic approaches to monitor fundamental electrochemical processes, including electroabsorbance measurements coupled with impedance spectroscopy to track charge motion in π-conjugated polymers as a function of microstructure and electrolyte composition.

In π-conjugated polymers, the three-dimensional electronic structure governing energy/charge transport and transfer is not well-captured by a band-like picture: rather, the electronic structure and charge carriers (i.e., polarons and bipolarons) are highly sensitive to local perturbations and nano-to-microenvironments that derive from intermolecular and interionic interactions. For the prototypical homopolymer poly(3-hexylthiophene), polaron and bipolaron signals exist in the visible to near-IR regions of the electromagnetic spectrum and are highly sensitive to nanometer-length scale interactions including interchain aggregation. Tracking these signatures using spectroelectrochemical methods allows one to resolve carrier motion in both energy and frequency domains to better understand charge transport and charge transfer.

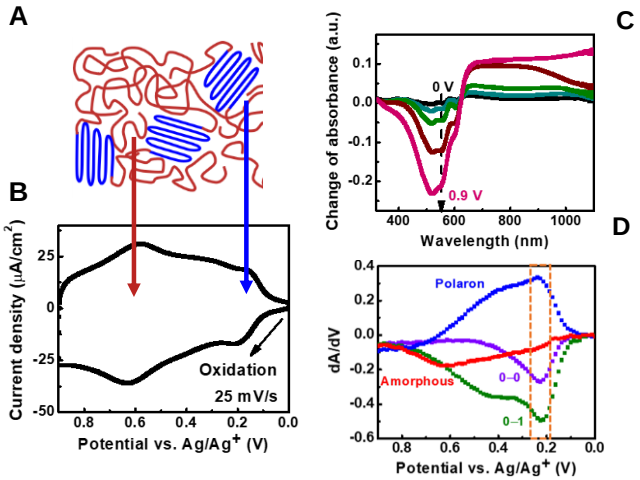

Figure 1. A) Schematic representation of semicrystalline P3HT with crystallites (blue) and amorphous domains (red). B) Cyclic voltammogram of semicrystalline P3HT collected at a scan rate of 25 mV/s in 0.1 M tetrabutylammonium hexafluorophosphate versus Ag/(10 mM) $AgNO_3$ in acetonitrile. C) Potential-dependent change of absorbance of rrP3HT as a function of wavelength with respect to the undoped film (0 V). D) Change in absorbance of the 0−0 transition (610 nm), 0−1 transition (560 nm), amorphous (440 nm), and polaron (730 nm) as a function of applied potentials.

A schematic of the microstructure of the semicrystalline polymer system is shown in Figure 1A, which is comprised of regions of crystallites (blue) and amorphous domains (red). The differences in the wavefunction overlap between polymer chains results in the two sub-populations having electrochemically resolvable redox properties, as indicated in the cyclic voltammogram in Figure 1B. Likewise, the sub-populations are spectroscopically resolvable with the bleaching of π–π* transition states (i.e., 0–0 transition at 610 nm and 0–1 transition at 560 nm), and is associated with the evolutions of polarons (730 nm) and bipolarons (1100 nm). Figure 1D shows the derivative of the change in absorbance with change in potential, which demonstrates that the formation of polarons is originated from the electrochemically consumed population of ground-state rrP3HT. The electroabsorbance response

is most sensitive to the amorphous fraction at ~440 nm, also plotted for reference in Figure 1D.

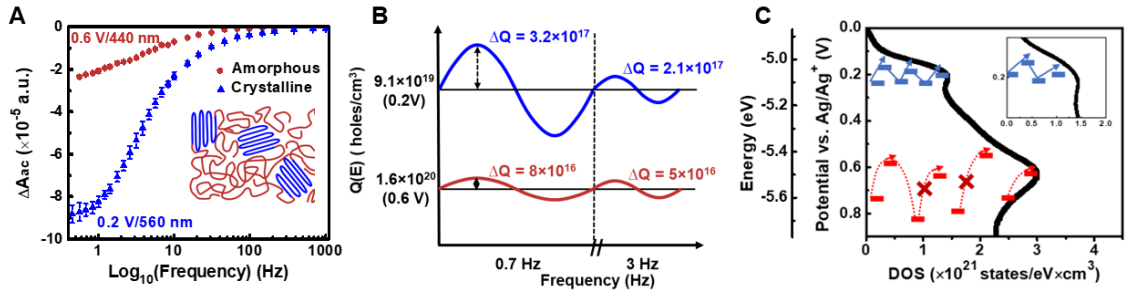

Figure 2. A) Frequency-dependent changes in absorbance for the two subpopulations of semicrystalline poly(3-hexylthiophene). B) Schematic interpretation of frequency-dependent charge modulation for the two sub-populations. C) Schematic of the density of states, with approximately 20% of the redox volume of the film responsible for the majority of charge modulation and transport.

Color impedance spectroscopy (CIS) follows the optical modulation of a spectroscopic signature during sinusoidal modulation of the local potential. Our CIS approach allows for resolution of relative carrier motion as a function of local environment (crystallites versus amorphous domains) in both energy and frequency, summarized in Figure 2. Figure 2A shows the change in absorbance for the two sub-populations as a function of frequency, notably at different steady-state (DC) bias. A schematic interpretation is provided in Figure 2B. The potential sets the net DC concentration of holes per volume, while the AC response describes oscillating charges within the respective domains. For example, at a potential of 0.2 V, there is a net carrier density of 9.1×10^{19} holes/cm^3, with an oscillating population of 3.2×10^{17} holes/cm^3 at 0.7 Hz in the crystallites. Increasing the DC bias to 0.6 V increases the volumetric carrier density to 1.6×10^{20} holes/cm^3, with only 8×10^{16} holes/cm^3 moving with potential modulation within the amorphous fraction at 0.7 Hz. Figure 2C shows a schematic representation of the density of states of the two subpopulations, as a function of energy (eV) and applied potential (V). We emphasize that the narrow distributions of states for the crystallites, which comprise approximately 20% of the redox-active volume. Alternatively, the amorphous domains are hypothesized to be significantly more heterogeneous in energy-DOS distributions, which will give rise to decreased transport properties. Future work will focus on charge oscillations in the presence of an outer sphere redox probe.

This work was supported by the U.S. Department of Energy (DOE), Office of Science, Basic Energy Sciences (BES), under Award # DE-SC0020208.

DOE Solar Photochemistry Sponsored Publications 2020-2023

1. Chen, Z. Ratcliff, E.L. "Watching polarons move in the energy and frequency domains using color impedance spectroscopy" *Chem. Mater.* **2022**, 34, 10691-10700. https://doi.org/10.1021/acs.chemmater.2c02831

2. Hill, L.D., DeKeersmaecker, M., Colbert, A.E., Hill, J.W., Placencia, D., Boercker, J.E., Armstrong, N.R., Ratcliff, E.L. "Rationalizing energy level alignment by characterizing Lewis acid/base and ionic interactions at printable semiconductor/ionic liquid interfaces" *Mat. Horiz.* **2022,** 9, 471-481. https://doi.org/10.1039/D1MH01306H

3. Harris, J.K., Ratcliff, E.L. "Ion diffusion coefficients in poly(3-alkylthiophenes) for energy conversion and biosensing: role of side-chain length and microstructure" *J. Mat. Chem. C.* **2020**, 8, 13319-13327. DOI https://doi.org/10.1039/D0TC03690K

Charge-Transfer States in Organic Solid-State Systems: Friend or Foe?

Garry Rumbles, Obadiah Reid, Nick Hight-Huff, Joshua Carr, Leo Romanetz
Chemistry and Nanoscience Centre
National Renewable Energy Laboratory
Golden, Colorado, 80401

We recently proposed a new model to describe the formation of free carriers (FC) in solid-state organic systems (10.1039/D1MH01331A). The model, distributed range electron transfer (DRET), differs from conventional models by proposing the formation of a charge transfer (CT) state that competes with the formation of free carriers (FC) and does not serve as a mediator in the process, which is its commonly accepted role. The model uses a simple Marcus formulation to describe the rate constant for photoinduced electron transfer (PET) to create both the short-range CT state and the long-range free carriers. A key component of the model is the ability to allow the rate of formation of the free carriers to outcompete the CT state, which according to the mediating model should dominate the PET process. The model predicts that a large reorganization energy for the CT state in comparison to a small value for the formation of free carriers, combined with a greater number of acceptors for the long-range process to produce free carriers, this last point is an entropy term previously proposed but not verified by Gregg at al (10.1021/jz2012403). The model describes well data from sensitized films of the C_{60} derivative, PCBM, as the host, but it requires further testing and validation to establish universality. It is some of these additional efforts that will be reported in this presentation.

Our systems to date have focused on using sensitized systems as they provide greater control over the distribution of acceptors around the sensitizer and have facilitated in ease of calculating the driving force for the PET process using standard electrochemical data. We have begun testing the DRET model using other so-called non-fullerene acceptors (NFAs), and also examined how aggregation of the sensitizer to approach the high blend concentrations required for organic photovoltaic solar cells, the connection to which provides an important motivation for our studies. One of the challenges of using new host molecules and aggregated sensitizers is the difficulty in determining the microwave electron and hole mobilities, which is required to enable our time-resolved microwave conductivity (TRMC) experiment to make the quantitative determinations of charge yields that were critical for proposing the DRET model. Although we have some initial data, it is currently a challenge to identify sensitizing molecules that enable the high driving force, inverted Marcus region to be probed in these systems.

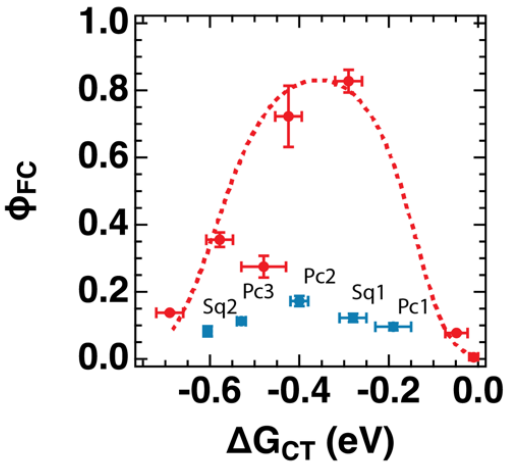

Figure 1 - Yield of free charges as a function of driving force for red sensitizers and where the dotted line represents the previously published DRET model prediction. The FC yields for the blue sensitizers is noticeably lower ,even though the driving force falls into the same window as that of the red sensitizers.

During our initial work, it was observed that sensitizers that absorbed to the blue of the PCBM host did not fit the DRET model. We have identified this as a complication of energy transfer from the sensitizer to the host that competes with PET and reduces the yield of free charges. Modelling of this process using a Förster model does not completely explain the data, and suggests a greater role of, perhaps, a Dexter energy transfer process. These data and the modelling will also be discussed in the presentation.

One of the bigger challenges for the model is the absence of how the CT state fits into the equation, as there is unequivocal evidence that the species can be seen in absorption and frequently in emission too. It is therefore imperative that in addition to spectroscopically tracing the free carriers, identifying the CT state and examining its role is important to enable a full picture of the PET process in these sensitized systems as well as the device-relevant blends. We have therefore established a new optically-detected magnetic resonance (ODMR) experiment based on transient absorption detection (PADMR) to uniquely track these states. Three samples from our initial DRET study: a Zinc (Pc3) and free-base (Pc1) Phthalocyanine, and a silyl naphthalocyanine (Nc1) have been studied as sensitizers in PCBM. Some data are shown in Figure 2 and demonstrate how we are using this technique to observe and model the degree of charge separation in the three samples. The data in the top row depict how the transient bleach signal is modulated using differing rf driving frequencies, as a function of magnetic field, where the signals are dependent on the separation and coupling strength of the triplet levels of the CT state.

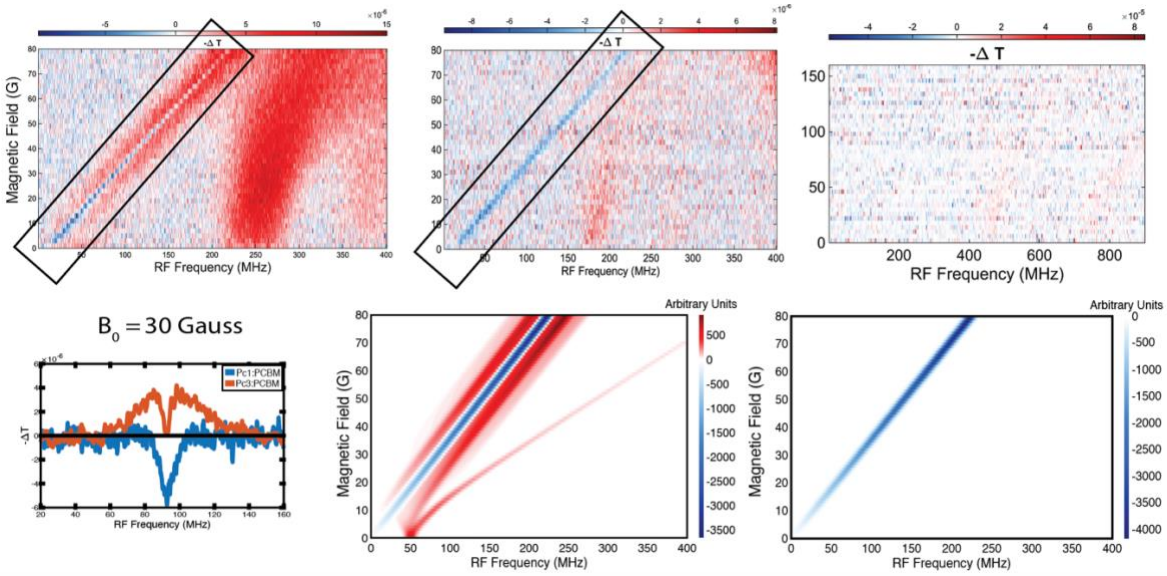

Figure 2 - Top row: PADMR spectra at 5 K for (from left to right) Pc3, Pc1 and Nc1 in PCBM-sensitized films with CW excitation at 787 nm and probe set 760, 760, and 812 nm, respectively. The highlighted signals are characteristic of radical-pair ODMR signals. Bottom row, left: single field slice of the above 2D scans at 30 G magnetic field. Bottom row, center: EasySpin simulation of a pair of radicals with zero-field splitting parameters: D = 50 MHz and E = 0 that gives a positive ODMR signal and a pair of radicals with no zero-field splitting that gives a negative ODMR signal. Bottom row, right: Simulation of a single pair of radicals with no zero-field splitting that gives a negative ODMR signal.

DOE Solar Photochemistry Sponsored Publications 2020-2023

1. O'Connor, Max M., Taylor J. Aubry, Obadiah G. Reid, and Garry Rumbles. "Charge Concentration Limits the Hydrogen Evolution Rate in Organic Nanoparticle Photocatalysts." *Advanced Materials*, (2023): 2210481. https://doi.org/10.1002/adma.202210481.
2. Evans, Austin M., Kelsey A. Collins, Sangni Xun, Taylor G. Allen, Samik Jhulki, Ioannina Castano, Hannah L. Smith, et al. "Controlled N-Doping of Naphthalene-Diimide-Based 2D Polymers." *Advanced Materials* 34, no. 22 (2022): 2101932. https://doi.org/10.1002/adma.202101932.
3. Stingelin, Natalie, and Garry Rumbles. "In Memoriam of Alasdair James Campbell." *Journal of Materials Chemistry C* 10, no. 23 (2022): 8894–8894. https://doi.org/10.1039/D2TC90098J.
4. Zieleniewska, Anna, Fabian Lodermeyer, Maurizio Prato, Garry Rumbles, Dirk M. Guldi, and Jeffrey L. Blackburn. "Elucidating the Electronic Properties of Single-Wall Carbon Nanohorns." *Journal of Materials Chemistry C* 10, no. 15 (2022): 5783–86. https://doi.org/10.1039/D2TC00179A.
5. Rumbles, Garry. "Sustainable Energy & Fuels: 2022 and Beyond." *Sustainable Energy & Fuels* 6, no. 1 (2022): 10–10. https://doi.org/10.1039/D1SE90084F.
6. Carr, Joshua M., Taylor G. Allen, Bryon W. Larson, Iryna G. Davydenko, Raghunath R. Dasari, Stephen Barlow, Seth R. Marder, Obadiah G. Reid, and Garry Rumbles. "Short and Long-Range Electron Transfer Compete to Determine Free-Charge Yield in Organic Semiconductors." *Materials Horizons* 9, no. 1 (January 4, 2022): 312–24. https://doi.org/10.1039/D1MH01331A.
7. Allen, Taylor G., Panagiota Kafourou, Bryon W. Larson, Martin Heeney, Obadiah G. Reid, and Garry Rumbles. "Reconciling the Driving Force and the Barrier to Charge Separation in Donor–Nonfullerene Acceptor Films." *ACS Energy Letters* 6, no. 10 (October 8, 2021): 3572–81. https://doi.org/10.1021/acsenergylett.1c01563.
8. Pace, Natalie A., Tyler T. Clikeman, Steven H. Strauss, Olga V. Boltalina, Justin C. Johnson, Garry Rumbles, and Obadiah G. Reid. "Triplet Excitons in Pentacene Are Intrinsically Difficult to Dissociate via Charge Transfer." *The Journal of Physical Chemistry C* 124, no. 48 (December 3, 2020): 26153–64. https://doi.org/10.1021/acs.jpcc.0c08537.
9. Rosales, Bryan A., Laura E. Mundt, Taylor G. Allen, David T. Moore, Kevin J. Prince, Colin A. Wolden, Garry Rumbles, Laura T. Schelhas, and Lance M. Wheeler. "Reversible Multicolor Chromism in Layered Formamidinium Metal Halide Perovskites." *Nature Communications* 11, no. 1 (December 2020): 5234. https://doi.org/10.1038/s41467-020-19009-z.
10. Pace, Natalie A, Nadezhda V Korovina, Tyler T Clikeman, Sarah Holliday, Devin B Granger, Gerard M Carroll, Sanjini U Nanayakkara, ...Obadiah G Reid and Garry Rumbles, "Slow Charge Transfer from Pentacene Triplet States at the Marcus Optimum." *Nature Chemistry* 100, no. 1 (November 2019): 1–8. https://doi.org/10.1038/s41557-019-0367-x.

Towards a Molecular Understanding of the Spin-statistical Factor during Triplet-Triplet Annihilation for Photon Upconversion

Tsumugi Miyashita[1], Maria Fumanal[2] and Ming Lee Tang[1,3]
[1]Dept. of Biomedical Engineering, The University of Utah, Salt Lake City, UT 84112
[2]Departament de Ciència de Materials i Química Física and IQTCUB, Universitat de Barcelona, Barcelona, Spain, E-08028
[3]Dept. of Chemistry, The University of Utah, Salt Lake City, UT 84112

The goal of this research is to enable all the energy contained in sunlight to be harvested. Current systems are unable to extract all of the energy available from sunlight due to rapid relaxation processes that dissipate some of the energy as heat. In this work, inexpensive, earth-abundant components capable of supporting multi-excitonic processes involving more than one tightly bound excited state are investigated as a way to exceed the Shockley-Queisser limit. This research focuses on hybrid organic-inorganic nanostructures capable of singlet fission and photon upconversion. A variety of steady-state and time-resolved spectroscopic techniques are used to study the transfer of energy from spin-triplet excitons that are created in either the organic molecules, or the nanoparticle.

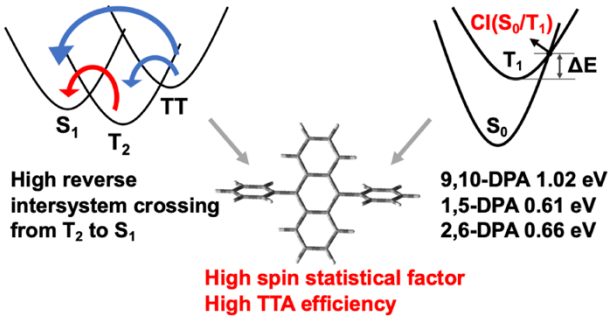

Though triplet-triplet annihilation (TTA) is currently used in high performance organic light emitting diodes (OLEDs), the structural factors affecting TTA are not well-understood. TTA can be used to convert low energy near-infrared light to high energy UV or visible light. The low spin statistical factor and low TTA efficiency, however, are bottlenecks in TTA-based photon upconversion. The spin statistical factor is the probability that the singlet is formed through TTA and is thus important in improving any TTA-based photon upconversion system. In this study, we investigate the spin statistical factor and TTA efficiency in three diphenylanthrene (DPA) isomers (9,10-DPA, 1,5-DPA and 2,6-DPA). The 9,10-DPA isomer, in the presence of the platinum octaethylporphyrin sensitizer, gives the highest photon upconversion efficiency of 0.221 out of a maximum theoretical value of 0.5. Both steady-state and time-resolved transient absorption results demonstrate that TTA efficiencies for 9,10-DPA and 1,5-DPA are comparable around 0.32, whereas it is 0.7 times lower for 2,6-DPA at 0.23. Additionally, the spin statistical factor decreases from 9,10-DPA to 1,5-DPA to 2,6-DPA, from 0.85 to 0.72 and 0.29 respectively. The higher TTA efficiency and spin-statistical factor of 9,10-DPA compared to its isomers is rationalized at the molecular level based on DFT and time-dependent DFT (TDDFT) calculations. On the one side, the conical intersection between the S_0 and T_1 states for 9,10-DPA is significantly higher in energy resulting in a longer triplet lifetime, which ultimately serves to enhance the TTA efficiency. On the other side, TDDFT calculations show that 9,10-DPA can undergo high reverse intersystem crossing from T_2 to the bright S_1 state therefore increasing the spin statistical factor with respect to the other two isomers. Both unique features of 9,10-DPA isomer originate in the appropriate position of the phenyl groups, providing rigidity and favorable triplet energetics for efficient TTA.

This work provides insight into designing molecules for efficient photon upconversion, light emission or quantum information science applications. The effect of molecular and nanocrystal structure on the electronic coupling between the hybrid components will be examined to establish fundamental relationships between structure and triplet energy transfer efficiency. The findings will be directly applicable to a potential acene-silicon platform that may ultimately enhance the power conversion efficiency of silicon solar cells.

DOE Solar Photochemistry Sponsored Publications 2020-2023

1. T. Miyashita, P. Jaimes, T. Lian, **M. L. Tang**, Z. Xu, "Quantifying the Ligand-Induced Triplet Energy Transfer Barrier in a Quantum Dot-Based Upconversion System", *J. Phys. Chem. Lett.,* 13, 3002, **2022**. (selected for supplementary journal cover)

2. Z. Xu, Z. Huang, T. Jin, T. Lian, **M. L. Tang** "Mechanistic understanding and rational design of quantum dot/mediator interfaces for efficient photon upconversion", *Acc. Chem. Res.*, 12, 36558, **2021**. (invited, selected for journal cover).

3. P. Xia, E. K. Raulerson, D. Coleman, C. S. Gerke, L. Mangolini, **M. L. Tang**, S. T. Roberts, "Achieving Spin-triplet Exciton Transfer between Silicon and Molecular Acceptors for Photon Upconversion" *Nature Chem.*, 12, 137, **2020**.

4. T. Huang, T. Koh, J. Schwan, T. Tran, P. Xia, L. Mangolini, **M. L. Tang**, S. T. Roberts, " Bidirectional Triplet Exciton Transfer Between Silicon Quantum Dots and Perylene Molecules in a Red-to-Blue Photon Upconversion System" **2021** (in press).

5. Z. Huang, Z. Xu, T. Huang, V. Gray, K. Moth-Poulsen, T. Lian, **M. L. Tang** "Evolution from tunneling to hopping mediated triplet energy transfer from quantum dots to molecules", *J. Am. Chem. Soc.*, 142, 17581, **2020**.

6. Z. Xu, Z. Huang, C. Li, T. Huang, F. A. Evangelista, **M. L. Tang**, T. Lian, " Tuning the quantum dot (QD)/mediator interface for optimal efficiency of QD-sensitized near-infrared-to-visible photon upconversion systems", *ACS Appl. Mater. Interfaces,* 12, 36558, **2020**.

7. J. De Roo, Z. Huang, N. J. Schuster, L. Hamachi, D. N. Congreve, Z. Xu, D. A. Fishman, T. Lian, J. Owen, **M. L. Tang**, "Anthracene Diphosphate Ligands for CdSe Nanocrystals: Molecular Design for Efficient Upconversion" *Chem. Mater.,*32, 1461, **2020**.

8. P. Xia, E. K. Raulerson, D. Coleman, C. S. Gerke, L. Mangolini, **M. L. Tang**, S. T. Roberts, "Achieving Spin-triplet Exciton Transfer between Silicon and Molecular Acceptors for Photon Upconversion" *Nature Chem.*, 12, 137, **2020**.

Dexter Energy Transfer Pathways

S. Bai[1], S.N. Chowdhury[1], K. Liu[1], S.A. Mavrommati[2], J. Valdiviezo[1], J.Y. Yuly[1], P. Zhang[1], Z. Zhang[1], S.S. Skourtis[2], and D.N. Beratan[1]
[1]Department of Chemistry, Duke University, Durham, NC 27708 USA
[2]Department of Physics, University of Cyprus, Nicosia 1678, Cyprus

Our team is studying the molecular mechanisms of Dexter (spin-forbidden) electronic excitation energy transfer at the nanoscale. We are developing approaches to describe the contributions of charge-transfer and exchange contributions to the coupling, and we are examining the balance of coherent and incoherent mechanisms for long range Dexter energy transfer in novel structures. We have established significant experimental collaboration that are allowing us to begin to understand the atomistic control of Dexter transport in both nanoparticle and organic molecular structures, and we are exploring the viability of using cold-atom quantum computers to simulate the quantum dynamics of energy and charge transport in the condensed phase.

A Trapped-ion Qutrit quantum simulator for electron and energy transfer dynamics.
The quantum dynamics of Dexter transfer and transport in the condense phase is poorly understood because of the formidable computational scaling required to describe quantum systems in contact with a dissipative condensed phase environment. The promise of emerging quantum-based simulators is to offer strategies to explore complex condensed phase quantum dynamics with more favorable cost scaling with system size compared to classical computers. As a result, we are exploring the viability of modeling condensed phase electronic energy transfer and electron transfer using cold trapped ion quantum computers. In collaboration with the groups of K.R Brown and J. Kim at Duke, we demonstrated the feasibility of using trapped-ion quantum simulators to describe the influence of excitation light polarization on the quantum dynamics and electron transport in model donor acceptor systems. We use d-level systems (qudits), rather than traditional two-level quantum systems (qubits) to enhance the efficiency of the simulations. The accuracy of quantum simulations using qubits is limited, in part, by decoherence as the system size grows. This limitation can be reduced by utilizing multi-level qudit structures when encoding a molecular Hamiltonian in a trapped-ion system. By using single-qutrit operations, we decrease the number of ions that is required for the quantum simulations, and we replace multi-ion entangling operations with operations that manipulate the atomic levels of a single ion. This produces significantly faster compute operations, with a longer coherence time and higher accuracy for tracking the dynamics being modeled. The simulations are realized with d=3, namely a qutrit trapped-ion quantum simulator, producing high fidelity simulations of ET induced by polarized light in our model donor-acceptor structures. The system studied has novel coupling pathway interferences, arising from the donor excited state degeneracy, and the results found are consistent with those produced on classical computers. We also studied potential sources of error that enter these quantum simulations. We aim to build upon this first study to explore how the quantum computations will scale as increasing realism is added to the system, bath, and system-bath interaction Hamiltonians.

Triplet energy transfer in quantum dot core-shell structure. Quantum dot sensitized triplet energy transfer has found promising applications in photon up-conversion and photocatalysis. Yet, it remains unclear whether triplet energy transfer from quantum dots is mediated by charge transfer virtual states or by direct two-particle exchange. Charge transfer state mediated triplet energy transfer was recently observed in CdSe/CdS–anthracene carboxylic acid (ACA) complexes. We have found that the two-particle exchange interaction mediates triplet energy transfer in the CdSe/CdS–ACA assemblies. Joint experimental and theoretical studies in collaboration with T. Lian (Emory) find that the measured triplet energy transfer distance dependent coupling decay constant (β_{TET}) as a function of the CdS shell thickness is much weaker than is found for electron and hole transfer. That is, $\beta_{TET} << \beta_e + \beta_h$. Theoretical analysis finds that the bridge-exciton states interact strongly the donor exciton and the surface acceptor through wave function delocalization in the core and shell regions. The strong wave function overlap of the donor and bridge exciton does not decay significantly with the shell thickness. The strong overlap leads to the two-particle exchange interaction dominating the donor-bridge exciton coupling, which is described well by typical exponential decay models. Consideration of the electron and hole coupling through the shell region, together with analysis of particle size distributions of the nanoparticles is leading to a comprehensive understanding of triplet energy transfer in chemically modified core-shell nanoparticle structures.

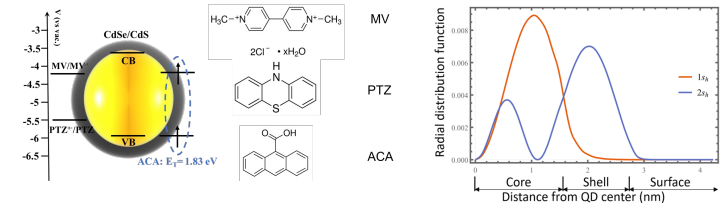

Figure 1. Radial wave functions of CdSe/CdS quantum dots (1.5 nm core; 1.3 nm shell thickness). The wave functions of the $1s_h$ and $2s_h$ strongly overlap, producing a strong two-particle exchange dominated coupling. The wave function of the $2s_h$ state has large amplitude near the surface (strongly interacting with the surface-bound acceptor).

Design of Dexter Energy Transport Wires. We have developed design principles for organic π-stacked molecular bridges that may enable rapid and efficient triplet exciton transfer over long distances. The rules indicate that low inner-sphere reorganization energies, low static and dynamic disorder, and enhanced π-stacking interactions among nearest-neighbor chromophores favor the persistence of coherent triplet exciton transfer, even at room temperature. We have proposed several candidate molecular structures that satisfy these criteria, and the designs are being explored synthetically in a collaboration with C. Nuckolls (Columbia). Our analysis and designs are based on electronic structure analysis, molecular dynamic, and density matrix based dynamical simulations. We predict fast triplet energy transfer through the designed bridges, with effective intra-bridge triplet energy transfer rates on the scale of 2 psec for bridges up to 50 chromophore units. Ongoing studies involve the development of a flickering resonance theory for Dexter energy transfer and molecular design/redesign as part of the collaboration with the Nuckolls group.

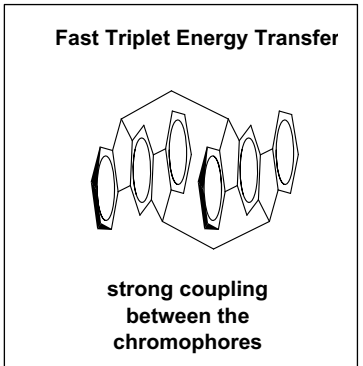

Figure 2. Example of proposed Dexter exciton wire.

Toward improved energy splitting methods to compute Dexter couplings. The computation of intermolecular Dexter couplings is a first step toward modeling of transport in extended energy transport networks. An economical approach to estimating Dexter couplings is to compute excitons splitting. For high symmetry donors and acceptors, the Dexter coupling is the half of the adiabatic energy splitting. When the structures have lowered symmetry, the simple energy splitting method fails. To address this issue and retain the power and simplicity of the splitting method, use small molecular geometry changes to determine the minimum energy splitting associated with the splitting between the singlet and triplet adiabatic energy surfaces. The minimum energy splitting thus obtained provides useful estimates of the Dexter coupling. The validity of this approach is confirmed by comparing our approach to computations using the fragment spin difference method. We explored the performance of this computational approach to compute Dexter energy transfer couplings in noncovalent aromatic assemblies. These benchmark studies inform methods chosen in ongoing computations of Dexter couplings.

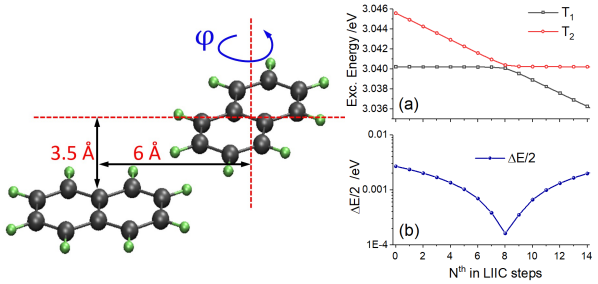

Figure 3. The T_1 and T_2 energy variations when tuning the **n**aphthalene geometry towards the S_0/T_1 crossing point. The T_1 and T_2 energy splitting minimum defines the DET coupling.

Modulating Dexter energy transfer with chirality. Electron transfer kinetics has been found to be modulated by molecular chirality, through the so-called chirality induced spin selectivity effect (CISS). Since triplet excitation energy transfer at long-distances can be controlled by virtual charge transfer events, Dexter energy transfer might also be impacted by molecular chirality. There is recent experimental evidence that chirality may influence Dexter transfer (B. Chen et al., *Nat. Commun.*, 14, 1514, 2023). In these experiments, the phosphorescence intensity was found to change by more than 100-fold in host-guest frameworks with different chirality pairings. A theory for chirality-dependent Dexter and Förster energy transfer is being developed to understand the origins of these novel findings.

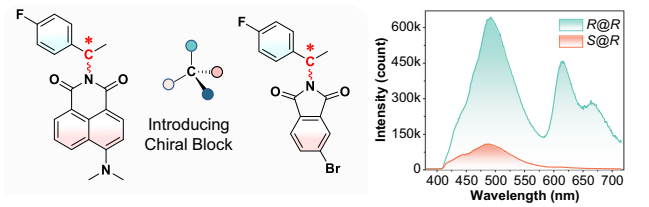

Figure 4. A chiral amine was introduced in a naphthalimide (D) - phthalimide (A) host-guest assembly, enhancing the steady-state photoluminescence.

DOE Solar Photochemistrhy Sponsored Publications

1. M. Kang, K.T. Liu, S.N. Chowdhury, J.L. Yuly, K. Sun, J. Whitlow, J. Valdiviezo, Zhendian Zhang, P. Zhang, D.N. Beratan, and K. R. Brown, "Trapped-ion quantum simulations for condensed-phase chemical dynamics: seeking a quantum advantage," in preparation (2023).
2. K. Sun, C. Fang, M. Kang, Z. Zhang, P. Zhang, D.N. Beratan, K.R. Brown, and J. Kim, "High-fidelity Simulation of Polarized Light-induced Electron Transfer on A Trapped-ion

Qutrit System," in preparation (2023).
3. S. Bai, P. Zhang, and D.N. Beratan, "Using adiabatic Energy Splitting to Compute Dexter Energy Transfer Couplings," in preparation (2023).
4. S. A. Mavrommati and S. S. Skourtis, Molecular wires for efficient long-distance triplet energy transfer, *J. Phys. Chem. Lett.* 13, 9679-9687 (2022).

Rational Design of Metal-tipped Semiconductor Quantum Rod Heterostructures for Efficient Light-driven Charge Separation and H_2 Evolution

Tianquan (Tim) Lian
Department of Chemistry
Emory University
Atlanta, Georgia 30322

One of the goals of our DOE funded project is to advance fundamental understanding of light driven charge separation and recombination processes in nano-heterostructures and to provide design principle to guide the rational development of these materials for efficient solar fuel generation. Colloidal quantum confined semiconductor-metal nanocrystal heterostructures are promising candidates for solar energy conversion because their light absorbing semiconductor and catalytic metal domains can be independently tuned and optimized. Although their overall light-to-hydrogen generation quantum efficiencies have been reported to show interesting dependences on the morphologies of the semiconductor and metal domains, the mechanisms of such dependences are poorly understood. Using Pt nanoparticle tipped CdS nanorods (CdS-Pt NRs) as a model system, we have examined how the morphology of the nanorods affect the light driven H_2 generation performance in this system. In these studies, we directly measure the quantum efficiency of light-driven H_2 generation as well as elementary charge separation and recombination processes. The comparison of these processes allows us to develop a simplified kinetics model that account for key elementary steps involved in the overall light-to-H_2 generation and gain deeper insight into how the nanorod morphologies affect the H_2 generation performance.

1). Pt particle size affects both the charge separation and water reduction efficiencies of CdS-Pt nanorod photocatalysts for light-driven H_2 generation. Decreasing the metal catalyst size into nanoclusters or even single atom is an emerging direction of developing more efficient and cost-effective catalysts, especially in electro- or heterogeneous catalysis. It is unclear how to incorporate similar ideas into photocatalyst design because the catalyst particle size affects both the catalyst activity and interfacial charge separation. To answer this question, we study the effect of the Pt catalyst size on light driven H_2 generation quantum efficiency (QE_{H_2}) of CdS-Pt NRs in the presence of sacrificial electron donors. With the increase of the Pt catalyst size from 0.7±0.3 to 3.0±0.8 nm, the QE_{H_2} of CdS-Pt increases from 0.5±0.2% to 38.3±5.1%, by nearly two orders of magnitude (Fig. 1 left panel). Transient absorption spectroscopy measurement reveals that the electron transfer rate from the CdS NR to the Pt tip increase with the Pt diameter following a scaling law of $d^{5.6}$, giving rise to the increase of electron transfer efficiency at larger Pt sizes. The observed trend can be understood by a simplified kinetic model that assumes the overall efficiency is the product of the quantum efficiencies of charge separation (including hole transfer, electron transfer

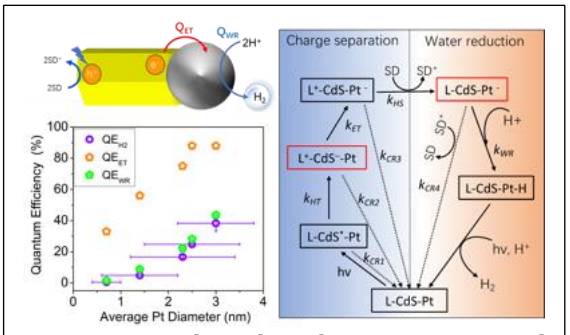

Fig. 1. Pt size dependent charge separation and H2 generation in CdS-Pt NRs. (left) scheme of CdS-Pt nanorod and Pt size dependent charge separation, water reduction and H2 generation quantum efficiency. (right) A simplified kinetics model that account for key steps in the overall light-to-H_2 conversion process.

and hole scavenging) and water reduction steps, and for CdS-Pt NRs, the quantum efficiencies of electron transfer and water reduction steps increase with the Pt sizes. Our findings suggest the importance of improving the quantum efficiencies charge separation and catalysis speed in designing efficient semiconductor-metal hybrid photocatalysts, especially in the regime of small metal particle sizes.

2) Nanorod length-dependent photodriven H_2 production in 1D CdS-Pt heterostructures. Another key morphological control is the length of CdS nanorod. We use heterostructures of Pt tipped 0D CdS quantum dots (with ~4.6 nm diameter) and 1D CdS nanorods (of ~13.8, 27.8, 66.6, and 88.9 nm average rod lengths, Figure 2 left panel) as a model system to study the rod length-dependence of charge separation and charge recombination times and their impacts on photo-driven H_2 production. The H_2 generation quantum efficiency increases from 0.2±0.0% in quantum dots to 27.8±0.4% at the rod length of 28 nm and show negligible changes at longer rod lengths(Figure 2 right). The electron transfer half lifetime increases monotonically with the rod length from 0.7±0.1 in quantum dots to 170.2±29.5 ps in the longest rods, corresponding to a decreases of electron transfer quantum efficiency from 92% to 70% (Figure 2 right). The average lifetime of charge separated state increases from 4.7±0.4 μs in quantum dots to 149±34 μs in 28nm nanorods, and the lifetime does not increase further in longer rods, resembling the trend in the observed H_2 generation quantum efficiency. Detailed analysis suggests that in these samples, the charge separation lifetime determines the quantum efficiency for hole removal by the sacrificial electron donor and is the key factor for the overall light driven H_2 generation quantum efficiency.

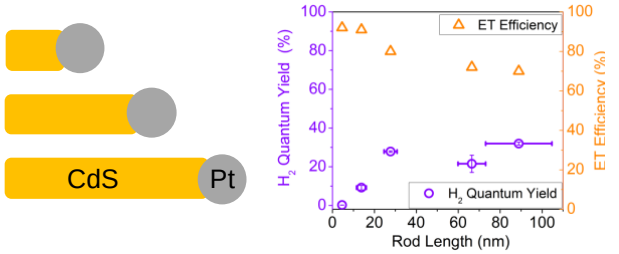

Figure 2. CdS nanorod length dependent charge separation and H_2 generation in CdS-Pt NRs. (left) scheme of CdS-Pt nanorod of different rod length. (right) Rod length dependent charge separation and H2 generation quantum efficiency.

3)Multiple electron transfer from the CdS nanorod to Pt tip. Solar-to-fuel conversion often requires multiple proton-coupled electron transfer (PCET) processes powered by the energetic electrons and/or holes generated by the absorption of multiple photons. The effective coupling of multiple electron transfer from the light absorber with the multiple PCET reactions at the catalytic center is one of the key challenges in efficient and selective conversion of solar energy to chemical fuels. In this work, we examine the dynamics of multiple electron transfer in CdS nanorods with a Pt tip. By excitation-fluence dependent transient absorption measurement, we show that multi-exciton Auger recombination rate follows a carrier-collision model, $k_n^A =$

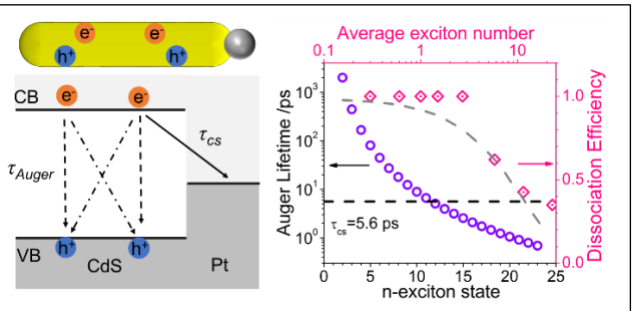

Figure 5. (Left) Schematic of multiple electron transfer from the CdS NR to Pt tip and competitive processes. (right) The lifetime of n-exciton states (purple circles, left axis) and dissociation efficiency of multiple-exciton states (red diamond, right axis). Long-lived multiexciton states in CdS and fast ET time to Pt (horizontal dashed line) enables efficient multiple ET to the Pt.

$n^2(n-1)/4k_2^A$, with a biexciton lifetime ($1/k_2^A$) of 2.0±0.2 ns (Figure 5). In CdS-Pt nanorods, electron transfer kinetics does not change with the excitation fluence and ET from the CdS to Pt has a half-life time of 5.6±0.6 ps, independent of the number of transferred electrons. Because the ET time is faster than the multiple exciton Auger decay time, efficient multiple ET can be achieved. Under the highest fluence, where 22.9 excitons are generated per nanorod, dissociation of 8 excitons is observed. However, the half lifetime of the charge separated state recombination (with n electrons in the Pt and n holes in the CdS) decreases from 10 μs in single charge separated state to 42 ns with 8 charge separated states. Our findings suggest the possibility of driving multielectron photocatalytic reactions under intense light illumination and controlling product selectivity through the transient concentration of electrons.

DOE Solar Photochemistry Sponsored Publications 2020-2023 (DOE DE-SC0008798)

1) Taghinejad, M., Xu, Z., Lee, K. T., Lian, T., & Cai, W. Transient second-order nonlinear media: Breaking the spatial symmetry in the time domain via hot-electron transfer. ***Phys. Rev. Lett (2020)***, 124, 013901
2) Taghinejad, M., Xu, Z., Lee, K. T., Lian, T., & Cai, W. Photocarrier-Induced Active Control of Second-Order Optical Nonlinearity in Monolayer MoS_2. **Small (2020),** 1906347 (https://doi.org/10.1002/smll.201906347)
3) Qiuyang Li, Wenxing Yang, Tianquan Lian, "Exciton Transport and Interfacial Charge Transfer in Semiconductor Nanocrystals and Heterostructures ", ***Springer Verlag Handbook on Photochemistry (2020), accepted***
4) De Roo, J., Huang, Z., Schuster, N., Hamachi, L., Congreve, D., Xu, Z., Fishman, D., Lian, T., Owen, J., Tang, M. Anthracene Diphosphate Ligands for CdSe Quantum Dots; Molecular Design for Efficient Upconversion. ***Chemistry of Materials (2020), 32, 1461***.
5) Yawei Liu, Qiaoli Chen, David Cullen, Zhaoxiong Xie, and Tianquan Lian, "Size Dependent Hot Electron Transfer in CdS Nanorod-Au Heterostructures", **Nano Letters** (2020), 20 (6), 4322, http://dx.doi.org/10.1021/acs.nanolett.0c01050
6) Wenxing Yang, Gregory E. Vansuch, Yawei Liu, Jin Tao, Qiliang Liu, Aimin Ge, Monica L. K. Sanchez, Michael W. W. Adams, R. Brian Dyer, and Tianquan Lian, "Surface ligand "liquid" to "crystalline" phase transition modulates the solar H_2 production quantum efficiency of CdS nanorod/mediator/Hydrogenases assemblies", ***ACS AMI*** (2020), 13 (32), 36558-36567
7) Zihao Xu, Zhiyuan Huang, Chenyang Li, Tingting Huang, Francesco A. Evangelista, Ming L. Tang, and Tianquan Lian, "Tuning QD/Mediator interface for Optimal Efficiency of Quantum Dot Sensitized Near Infrared to Visible Photon Upconversion Systems", ***ACS AMI*** (2020), 12 (31), 35614-35625
8) Xu Guo, Qiuyang Li, Yawei Liu, Tao Jin, Yubin Chen, Liejin Guo and Tianquan Lian "Enhanced Light-Driven Charge Separation and H_2 Generation Efficiency in WSe_2 Nanosheet-Semiconductor Nanocrystal Heterostructures", ***ACS AMI (2020)*** 12, 44769. ***(https://doi.org/10.1021/acsami.0c12931)***
9) Zhiyuan Huang, Zihao Xu, Tingting Huang, Victor Gray, Kasper Moth-Poulsen, Tianquan Lian, Ming Lee Tang, "Evolution from tunneling to hopping mediated triplet energy transfer from quantum dots to molecules", ***JACS (2020)*** 142,41,17581. https://doi.org/10.1021/jacs.0c07727

10) Zihao Xu, Zhiyuan Huang, Tao Jina, Tianquan Lian, Ming L. Tang, "Mechanistic Understanding and Rational Design of Quantum Dot/Mediator Interfaces for Efficient Photon Upconversion" ***Account of Chemical Research (2021)***, 54, 70-80, https://doi.org/10.1021/acs.accounts.0c00526
11) Wenxing Yang, Yawei Liu, James R. McBride, Tianquan Lian, "Ultrafast and long-lived transient heating of surface adsorbates on plasmonic semiconductor nanocrystals", Nano Lett.(2021), 21, 453. https://doi.org/10.1021/acs.nanolett.0c03911
12) Sean S. E. Collins, Emily K. Searles, Lawrence J. Tauzin, Minhan Lou, Luca Bursi, Yawei Liu, Jia Song, Charlotte Flatebo, Rashad Baiyasi, Yi-Yu Cai, Benjamin Foerster, Tianquan Lian, Peter Nordlander, Stephan Link, and Christy F. Landes, "Plasmon Energy Transfer in Hybrid Nanoantennas", **ACS Nano (2021) 15, 9522-30 (**https://doi.org/10.1021/acsnano.0c08982)
13) W. Yang, Y. Liu, D.A. Cullen, J.R. McBride, T. Lian, "Harvesting Sub-bandgap IR Photons by Photothermionic Hot Electron Transfer in a Plasmonic p-n Junction, Nano Letters (2021), 21, 9, 4036. https://doi.org/10.1021/acs.nanolett.1c00932
14) J. Song, J. Long, Y. Liu, Z. Xu, A. Ge, B.D. Piercy, D.A. Cullen, I. N. Ivanov, M. D. Losego, T. Lian, "Highly Efficient Plasmon Induced Hot-Electron Transfer at Ag/TiO2 interface", ACS Photonics (2021), 8, 1497, https://doi.org/10.1021/acsphotonics.1c00321
15) R. Lemasters, M. R. Shcherbakov, G. Yang, J. Song, T. Lian, H. Harutyunyan, and G. Shvets, "Deep Optical Switching on Subpicosecond Timescales in an Amorphous Ge Metasurface", Advanced Optical Materials (2021), 2100240, https://doi.org/10.1002/adom.202100240
16) Wenxing Yang, Yawei Liu, Tomas Edvinsson, Ashleigh Castner, Shihuai Wang, Sheng He, Sascha Ott, Leif Hammarström, and Tianquan Lian, Photoinduced Fano Resonances between Quantum Confined Nanocrystals and Adsorbed Molecular Catalysts, Nano Lett (2021), 21, 5813. https://doi.org/10.1021/acs.nanolett.1c01739
17) Liu, Yawei; Yang, Wenxing; Chen, Qiaoli; Cullen, David; Xie, Zhaoxiong; Lian, Tianquan, "Pt particle size affects both the charge separation and water reduction efficiencies of CdS-Pt nanorod photocatalysts for light-driven H2 generation", JACS (2022), https://doi.org/10.1021/jacs.1c11745
18) Li Zhai, Sara T. Gebre, Bo Chen, Dan Xu, Junze Chen, Zijian Li, Yawei Liu, Hua Yang, Chongyi Ling, Yiyao Ge, Wei Zhai, Changsheng Chen, Lu Ma, Qinghua Zhang, Xuefei Li, Yujie Yan, Xinyu Huang, Lujiang Li, Zhiqiang Guan, Chen-lei Tao, Zhiqi Huang, Hongyi Wang, Jinze Liang, Ye Zhu, Chun-Sing Lee, Peng Wang, Chunfeng Zhang, Lin Gu, Yonghua Du, Tianquan Lian, Xue-Jun Wu, Hua Zhang, "Epitaxial Growth of Highly Symmetrical Branched Noble Metal-Semiconductor Heterostructures with Efficient Plasmon-Induced Hot-Electron Transfer". Nature Communication (2023) accepted.
19) Liu, Yawei; Yang, Wenxing; Chen, Qiaoli; Xie, Zhaoxiong; Lian, Tianquan, "Nanorod length-dependent photodriven H2 production in 1D CdS-Pt heterostructures", under review in JACS.
20) Wenxing Yang, Sheng He, Tianquan Lian, "Doping of colloidal nanocrystals for optimizing interfacial charge transfer: a double-edged sword", to be submitted

Multi-Electron and Triplet Energy Transfer at the Interface of Two-Dimensional Semiconductors

Victoria A. Lumsargis, Angana De, Daria D. Blach, Shibin Deng, and Libai Huang
Department of Chemistry
Purdue University
West Lafayette, IN 47907

Scope of the Project: Exciton transfer, transport, and dissociation at hetero-interfaces play a critical role in converting light into electricity and fuels using organic and nanostructured materials. Two-dimensional (2D) transition metal dichalcogenides (TMDCs) and hybrid perovskites are excitonic structures characterized by their tunable interfacial energy landscapes, which facilitate fast charge and energy transfer processes. Heterostructures that integrate 2D semiconductors with other excitonic materials present new opportunities for developing solar energy functionalities. The overarching goal of this program is to build a fundamental knowledge base for energy and charge transfer at these 2D interfaces, using ultrafast microscopy and spectroscopy. In this context, we highlight our recent results on leveraging the unique electronic properties of 2D materials to interact with singlet and triplet excitons in acene and pyrene molecules, achieving efficient charge separation, multi-electron transfer, and triplet exciton sensitization.

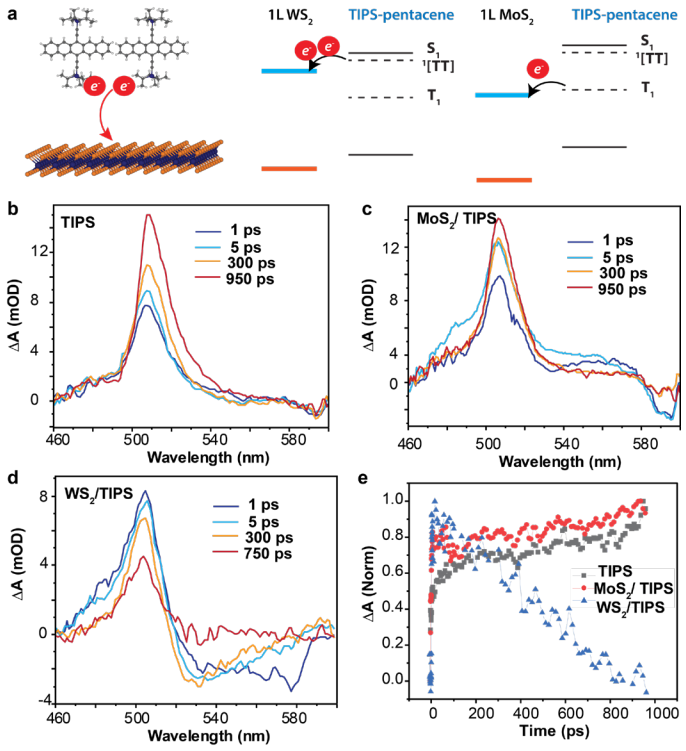

Figure 1. Charge separation of triplet excitons generated from singlet fission at TMDC-acene Interfaces. (a) Energy antialignment of MoS_2 and WS_2 and TIPS-pentacene heterostructures. (b-d) Transient absorption spectra taken at 8K with 620 nm excitation at different delay times for TIPS pentacene only, MoS_2-,WS_2 -TIPS-pentacene heterostructures, respectively. (e) Comparison of triplet dynamics at 507 nm in different sample at 8 K.

Recent Results:

Multi-electron transfer from triplet pairs at TMDC-acene Interfaces. Singlet fission, a process in which an excited singlet state shares its excitation energy with a neighboring ground-state chromophore, converting both into triplet excited states, has the potential to surpass the Shockley-Queisser limit by generating additional photocurrent from high-energy photons. To harness the triplet excitons, it is desirable to directly dissociate the bound triplet pair states. Recently, we demonstrated that TMDC layers can serve as effective triplet acceptors for singlet fission.

We investigated electron transfer initiated from ^{1}[TT] and T_1 states by fabricating heterostructures consisting of monolayer MoS_2, WS_2 and TIPS-pentacene (6,13-Bis(triisopropylsilylethynyl)pentacene) (**Figure 1a**). Electron transfer can occur from the S_1, ^{1}[TT], and T_1 states of TIPS pentacene to

MoS_2. However, in contrast, electron transfer to WS_2 is only possible from the ^{1}[TT] or S_1 states. To achieve efficient triplet exciton dissociation and prevent singlet transfer, singlet fission needs to outcompete electron transfer from S_1. The initial step of singlet fission in TIPS-pentacene thin films is fast on the sub-ps timescale, which can outcompete charge transfer from S_1 (~ 2 ps). The separation of the triplet pair state ^{1}[TT], on the other hand, can be much slower; therefore, concerted two-electron transfer from ^{1}[TT] is an important pathway. Such multi-charge transfer can benefit solar energy conversion to chemical fuel because the lifetimes of one-electron intermediates do not limit the efficiency of the photocatalytic reactions.

We performed temperature-dependent transient absorption spectroscopy to probe these pathways, tracking the dynamics of ^{1}[TT] and T_1 excited stated absorption band near 500 nm. As shown in **Figure 1b**, T_1 formation in TIPS-pentacene is on the order of a few hundred picoseconds at 8 K, because the dissociation of ^{1}[TT] to T_1 is a temperature-activated process. Remarkably, WS_2/TIPS-pentacene and MoS_2/TIPS-pentacene heterostructures exhibit distinctly different triplet dynamics at low temperature (**Figure 1c-d**). The triplet dynamics in MoS_2/TIPS-pentacene heterostructure is overall similar to that of TIPS pentacene, implying minimal charge transfer from either ^{1}[TT] or T_1, likely due to the lack of thermal energy needed to overcome the energy barrier at 8 K. Conversely, a much faster triplet decay is observed in WS_2/TIPS-pentacene (**Figure 1e**), indicating the charge transfer from ^{1}[TT] because the transfer from T_1 is not energetically favorable. At 8K, we extracted the electron transfer time from the ^{1}[TT] state to be ~ 10 ps by monitoring the rise of exciton bleach of WS_2 when selectively exciting TIPS pentacene. These results showcase the promise of TMDCs as electron acceptors for ^{1}[TT] state from singlet fission.

Triplet exciton transfer dominated by quantum tunneling in 2D organic-inorganic hybrid perovskites. Triplet energy transfer at organic-inorganic interfaces has recently garnered significant research interest due to the success of hybrid structures in photon upconversion and downconversion applications. In addition to highly programmable lattices with strong electronic coupling between organic and inorganic components, excitons residing in the inorganic lattice of 2D perovskites have advantages in sensitizing triplet excitons in organic molecules. This is due to the strong spin-orbit interaction, resulting in an exciton fine structure with small energy splitting between singlet-like and triplet-like states. In collaboration with Prof. Prezhdo at the University of Southern California, we demonstrated rapid energy transfer from the 2D lead iodide sublattice to the triplet excitons in pyrene ligands (**Figure 2a**). Phosphorescence from triplet excitons in pyrene was observed upon exciting the excitons in 2D perovskites, displaying a narrow linewidth with well-resolved vibrational features at low temperatures (**Figure 2b**). Energy transfer from the lead iodide sublattice to the pyrene cations is remarkably fast, showing weak temperature dependence and

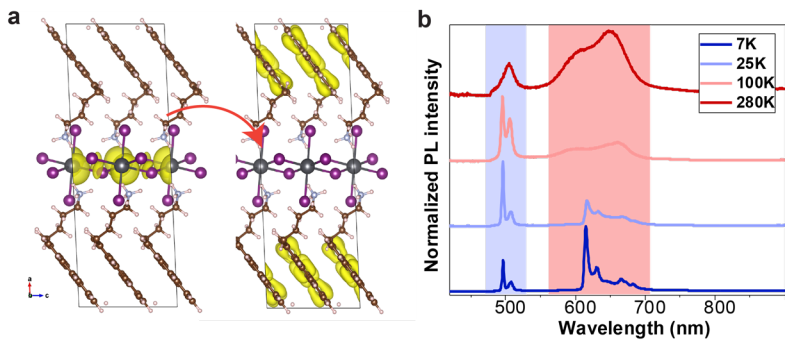

Figure 2. Energy transfer from 2D lead iodide perovskite to the triplet excitons in pyrene ligands. (a) Calculations of excitons resides in the lead iodide sublattice (left) and triplet excitons in the pyrene ligands (right). Provided by Prof. Prezhdo group. (b) Temperature-dependent emission spectra showing both excitons in the lead iodide sublattice (blue shaded area) and triplet emission from pyrene (red shaded area).

energy transfer timescales of approximately 50-70 ps across a temperature range of 7-295 K. Theoretical modeling revealed that triplet energy transfer was dominated by quantum tunneling in the Marcus inverted regime. These results provide insights into how a suitable design of the energy landscape at 2D organic-inorganic interfaces can enable efficient energy transfer functions.

DOE Solar Photochemistry Sponsored Publications 2020-2023

1. Daria D. Blach, Dana B. Sulas-Kern, Oleg Prezhdo, Jeffrey L. Blackburn, and Libai Huang*, Long-Range Interfacial Charge Transport in Heterostructures of MoS_2 and Carbon Nanotubes, manuscript in preparation, (2023).
2. Shibin Deng, Ti Wang, Jinying Wang, Daniele Meggiolaro, Yongping Fu, Linrui Jin, Jee Yung Park, Francesco Ambrosio, Letian Dou, Song Jin, Filippo De Angelis, and Libai Huang*, Polaron Repulsion in Lead Halide Perovskites, submitted (2023).
3. Long Yuan, Biyuan Zheng, Qiuchen Zhao, Roman Kempt, Thomas Brumme, Agnieszka Beata Kuc*, Chao Ma, Shibin Deng, Anlian Pan* and Libai Huang*, Strong Dipolar Repulsion of One-Dimensional Interfacial Excitons in Monolayer Lateral Heterojunctions, *ACS Nano*, Accepted (2023).
4. Maja Feierabend, Victoria Lumsargis, Joshua JP Thompson, Kang Wang, Letian Dou, Libai Huang, Ermin Malic*, Dark interlayer excitons in WS/tetracene heterostructures, *Nanoscale* 15, 1730-1738 (2023).
5. Sandhya Susarla, Daria Blach, Mit Naik, Zhenglu Li, Johan Carlstroem, Takashi Taniguchi, Kenji Watanabe, Libai Huang, Felipe da Jornada, Ramamoorthy Ramesh, Steven Louie*, Peter Ercius*, Archana Raja*, Hyperspectral imaging of excitons within a moiré unit-cell with a subnanometer electron probe, *Science* 378, 1235-1239, (2022).
6. Yuming Deng, Lan Jiang, Libai Huang, Tong Zhu, Energy flow in hybrid organic/inorganic systems for triplet–triplet annihilation upconversion, *ACS Energy Letters*, 7, 847–861, (2022).
7. Long Yuan, Biyuan Zheng, Qiuchen Zhao, Roman Kempt, Thomas Brumme, Agnieszka Beata Kuc, Chao Ma, Shibin Deng, Anlian Pan, Libai Huang*, Non-Equilibrium First-Order Exciton Mott Transition at Monolayer Lateral Heterojunctions Visualized by Ultrafast Microscopy, arXiv preprint arXiv:2111.07887, (2021).
8. Ke Ma, Harindi R. Atapattu, Qiuchen Zhao, Yao Gao, Blake P. Finkenauer, Kang Wang, Ke Chen, So Min Park, Aidan H. Coffey, Chenhui Zhu, Libai Huang, Kenneth R. Graham, Jianguo Mei, Letian Dou, Multifunctional Conjugated Ligand Engineering for Stable and Efficient Perovskite Solar Cells, *Advanced Materials*, 33, 2100791, (2021).
9. Ke Ma, Sheng-Ning Hsu, Yao Gao, Zitang Wei, Linrui Jin, Blake P. Finkenauer, Libai Huang, Bryan W. Boudouris, Jianguo Mei, Letian Dou, Organic Cation Engineering for Vertical Charge Transport in Lead-Free Perovskite Quantum Wells, *Small Science*,1, 2000024, (2021).
10. Scott A McClary, Mohammad M Taheri, Daria D Blach, Apurva A Pradhan, Siming Li, Libai Huang, Jason B Baxter, Rakesh Agrawal, Nanosecond carrier lifetimes in solution-processed enargite (Cu3AsS4) thin films, *Applied Physics Letters*, *117*, 162102, (2020).
11. Ti Wang, Linrui Jin, Juanita Hidalgo, Weibin Chu, Jordan M Snaider, Shibin Deng, Tong Zhu, Barry Lai, Oleg Prezhdo, Juan-Pablo Correa-Baena, Libai Huang*, Protecting hot carriers by tuning hybrid perovskite structures with alkali cations, Science Advances, eabb1336, 2020.
12. Ti Wang, Yongping Fu, Linrui Jin, Shibin Deng, Dongxu Pan, Liang Dong, Song Jin*, Libai Huang*, Phenethylammonium Functionalization Enhances Near-Surface Carrier Diffusion in Hybrid Perovskites, *Journal of the American Chemical Society*, 142, 16254–16264, (2020).

13. Long Yuan, Biyuan Zheng, Jens Kunstmann, Thomas Brumme, Agnieszka Beata Kuc, Chao Ma, Anlian Pan, and Libai Huang*, Twist-angle-dependent interlayer exciton diffusion in WS2–WSe2 heterobilayers, *Nature Materials*, 19, 617-623, (2020).
14. Daria Blach, Weihao Zheng, Huawei Liu, Anlian Pan, Libai Huang*, Carrier Transport Across a CdSxSe1-x Lateral Heterojunction Visualized by Ultrafast Microscopy, *Journal of Physical Chemistry C*, 124, 11325–11332, (2020).
15. Shibin Deng, Jordan M Snaider, Yao Gao, Enzheng Shi, Linrui Jin, Richard D Schaller, Letian Dou, Libai Huang*, Long-lived charge separation in two-dimensional ligand-perovskite heterostructures, *Journal of Chemical Physics*, 152, 044711, (2020).
16. Shibin Deng, Enzheng Shi, Long Yuan, Linrui Jin, Letian Dou, and Libai Huang*, Long-Range Exciton Transport and Slow Annihilation in Two-Dimensional Hybrid Perovskites, *Nature Communications* 11, 664, (2020).
17. Shibin Deng, Daria D Blach, Linrui Jin, Libai Huang*, Imaging Carrier Dynamics and Transport in Hybrid Perovskites with Transient Absorption Microscopy, *Advanced Energy Materials*, 71, 1903781, (2020).

Managing Excited-State Interactions in Semiconductor Nanocrystal–Molecular Hybrids. Energy Versus Electron Transfer

Jeffrey DuBose, Jishnudas Chakkamalayath, Anthony Kipkorir and Prashant V. Kamat
Radiation Laboratory and Department of Chemistry and Biochemistry
University of Notre Dame, Notre Dame, IN 46556, USA

The flow of energy and electron transfer processes in semiconductor nanocrystal based light harvesting assemblies is dictated by the energetics of the excited state interactions (Figure 1). Singlet and triplet excited state energies and redox properties of the chromophore dictate the efficiency of energy/electron transfer. Hence, it is important to obtain fundamental understanding of excited state interactions in semiconductor-molecular hybrids before employing them in photocatalytic and optoelectronic applications. Metal halide perovskite nanocrystals are interesting in the sense that they can either transfer energy or electrons/holes to the adsorbed organic molecules.

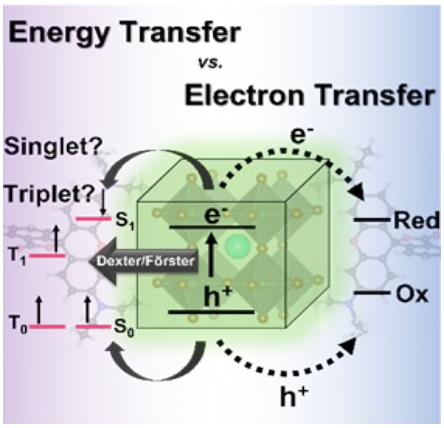

Figure 1 Excited state interactions dictating energy and electron transfer.

Our recent research efforts focus on two specific scenarios of the flow of energy and electron processes in $CsPbBr_3$ nanocrystal-molecular hybrids. The energy transfer is probed through three molecular acceptors – rhodamine B (RhB), rhodamine isothiocyanate (RhB-NCS), and rose Bengal (RoseB), which contain an increasing degree of heavy atom pendant groups. When interacting with $CsPbBr_3$ as an energy donor, photoluminescence excitation spectroscopy reveals that singlet energy transfer occurs with all three acceptors. However, the acceptor functionalization directly influences several key parameters that dictate the excited state interactions.

Both long-range dipole-based Förster resonance energy transfer (FRET) and short-range Dexter energy transfer (DET) mechanisms were found to be responsible for the generation of the singlet excited dye. The time-resolved difference absorption spectra recorded with excited $CsPbBr_3$ interacting with RhB are shown in Figures 2A and B. The transient bleaching recovery of

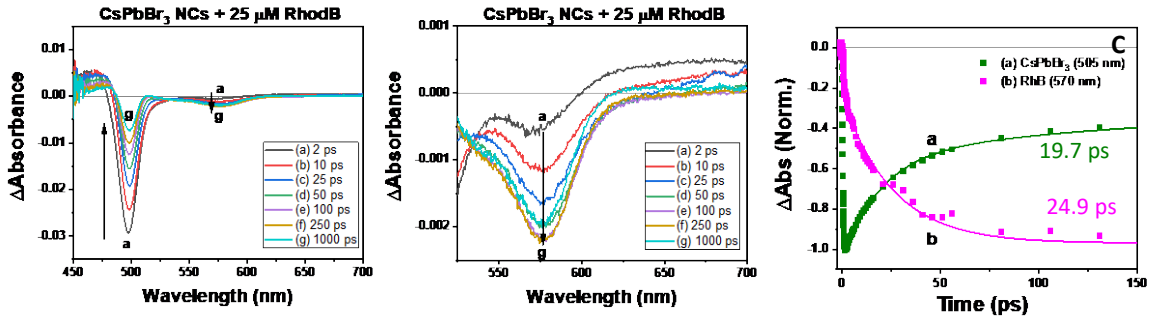

Figure 2. Time-resolved difference absorbance spectra recorded after 400 nm laser pulse excitation for (A) $CsPbBr_3$ with RhB. (B) Zoomed region corresponding to RhB absorption (545-700 nm) showing the growth of bleach. (C) Transient decay of CsPbBr3 bleach and growth of RhB bleach, fitted to first order kinetics.

$CsPbBr_3$ at 505 nm and bleach growth of RhB at 570 nm recorded after 400 nm laser pulse excitation of the solution containing 30 nM $CsPbBr_3$ and 25 μM RhB are compared in Figure 2C. It is interesting to note the similarity of the kinetics of the fast components of these two traces, indicates the time scale with which we observe energy transfer between the two. The kinetic analysis of the fast rise component (trace b) suggests the rate constant for energy transfer to be 5.9×10^{10} s^{-1}. In addition to energy transfer, each acceptor had a subpopulation of molecules (~30%) that underwent electron transfer as a competing pathway. The structural influence of acceptor moieties needs be considered for both excited state energy and electron transfer in nanocrystal-molecular hybrids.

Electron and/or hole transfer from excited $CsPbBr_3$ nanocrystals to a molecular relay present near the interface offers another avenue to directly convert light energy into chemical energy. Such interfacial electron transfer of semiconductor nanocrystals has been widely explored in photocatalytic chemical fuel generation. The relative energy level alignment of donors and acceptors to direct the flow of charge carriers becomes important in dictating electron transfer. By employing viologen as a probe, we elucidated the factors controlling the interfacial electron transfer processes. The laser pulse irradiation and steady-state irradiation of $CsPbBr_3$-viologen hybrids map out timescales of forward and back electron transfer events that dictate the overall production of photocatalytic reduction product (Figure 3). The initial charge-separated pair has a lifetime of microseconds as it underwent recombination. A significant fraction of the charge-separated pair escapes the initial charge recombination and produces a net yield of electron transfer product (viologen radical) under steady-state irradiation. Although the initial electron transfer from the excited semiconductor into the electron acceptor such as viologen moiety is an ultrafast process, it is the back electron transfer process that occurs at different time scales that eventually determines the net electron transfer yield.

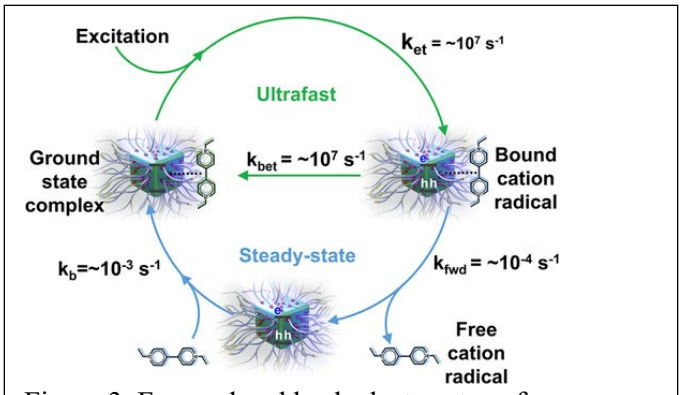

Figure 3. Forward and back electron transfer processes dictating the net electron transfer yield in a $CsPbBr_3$-Viologen hybrid under laser pulse and steady state irradiation.

The competition between electron and energy transfer further highlights the complexity of excited state interactions in semiconductor nanocrystal-molecular assemblies and the need for careful spectroscopic analysis to elucidate competitive pathways. A basic understanding of the fundamental differences between the two excited deactivation processes (energy and charge transfer) and ways to modulate them should enable design of more efficient light harvesting assemblies with semiconductor and molecular systems.

Future work will focus on directing energy and electron transfer pathways through modulation of spectral overlap, control of the surface ligand environment, and varying the nanocrystal size. Acceptor molecule functionalization will also provide an additional knob to improve interactions and, thus, aid in designing light harvesting assemblies with desirable properties.

DOE Solar Photochemistry Sponsored Publications 2020-2023

1. Kipkorir, A.; Jin, X. Gao, H.; Kamat, P. V. Photoinduced electron transfer across the polymer-capped $CsPbBr_3$ interface in a polar medium, J. Chem. Phys. 2023, 158, Art. No. 144702.
2. DuBose, J. T.; Kamat, P. V. How Pendant Groups Dictate Energy and Electron Transfer in Perovskite–Rhodamine Light Harvesting Assemblies, Journal of the American Chemical Society 2023, 145, 4601–4612
3. Chakkamalayath, J.; Hiott, N.; Kamat, P. V., How Stable Is the 2D/3D Interface of Metal Halide Perovskite under Light and Heat? ACS Energy Letters 2023, 8, 169-171
4. Chakkamalayath, J.; Szabó, G.; DuBose, J. T.; Kamat, P. V., Excited State and Transient Chemistry of a Perylene Derivative (DBP). An Untold Story. The Journal of Physical Chemistry A 2023, 127, 99–106
5. DuBose, J. T.; Kamat, P. V., Efficacy of Perovskite Photocatalysis: Challenges to Overcome. ACS Energy Letters 2022, 7, 1994-2011
6. DuBose, J. T.; Kamat, P. V., Hole Trapping in Halide Perovskites Induces Phase Segregation. Accounts of Materials Research 2022, 3, 761-771
7. DuBose, J. T.; Kamat, P. V., Energy Versus Electron Transfer: Managing Excited-State Interactions in Perovskite Nanocrystal–Molecular Hybrids. Chemical Reviews 2022, 122, 15, 12475–12494
8. Mathew, P. S.; Szabó, G.; Kuno, M.; Kamat, P. V., Phase Segregation and Sequential Expulsion of Iodide and Bromide in Photoirradiated Ruddlesden–Popper 2D Perovskite Films. ACS Energy Letters 2022, 7, 3982-3988
9. DuBose, J. T.; Szabó, G.; Chakkamalayath, J.; Kamat, P. V., Excited-State Transient Chemistry of Rubrene: A Whole Story. The Journal of Physical Chemistry A 2022, 126, 7147-7158
10. Chen, B.-A.; Ptasinska, S.; Kamat, P. V., Metal Cocatalyst Dictates Electron Transfer in Ag-Decorated MoS_2 Nanosheets. The Journal of Physical Chemistry C 2022, 129, 11907–11914
11. Kipkorir, A.; Kamat, P. V., Managing Photoinduced Electron Transfer in $AgInS_2$-CdS Heterostructures. The Journal of Chemical Physics 2022, 156, Art. No. 174703
12. Chakkamalayath, J.; Hartland, G. V.; Kamat, P. V., Photoinduced Transformation of Cs_2Au2Br_6 into $CsPbBr_3$ Nanocrystals. The Journal of Physical Chemistry Letters 2022, 13, 2921-2927
13. Cho, J.; Mathew, P. S.; DuBose, J. T.; Kamat, P. V., Photoinduced Halide Segregation in Ruddlesden–Popper 2D Mixed Halide Perovskite Films. Advanced Materials 2022, 2105585.
14. DuBose, J. T.; Christy, A.; Chakkamalayath, J.; Kamat, P. V., Transformation of Perovskite Nanoplatelets to Large Nanostructures Driven by Solvent Polarity. ACS Materials Letters 2022, 4, 93-101.
15. Costantino, F.; Gavioli, L.; Kamat, P. V., Bipolar CdS/Pd Photocatalytic Membrane for Selective Segregation of Reduction and Oxidation Processes. ACS Physical Chemistry Au 2022, 2.
16. DuBose, J. T.; Kamat, P. V., Directing Energy Transfer in Halide Perovskite–Chromophore Hybrid Assemblies. Journal of the American Chemical Society 2021, 143 (45), 19214–19223.
17. Kipkorir, A.; DuBose, J.; Cho, J.; Kamat, P. V., CsPbBr3–CdS Heterostructure: Stabilizing

Perovskite Nanocrystals for Photocatalysis. Chemical Science 2021, 12, 14815-14825.
18. Chakkamalayath, J.; Hartland, G. V.; Kamat, P. V. Light Induced Processes in CsPbBr3–Au Hybrid Nanocrystals: Electron Transfer and Expulsion of Au, J. Phys. Chem. C 2021, 125, 17881-17889.
19. Mathew, P. S.; DuBose, J. T.; Cho, J.; Kamat, P. V. Spacer Cations Dictate Photoinduced Phase Segregation in 2D Mixed Halide Perovskites, ACS Energy Letters 2021, 6, 2499-2501.
20. Cho, J.; DuBose, J. T.; Mathew, P. S.; Kamat, P. V. Electrochemically induced iodine migration in mixed halide perovskites: suppression through chloride insertion, Chemical Communications 2021, 57, 235-238.
21. DuBose, J. T.; Mathew, P. S.; Cho, J.; Kuno, M.; Kamat, P. V. Modulation of Photoinduced Iodine Expulsion in Mixed Halide Perovskites with Electrochemical Bias, J. Phys. Chem. Lett. 2021, 12, 2615-2621.
22. Chhetri, M.; Kamat, P. V. Vectorial Charge Transfer across Bipolar Membrane Loaded with CdS and Au Nanoparticles, J. Phys. Chem. C 2021, 125, 6870-6876.
23. Dey, A., et al. State of the Art and Prospects for Halide Perovskite Nanocrystals, ACS Nano 2021, 15, 10775–10981.
24. Kamat, P. V.; Kuno, M., Halide Ion Migration in Perovskite Nanocrystals and Nanostructures. Accounts of Chemical Research 2021, 54, 520-531.
25. Brennan, M. C.; Ruth,A.; Kamat, P. V.; Kuno, M. Photoinduced Anion Segregation in Mixed Halide Perovskites, Trends in Chemistry (Cell Press), 2020, 2, 282-301
26. Cho, J.; Kamat, P. V. How Chloride Suppresses Photoinduced Phase Segregation in Mixed Halide Perovskites, Chem. Mater. 2020, 32, 6206–6212.
27. Cho, J.; Kamat, P. V. Photoinduced Phase Segregation in Mixed Halide Perovskites: Thermodynamic and Kinetic Aspects of Cl–Br Segregation, Advanced Optical Materials 2020, 8, Art. no. 2001440.
28. Cho, J.; DuBose, J. T.; Kamat, P. V. Charge Carrier Recombination Dynamics of Two-Dimensional Lead Halide Perovskites, J. Phys. Chem. Lett. 2020, 11, 2570-2576.
29. Mathew P.S.; Samu, G. F.; Janaky, C.; Kamat, P. Iodine (I) Expulsion at Photoirradiated Mixed Halide Perovskite Interface. Should I Stay or Should I Go, ACS Energy Lett, 2020, 5, 1872–1880.
30. Cho, J.; DuBose, J. T.; Le, A. N. T., Kamat., P. V. Suppressed Halide Ion Migration in 2D Lead Halide Perovskites, ACS Materials Lett. 2020, 2, 565-570
31. DuBose, J. T..; Kamat, P.V. Surface Chemistry Matters. How Ligands Influence Excited State Interactions between CsPbBr3 and Methyl Viologen, J. Phys. Chem. C.2020, 124, 12990-12998
32. Elmelund, T.; Seger, B.; Kuno, M.; Kamat, P. V. How Interplay between Photo and Thermal Activation Dictates Halide Ion Segregation in Mixed Halide Perovskites, ACS Energy Lett. 2020, 5, 56-63.
33. Kobosko, S. M.; DuBose, J. T.; Kamat, P. V. Perovskite Photocatalysis. Methyl Viologen Induces Unusually Long-Lived Charge Carrier Separation in CsPbBr3 Nanocrystals, ACS Energy Letters 2020, 5, 221-223.
34. Cho, J.; DuBose, J. T.; Kamat, P. V. Charge Injection from Excited Cs2AgBiBr6 Quantum Dots into Semiconductor Oxides, Chem. Mater. 2020, 32, 510-517.

Controlling Charge-Transfer Reactions with First Row Transition Metal Complexes

A.L. Raithel, E. Firestone, S. Kaushik, T.Y. Kim, T.W. Hamann
Department of Chemistry
Michigan State University
East Lansing, MI 48823

All photochemical energy conversion systems involve the fundamental processes of light absorption, charge separation, and collection. Dye-sensitized solar cells (DSSCs) are an excellent platform to investigate the subtle interplay of various electron-transfer reactions that give rise to charge separation and collection following light absorption by molecular chromophores. This talk will highlight our recent efforts to design first-row transition metal coordination complexes to control the kinetics of such electron-transfer reactions in the context of DSSCs and introduce alternative hybrid solar energy conversion schemes.

In the first part of this talk, our latest efforts to control the spin state of Co redox couples to affect the inner-sphere reorganization energy and thus electron-transfer kinetics will be presented. We synthesized a new family of strong-field hexadentate ligands in order to induce low-spin Co(II) complexes that are stable with tunable redox potentials. By introducing 0, 1 or 2 dimethyl amino groups onto the PY5Im ligand backbone, redox potentials of the Co(II/III) couples can be controlled. Interestingly, crystal structures of the complexes show a geometry change from distorted square pyramidal in the Co(II) complexes to octahedral in the Co(III) complexes. This unusual geometry change is attributed to a strong Jahn-Teller distortion due to the low-spin d7 electronic configuration. We will discuss the implications of this geometry change on the electron-transfer kinetics of cobalt metal centers by utilizing cross-exchange reaction measurements with ferrocene derivatives as well as data on these new redox couples employed in DSSCs.

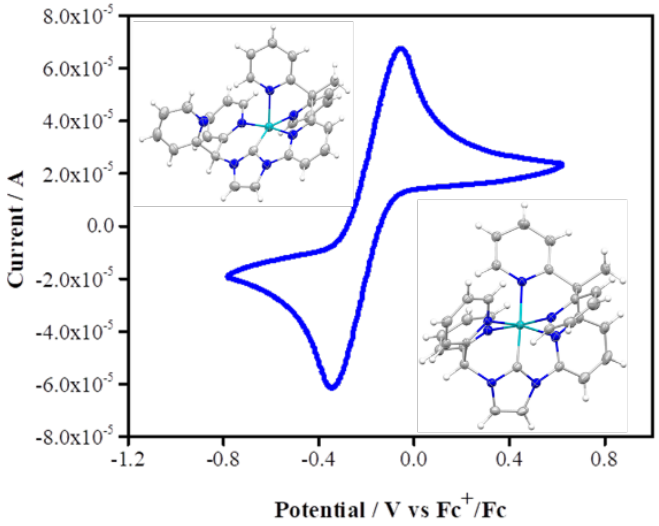

In the second part of this talk, our parallel effort of using polydentate ligands to form unique copper cage complexes will be presented. The hypothesis is that the resulting complexes should be stable, inert to ligand substitution by 4-*tert*-butylprydine (TBP) that occurs other copper redox couples reported in DSSCs, as well as offering the possibility to control the potential and reorganization energy. In one example, we have synthesized and isolated both oxidation states of the $[Cu(bpyPY4)]^{2+/+}$ redox couple, where bpyPY4 is the hexadentate ligand 6,6′-bis(1,1-di(pyridin-2-yl)ethyl)-2,2′-bipyridine. Titrations of the $[Cu(bpyPY4)]^{2+}$ cage complex with TBP, measured with UV-Vis spectroscopy, cyclic voltammetry and ^{1}H-NMR, we were able to determine that the cage complex does not undergo ligand substitution as predicted. Surprisingly, the copper complex has a very negative Cu(II/I) redox potential of ca. -0.5 V vs Fc^{+}/Fc. The redox potential of a Cu(II/I) redox couples is correlated with the stability of the Cu(II) form; this relationship is Nernstian with

a 0.059 V negative shift in potential for each 10-fold increase in the stability constant. Thus, the negative redox potential indicates a very stable Cu complex. These results suggest new design rules for copper complex redox shuttles in combination with exogeneous bases, which will also be discussed.

In the third part of this talk, the remarkable behavior of copper complexes transforming from liquid-based to solid-state hole transport materials (HTMs) will be presented. We applied an in-situ solidification analysis of the $[Cu(dmbpy)_2]^{2+/+}$ (dmbpy = 6,6′-dimethyl-2,2′-bipyridine) charge transport changes from ionic to electronic diffusion. Through use of the modified Dahms-Luff equation, a fast self-exchange rate constant of hole-hopping in the HTM of 8.3×10^8 ($\pm 5 \times 10^7$) $M^{-1}s^{-1}$ is calculated, which indicates a small reorganization energy of 0.47 eV. The behavior is quite different when TBP is present, however. EPR measurements were employed to monitor the effect of titrating TBP in both liquid solutions and solid films of $[Cu(dmbpy)_2]^{2+}$; we found strong evidence of a ligand exchange reaction, converting $[Cu(dmbpy)_2]^{2+}$ to $[Cu(TBP)_4]^{2+}$. Increased concentrations of $[Cu(TBP)_4]^{2+}$ decrease the conductivity of the liquid electrolyte, in accord with reports by others, however in the solid thin films of $[Cu(dmbpy)_2]^{2+/+}$, addition of TBP increases the hole mobility and conductivity. Variable temperature conductivity measurements indicate that the charge transport mechanism of these molecular solids changes from a hopping mechanism to band-like transport mechanism upon addition of TBP. These results provide the first mechanistic underpinnings of the complex interplay of TBP that appears to be critical in making high conductivity films of these $[Cu(dmbpy)_2]^{2+/+}$ molecules utilized in high-efficiency solid-state DSSCs.

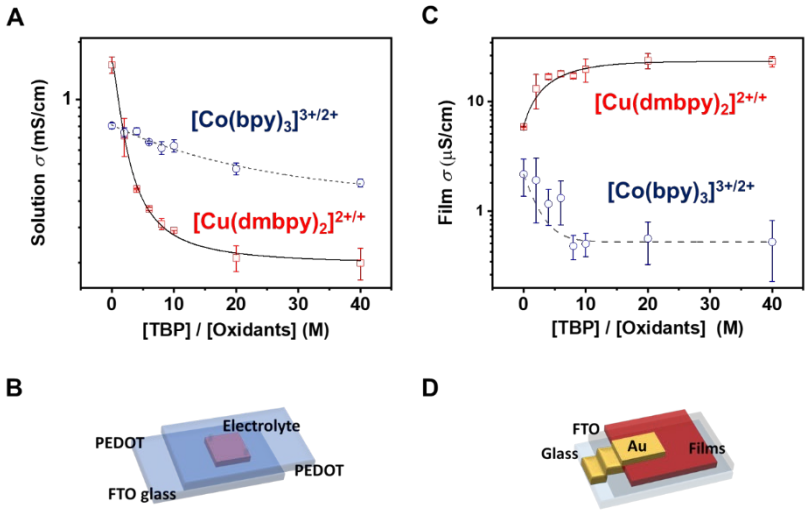

Finally, initial results will be presented of a single-component solar photochemical system by exploiting another interesting property of copper complexes. The concept is analogous to a DSSC, however the chromophore is dissolved in solution and also acts as redox shuttle (thus the name single-component). The advantages and challenges of such a system will be presented. We have synthesized several copper complexes reported by the Castellano group, for example $[Cu(dsbtmp)_2]^+$ (dsbtmp = 2,9-di(secbutyl)-3,4,7,8-tetramethyl-1,10-phenanthroline), which have long excited state lifetimes. Measurements of the electron-transfer self-exchange kinetics will be shown which we hypothesize correlate with excited state lifetime. Ligand exchange reactions of the Cu^{2+} complexes are also investigated, which have a net beneficial effect. Preliminary measurements of single component systems have demonstrated promising photocurrent-voltage responses showing the concept is viable. Finally, ongoing and future efforts to further understand the operational details of the photochemical and electron-transfer reactions of copper complexes and determine the rate-limiting steps to guide further development of this intriguing new concept.

DOE Solar Photochemistry Sponsored Publications 2020-2023

1. Kim, T.Y., Wang, Y., Raithel, A.L., Hamann, T.W.; "Real-Time Observation of the Diffusion Mechanism Progression from Liquid to Solid-State of Transition Metal Complexes" *ACS Energy Letters* **2020**, 5, 2, 583–588
2. Raithel, A.L., Kim, T.Y., Nielsen, K., Staples, R.J., Hamann, T.W.; "Low-Spin Cobalt(II) Redox Shuttle by Isocyanide Coordination" *Sustainable Energy & Fuels* **2020** 4, 2497–2507
3. Han, R., Kim, T.Y., Hamann, T.W., Osterloh, F.; "Photochemical Charge Separation and Dye Self-Oxidation Control Performance of Fluorescein, Rose Bengal, and Triphenylamine Dye-Sensitized Solar Cells" *Journal of Physical Chemistry* **2020** 124, 48, 26174–26183
4. Kim, T.Y., Kim, B.S., Oh, J.G., Park, S.C., Jang, J., Hamann, T.W., Kang, Y.S., Bang, J.H., Giménez, S., Kang Y.S.; "Interfacial Engineering at Quantum Dot-Sensitized TiO2 Photoelectrodes for Ultrahigh Photocurrent Generation" *ACS Applied Materials and Interfaces* **2021**, 13 (5), 6208–6218
5. Velore, J., Pradhan, S.C., Hamann, T.W., Hagfeldt, A., Unni, K.N.N., Soman, S.; "Understanding Mass Transport in Copper Electrolyte-Based Dye-Sensitized Solar Cells: *ACS Applied Energy Materials* **2022**, 5, 3, 2647–2654
6. Devdass, A., Watson, J., Firestone, E., Hamann, T.W., Delcamp, J.H., Jurss, J.W.; "An Efficient Copper-based Redox Shuttle Bearing a Hexadentate Polypyridyl Ligand for DSCs Under Low-Light Conditions" *ACS Applied Energy Materials*, **2022**, 5, 5964–5973
7. Raithel, A.L., Meador, W., Kim, T.Y., Staples, R.J., Delcamp, J., Hamann, T.W.; "Molecular Switch Cobalt Redox Shuttle with a Tunable Hexadentate Ligand" *Journal of the American Chemical Society* **2023**, 145, 2, 1367–1377
8. Kim, T.Y., Suh, E.H., Firestone, E., Raithel,A.L, Xu, C.Q., Ke, X., Jang, J., McCracken, J., and Hamann, T.W.; "Metal complex molecular solids showing band-like transport driven by in situ ligand exchange" *under review, Materials Chemistry*

‘Dark’ Voltammetry with Semiconductor Electrodes

Robert Vasquez, Jacob Waelder, Yifan Liu, Dylan Vitt, and Stephen Maldonado
Department of Chemistry
University of Michigan
Ann Arbor, MI 48109-1055

The semiconductor/electrolyte interface is the defining feature of photoelectrochemical cells. Although numerous theoretical and spectroscopic studies over the past six decades have informed on the microscopic details of these junctions, electrochemical measurements have proven less popular and useful. A persistent impediment in electroanalysis with semiconductor electrodes is that the corresponding data do not typically conform to the familiar behaviors of metal electrodes and are thus often considered unusable.

The overarching thesis of this work is that there is an abundance of useful information embedded in every voltammetric measurement with semiconductor electrodes, especially and specifically when the response does not look ‘ideal.’ This presentation will implicitly argue three points of increasing significance regarding these two approaches. First, the use of expressions derived for metal electrodes to analyze the data from semiconductor electrodes is unjustifiable and likely will lead to gross inaccuracies/misconceptions. Second, devising experiments to ensure voltammetric data look identical to the response of a solid-state diode is not necessary. Third, the way forward to understand every aspect of otherwise ‘ugly’ voltammetric data from a semiconductor electrode is to recognize that the applied potential is always distributed across several locales that comprise the semiconductor/electrolyte junction.

This presentation will describe the response characteristics of data collected from various configurations of semiconductor electrodes in contact with electrolytes that support heterogeneous charge transfer with putatively outer-sphere redox species in the absence of illumination (Figure 1). Although relevant to both dye-sensitized photovoltaic systems and electro-catalyzed photoelectrochemical cells, this discussion will not dwell on photo-effects purposely. Rather, the focus is on establishing a baseline intuition for recognizing and for interpreting the operation of semiconductor electrodes in the dark. Three vignettes will be highlighted that all utilize a multi-layer model for understanding and interpreting voltammetric data of semiconductors operating in depletion and accumulation.

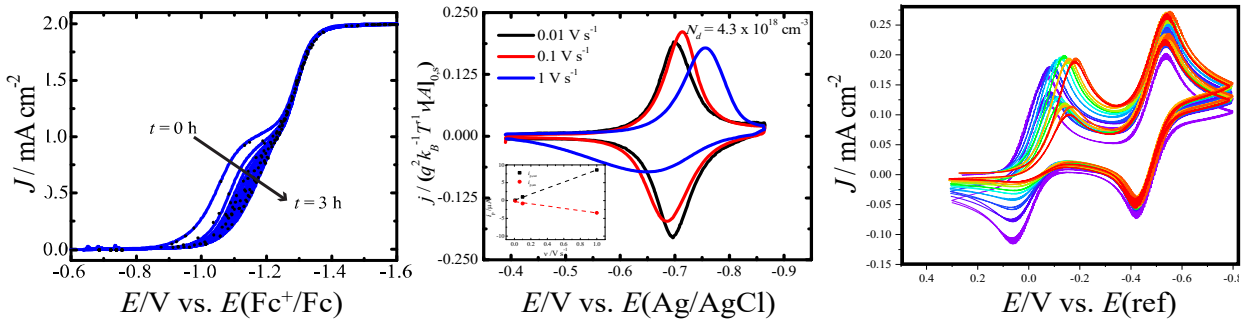

Figure 1. Representative voltammetric data from n-Si electrodes in a variety of experimental configurations. (bottom left) Evolution of Si ultramicroelectrode steady-state voltammograms for a redox species dissolved in a liquid electrolyte. (bottom middle) Scan-rate dependence of Si macroelectrode voltammograms for a redox adsorbate. (bottom right) Evolution of Si macroelectrode voltammograms for a redox species dissolved in a liquid electrolyte.

The first part of the talk will discuss the use of semiconductor ultramicroelectrodes (SUMEs). Data will be shown that illustrate these platforms are useful for monitoring surface reactions such as methoxylation of H-terminated Si immersed in methanol. The unique variations of the voltammetric responses in depletion and accumulation conditions collectively inform on the rate of methoxy layer growth as a function of electrolyte composition.

The second component of the talk will focus on the responses of redox adsorbates on n-Si. Three points will be discussed. First, the overall character of a voltammogram for a redox adsorbate on a semiconductor electrode implicitly reports on the operative charge-transfer kinetics between the semiconductor and the molecule. For a set of voltammograms collected over several scan rates, the transition from 'reversible' to 'irreversible' allows estimate of the operative rate constant. Second, the exact form of the faradaic current depends on the fractional potential drops across the space-charge, surface, Helmholtz, and diffuse layers. Third, possibility of coupling between the charging and faradaic currents exists, affording secondary measurement of surface energetics from a single voltammogram.

The third portion of the talk will communicate a semi-integration method to model the voltammetric response of semiconductor macroelectrodes interacting with freely diffusing redox species. An algorithm that can describe the expected and observed data features will be introduced.

DOE Solar Photochemistry Sponsored Publications 2020-2023

1. Liu, Z; Pishgar, S.; Lancaster, M.; and Maldonado, S. "Voltammetric Measurement of Rates and Energetics for Surface Methoxylation of Si(100) in Methanol with Dissolved Electron Acceptors using Si Ultramicroelectrodes" *Anal. Chem.*, **2023**, *accepted*
2.Vasquez, R.; Waelder, J.; Liu, Y.; Bartels, H.; and Maldonado, S. " A Gauss's Law Analysis of Redox Active Adsorbates on Semiconductor Electrodes: The Charging and Faradaic Currents are Not Independent " *Proc. Natl. Acad. Sci. U.S.A.*, **2022**, *119(36)*, ee2202395119
3. Waelder, J.; Vasquez, R.; Liu, Y.; and Maldonado, S. "A Description of the Faradaic Current in Cyclic Voltammetry of Absorbed Redox Species on Semiconductor Electrodes" *J. Am. Chem. Soc.*, **2022**, *144(14)*, 6410-6419
4. Waelder, J. and Maldonado, S. "Beyond the Laviron Method: A New Mathematical Treatment for Analyzing the Faradaic Current in Reversible, Quasi-Reversible, and Irreversible Cyclic Voltammetry of Adsorbed Redox Species" *Anal. Chem.*, **2021**, *93(37)*, 126720-1268
5. Breuhaus-Alvarez, A.G.; Cheek, Q.; Cooper, J.J.; Maldonado, S.; Barlett, B.M.* "Chloride Oxidation as an Alternative to the Oxygen-Evolution Reaction on HxWO3 Photoelectrodes" *J. Phys. Chem. C*, **2021**, *125(16)*, 8543-8550
6. Vasquez, M. R.; Hlynchuk, S.; Maldonado, S. "Effect of Covalent Surface Functionalization of Si on the Activity of Trifluoromethanesulfonic Anhydride for Suppressing Surface Recombination" *ACS Appl. Mater. Interfaces.*, **2020**, *12*, 57560-57568
7. Lancaster, M.; AlQurashi, A.; Selvakumar, C. R.; and Maldonado, S. "Quantitative Analysis of Semiconductor Electrode Voltammetry: A Theoretical and Operational Framework for Semiconductor Ultramicroelectrodes" *J. Phys. Chem. C*, **2020**, *124(9)*, 5021-5035
8. Spitler, M. T.; Modestino, M. A.; Deutsch, T. G.; Xiang, C. X.; Durrant, J. R.; Esposito, D. V.; Haussener, S.; Maldonado, S.; Sharp, I. D.; Parkinson, B. A.; Ginley, D. S.; Houle, F. A.; Hanappe, T.; Neale, N. R.; Nocera, D. G.; and McIntyre, P. C. "Practical Challenges in the Development of Photoelectrochemical Solar Fuels Productions" *Sustainable Energy Fuels*, **2020**, *4*, 985-995

The determination of referenced HOMO/LUMO levels with pulse radiolysis

Michele Myong, Mrinalni Iyer, Yaejin Kim, John Miller and Matthew Bird
Chemistry Division
Brookhaven National Laboratory
Upton, NY 11782

Scope

Our research centers around leveraging the unique capabilities of pulse radiolysis to study fundamental processes relevant to solar photochemistry. Specifically, we are currently investigating redox beyond electrochemistry, charge escape and transport, and charge recombination and electronic coupling. Common themes across these topics are the study of processes in nonpolar media and the use of conjugated materials to investigate effects of charge delocalization. Here we focus on redox beyond electrochemistry.

Knowledge of redox potentials is vital for the design and mechanistic understanding of molecular systems for solar energy conversion. They are typically determined with relative ease by cyclic voltammetry (CV). Some constraints of this method include the need for moderately polar solvents with large concentrations of electrolyte and analytes with reversible waves. There is also variability in reported redox potentials and sometimes limitations due to electrochemical potential windows. We seek to use pulse radiolysis to complement CV by addressing these limitations, particularly in areas of relevance to solar photochemistry.

Pulse radiolysis enables the rapid generation of excess, free charges in any solvent without the need for electrolyte or electrodes. Relative one-electron redox potentials of pairs of solutes can be determined through charge transfer equilibria measurements. This approach enables us to measure the following: 1) Redox potentials without electrolyte, 2) Redox potentials beyond typical electrochemical windows 3) Redox potentials in cases where CV gives irreversible voltammograms and 4) Redox potentials in nonpolar solvents.

Recent results

We have recently looked at examples of the first three cases[2,3,4,7] and here we address the fourth topic of nonpolar media. This is particularly relevant to molecular films where the accurate determination of HOMO/LUMO levels of conjugated molecules and polymers has been a long-standing unsolved problem. With organic photovoltaic (OPV) power conversion efficiencies nearly at 20%, and their emerging applications in photocatalysis, knowledge of the driving force for electron transfer is vital for understanding how to further optimize these materials.

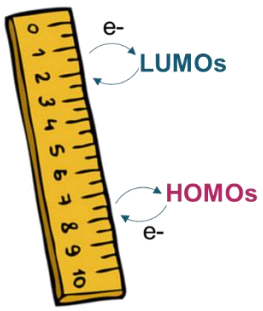

Figure 1. Redox ladder measuring stick to determine accurate and referenced redox potentials in nonpolar media with pulse radiolysis.

The two leading approaches for estimating HOMO and LUMO levels in these highly conjugated materials come from onset potentials obtained by CV or UPS/IPES measurements on films. Both methods give important information but, even in the best case, we expect 50-100 mV accuracy which could correspond to orders of magnitude variation in electron

transfer rates. Remarkably, one of the leading OPV blends of PM6 and Y6 has been reported to have a HOMO offset of 90 meV with CV but 700 meV with UPS.

We have developed a "redox ladder" in o-xylene to serve as a measuring stick (fig. 1) to get internally referenced redox potentials in a nonpolar media. The ladder is constructed from equilibrium constants for electron or hole transfer between numerous pairs of molecules. The choice of o-xylene gives nonpolar redox potentials and enables both reduction and oxidation processes to be studied. Newer "green" OPV materials are designed to be soluble in o-xylene.

Redox equilibria have the potential to determine relative redox potentials to a high accuracy because even a 10% error in the determination of K_{eq} only corresponds to a 2.4 mV change in estimated redox potential.

Due to the two types of equilibria for electrons or holes (fig. 2a), we end up with two redox ladders and uniting them to a common potential presents a unique challenge to this technique. We will discuss various potential approaches to connecting these ladders including the use of ground state charge transfer equilibria, analyzed with both optical spectroscopy and DC conductivity (fig. 2b). We will report our results from this approach (fig 2b) for a series of pairs of molecules that provide connections between the ladders.

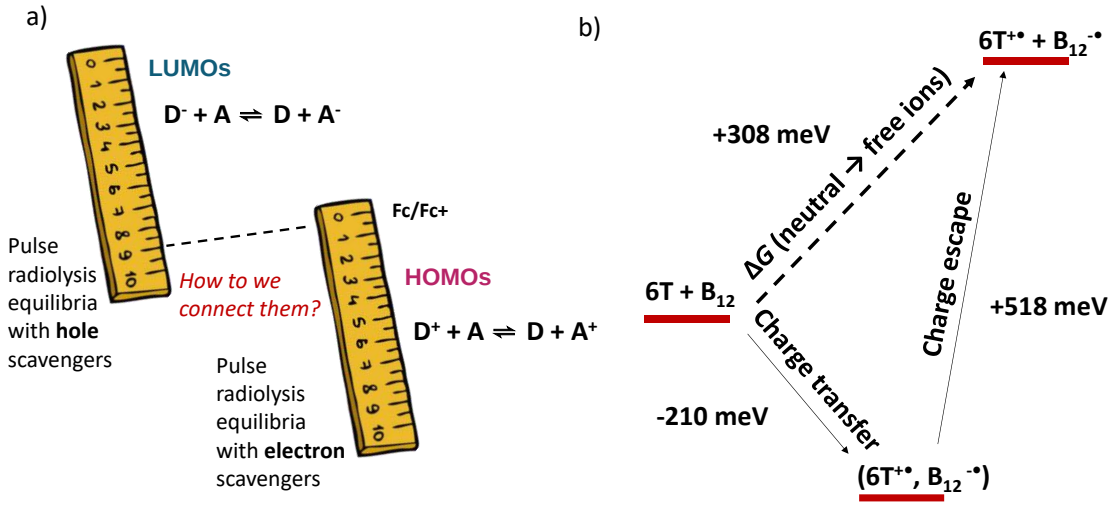

Figure 2. a) A universal redox ladder must connect electron and hole transfer ladders. b) An approach we have studied measures two equilibria for charge transfer and escape between molecular pairs in the ground state in o-xylene. The energy diagram reports values from such a measurement between an oliogothiophene (6T) and a strong dodecaborane electron acceptor (B_{12}). The free energy change going from separated neutral molecules to separated ions implies that the B_{12}(0/-) potential is 0.308 mV more negative than 6T(+/0).

Future Plans

On this topic, we plan to maintain and update a library of redox potentials where each subsequent measurement enhances the accuracy of the previous ones, by adding more linkages to the ladder. We will use these values to help to better interpret CV and UPS/IPES experiments. We plan to further investigate the effect of intermolecular interactions on redox potentials to make the final connection to the film environment where these interactions are important.

DOE Solar Photochemistry Sponsored Publications 2020-2023

1. Aubry, T. J.; Winchell, K. J.; Salamat, C. Z.; Basile, V. M.; Lindemuth, J. R.; Stauber, J. M.; Axtell, J. C.; Kubena, R. M.; Phan, M. D.; Bird, M. J.; Spokoyny, A. M.; Tolbert, S. H.; Schwartz, B. J. "Tunable Dopants with Intrinsic Counterion Separation Reveal the Effects of Electron Affinity on Dopant Intercalation and Free Carrier Production in Sequentially Doped Conjugated Polymer Films" Adv. Funct. Mater. 2020, 30, 2001800. DOI:10.1002/adfm.202001800

2. Bird, M. J.; Cook, A. R.; Zamadar, M.; Asaoka, S.; Miller, J. R. "Pushing the Limits of the Electrochemical Window with Pulse Radiolysis in Chloroform" Phys. Chem. Chem. Phys. 2020, 22, 14660-14670. DOI:10.1039/D0CP01948H

3. Bird, M. J.; Pearson, M. A.; Asaoka, S.; Miller, J. R. "General Method for Determining Redox Potentials without Electrolyte" J. Phys. Chem. A 2020, 124, 5487 DOI:10.1021/acs.jpca.0c02948

4. Bird, M. J.; Miller, J. R. "Effects of Electrolyte on Redox Potentials" Redox Chemistry – From Molecules to Energy Storage, IntechOpen 2022 ISBN: 978-1-80355-537-9, DOI: 10.5772/intechopen.103003

5. Myong, M. S.; Bird, M. J.; Miller, J. R. "Kinetics and Energetics of Electron Transfer to Dimer Radical Cations" J. Phys. Chem. B 2023, 127, 13, 2881–2886 DOI: 10.1021/acs.jpcb.2c07302

6. Kellogg, M.; Mencke, A.; Muniz, C.; Ahammad, R.; Cardoso-Delgado, F.; Baluyot-Reyes, N.; Sewell, M.; Bird, M.; Bradforth, S.; Thompson, M.; "Intra- and Inter-Molecular Charge Transfer Dynamics of Carbene-Metal-Amide Photosensitizers" 2023 ChemRxiv. DOI: 10.26434/chemrxiv-2023-6tqv9

Solar Photochemistry-supported use of the Accelerator Center for Energy Research (ACER)

7. Sandoval, B.A.; Clayman, P.D.; Oblinsky, D.G.; Oh, S.; Nakano, Y.; Bird, M.; Scholes, G.D.; Hyster, T.K. "Photoenzymatic Reductions Enabled by Direct Excitation of Flavin-Dependent "Ene"-Reductases" J. Am. Chem. Soc. 2021 143, 1735-1739. DOI: 10.1021/jacs.0c11494

8. Till, N.A.; Oh, S.; MacMillan, D.W.C.; Bird, M.J. "The Application of Pulse Radiolysis to the Study of Ni(I) Intermediates in Ni-Catalyzed Cross-Coupling Reactions" J. Am. Chem. Soc. 2021 143, 9332-9337. DOI: 10.1021/jacs.1c04652

9. Shin N. Y.; Tsui E.; Reinhold A.; Scholes, G. D.; Bird, M. J.; Knowles, R. R. "Radicals as Exceptional Electron-Withdrawing Groups: Nucleophilic Aromatic Substitution of Halophenols Via Homolysis-Enabled Electronic Activation" J. Am. Chem. Soc. 2022 144, 21783-21790. DOI: 10.1021/jacs.2c10296

In Situ Spectroscopy of Electrochemical and Photoelectrochemical Interfaces

Ruoxi Li, Bofan Zhao, Zhi Cai, Zihao Xu, Sa Suo, Jahan Dawlaty, Lasse Jensen, Tianquan Lian and Stephen B. Cronin
Departments of Chemistry, Physics, and Electrical Engineering
University of Southern California
Los Angeles, CA 90089

We present the novel use of surface enhanced Raman scattering (SERS) spectroscopy to detect charge transfer in ferrocene/ferrocenium (Fc/Fc^+) bound to an active electrode under electrochemical working conditions. The ferrocene has a 6-carbon linker with a thiol tether (6-(ferrocenyl)hexanethiol) and produces Fc/Fc^+ couple voltammograms exhibiting charge transfer above 0.4V vs. Ag/AgCl. By observing *in situ* micro-Raman spectroscopy with a water immersion lens, we observe significant changes in the spectra that corresponds to the charge state oxidation to ferrocenium (Fc^+). In particular, the Fc^+ state is characterized by the disappearance of the C_p-breathing mode (1104 cm^{-1} peak) and an 11-fold increase in the hexanethiol tail mode around 1072 cm^{-1}. Raman spectra calculated by density functional theory exhibit predominant peaks that agree well with our experimental observations and indicate that the $Fc \rightarrow Fc^+$ transition is associated with a change in the orientation, which gives rise to dramatic changes in the Raman spectra.

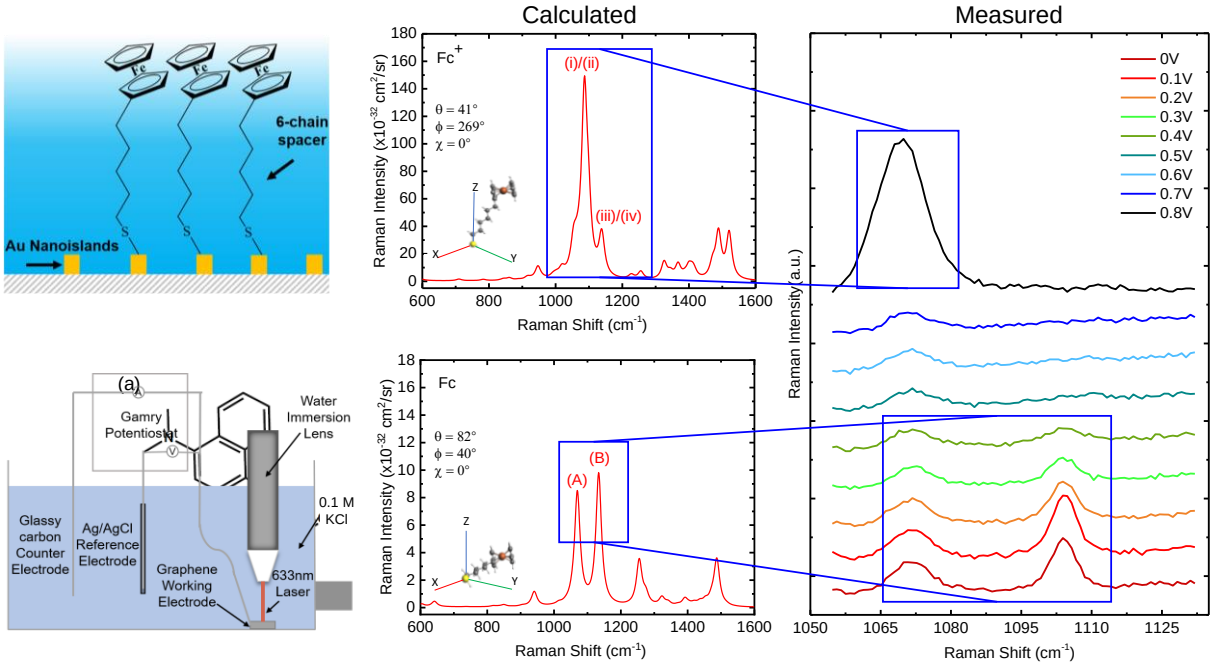

Figure 1. Calculated and measured Raman spectra of the (a) 6-(ferrocenium)hexanethiol and (b) 6-(ferrocenyl)hexanethiol.

Photocatalysis at the semiconductor-liquid interface represents a complex multiple step process. While the overall incident light-to-current conversion efficiency (IPCE) can be readily measured, identifying the microscopic efficiency loss processes remains difficult. Here, we report simultaneous *in-situ* photocurrent and transient reflectance spectroscopy (TRS) measured to directly observe photoinduced charge separation in the photocatalytic proton reduction process on GaP photocathodes protected by TiO_2. The separated charge carriers responsible for water

reduction can be directly probed to follow their kinetics and efficiency (ϕ_{CS}). Here, Franz−Keldysh Oscillations (FKO) observed in the TR spectra are caused by the photoinduced change of the built-in electric field at the semiconductor surface due to charge separation. The rate and efficiency increase at more negative applied bias and decrease at higher excitation fluence. The reduction efficiency (ϕ_{red}) is calculated by IPCE/ϕ_{CS}, and the result measures two key loss mechanisms: recombination within the bulk GaP and interfacial recombination at the junction, both of which can be suppressed with applied bias. This study provides an insight on the main loss pathways in photoelectrochemical system.

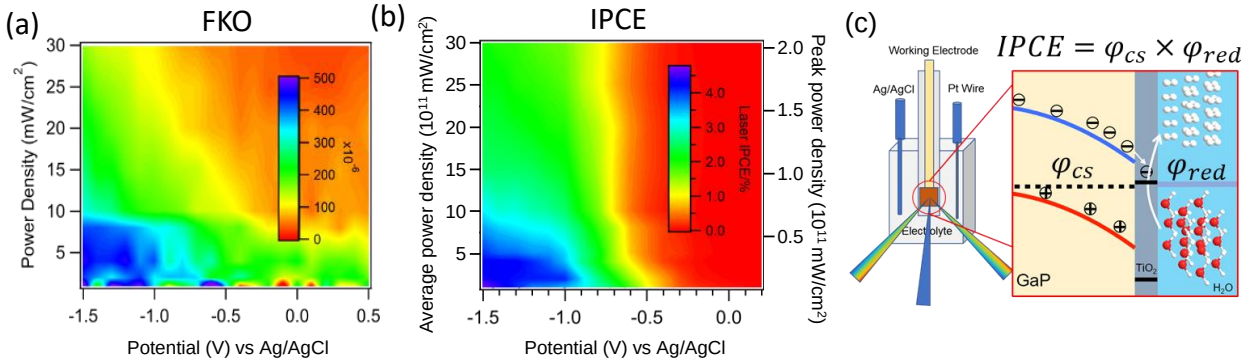

Figure 2. (a) Franz–Keldysh oscillation (FKO) magnitude and incident light-to-current conversion efficiency (IPCE) plotted as a function of optical power density and electrode potential. (c) Photoelectrochemical cell setup coupled with transient reflectance spectroscopy setup. The 3-electrode cell consists of 5 nm atomic layer deposited (ALD) TiO_2 on GaP working electrode, Pt wire counter electrode and Ag/AgCl reference electrode.

DOE Solar Photochemistry Sponsored Publications 2020-2023

1. Zihao Xu, et al., "Direct *In Situ* Observation of the Quantum Efficiencies of Charge Separation and Proton Reduction at TiO_2 protected GaP Photocathodes" Journal of the American Chemical Society 145, 2860-2869 (2023).
2. Yu Wang and Stephen Cronin. "Performance Enhancement of TiO_2-encapsulated Photoelectrodes Based on III–V Compound Semiconductors" Book title: Ultrathin Oxide Layers for Solar and Electrocatalytic Systems, Chapter 5, Royal Society of Chemistry, 103-134 (2022).
3. Angelo Montenegro, et al., "Field-Dependent Orientation and Free Energy of D_2O at an Electrode Surface Observed via SFG Spectroscopy", Journal of Physical Chemistry C, 126, 20831-20839 (2022).
4. Yu Wang, et al., "In Situ Investigation of Ultrafast Dynamics of Hot Electron-Driven Photocatalysis in Plasmon-Resonant Grating Structures", Journal of the American Chemical Society, 144, 3517-3526, (2022).
5. Sisi Yang, et al., "CO_2 Reduction to Higher Hydrocarbons by Plasma Discharge in Carbonated Water", ACS Energy Letters, 6, 3924-3930, (2021).
6. Zihao Xu, et al., "Nanoscale TiO_2 Protection Layer Enhances the Built-In Field and Charge Separation Performance of GaP Photoelectrodes", Nano Letters, 21, 8017-8024, (2021).
7. Angelo Montenegro, et al., "Asymmetric response of interfacial water to applied electric fields", Nature, 594, 62–65, (2021).
8. Shujin Li, et al., "Monitoring Reaction Intermediates in Plasma-Driven SO_2, NO, and NO_2 Remediation Chemistry Using *in Situ* SERS Spectroscopy", Analytical Chemistry, 93, 6421-6427 (2021).

Elucidating Design Principles of Semiconductor|Molecule Electronic Coupling for Improved Photoelectrochemical Function

Michael J. Rose
Department of Chemistry
The University of Texas at Austin
Austin, TX 78712

Semiconductor surface functionalization has long been used as a means to control charge equilibration, mitigate and alleviate surface states, and maximize band bending at semiconductor|electrolyte interfaces. The more recent advent of connecting molecular catalysts and molecular light absorbers to photoelectrodes has underscored the need to improve our fundamental understanding of the bonding, covalency and electronic coupling between a photo-activate material and a molecular component. Since Roald Hoffmann's descriptions of the binding of molecular ligands (like CO) to metallic electrodes, chemists have been interested in the interaction of molecules with materials. The need to control semiconductor band edge energetics, efficiently relay electrons to/from catalysts, and the long-standing challenge of extracting 'hot electrons' all motivate a deeper understanding of material|molecule bonding (**Figure 1**).

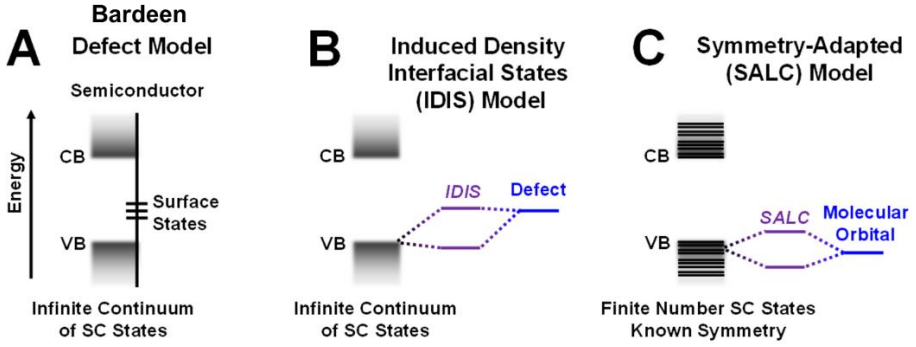

Figure 1. The continuum of evolving schemes for understanding surface defects versus well-defined molecular bonding at semiconductor|molecule interfaces.

We recently observed a remarkable photoelectrochemical effect of semiconductor|molecule electronic coupling on HER activity. In short, silicon photoelectrodes of the Si(111) variety were functionalized with a series of organic molecules, including anthracene and nitrated anthracene derivatives. The strongly dipolar nitro-anthracene functionalized surface provided the most positive onset potential (V_{onset}) in a photogenerative methyl-viologen cell (*p*-Si, $MV^{2+}/MV^{+\bullet}$), consistent with expectation for vacuum level shift based on the interfacial dipole. In contrast, in an HER device of formulation *p*-Si(111)|**R**|TiO_2|Pt the non-polar anthracene surface unexpectedly provided the highest V_{onset} (**Figure 2**). DFT/VASP calculations revealed a high extent of hybridization between the valence-band (VB) and conduction-band (CB) of Si (E_g = 1.1 eV) with the HOMO and LUMO (E_g = 3.3 eV) of anthracene

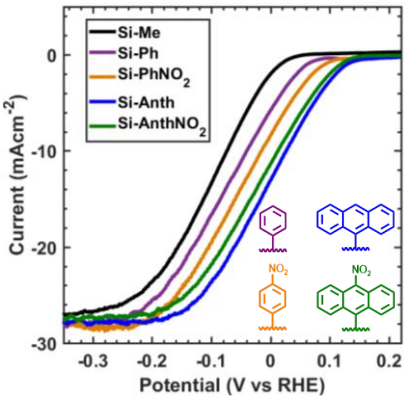

Figure 2. PEC-HER performance of anthracene-functionalized *p*-Si(111) electrodes compared with dipolar $PhNO_2$ and $AnthNO_2$ (1 sun, 0.5 M H_2SO_4, 100 mV/s). (*JACS* **2021**, *143*, 2567)

(**Figure 3**). We hypothesize that the very positive V_{onset} value in this sample was due to the enhanced polarizability of the molecule|material interface, which gave rise to a strong induced dipole that is more effective than the static dipole of nitrophenyl or nitro-anthracene. In this way, the covalently attached anthracene was interpreted to be 'part of the electrode', rather than an independent molecular entity. A group theoretical analysis of the silicon band structure and anthracene electronic structure revealed a symmetry-based rationale for the high extent of electronic coupling between molecule and material. On this basis, we hypothesize that determining how to build symmetry-adapted MO diagrams is an under-appreciated mechanism for understanding and optimizing charge transfer and catalytic efficiencies in photoelectrochemical systems. In this regime, both the symmetries of the semiconductor VB/CB and molecular HOMO/LUMO are required to provide an accurate MO diagram of the interface.

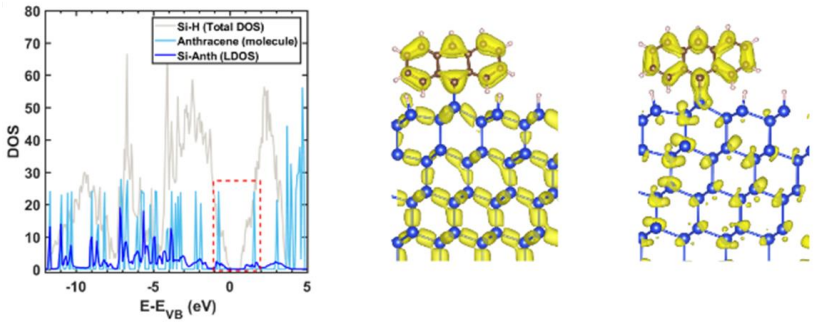

Figure 3. Calculated DOS plots and orbital hybridization for the Si(111)|Anth surface, namely Si|Anth. (*JACS* **2021**, *143*, 2567)

The present research program is designed to test the importance of energetic versus symmetry matching in driving hybridization and functional photoelectrochemical benefits at semiconductor|molecule interfaces. Firstly, we will utilize a series of simple hydrocarbon acenes as model systems wherein parameters — such as HOMO-LUMO bandgap, point group, symmetry of HOMO vs LUMO, and orbital lobe versus node — can be systematically evaluated to determine their effect on (*i*) V_{onset}, (both in MV^{2+} cell and HER); (*ii*) extent of band-bending induced; and (*iii*) the spectroscopically and electrochemically determined density of states (DOS). Our preliminary experiments have focused on adapting electrochemical impedance spectroscopy (EIS) methods for the quantification of silicon|molecule DOS. Spectroscopic determination of silicon|molecule DOS is also ongoing using UPS and low-energy inverse photoelectron spectroscopy (LEIPS). We hypothesize that surface functionalization with molecules that provide the best (*i*) symmetry match between molecule HOMO|LUMO and silicon VB|CB, and (*ii*) best energetic bandgap match (**Figure 4**), will provide the highest V_{onset} in HER experiments in the *p*-Si(111)|**R**|TiO_2|Pt system. In this way, our goal is to deliver new design principles to the photoelectrochemistry community regarding the best mechanisms, structures and design principles to attach catalysts, drive high ΔG electron transfer vis a vis large extent of band-bending, and provide rational mechanisms for the extraction of hot electrons.

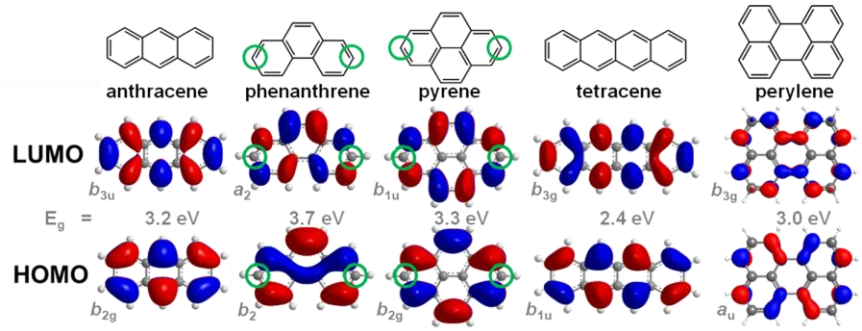

Figure 4. Proposed surface attachment molecules designed to test the effects of bandgap, HOMO/LUMO symmetry, and 'lobe vs. node' attachment point on PEC function of *p*-Si|**R**|TiO_2|Pt HER systems.

Elucidating the Dynamic Surfaces of Solar Photocatalysts

John M. Gregoire, Kevin Kan, Ryan J. R. Jones, Lan Zhou, Dan Guevarra
Division of Engineering and Applied Science
California Institute of Technology
Pasadena, CA 91125

Photocatalyst materials are central to solar fuels science and technology, providing multiple functionalities from solar harvesting, carrier transport, and catalysis of the desired chemical transformation. Nearly all photocatalysts, especially those that harvest visible light, have dynamic surfaces under operation due to interfacial reactions with the electrolyte. While scientific understanding and design principles for the semiconductor aspects of photocatalysts are well established, the dynamics of the photocatalyst-electrolyte interface and the implications for durability are relatively underexplored. The molecular-level processes that underlie the dynamics of this interface are not amenable to direct observation, motivating an approach to understand the molecular processes by establishing models that describe the consequences of an ensemble of molecular processes. Characterizing the ensemble effects and establishing the pertinent electrochemical environment parameters may be achieved by measuring the performance and aqueous concentrations of the photocatalyst's constituent elements, especially the metal elements. The environmental parameters include illumination intensity and wavelength, temperature, electrochemical potential, pH, and other aspects of the electrolyte composition.

Establishing a predictive model for the performance and aqueous metals concentrations as a function of these multiple parameters requires the combination of kinetic rate models and experimental data from which the model parameters can be learned. By developing data science methods to guide and learn from automated experiments, we will accelerate the durability characterize of operational photocatalysts 100-fold. The resulting *operational durability maps* will provide unprecedented understanding of photocatalyst dynamics. The models will also be deployed to predict pairings of photocatalysts and electrochemical conditions that give rise to solid-electrolyte interfaces with efficient solar chemical conversion, which comprises the greatest opportunity for achieving the requisite decades-long durability for a deployable solar fuels technology.

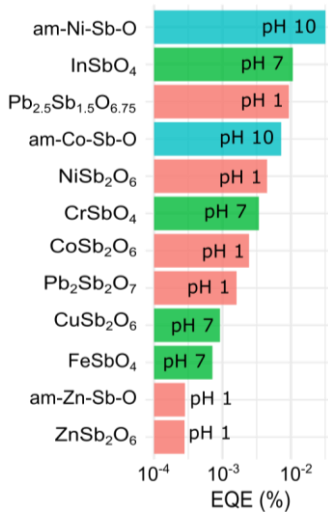

Figure 1: Survey of 12 discovered Sb-X-O photoanodes with external quantum efficiency (EQE) under 2.4 eV illumination and favorable Pourbaix energetics under OER conditions at the noted pH.

This project is uniquely enabled by the state-of-the-art experiment automation and data science capabilities that have been developed over the past decade in Caltech's High Throughput Experimentation group. The use of these capabilities for accelerated photoanode discovery also provides the basis for selection of initial metal oxides for establishing operational durability maps (Figure 1).[doi: 10.1021/acssuschemeng.2c05239]

In the first year of the project, we are establishing 2 new experimental capabilities for mapping durability. The first is a rapid screening technique that leverages scanning droplet cell technology previously established for high throughput photoelectrochemistry.

By introducing broad-band illumination and spectral transmission measurements, the instrument will perform on-the-fly analysis to detect changes in the spectral transmission, which may occur from oxidation of the photoanode material and/or its dissolution via corrosion reactions (Figure 2). In addition to finding pH and potential windows at which "optical stability" is achieved, this instrument will also provide a platform for developing active learning algorithms. Once a photoanode sample is deemed to have undergone an "instability event", any further testing for stability would occur on a material that is distinct from the as-prepared material. The implication for the number of possible experiments to determine stable operation windows is that a fresh sample will be needed for every pH and potential, for which comprehensive experimentation would be very resource intensive. Active learning algorithms will be established via machine learning collaborations to enable more efficient use of the samples, where the algorithms are anticipated to generalize to a broad range of stability evaluation experiments.

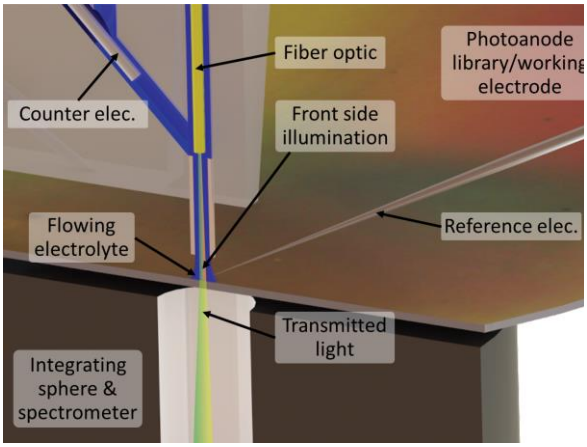

Figure 2: Scanning droplet electrochemical cell with spectral transmission as an *in situ* stability diagnostic.

The second instrument is an extension of the Accelerated Durability Screening System (ADSS) established in the Liquid Sunlight Alliance. The quest for durability is not one of eliminating all metal species from the electrolyte, but rather finding a catalyst and operating condition where the equilibrium dissolved metals concentrations are not problematic for device-level durability. Using the durability screening instrument of Figure 3, photoanodes will be equilibrated with dissolved metals concentrations via electrolyte recirculation. At scheduled times, or per automated decision algorithms, aliquots will be extracted from the electrolyte, followed by preparation for and injection into ICP-MS to characterize the dissolved metals concentrations. Experiments will be initially performed at ambient temperature and, when warranted, the electrolyte recirculation systems will be placed in a temperature-controlled bath for measurements at elevated temperature.

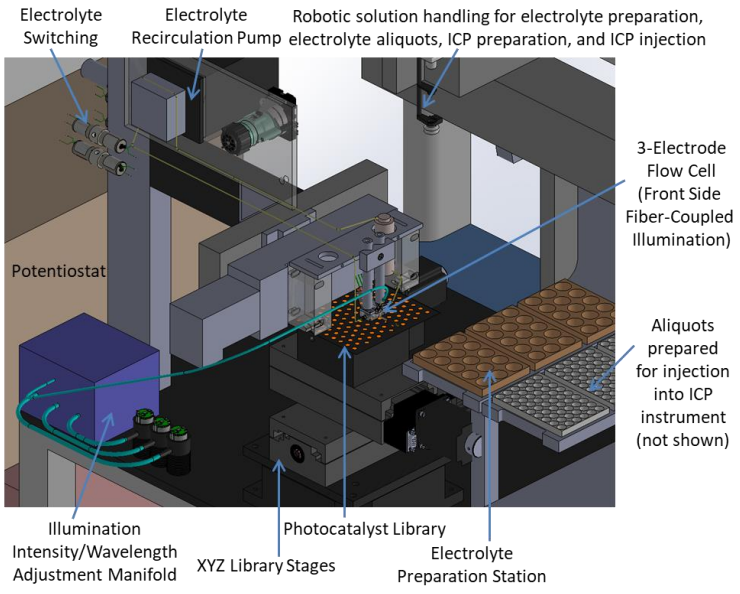

Figure 3: Schematic of the custom high throughput durability screening instrument. A robotic liquid handling robot couples electrolyte preparation, aliquots from an electrochemical flow cell, and preparation of ICP-MS injection.

Photophysics of Co(III) Polypyridyl Complexes: Ligand Field Excited State Dynamics in the Marcus Inverted Region

Atanu Ghosh, Jonathan T. Yarranton, and James K. McCusker*
Department of Chemistry
Michigan State University
East Lansing, Michigan 48824

Our research program is focused on developing an understanding of the factors governing structure-property relationships in the excited-state dynamics of transition metal complexes. A particular emphasis is on elements of the first transition series, whose large natural abundance makes it possible to envision scaling up results we obtain from our fundamental studies that portend applications in energy science. The work is carried out through a confluence of synthetic chemistry (both organic and inorganic) as well as the application of a wide variety of steady-state and time-resolved spectroscopies (in particular ultrafast time-resolved optical studies), all of which are complimented by theory. This synergy places us in a unique position to synthesize molecules, thoroughly characterize their physical and photophysical properties, then prepare new chromophores based on the information gleaned from those studies. The overriding goal is to create a research platform by which first-row metal complexes can be created with design-specific photophysical properties than can be coupled to energy conversion processes of interest (e.g., solar energy conversion, photoredox catalysis, etc.).

Research efforts over the past few grant cycles have focused on complexes possessing a d^6 configuration, specifically those containing Fe(II) and, more recently, Co(III). In the case of Fe(II), the initially formed ^{1}MLCT excited state typically decays to lower-lying ligand-field excited states on a sub-picosecond time scale due to, among other reasons, the primogenic effect associated with the 3d orbitals. Proper design of chromophores whose excited-state energetics are positioned such that the charge-transfer states can be stabilized relative to the metal-centered states requires knowledge of the energies of those ligand-field states. Unfortunately, these ligand-field transitions are obscured in Fe(II) complexes due to the overlapping presence of the strongly allowed $^1A_1 \rightarrow {}^1$MLCT absorption in the mid-visible region. This motivated us to begin examining isoelectronic Co(III) complexes, where the blue-shifted LMCT absorption(s) characteristic of this ion opens up the visible region for direct observation of the ligand-field transitions (Figure 1). This allowed us to apply ligand-field theory for a series of Co(III) polypyridyl-based chromophores and create a spectrochemical series for d^6 charge-transfer complexes with quantitative knowledge of the ligand-field states.

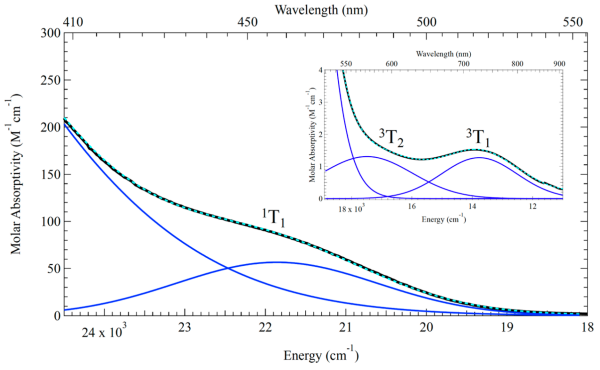

Figure 1. *Electronic absorption spectrum of $[Co(bpy)_3](PF_6)_3$ in CH_3CN solution. The inset shows absorptions toward the red acquired at higher concentration in 10-cm pathlength cells, revealing spin-forbidden d-d absorptions.*

The availability of this unprecedented information about the energetics of the metal-centered excited states of these Co(III) complexes motivated us to look at the photophysics of this relatively

unexplored class of chromophores in more detail. The first system studied was $[Co(bpy)_3]^{3+}$. We had determined from our steady-state studies that Co(III) complexes present with an increase in the ligand-field strength (i.e., 10 Dq) of ~3000 cm^{-1} relative to the corresponding Fe(II) complex. The excited-state lifetime of ~1 ns for $[Fe(bpy)_3]^{2+}$ in CH_3CN solution therefore created the expectation of a sub-nanosecond lifetime for $[Co(bpy)_3]^{3+}$ given the increase in the zero-point energy of the ligand-field state(s). In stark contrast, a ground-state recovery time of ~4 ns was observed, prompting a more extensive examination of this system.

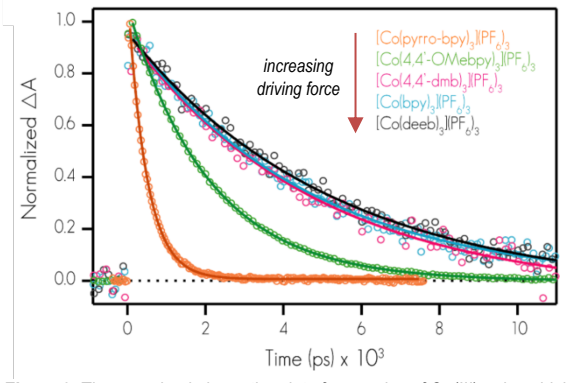

Figure 2. *Time-resolved absorption data for a series of Co(III) polypyridyl complexes in CH_3CN solution at 298 K. The data show an increase in the time constant for ground-state recovery with increasing ligand-field state energy, consistent with Marcus inverted region behavior.*

Time-resolved absorption measurements on several Co(III) polypyridyl complexes whose variations in ligand-field strength had already been determined from our steady-state absorption studies are shown in Figure 2. The unmistakable signature of Marcus inverted region behavior is evident in these data, as the rate of ground-state recovery from the lowest-energy ligand-field excited state of these compounds decreases with increasing ligand-field strength (i.e., increasing driving force). Previous work from our group has demonstrated the utility of variable-temperature ultrafast spectroscopy to quantify parameters such as electronic coupling (H_{ab}), driving force, and reorganization energy that serve to define the non-radiative decay dynamics that dominate the excited-state properties of this class of chromophores. We therefore carried out variable-temperature time-resolved absorption measurements on these same compounds; plots of $\ln(k_{obs} T^{1/2})$ v. T^{-1} yielded the expected linear correlation predicted by semi-classical Marcus Theory. The intercept affords information concerning the electronic coupling, while the slope reflects the influence of both the driving force and reorganization energy. From this analysis it was determined that H_{ab} decreases with increasing 10 Dq, indicating direct coupling between the lowest-energy excited state of the Co(III) complex and the ground state. This trend is opposite to what is observed for Fe(II) polypyridyl complexes, where one observes a modest increase in H_{ab} with increasing driving force due to the second-order nature of the coupling between the $^1A_1$ and $^5T_2$ states associated with the dynamics of those compounds. This observation allows us to conclude that the lowest energy excited state of these Co(III) complexes corresponds to the $^3T_1$ ligand-field state, implying the increase in ligand-field strength upon shifting from Fe(II) to Co(III) pushes the system past the $^5T_2/^3T_1$ crossing point to yield the energy landscape represented in Figure 3. The implications of the inverted region behavior of Co(III) chromophores as it pertains to applications in solar energy conversion in general and photoredox catalysis in particular will be discussed.

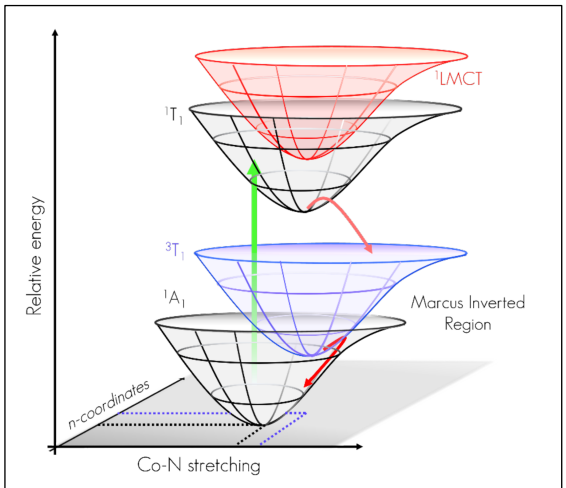

Figure 3. *Schematic potential energy surface diagram for excited ligand field-state dynamics of Co(III) polypyridyl complexes.*

DOE Solar Photochemistry Sponsored Publications 2020-2023

1. Miller, J.N.; McCusker, J.K. "Outer-sphere Effects on Ligand-field Excited-state Dynamics: Solvent Dependence of High-spin to Low-spin Conversion in $[Fe(bpy)_3]^{2+}$", *Chem. Sci.* **2020**, *11*, 5191 - 5204.
2. Paulus, B.C.; Adelman, S.L.; Jamula, L.L.; McCusker, J.K. "Leveraging Excited-state Coherence for Synthetic Control of Ultrafast Dynamics", *Nature* **2020**, *582*, 214 – 218.
3. Taylor, J.O.; Pižl, M.; Kloz, M.; Rebarz, M.; McCusker, C.E.; McCusker, J.K.; Záliš, S.; Hartl, F.; Vlček, A. "Optical and Infrared Spectroelectrochemical Studies of CN-substituted Bipyridyl Complexes of Ru(II)", *Inorg. Chem.* **2021**, *60*, 3514 – 3523.
4. Paulus, B.C.; Nielsen, K.C.; Tichnell, C.R.; Carey, M.C.; McCusker, J.K. "A Modular Approach to Light Capture and Synthetic Tuning of the Excited-state Properties of Fe(II)-based Chromophores", *J. Am. Chem. Soc.* **2021**, *143*, 8086 – 8098.
5. Yarranton, J.T.; McCusker, J.K. "Ligand-field Spectroscopy of Co(III) Complexes and the Development of a Spectrochemical Series for Low-spin d^6 Charge-transfer Complexes", *J. Am. Chem. Soc.* **2022**, *144*, 12488 – 12500.
6. Paulus, B.C.; McCusker, J.K. "On the Use of Vibronic Coherence to Identify Reaction Coordinates for Ultrafast Excited-state Dynamics in Transition Metal-based Chromophores", *Faraday Discuss.* **2022**, *237*, 274 – 299.
7. Ghosh, A.; Yarranton, J.T.; McCusker, J.K.; "Photophysics of Co(III) Polypyridyl Complexes: Ligand-field Excited State Dynamics in the Marcus Inverted Region", *Nature Chemistry*, submitted for publication.
8. McCusker, J.K. "The Ultrafast Science of Inorganic Chemistry: Past, Present, and Future", manuscript in preparation as an invited Outlook article in *ACS Central Science*.
9. McCusker, J.K. "Then and Now: The Photophysics of Group 8 Tris-bipyridine Complexes and the Legacy of Creutz-Sutin", manuscript in preparation as an invited contribution to *Chem. Phys. Rev.*

Toward Conformational Control over Charge Separation

Paul J. Griffin, Bronte J. Charette, Shelby R. King, Matthew Dake, Claire M. Zimmerman, Annika R. Holm, Laura Smith, Robert Cook, Alex Remolina, Nick E. Jackson, Josh Vura-Weis, and Lisa Olshansky
Department of Chemistry
University of Illinois, Urbana-Champaign
Urbana, IL 61820

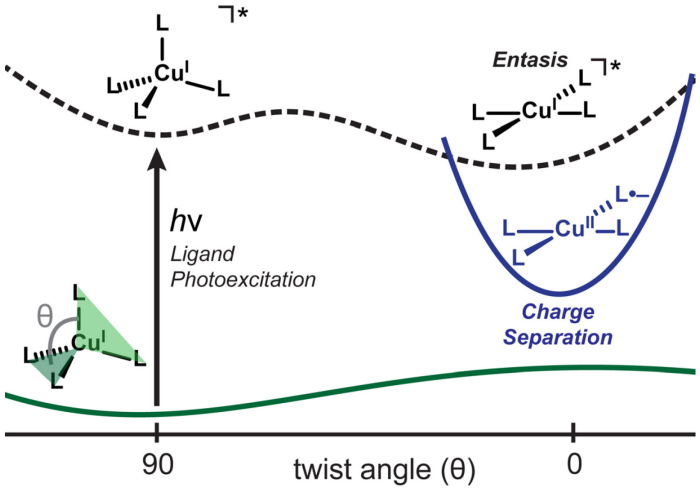

Operating under ambient conditions, biological systems for electron transfer (ET) cannot exert control over ET by changing bulk properties like temperature, pH, or reduction potential. Instead, they may have evolved to rely on triggered and distinct structural rearrangements in order to attain this control. To test the validity of this hypothesis, and employ it for the generation of long-lived charge separated (CS) states, we have prepared a series of copper coordination complexes in which distinct coordination modes for Cu(II) versus Cu(I) are operative. With these systems, we seek to drive photo-induced conformational changes that will lower the reorganization energy incurred going from Cu(I) to Cu(II) during CS, and simultaneously increase this reorganization energy for charge recombination, achieving long-lived CS.

To these ends, we have developed a series of ligands that exhibit unique coordination modes for Cu(II) relative to Cu(I). Ground state structural and spectroscopic characterization of these complexes serve as important benchmarks for related photophysical measurements. Through these characterizations, we have shown that in one of our ligand systems, Cu(I) exhibits conformational fluxionality in solution, and Cu(II) is locked into place as a square pyramid. In another system, Cu(II) exhibits conformational fluxionality in solution, while Cu(I) is locked into place as tetrahedral. With an aim to understand the ground state reorganization energies in these systems, and more specifically, to understand how these energies are effected by the observed conformational dynamicity, we performed a series of NMR line-broadening experiments to extract self-exchange ET rate constants. We found that our dynamical Cu complexes produce the fastest known Cu(II/I) ET self-exchange rate constants among all reported molecular species. With k_{11} values $>10^6$ $M^{-1}s^{-1}$, our ET rate constants are similar to those observed in the fastest known blue copper proteins and are 10-fold faster than the fasted previously reported (also dynamical) Cu(II/I)

molecular complex. From these data, we calculate an inner sphere reorganization energy of 0.62 eV for our fastest ET process. These findings support the molecular design principles proposed, in which a lowered reorganization energy for CS and a high reorganization energy for charge recombination together could result in the generation of long-lived CS states.

Using photo-active versions of these ligands that are modified to contain TICT (twisted intramolecular charge transfer) fluorophores, we have also performed a series of spectroscopic and computational investigations into our potential ability to drive CS. In our initial efforts we found that unlike the current 'gold standard' in first-row transitional metal-mediated CS, $[Cu(phen)_2]^+$, our systems are extremely stable under photochemical conditions, decaying by only 1 % after 10^7 laser shots (at ~0.2 μJ/pulse). However, we observed that the primary differences between the photophysics of ligands versus complexes resulted from slowed radiative rate constants in the presence of Cu, rather than increase nonradiative contributions that would be indicative of CS. These first studies also revealed that our choice of TICT fluorophore was problematic in that it gave rise to a number of unproductive 'off-pathway' ligand-centered transitions.

We have now made a modified family of complexes in which the robustness of our complexes is retained, but where the unwanted ligand-centered transitions are diminished. With these new systems, we do now observe differences between the transients of ligands relative to those of complexes, and in the presence of Cu, a longer-lived transient is sustained. These works are ongoing and though the differences we observe are small, we are encouraged further by support from computational results. Here, we have made two exciting observations. 1) TD-DFT and NTO analyses reveal that the excitation wavelengths we use give rise to an unpredicted and unusual metal-to-TICT transition that has only been reported once before. We think that this information can be critically incorporated to improve our quantum efficiencies. 2) Excited state geometry optimizations reveal that the relaxed excited state with our dynamical ligands exhibit the distinct coordination features of the corresponding Cu(II) complexes, rather than the Cu(I) analogues from which they arise. Given the distinct geometry and bond distance changes we see between ground state Cu(I) and Cu(II) complexes, it is noteworthy and clear that following excitation of Cu(I), the predicted relaxed state has significant Cu(II) character, suggesting that CS may be supported. Work is underway to compile, publish, and then build on these preliminary findings and others.

DOE Solar Photochemistry Sponsored Publications

1. Bronte J. Charette, Paul J. Griffin, Claire M. Zimmerman, and **Lisa Olshansky** "Conformationally Dynamic Copper Coordination Complexes" *Dalton Trans.* **2022**, *51*, 6212.
2. Paul J. Griffin, Bronte J. Charette, John H. Burke, Josh Vura-Weis, Richard D. Schaller, David J. Gosztola, and **Lisa Olshansky** "Toward Improved Charge Separation through Conformational Control in Copper Coordination Complexes" *J. Am. Chem. Soc.* **2022**, *144*, 12116.
3. Paul J. Griffin, Matthew Dake, Alex Remolina, and **Lisa Olshansky** "Unprecedented Rates of Electron Transfer in Copper Coordination Complexes through Conformational Dynamicity" *In preparation.*
4. Shelby R. King, Bronte Charette, Annika Holm, Richard D. Schaller, Matthew Dake, Robert Cook, and **Lisa Olshansky** "Excited State Dynamics in Copper Coordination Complexes" *In preparation.*

Earth Abundant Transition Metal Photosensitizers Based on Cu(I) and Cr(III) Phenanthrolines

Michael C. Rosko, Jonathan P. Wheeler, Adrienne P. Faulkner, Alexandra T. Barth, Sarah Arteta, Sarah Kromer, Eli M. Espinoza, and Felix N. Castellano*
Department of Chemistry
North Carolina State University
Raleigh, NC 27695-8204

Five Cu(I) *bis*(phenanthroline) photosensitizers formulated from a new ligand structural motif (**Cu1–Cu5**) coded according to their 2,9-substituents were synthesized, structurally characterized, and fully evaluated using steady-state and time-resolved absorption and photoluminescence (PL) measurements as well as electrochemistry. The 2,9-disubstituted-3,4,7,8-tetramethyl-1,10-phenanthroline ligands feature the following six-membered ring systems prepared through photochemical synthesis: 4,4-dimethylcyclohexyl (**1**), tetrahydro-2H-pyran-4-yl (**2**), tetrahydro-2H-thiopyran-4-yl (**3**), 4,4-difluorocyclohexyl (**4**), and cyclohexyl (**5**). Universally, these Cu(I) metal-to-ligand charge transfer (MLCT) chromophores display excited-state lifetimes on the microsecond time scale at room temperature, including the three longest-lived homoleptic cuprous phenanthroline excited states measured to date in deaerated CH_2Cl_2, $\tau = 2.5 – 4.3$ μs, while featuring high PL quantum efficiencies ($\Phi_{PL} = 5.3 – 12\%$). The corresponding absorption and PL spectra measured in CH_2Cl_2 are presented in **Figure 1**. Ultrafast and conventional transient absorption measurements confirmed that the PL originates from the MLCT excited state, which remains sterically arrested, preventing an excessive flattening distortion even when dissolved in Lewis basic CH_3CN. Combined PL and electrochemical data provided evidence that **Cu1–Cu5** are potent photoreductants (E^* = −1.73 to −1.62 V vs. $Fc^{+/0}$ in CH_3CN), whose potentials are altered solely based on which heteroatoms or substituents reside on the 2,9-appended ring derivatives. It is proposed that long-range electronic inductive effects are responsible for the systematic modulation observed in the PL spectra, excited-state lifetimes, and the ground state absorption spectra and redox potentials. Excited state triplet-triplet and triplet-doublet energy transfer reactions were readily accessed using these Cu(I) photosensitizers. Data will also be presented on newly conceived *bis*(heteroleptic) Cu(I) complexes leveraging the HETPHEN strategy in concert

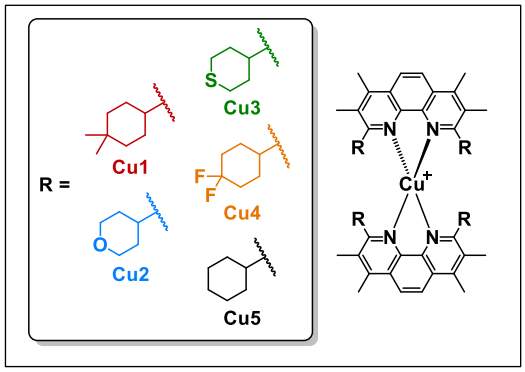

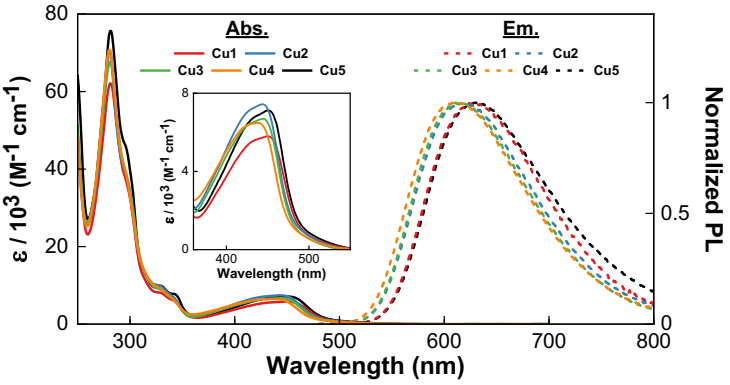

Figure 1. The absorption (solid lines) and PL emission spectra (dashed lines) of **Cu1-Cu5** recorded in CH_2Cl_2 at room temperature.

with π-conjugated phenanthroline ligands to promote panchromatic light absorption.

A new class of visible light-harvesting, homoleptic, paramagnetic Cr(III) photosensitizers, have been synthesized, photophysically characterized, and successfully applied in photoredox-driven oxidation chemistry; **[Cr(dm2nep)$_3$](BF$_4$)$_3$** (**dm2nep** = 4,7-bis(naphthelen-2-ylethynyl)-3,8-dimethyl-1,10-phenanthroline) serves as a representative example of the series, **Figure 2**. Static spectroscopic methods (UV-Vis absorption and photoluminescence), revealed a Cr(III) species with improved visible-light harvesting over all previously reported homoleptic phenanthroline-based Cr(III) species, while possessing the signature intraconfigurational "spin-flip" ^{2}E ligand-field PL emission in CH_3CN (λ_{em} = 760 nm, Φ_{PL} = 1.8%, τ = 172 μs), **Figure 2**. This chromophore also sensitizes $^1O_2$ phosphorescence at 1270 nm with quantum yields exceeding 90% in aerated CH_3CN. Electrochemical measurements revealed this compound to be a potent photooxidant (E^* = 1.78 V vs. SCE in MeCN) and preliminary photoredox studies were conducted. The challenging [4+2] model cycloaddition reaction between *trans*-anethole and isoprene was efficiently driven to 100% yield and 100% conversion in 3 hours upon irradiation with 456 nm light in $MeNO_2$ with a TON of 1000 at 0.1% photocatalyst loading. These experimental conditions enabled *in-situ* reaction monitoring and quantitation using ^{1}H NMR spectroscopy. Spectroelectrochemistry, conventional and ultrafast transient absorption measurements are currently underway to better comprehend the excited state evolution occurring in this and numerous related light-harvesting spin-flip Cr(III) *tris*(phenanthroline) complexes that are being conceived or have already been prepared.

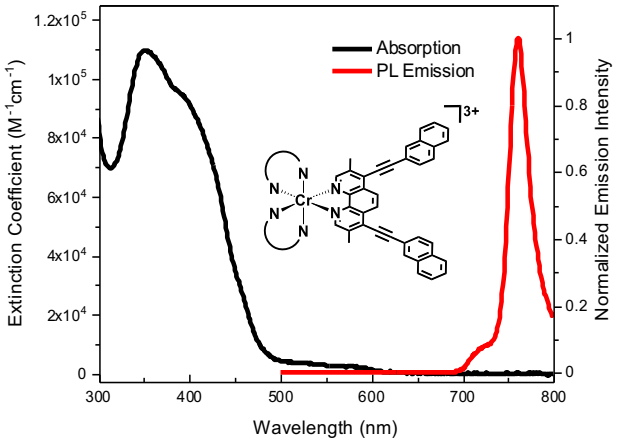

Figure 2. The absorption (black line) and PL emission spectrum (red line) of **[Cr(dm2nep)$_3$](BF$_4$)$_3$** recorded in CH_3CN at room temperature. The PL spectrum was recorded using 420 nm excitation.

DOE Solar Photochemistry Sponsored Publications 2020-2023

1. *A Robust Visible-Light-Harvesting Cyclometalated Ir(III) Diimine Sensitizer for Homogeneous Photocatalytic Hydrogen Production.* Yang, M.; Yarnell, J.E.; El Roz, K.; Castellano, F.N. *ACS Appl. Energy Mater.* **2020**, *3*, 1842-1853. https://pubs.acs.org/doi/10.1021/acsaem.9b02269

2. *Delayed Fluorescence in a Zr(IV) Photosensitizer with Ligand-to-Metal Charge Transfer Excited States.* Zhang, Y.; Lee, T.S.; Favale, J.M.; Petersen, J.L.; Scholes, G.D.; Castellano, F.N.; Milsmann, C. *Nat. Chem.* **2020**, *12*, 345-352. https://doi.org/10.1038/s41557-020-0430-7

3. *Energy Migration Processes in Re(I) MLCT Complexes Featuring a Chromophoric Ancillary Ligand.* Wells, K.A.; Yarnell, J.E.; Palmer, J.R.; Lee, T.S.; Papa, C.M.; Castellano, F.N. *Inorg. Chem.* **2020**, *59*, 8259-8271. https://pubs.acs.org/doi/abs/10.1021/acs.inorgchem.0c00644

4. *On the Quantum Yield of Photon Upconversion via Triplet-Triplet Annihilation.* Zhou, Y.; Castellano, F.N.; Schmidt, T.W.; Hanson, K. *ACS Energy Lett.* **2020**, *5*, 2322-2326.

https://dx.doi.org/10.1021/acsenergylett.0c01150

5. *Visible-Light-Driven Triplet Sensitization of Polycyclic Aromatic Hydrocarbons Using Thionated Perinones.* Palmer, J.R.; Wells, K.A.; Yarnell, J.E.; Favale, J.M.; Castellano, F.N. *J. Phys. Chem. Lett.* **2020**, *11*, 5092-5099. https://doi.org/10.1021/acs.jpclett.0c01634

6. *Direct Evidence of Visible-Light Induced Homolysis in Chlorobis(2,9-dimethyl-1,10-phenanthroline)copper(II).* Fayed, R.; Engl, S.; Danilov, E.O.; Hauke, C.; Reiser, O.; Castellano, F.N. *J. Phys. Chem. Lett.* **2020**, *11*, 5345-5349. https://dx.doi.org/10.1021/acs.jpclett.0c01601

7. *Ligand-Triplet Migration in Iridium(III) Cyclometalates Featuring π-Conjugated Isocyanide Ligands*. Favale, J.M.; Hauke, C.E.; Danilov, E.O.; Yarnell, J.E.; Castellano, F.N. *Dalton Trans.* **2020**, *49*, 9995-10002. https://doi.org/10.1039/D0DT02100H

8. *Photophysical and Ultrafast Processes in Rhenium(I) Diimine Dicarbonyls.* Atallah, H.; Taliaferro, C.M.; Wells, K. A.; Castellano, F.N. *Dalton Trans.* **2020**, *49*, 11565-11576. https://doi.org/10.1039/D0DT01765E

9. *Low Power Threshold Photochemical Upconversion using a Zirconium(IV) LMCT Photosensitizer.* Yang, M.; Sheykhi, S.; Zhang, Y.; Milsmann, C.; Castellano, F.N. *Chem. Sci.* **2021**, *12*, 9069-9077. https://doi.org/10.1039/D1SC01662H

10. *Next Generation Cuprous Phenanthroline MLCT Photosensitizer Featuring Cyclohexyl Substituents*. Rosko, M.C.; Wells, K.A.; Hauke, C.E.; Castellano, F.N. *Inorg. Chem.* **2021**, *60*, 8394-8403. https://pubs.acs.org/doi/10.1021/acs.inorgchem.1c01242

11. *Accessing the Triplet Manifold of Naphthalenebenzimidazole-phenanthroline in Rhenium(I) Bichromophores.* Wells, K.A.; Yarnell, J.E.; Sheykhi, S.; Palmer, J.R.; Yonemoto, D.T.; Joyce, R.; Garakyaraghi, S.; Castellano, F.N. *Dalton Trans.* **2021**, *50*, 13086-13095. https://doi.org/10.1039/D1DT02329B

12. *High-Efficiency Deep Red to Yellow Photochemical Upconversion under Solar Irradiance.* Gallaher, J.K.; Wright, K.M.; Frazer, N.L.; MacQueen, R.W.; Crossley, M.J.; Castellano, F.N.; Schmidt, T.W. *Energy Environ. Sci.* **2021**, *14*, 5541-5551. https://doi.org/10.1039/D1EE02197D

13. *Long-lived Photoluminescence of Molecular Group 14 Compounds through Thermally Activated Delayed Fluorescence.* Gowda, A.S.; Lee, T.S.; Petersen, J.L.; Rosko, M.C.; Castellano, F.N.; Milsmann, C. *Inorg. Chem.* **2022**, *61*, 7338-7348. https://pubs.acs.org/doi/10.1021/acs.inorgchem.2c00182

14. *Real-Time and In Situ Viscosity Monitoring in Industrial Adhesives Using Luminescent Cu(I) Phenanthroline Molecular Sensors*. Dara, A.; Mast, D.M.; Razgoniaev, A.O.; Hauke, C.E.; Castellano, F.N.; Ostrowski, A.D. *ACS Appl. Mater. Interfaces* **2022**, *14*, 33976-33983. https://pubs.acs.org/doi/10.1021/acsami.2c06554

15. *Employing Long Range Inductive Effects to Modulate MLCT Photoluminescence in Homoleptic Cu(I) Complexes.* Rosko, M.C.; Espinoza, E.M.; Arteta, S.; Kromer, S.E.; Wheeler, J.P.; Castellano, F.N. *Inorg. Chem.* **2023**, *62*, 3248-3259. https://doi.org/10.1021/acs.inorgchem.2c04315

Photo- and Electrochemical Hydrogen Evolution by Rh2(II,II) Complexes Containing a Benzo[*c*]cynnoline (bncn) Ligand

Claudia Turro
Department of Chemistry and Biochemistry
The Ohio State University
Columbus, OH 43210

We recently discovered the photochemical proton reduction and H_2 evolution by a new, air-stable single-molecule photocatalyst, *cis*–$[Rh_2(DPhF)_2(bncn)_2]^{2+}$ (bncn = benzo[*c*]cinnoline,DPhF = N,N-diphenylformamidinate; Figure 1, top left) that operates with red light, with turnover numbers, TONs, of over 200 (λ_{irr} = 670 nm, 24 hours) in the presence of *p*-toluenesulfonic acid (TsOH) and BNAH (1-benzyl-1,4-dihydronicotinamide) as a sacrificial electron donor. Mechanistic studies revealed that the excited state of *cis*–$[Rh_2(DPhF)_2(bncn)_2]^{2+}$, $\mathbf{[Rh_2]^{2+}}$, is able to oxidize the sacrificial donor in solution, BNAH, to produce the one-electron reduced complex, $\mathbf{[Rh_2]^{+}}$, where the unpaired electron resides on the bncn ligand. Importantly, $\mathbf{[Rh_2]^{+}}$ is able to absorb another red photon and undergo a second excited state charge transfer event to generate $\mathbf{[Rh_2]}$, and the latter has been shown independently to produce H_2 in acidic solutions. Similar results were later observed for related dirhodium(II,II) complexes containing bncn ligands, one of which exhibits a longer excited state lifetime and greater TONs under similar conditions as $\mathbf{[Rh_2]^{2+}}$. In addition, a derivative of $\mathbf{[Rh_2]^{2+}}$ was bound to NiO films on an electrode, such that hole injection/ current generation replaced the sacrificial electron donor.

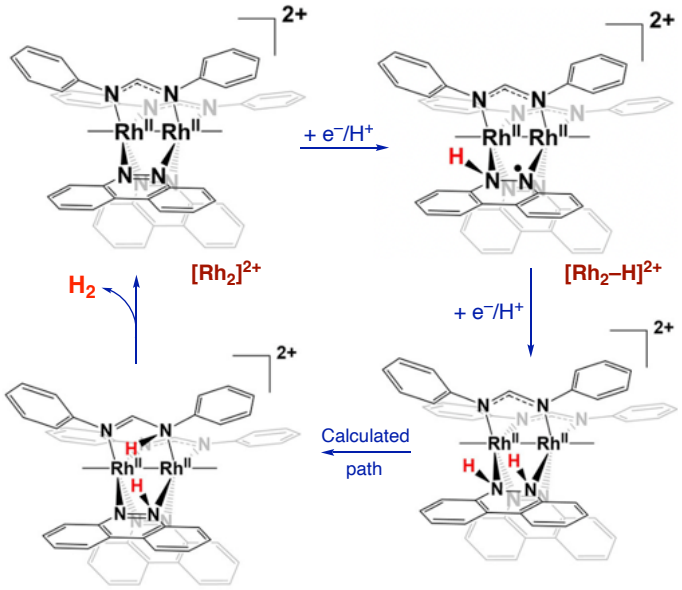

Figure 1. Structure of $\mathbf{[Rh_2]^{2+}}$ and electrocatalytic mechanism for hydrogen evolution, including calculated pathway for H–H bond forming.

More recently, electrocatalytic studies with $\mathbf{[Rh_2]^{2+}}$ in combination with theoretical calculations revealed that the first reduction of the bncn ligand in the complex results in a ligand-centered proton coupled electron transfer step, producing $\mathbf{[Rh_2–H]^{2+}}$ (Figure 1). Experimental evidence and theoretical predictions reveal that the protonated and reduced bncn ligand is the site of the second reduction, and that the doubly-reduced, protonated bncn ligand in $\mathbf{[Rh_2–H]^{2+}}$ is then protonated, resulting in H_2 evolution (Figure 1). This finding is critical, because if the observed photo- and electrocatalytic hydrogen evolution is indeed ligand-centered, then the scarce and expensive rhodium may be substituted for more earth-abundant metals. It should be noted that bncn alone does not act as a photo- or electrocatalyst since it decomposes upon reduction in the presence of acid. Therefore, it appears that the bimetallic scaffold is crucial to allow the chemistry to take place without decomposition of the catalyst.

The presentation will focus on establishing that indeed the observed chemistry is ligand-centered, investigating the role of the DPhF ligand(s) on the reaction, improving the photocatalytic activity, and developing strategies to couple the bncn ligand and earth-abundant platforms. In addition, future plans will be discussed. To begin addressing these points, the series of complexes *cis*–$[Rh_2(DTolF)_2(bpnp)(L)]^{2+}$ (DTolF = N,N'-di-p-tolylformamidinate, bpnp = 2,7-dipyridyl-1,8-naphthiridine), where L = pyrazine (**Rh_2–pyz**), cinnoline (**Rh_2–cin**), and bncn (**Rh_2–bncn**), was prepared and their structures are shown in Figure 2a. In **Rh_2–bncn**, only one bncn ligand is present and both axial sites are blocked by the pyridine units of the bpnp ligand, such that catalysis by this complex would not proceed through an axial Rh–H hydride intermediate. This complex exhibits charge transfer transitions from $Rh_2(\delta^*)$/DTolF(nb) to bnpn at 770 nm (ε = 1,800 $M^{-1}cm^{-1}$) and to bncn at 720 nm (ε = 5,200 $M^{-1}cm^{-1}$) and irradiation with 670 nm light results in the production of H_2 in the presence of TsOH and BNAH with TON = 16 (24 h). In addition, the complexes *cis*–$[Rh_2(O_2CCH_3)(DPhF)(bncn)_2]^{2+}$ (**Rh_2-OAc-bncn$_2$**) and *cis*–$[Rh_2(O_2CCH_3)(DPhF)(bncn)\text{-}(CH_3CN)_2]^{2+}$ were prepared and characterized, where one formamidinate ligand was replaced with acetate. Both complexes exhibit $Rh_2(\delta^*)$/DTolF(nb) → bncn transitions at ~560 nm and undergo photocatalytic H_2 evolution with TONs of 41 and 166 (λ_{irr} = 595 nm, 0.1 M BNAH, 0.1 M TsOH, in DMF). For these complexes and the Rh2–L series, excited state and electrochemical measurements will be presented, which can be used to understand the reduced production of H_2 observed in these systems relative to **$[Rh_2]^{2+}$**. These results, taken together, point at a bncn-localized mechanism for H_2 evolution, modulated by the accumulated charge on the ligand following excited state reduction from the sacrificial donor or electrochemical reduction.

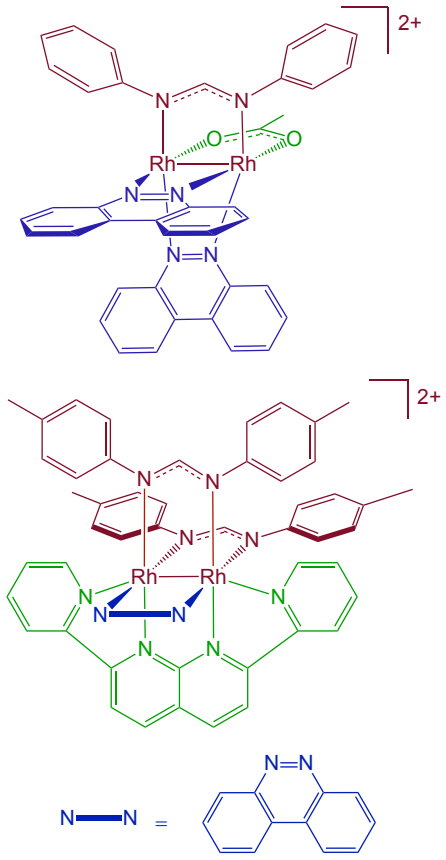

Figure 2. Structures of **Rh_2-OAc-bncn$_2$** (top) and **Rh_2-bncn** (bottom).

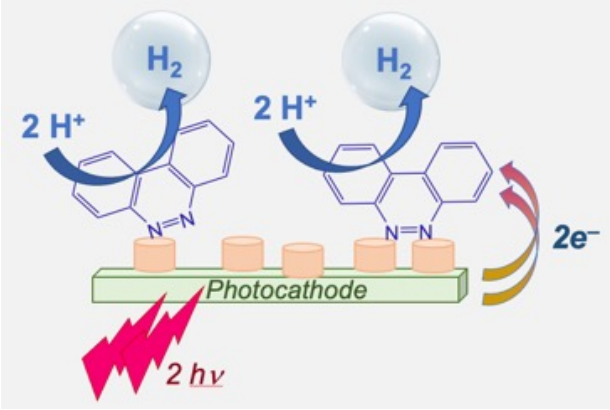

Figure 3. Schematic representation of photocatalytic hydrogen evolution by bncn on photocathode.

Current experiments will be discussed, which include electrocatalysis using bncn in the presence of first-row transition metals, as well as the coordination of a tridentate ligand containing a bncn unit to a Co_3 cluster. In addition, experiments are underway using a photocathode and anchoring the bncn ligand either directly or through an earth-abundant metal to achieve hydrogen production, as shown in Figure 3.

DOE Solar Photochemistry Sponsored Publications 2020-2023

1. Whittemore, Tyler J.; Xue, Congcong; Huang, Jie; Gallucci, Judith C.; Turro, C. Single-chromophore single-molecule photocatalyst for the production of dihydrogen using low-energy light. *Nature Chemistry* **2020,** *12*, 180-185.

2. Millet, A.; Xue, C.; Song, E.; Turro, C.; Dunbar, K. R. Synthetic Strategy for Trapping the Elusive Trans-Dirhodium(II,II) Formamidinate Isomer: Effects of *Cis* versus *Trans* Geometry on the Photophysical Properties. *Inorg. Chem.* **2020**, *59*, 2255-2265.

3. Huang, J.; Gallucci, J. C.; Turro, C. Panchromatic Dirhodium Photocatalysts for Dihydrogen Generation with Red Light. *Chem. Sci.* **2020**, 11, 9775-9783.

4. Manamperi, H.; Moore, C. E.; Turro, C. Dirhodium Complexes as Electrocatalysts for CO_2 Reduction to HCOOH: Role of Steric Hindrance on Selectivity. *Chem. Commun.* **2021**, 57, 1635-1638.

5. Huang, J.; Sun, J.; Wu, Y.; Turro, C. Dirhodium(II,II)/NiO Photocathode for Photoelectrocatalytic Hydrogen Evolution with Red Light. *J. Am. Chem. Soc.* **2021**, *143*, 1610-1617.

6. Lin, S.; Turro, C. Dirhodium Complexes as Panchromatic Sensitizers, Electrocatalysts, and Photocatalysts. *Chem. Eur. J.* **2021**, *27*, 5379-5387.

7. Millet, A.; Xue, C.; Turro, C.; Dunbar, K. R. Unsymmetric Dirhodium Single Molecule Photocatalysts for Hydrogen Production with Low-Energy Light. *Chem. Commun.* **2021**, *57*, 2061-2064.

8. Lin, S.; Banerjee, S.; Fortunato, M. T.; Xue, C. ; Huang, J.; Sokolov, A. Yu.; Turro, C. Electrochemical Strategy for Proton Relay Installation Enhances the Activity of a Hydrogen Evolution Catalyst. *J. Am. Chem. Soc.* **2022**, *144*, 20267-20277.

Photohydrides: Mechanism-Guided Development of Molecular Photoelectrocatalysts

Isaac Cloward, Tamara Jurado, Eamon Reynolds, Bethany Stratakes, Kaylee Wells, Felix Castellano, and Alexander Miller
Department of Chemistry
University of North Carolina at Chapel Hill
Chapel Hill, NC 27516

This project seeks to identify transition metal hydride complexes that can be generated electrochemically at mild potentials and that are capable of photochemical H_2 release or hydride transfer reactions. Photoexcitation can help traverse high kinetic barriers to access desired products, lower electrochemical overpotential, or achieve distinct product selectivity compared to thermal (dark) electrocatalysis. A combination of kinetic and thermodynamic studies provides insight into the photochemical and electrochemical steps that underpin molecular photoelectrocatalysis. Recent research has focused on understanding how to control bimolecular photochemical H_2 evolution mechanisms, developing new single-component photoelectrocatalysts based on 3d transition metal complexes for hydrogen atom transfer, and furthering fundamental knowledge of hydricity, the hydride donor ability of a compound.

Controlling bimolecular H_2 evolution. Mechanistic studies of iridium complexes supported by cyclopentadienyl and bipyridine ligands established the bimolecular nature of photochemical H_2 evolution, wherein excited-state electron transfer is followed by H–H coupling of two Ir–H units. This mechanistic knowledge has guided two projects, one designed to enhance rates of H_2 evolution and one designed to redirect reactivity towards hydride transfer to organic substrates. To facilitate H_2 evolution, we prepared binucleating ligands that could hold the two metal hydrides in proximity.[8] As predicted, a marked enhancement in photoelectrocatalytic activity was observed — but not for the expected reason. Catalyst self-assembly, driven by hydrophobic groups on the organometallic complexes, produces "all-catalyst" nanoscale aggregates with strikingly enhanced catalytic behavior. Recognizing the power of ligand-induced aggregation enabled new monometallic designs that harness noncovalent interactions to bring catalysts into proximity and achieve faster rates at lower overpotential. **Figure 1** summarizes the evolution of catalysts leveraging self-assembly. In parallel, we have explored ways to prevent bimetallic H–H coupling and thus enable hydride transfer pathways. One such approach involves site isolation by surface attachment to transparent conductive oxides (e.g. mesoporous tin-doped indium oxide films). Upon surface attachment, a new mechanism of H_2

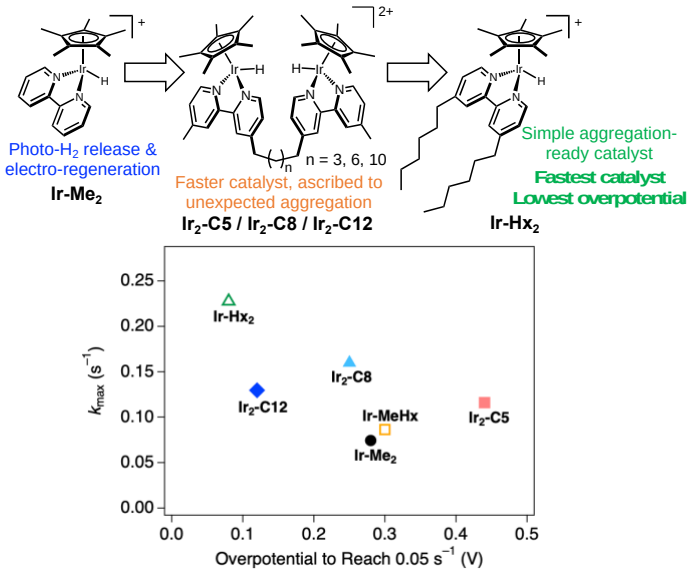

Figure 1. Hydrophobic linkers or appendages drive catalyst self-assembly into aggregates with high activity at low overpotential.

evolution was encountered featuring a monometallic (single-site) pathway. Initial studies have developed strategies to maximize surface stability, minimize background activity, and compare surface-anchored photoelectrocatalysis with solution systems. Current work is focused on tuning the acidity of the medium to enable hydride transfer via the single-site mechanism.

Nickel catalysts for photoelectrochemical hydrogen atom transfer. As shown in **Figure 2**, isolable nickel hydride complexes of the formula $[HNi(diphosphine)_2]^+$ were found to generate H_2 upon visible light illumination.[6] This rare example of photochemical H_2 evolution from a nickel hydride was leveraged to realize the first example of molecular photoelectrocatalysis by a first-row transition metal complex. Despite being short-lived, the excited state is proposed to have sufficient Ni–H σ* antibonding character to substantially weaken the Ni–H bond and promote H_2 evolution via hydrogen atom transfer. Consistent with the proposed mechanism, photolysis of nickel bis(diphosphine) hydride complexes in the presence of the persistent radical TEMPO• leads to exclusive hydrogen atom transfer to generate TEMPO–H in high yield (with the choice of solvent dictating the amount of competing H_2 evolution). These findings provide a platform for fundamental studies of nickel hydride photochemistry and thermochemistry-guided applications in fuel-forming electrochemical reductions at low overpotential.

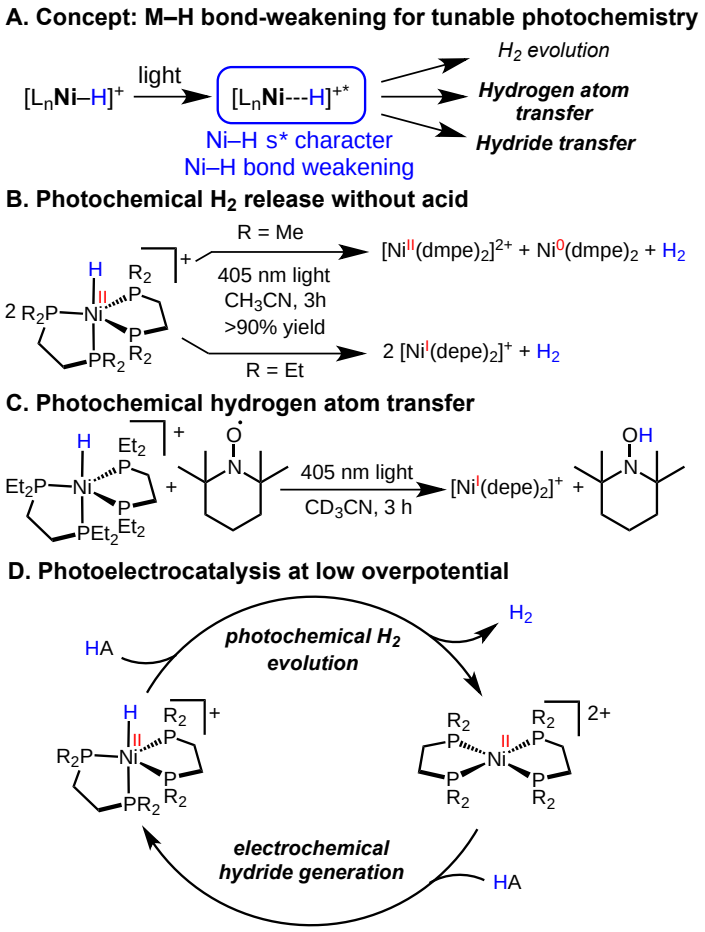

Figure 2. Concept and reactivity of nickel photohydrides.

Hydricity Studies. A longstanding goal of the project has been to develop fundamental tools associated with determining thermodynamic hydricity (hydride donor ability) of metal hydride complexes. Of particular interest have been factors such as how photoexcitation or changing temprature or solvent identity can influence the propensity of a hydride to react. A tutorial review introducing both thermodynamic and kinetic hydricity of transition metal complexes that highlights these remaining challenges was published recently.[3] A new method for determining hydricity at different temperatures was also introduced in the context of new strongly hydridic rhenium hydride complexes that can be formed from H_2 in various solvents.[4] Our group also collaborated to provide thermodynamic studies and Marcus analysis of hydride transfer from rhenium hydride complexes to various acceptors.[7] These studies can help researchers predict when metal hydrides will react with proton sources, CO_2, or other small molecules — both in the dark and under illumination.

DOE Solar Photochemistry Sponsored Publications 2020-2023

1. Barrett, S. M.; Stratakes, B. M.; Chambers, M.; Kurtz, D. A.; Pitman, C. L.; Dempsey, J. L.; Miller, A. J. M. "Mechanistic Basis for Tuning Iridium Hydride Photochemistry from H_2 Evolution to Hydride Transfer Hydrodechlorination." *Chem. Sci.* **2020**, 11, 6442-6449. https://doi.org/10.1039/D0SC00422G

2. Stratakes, B.M.; Miller, A.J.M. "H_2 Evolution at an Electrochemical "Underpotential" with an Iridium-Based Molecular Photoelectrocatalyst" *ACS Catal*. **2020**, 10, 9006-9018. https://doi.org/10.1021/acscatal.0c02265

3. Brereton, K.R.; Smith, N.E.; Hazari, N.; Miller, A.J.M. "Thermodynamic and kinetic hydricity of transition metal hydrides" *Chem. Soc. Rev*. **2020**, 49, 7929-7948. https://doi.org/10.1039/D0CS00405G

4. Hu, J.; Bruch, Q.J.; Miller, A.J.M. "Temperature and Solvent Effects on H_2 Splitting and Hydricity: Ramifications on CO_2 Hydrogenation by a Rhenium Pincer Catalyst." *J. Am. Chem. Soc.* **2021**, 143, 945-954. https://doi.org/10.1021/jacs.0c11110

5. Kaphan, D.; Brereton, K.; Klet, R.; Witzke, R.; Miller, A.J.M.; Mulfort, K.; Delferro, M.; Tiede, D. "Photocatalytic Transfer Hydrogenation in Water: Insight into Mechanism and Catalyst Speciation." *Organometallics.* **2021**, 40, 1482–1491. https://doi.org/10.1021/acs.organomet.1c00133

6. Stratakes, B.M.; Wells, K.A.; Kurtz, D.A.; Castellano, F.N.; Miller, A.J.M. "Photochemical H_2 Evolution from Bis(diphosphine) Nickel Hydrides Enables Low-Overpotential Electrocatalysis." *J. Am. Chem. Soc.* **2021**, 143, 21388–21401. http://doi.org/10.1021/jacs.1c10628

7. Espinosa, M.R.; Ertem, M.Z.; Barakat, M.; Bruch, Q.J.; Deziel, A.P.; Elsby, M.R.; Hasanayn, F.; Hazari, N.; Miller, A.J.M.; Pecoraro, M.V.; Smith, A.M.; Smith, N.E. "Correlating Thermodynamic and Kinetic Hydricities of Rhenium Hydrides." *J. Am. Chem. Soc.* **2022**, 144, 17939–17954. http://doi.org/10.1021/jacs.2c07192

8. Cloward, I.N.; Liu, T.; Rose, J.; Bonn, A.G.; Jurado, T.; Chambers, M.B.; Pitman, C.L.; ter Horst, M.; Miller, A.J.M. "Catalyst Self-Assembly Accelerates Bimetallic Light-Driven Electrocatalytic H_s Evolution in Water." *ChemRxiv preprint.* https://doi.org/10.26434/chemrxiv-2023-kf54s

Photooxidation of Hydroxymethylated Polycyclic Aromatic Dyes: Mechanism and Scope

Dugan Hayes, Carson Hasselbrink, Cali Antolini, Sophia Tiano, and Danielle Jacoby
Department of Chemistry
University of Rhode Island
Kingston, RI 02881

We recently discovered a novel photochemical reaction wherein polycyclic organic dyes bearing hydroxmethyl groups are oxidized to their corresponding aldehydes, some of which occur with concomitant elimination of dihydrogen as a byproduct. Our efforts are now focused on understanding the mechanism(s) of these photooxidations using 9-anthracenemethanol (AnMeOH) and 9-acridinemethanol (AcMeOH) as model reactants. By combining traditional steady-state physical organic chemistry techniques (isotope labeling, kinetic studies, and photophysical characterization) with ultrafast time-resolved spectroscopies (optical transient absorption, fluorescence upconversion, and time-correlated single photon counting) and time-dependent density functional theory, we aim to piece together a clear picture of the reaction from the initial photon absorption event to the formation of the products in their electronic ground states. Insights from this work will then allow us to identify the requisite properties of such constructs for photochemical dihydrogen release and thereby develop computational screening methods to design improved materials for molecular hydrogen storage, which we will experimentally validate by synthesizing these new dyes and evaluating their performance.

We have prepared three isotopologues of AnMeOH by substituting deuterium for the hydroxyl proton, one of the methylene protons, or both as shown in Fig. 1. Integration of the aldehyde peak in the ^{1}H NMR spectra taken following photochemical oxidation shows that while the -CH_2OD dye furnishes the -CHO product almost exclusively, the -CHDOH and -CHDOD dyes both preferentially furnish the -CDO product by approximately a factor of 5. This result confirms our hypothesis that one of the eliminated hydrogen atoms always originates from the hydroxyl group, while the other originates from the methylene group. Additionally, we have measured a kinetic isotope effect of ~5 for the cleavage of the methylene C-H bond. This value is consistent with the preservation of bending modes in the transition state, providing a crucial constraint on which H-H bond forming transition states are possible. We next plan to synthesize the corresponding isotopologues for AcMeOH to determine whether it likely follows a similar reaction trajectory.

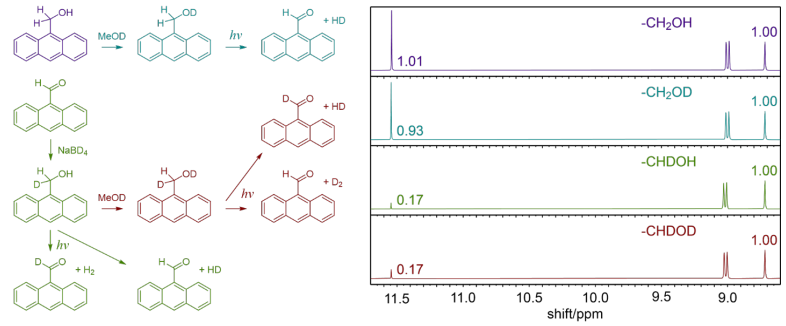

Figure 1. *Synthetic scheme and photochemical products of the isotopologues of AnMeOH prepared to date. Integration of the aldehyde peak in the ^{1}H NMR spectra allows us to quantify the relative amounts of -CHO and -CDO products.*

We have also measured the ultrafast optical transient absorption spectra of AcMeOH following excitation at 400 nm as shown in Fig. 2. At early delay times (< 20 ps), a broad, featureless excited state absorption spectrum is observed (blue trace), consistent with the excited state absorption spectrum of unsubstituted

acridine. Indeed, our preliminary TD-DFT calculations indicate that the initial excited state of AcMeOH is essentially identical to that of acridine, with the transition dipole oriented along the short axis of the dye. Notably, however, a sharp absorption feature at 660 nm (orange trace) grows in monoexponentially with a time constant of 730 ps, as shown in the corresponding kinetic trace. This spectrum is consistent with the spectra of the radical anions of several polycyclic heteroarenes such as 1,10-phenanthroline, and thus we assign this time constant to intramolecular charge transfer from the hydroxymethyl group to the acridine dye. However, 730 ps is remarkably slow for an intramolecular charge transfer, and we plan to explore the origin of this slow transfer rate using DFT calculations to quantify Marcus transfer rates for the accessible rotational landscape of the -CH_2OH rotor. We will use this approach to search for a transition state for the H-H bond formation in the charge-separated AnMeOH and AcMeOH diradicals.

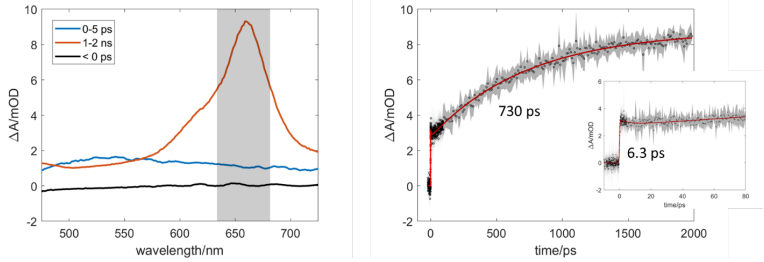

Figure 2. *(Left) Femtosecond transient absorption spectra of AcMeOH at various delay times. (Right) Kinetic trace averaged over the range indicated by the gray box in the left panel. Data points (open circles), one standard deviation error bars (gray shaded region), and the fit to a 6.3 ps decay and a 730 ps growth (red trace) are shown alongside the early time kinetics (inset).*

To follow the reaction further in time, we then measured the nanosecond optical transient absorption spectra of AcMeOH. Because our instrument response for this measurement is ~2 ns, the acridine radical anion is apparent even at the earliest delay times, but we also observe an additional excited state absorption feature at 780 nm corresponding to the initial excited state that is inaccessible in our ultrafast measurements. The kinetic trace at 660 nm shows a monoexponential decay with a 270 ns time constant and a small positive signal that persists for the 20 µs duration of the experiment that may correspond to irreversible formation of the aldehyde product. Careful steady-state characterization of the reactant and product will allow us to verify this assignment in the future.

Because AcMeOH is consumed over the course of these experiments, we are currently exploring alternate synthetic routes that may prove more easily scalable. Upon obtaining large quantities of material, we aim to perform variable temperature and visocity optical transient absorption measurements to determine whether charge transfer may be further retarded by slowing and/or kinetically trapping the hydroxymethyl rotor. We will also perform spectroelectrochemistry and cyclic voltammetry measurements of acridine and AcMeOH to confirm the assignment of the transient absorption spectrum at > 1 ns to the acridine radical anion and to determine the corresponding reduction potentials. Finally, we aim to better understand the potential scope of the photooxidation reaction by exploring other organic dyes as platforms and other saturated functional groups as reactive moieties. This will allow us to develop both a model of the reaction dynamics and a computational method for describing and predicting such reactivity.

Electrochemical Nitrogen and Proton Reduction using 2D Transition Metal Dichalcogenides

Logan Wilder[1], Nuwan H. Attanayake[1], Taylor Aubry[1], Jao van de Lagemaat[1], Derek Vigil-Fowler[1], Keenan Wyatt[1], Debjit Ghoshal[1], Hanyu Zhang[1], Tamara D. Koledin[1], Xiang Wang[2], Ji Hao[1], Sanjini U. Nanayakkara[1], Zhaodong Li[1], Michael V. Mirkin[2], and Elisa M. Miller[1]
[1]Materials, Chemical, and Computational Sciences, National Renewable Energy Laboratory Golden, CO 80401
[2]Department of Chemistry, Queens College-CUNY, Flushing, NY 11367

We use 2D transition metal dichalcogenide (TMDC) catalysts to facilitate the nitrogen (N_2) reduction to ammonia (NH_3) and proton reduction to hydrogen (H_2) via dark electrocatalysis in an aqueous based electrolyte. These two reduction pathways are important to understand and control for NH_3 and H_2 electrochemical production, as both products can be used as energy carriers, for energy storage, and as direct fuels. TMDCs are good catalyst candidates for these reactions because they can be reduced to 2D, where their quantum confined properties are easily manipulated for various applications. Transition metal-based catalysts offer a unique opportunity to exploit d electrons and orbitals as well as the chalcogenide plane for N_2 activation and/or H^+ adsorption, where we specifically aim to use theoretical calculations to guide design of MoS_2 and VS_2. In addition, the 2D TMDC catalysts are highly tunable 2D catalysts, where the band energetics, surface functionalization, defects, and phase can be tuned to control the reduction mechanisms.

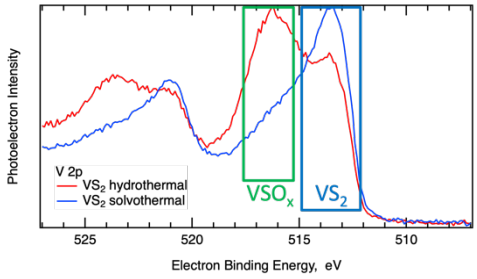

Figure 1. *XPS of 1T-VS_2 grown directly onto C paper via hydrothermal or solvothermal growth methods. The solvothermal growth shows a reduction in the VSO_x contribution compared to the VS_2 contribution.*

We have hydrothermally and solvothermally grown 1T-VS_2 nanoflowers directly on C-paper. We have characterized the 1T-VS_2 using Raman spectroscopy, X-ray diffraction (XRD), energy-dispersive X-ray spectroscopy (EDS), and X-ray photoelectron spectroscopy (XPS, Figure 1). The solvothermal growth yields more VS_2 and reduced VSO_X than the hydrothermal growth; however, both growth methods have S:V ratios greater than the expected 2:1 ratio. When testing both the hydrothermally and solvothermally grown VS_2 for electrochemical N_2 reduction, we do not detect any NH_3 generation. According to our theoretical density functional theory calculations performed at the meta-GGA level with treatment of spin, we need to have exposed metal sites at edges or sulfur vacancies to activate N_2 and for the N_2 reduction reaction (NRR) to proceed. Therefore, our next steps are to systematically reduce the amount of S in our grown samples and test for both NRR and hydrogen evolution reaction (HER) as a function of S:V ratio. Moreover, we will also evaluate the 1T-VS_2 for nitrate reduction to generation NH_3.

In preparing for electrochemical NRR, we also developed a more effective H-cell electrochemical cell design for aqueous-based NH_3 generating reactions in acidic or neutral conditions. An experimental design challenge in NRR is the selection of an ion-conductive membrane, which restricts NH_3/NH_4^+ crossover to preserve faradic efficiency and thus overall yield. Nafion cation exchange membranes (CEMs) are frequently used in NRR catalyst discovery experiments, but

recent reports suggest that Nafion CEMs allow NH_4^+ uptake and crossover. Here, we confirm experimentally that Nafion 212 shows high rates of NH_4^+ crossover in H-cell experiments (Figure 2a). Moreover, we determined that in H-cell experiments, anion exchange membranes (AEMs) show superior performance to Nafion in the restriction of NH_4^+ crossover while allowing sufficient ion conductivity for catalyst testing, and we have found that the commercially available AEM PiperION-A80 shows negligible NH_4^+ crossover and does not release measurable quantities of NH_3/NH_4^+ during a 6-h experiment (Figure 2b). In future studies, we will test AEMs in nitrate reduction electrolyzers, which will be useful as we explore other types of electrochemical reduction reactions for NH_3 generation.

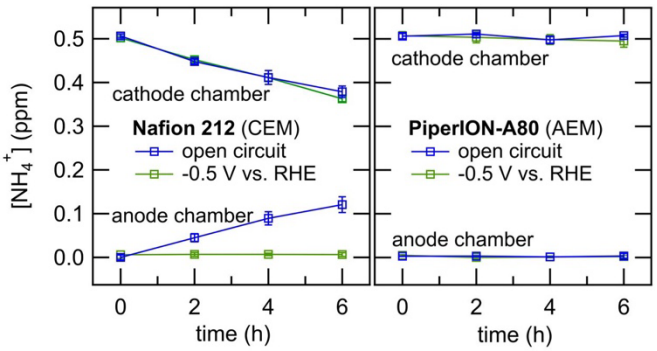

Figure 2. *Measurement of NH_4^+ membrane crossover of a) Nafion 212 and b) PiperION membranes in an H-cell with the membrane submerged in electrolyte at open circuit potential (OCP, blue traces) or with -0.5 V vs. RHE applied to the working electrode in the cathode chamber of the H-cell in three-electrode configuration (green traces).*

MoS_2 is one of the most heavily studied TMDCs and is thermodynamically stable in the semiconducting 2H state. However, these monolayers are more catalytically active and have greater electron conductivity in the unstable, metallic (1T/1T') state. Recently, we have demonstrated how to control the optoelectronic properties of MoS_2 monolayers using n-butyl lithium (BuLi) immersion treatments and functional groups, where shorter treatment times yield heavily n-type dope MoS_2 and longer treatment times fully convert the MoS_2 from the semiconducting to metallic (1T/1T') phase.[1] By adding functional groups to the MoS_2 (p-$(CH_3CH_2)_2$NPh-MoS_2, abbreviated Et_2N), the doped/converted MoS_2 is stable for up to two weeks. Using confocal Raman spectroscopy, we show the changes in the optoelectronic properties occur uniformly across the nanoflake (Figure 3), and this is also supported with additional microscopy measurements. Currently, we are growing via chemical vapor deposition even higher quality monolayers with full substrate coverage. Combining these higher quality monolayers with our technique to phase convert them to the catalytically active metallic phase, we propose to use these large-area monolayers as not only the protective layers for photoelectrodes but also as the catalyst for HER.

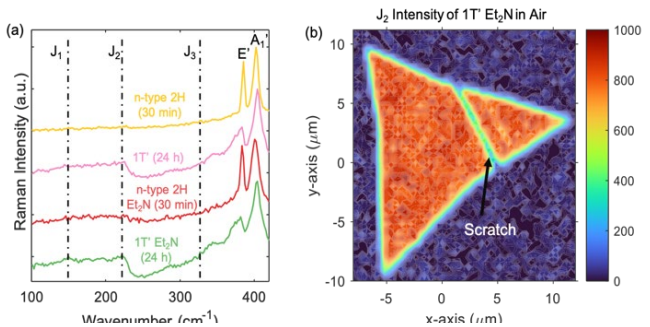

Figure 3. a) Raman Spectroscopy of MoS_2 monolayers following different BuLi immersion times (a) Raman spectra of MoS_2 monolayers immersed for 30 min or 24 h in BuLi with and without Et_2N surface functionalization. Measurements for the samples with Et_2N (red for 30 min BuLi soaking and green for 24 h) are conducted in air, while BuLi only treated samples (yellow and pink lines) are carried out under a N_2 environment (b) Raman mapping of the J2 mode (~225 cm^{-1}) intensity extracted from 1T' Et_2N MoS_2 measured in air.

DOE Solar Photochemistry Sponsored Publications 2020-2023

1. Hanyu Zhang, Tamara D. Koledin, Xiang Wang, Ji Hao, Sanjini U. Nanayakkara, Nuwan H. Attanayake, Zhaodong Li, Michael V. Mirkin, and Elisa M. Miller, "Stabilizing the Heavily-doped and Metallic Phase of MoS_2 Monolayers with Surface Functionalization"*2D Materials*, **9** 015033 (2022).
DOI: 10.1088/2053-1583/ac3f44

2. Soumyodip Banerjee, Xu Han, Maxime Siegler, Elisa M. Miller, Nicholas M. Bedford, Brandon C. Bukowski, and V. Sara Thoi, "A Flexible 2D Boron Imidazolate Framework for Polysulfide Adsorption in Lithium-Sulfur Batteries" Chemistry of Materials **34,** 10451 (2022).
DOI: 10.1021/acs.chemmater.2c02324

3. Zhaodong Li, Nuwan H. Attanayake, Jeffrey L. Blackburn, Elisa M. Miller "Carbon Dioxide and Nitrogen Reduction Reactions using 2D Transition Metal Dichalcogenide (TMDC) and Carbide/Nitride (MXene) Catalysts" *Energy and Environmental Science,* **14**, 6242 (2021).
DOI: 10.1039/D1EE03211A

4. Ian A. Murphy, Peter Rice, Madison Monahan, Leo P. Zasada, Elisa M. Miller, Simone Raugei, Brandi M. Cossairt "Covalent Functionalization of Nickel Phosphide Nanocrystals with Aryl-Diazonium Salts" *Chemistry of Materials*, **33** 9652 (2021).
DOI: 10.1021/acs.chemmater.1c03255

5. Tianyu Bo, Xiang Wang, Lili Han, Huolin Xin, Hanyu Zhang, Elisa M. Miller, and Michael V. Mirkin "Probing Activities of Individual Catalytic Nanoflakes by Tunneling Mode of Scanning Electrochemical Microscopy" *J. Chem. Phys. C,* **125**, 25525 (2021).
DOI: 10.1021/acs.jpcc.1c07309

6. Santu K. Bera, Megha Shrivastava, Khamari Bramhachari, Hanyu Zhang, Ajay K. Poonia, Dipendranath Mandal, Elisa. M. Miller, Matthew C. Beard, Amit Agarwal, and K. V. Adarsh, "Atomlike Interaction and Optically Tunable Giant Band-gap Renormalization in Large-area Atomically Thin MoS_2" *Physical Review B* **104** L201404 (2021).
DOI: 10.1103/PhysRevB.104.L201404

7. Gerard Michael Carroll**,** Rens Limpens, Gregory F. Pach, Yaxin Zhai, Matthew C. Beard, Elisa M. Miller, and Nathan R. Neale**, "**Suppressing Auger Recombination in Multiply Excited Colloidal Silicon Nanocrystals with Ligand-Induced Hole Traps**"** *Phys. Chem. C* **125**, 2565 (2021).
DOI: 10.1021/acs.jpcc.0c11388

8. Samuel Berweger, Hanyu Zhang, Prasana K. Sahoo, Benjamin M. Kupp, Jeffrey L. Blackburn, Elisa M. Miller, T. Mitch Wallis, Dmitri V. Voronine, Pavel Kabos, and Sanjini U. Nanayakkara, "Spatially Resolved Persistent Photoconductivity in MoS_2-WS_2 Lateral Heterostructures" *ACS Nano*, **14**, 14080 (2020).

DOI: 10.1021/acsnano.0c06745

9. Xu Han, Carter S. Gerke, Soumyodip Banerjee, Muhammad Zubair, Junjie Jiang, Nicholas M. Bedford, Elisa M. Miller, and V. Sara Thoi "Strategic design of MoO_2 nanoparticles supported by carbon nanowires for enhanced electrocatalytic nitrogen reduction" *ACS Energy Letters*, **5,** 3237 (2020).
DOI: 10.1021/acsenergylett.0c01857

10. Hanyu Zhang, Eric E. Benson, Kurt M. Van Allsburg, Elisa M. Miller, Drazenka Svedruzic, "Applying Dynamic Strain on Thin Oxide Films Immobilized on a Pseudoelastic Nickel-Titanium Alloy" *Journal of Visualized Experiments,* **161**, e61410 (2020).
DOI: 10.3791/61410

11. Dana B. Sulas-Kern, Elisa M. Miller, Jeffrey L. Blackburn, "Photoinduced Charge Transfer in Transition Metal Dichalcogenide Energy Technologies", *Energy and Environmental Science*, **13**, 2684 (2020).
DOI: 10.1039/d0ee01370f

12. Oren Elishav, Bar Mosevitzky Lis, Elisa M. Miller, Douglas Arent, Agustin Valera-Medina, Alon Grinberg Dana, Gennady Shter, Gideon Grader, "Progress and Prospective of Nitrogen-based Alternative Fuels" *Chemical Reviews*, **120**, 5352 (2020).
DOI: 10.1021/acs.chemrev.9b00538

13. Caitlin M. Hanna, Ryan T. Pekarek, Elisa M. Miller, Jenny Y. Yang, Nathan R. Neale, "Decoupling Kinetics and Thermodynamics of Interfacial Catalysis at a Chemically Modified Black Silicon Semiconductor Photoelectrode, *ACS Energy Letters*, **5**, 1848 (2020).
DOI: 10.1021/acsenergylett.0c00714

14. Hanyu Zhang, Jeremy R. Dunklin, Obadiah G. Reid, Seok Joon Yun, Sanjini U. Nanayakkara, Young Hee Lee, Jeffrey L. Blackburn, and Elisa M. Miller, "Disentangling Oxygen and Water Vapor Effects on Optoelectronic Properties of Monolayer Tungsten Disulfide" *Nanoscale* **12**, 8344 *(*2020).
DOI: 10.1039/c9nr09326e

15. Jeremy R. Dunklin, Aaron H. Rose, Hanyu Zhang, Elisa M. Miller, and Jao van de Lagemaat, "Plasmonic Hot Hole Transfer in Gold Nanoparticle-Decorated Transition Metal Dichalcogenide Nanosheets" *ACS Photonics* **7**, 197 (2020).
DOI: 10.1021/acsphotonics.9b01393

16. David M. Goggin, Hanyu Zhang, Elisa M. Miller, Joseph R. Samaniuk, “Interference Provides Clarity: Direct observation of 2D materials at fluid-fluid interfaces” ACS nano **14**, 777 (2020).
DOI: 10.1021/acsnano.9b07776

Contactless Measurement of Quasi-Fermi Level Splitting in Solar Fuel Photoelectrodes

Frank E. Osterloh, Sahar Daemi, Ye Cheng, Anna Kundmann, Kathleen Becker
Chemistry
University of California, Davis
Davis, CA and 95616

This project continues investigations of photocatalytic properties and charge separation in four solar fuel photocatalyst materials, n-$BiVO_4$, n-$CuWO_4$, n/p-GaP, and p-$CuGa_3Se_5$. These materials are studied with surface photovoltage spectroscopy (SPS) and electrochemistry to obtain information about the role of charge selective contacts, the effect of surface/interface states on charge transfer and trapping, and the role of band bending and Fermi level pinning on charge separation. In 2021 we performed the first quantitative Surface Photovoltage spectroscopy (SPS) measurements on semiconductor-liquid junctions (see Figure). We showed that the liquid-SPS data provides the quasi-Fermi Level Splitting (qFLS) of solar fuel electrodes. Obtaining this information in a contactless way may aid the search for improved solar fuel devices. This talk will demonstrate this approach for a $BiVO_4$ photoelectrode, [1] and show how it inspired the construction of the first $BiVO_4$-liquid solar cell [2]. The liquid SPS approach was also used to optimize $CuGa_3Se_5$ photocathodes for proton and methylviologen reduction [3] and to confirm a positive effect of pore ordering in $CuFe_2O_4$ water oxidation photoelectrodes on charge carrier trapping and photovoltage values. [4] In addition, vacuum-SPS determined the effective band gap and timescales for minority carrier trapping in a series of visible light active lanthanide oxysulfides $LnS_{14}O$ (Ln = La, Pr, Nd, Sm).[5] Insights into band gaps, majority carrier types and defects were obtained similarly for $Zn_4V_2O_9$ [6] and MV_2O_6 (M = Zn and Cu) [7] photoanodes, and for Al-doped $SrTiO_3$, [8] $Eu_{1-x}Ca_xTiO_3$, [9] and $LaTaO_2N$ photoactive oxides.[10] We also made progress in the construction of a GaP photocatalyst for H_2 evolution with a record quantum efficiency of 14.8% at 530 nm. [11] This became possible by considering the effects of surface states on recombination, the effect of solid-solid and solid-liquid junctions on charge separation, and the role of the reducing potential of the sacrificial donors in determining the overall reaction energetics. The study explains why most H_2-evolving photocatalysts in the literature are made of n-type, not p-type semiconductors. Lastly, we collaborated with Prof. Michael Mirkin to observe overall water splitting on single microscale particle photocatalysts for the first time. [12] In the future we plan to use liquid SPS to evaluate the effects of corrosion on qFLS in $CuWO_4$ and GaP. We also plan to expand the liquid SPS technique to allow measurements on photoelectrodes with applied bias.

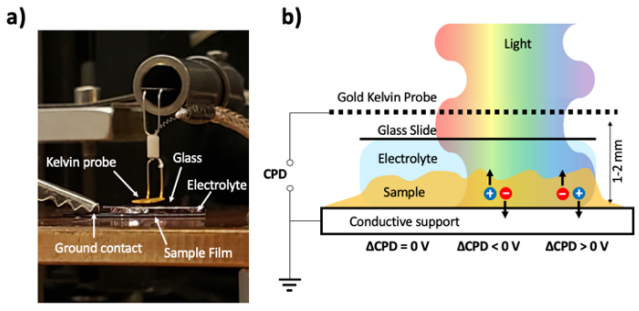

Figure. Vibrating Kelvin Probe Surface Photovoltage (VKP-SPV) Spectroscopy in liquids. a) Photo. b) Schematic of the measurement configuration. Illumination occurs through the 60% semi-transparent KP, placed 1-2 mm above the sample, and through the electrolyte, enclosed by a microscopy glass cover slide. The Contact Potential Difference (CPD) change under illumination equals the surface photovoltage signal SPV=CPD(light)-CPD(dark).

DOE Solar Photochemistry Sponsored Publications 2020-2023

1. Daemi, S., A. Kundmann, P. Cendula, K. Becker, and F.E. Osterloh, *Contactless Measurement of Quasi-Fermi Level Splitting in BiVO4 Photoelectrodes,* **submitted**.
2. Daemi, S., S. Kaushik, S. Das, T. Hamann, and F.E. Osterloh, *A BiVO4 liquid junction photovoltaic cell with 0.2% solar energy conversion efficiency,* **submitted**.
3. Cheng, Y., C. Xiao, B. Mahmoudi, R. Scheer, A.W. Maijenburg, and F.E. Osterloh, *Effect of charge selective contacts on the quasi Fermi level splitting of CuGa3Se5 thin film photocathodes for hydrogen evolution and methylviologen reduction*. EES Catalysis, **2023**, *1*, 74-83. http://dx.doi.org/10.1039/D2EY00062H
4. Einert, M., A. Waheed, D.C. Moritz, S. Lauterbach, A. Kundmann, S. Daemi, H. Schlaad, F.E. Osterloh, and J.P. Hofmann, *Mesoporous CuFe2O4 Photoanodes for Solar Water Oxidation: Impact of Surface Morphology on the Photoelectrochemical Properties*. Chemistry – A European Journal, **2023**, e202300277. http://dx.doi.org/https://doi.org/10.1002/chem.202300277
5. Wuille Bille, B.A., A.C. Kundmann, F.E. Osterloh, and J.M. Velázquez, *Ln10S14O (Ln = La, Pr, Nd, Sm) Oxysulfides: A Series of Direct n-Type Semiconductors*. Chemistry of Materials, **2022**, *34(16)*, 7553-7562. http://dx.doi.org/10.1021/acs.chemmater.2c01244
6. Hong, S., Y. Cheng, S. Hariyani, J. Li, R.M. Doughty, A. Mantravadi, A.N. Adeyemi, E.A. Smith, J. Brgoch, F.E. Osterloh, and J.V. Zaikina, *The Deep Eutectic Solvent Precipitation Synthesis of Metastable Zn4V2O9*. Inorganic Chemistry, **2022**, *61(1)*, 154-169. http://dx.doi.org/10.1021/acs.inorgchem.1c02511
7. Hong, S., S.J. Burkhow, R.M. Doughty, Y. Cheng, B.J. Ryan, A. Mantravadi, L.T. Roling, M.G. Panthani, F.E. Osterloh, E.A. Smith, and J.V. Zaikina, *Local Structural Disorder in Metavanadates MV2O6 (M = Zn and Cu) Synthesized by the Deep Eutectic Solvent Route: Photoactive Oxides with Oxygen Vacancies*. Chemistry of Materials, **2021**, *33(5)*, 1667-1682. http://dx.doi.org/10.1021/acs.chemmater.0c04155
8. Adeyemi, A.N., A. Venkatesh, C. Xiao, Z. Zhao, Y. Li, T. Cox, D. Jing, A.J. Rossini, F.E. Osterloh, and J.V. Zaikina, *Synthesis of SrTiO3 and Al-doped SrTiO3via the deep eutectic solvent route*. Materials Advances, **2022**, *3(11)*, 4736-4747. http://dx.doi.org/10.1039/D2MA00404F
9. Widenmeyer, M., T. Kohler, M. Samolis, A.T.D. Denko, X. Xiao, W. Xie, F.E. Osterloh, and A. Weidenkaff, *Band Gap Adjustment in Perovskite-type Eu1−xCaxTiO3 via Ammonolysis*. Zeitschrift für Physikalische Chemie, **2020**, *234(5)*, 887-909. http://dx.doi.org/10.1515/zpch-2019-1429
10. Bubeck, C., M. Widenmeyer, A.T. De Denko, G. Richter, M. Coduri, E.S. Colera, E. Goering, H. Zhang, S. Yoon, F.E. Osterloh, and A. Weidenkaff, *Bandgap-adjustment and enhanced surface photovoltage in Y-substituted LaTaIVO2N*. Journal of Materials Chemistry A, **2020**, *8(23)*, 11837-11848. http://dx.doi.org/10.1039/D0TA02136A
11. Becker, K., S. Assavachin, A. Kundmann, and F.E. Osterloh, *Junctions, Surface States, and Thermodynamics Control Hydrogen Evolution with a Gallium Phosphide Photocatalyst,* **submitted**.
12. Askarova, G., C. Xiao, K. Barman, X. Wang, L. Zhang, F.E. Osterloh, and M.V. Mirkin, *Photo-scanning Electrochemical Microscopy Observation of Overall Water Splitting at a Single Aluminum-Doped Strontium Titanium Oxide Microcrystal*. Journal of the American Chemical Society, **2023**, *145(11)*, 6526-6534. http://dx.doi.org/10.1021/jacs.3c00663
13. Segev, G., et al, *The 2022 solar fuels roadmap*. Journal of Physics D: Applied Physics, **2022**, *55(32)*, 323003. http://dx.doi.org/10.1088/1361-6463/ac6f97
14. Osterloh, F.E., *Kinetic and Thermodynamic Considerations for Photocatalyst Design (Chapter 1)*, in *Heterogeneous Photocatalysis. From Fundamentals to Applications in Energy Conversion and Depollution*, J. Strunk, Editor. 2021, Wiley VCH.
15. Roehrich, B.W., R. Han, and F.E. Osterloh, *Hydrogen evolution with fluorescein-sensitized Pt/SrTiO3 nanocrystal photocatalysts is limited by dye adsorption and regeneration*. Journal of Photochemistry and Photobiology A: Chemistry, **2020**, *400*, 112705. http://dx.doi.org/10.1016/j.jphotochem.2020.112705
16. Han, R., M.A. Melo Jr, Z. Zhao, Z. Wu, and F.E. Osterloh, *Light Intensity Dependence of Photochemical Charge Separation in the BiVO4/Ru-SrTiO3:Rh Direct Contact Tandem Photocatalyst for Overall Water Splitting*. The Journal of Physical Chemistry C, **2020**, *124*, 9724-9733. http://dx.doi.org/10.1021/acs.jpcc.0c00772
17. Han, R., T.-Y. Kim, T.W. Hamann, and F.E. Osterloh, *Photochemical Charge Separation and Dye Self-Oxidation Control Performance of Fluorescein, Rose Bengal, and Triphenylamine Dye-Sensitized Solar Cells*. The Journal of Physical Chemistry C, **2020**, *124(48)*, 26174-26183. http://dx.doi.org/10.1021/acs.jpcc.0c09052
18. Doughty, R.M., B. Hodges, J. Dominguez, R. Han, Z. Zhao, S. Assavachin, and F.E. Osterloh, *Fermi Level Pinning Controls Band Bending and Photochemical Charge Separation in Particles of n-SrTiO3, n-SrTiO3:Al, and n-GaAs:Te*. The Journal of Physical Chemistry C, **2020**, *124(34)*, 18426-18435. http://dx.doi.org/10.1021/acs.jpcc.0c04989
19. Doughty, R.M., F.A. Chowdhury, Z. Mi, and F.E. Osterloh, *Surface photovoltage spectroscopy observes junctions and carrier separation in gallium nitride nanowire arrays for overall water-splitting*. The Journal of Chemical Physics, **2020**, *153(14)*, 144707. http://dx.doi.org/10.1063/5.0021273

Rational design of light-driven proton pumps using knowledge from photoelectrochemical experiments, transient absorption spectroscopies, and detailed-balance simulations

Leanna Schulte,[1] Simon Luo,[1] Rohit Bhide,[1] Gabriel S. Phun,[1] Ethan J. Heffernan,[2] and Shane Ardo[1,2,3]
Dept. of [1]Chemistry, [2]Materials Science & Engineering, [3]Chemical & Biomolecular Engineering
University of California Irvine
Irvine, CA 92697-2025

Junctions that form at interfaces of solid-state electronic semiconductors generate space–charge regions. With proper design, diode behavior results, an important prerequisite for efficient photoconversion. Space–charge regions are not unique to semiconductor interfaces and also form at and across ion-exchange-membrane interfaces, with properties that can be tuned by varying the concentration of ions in the contacting phase(s). Leveraging this, we aim to demonstrate solar photochemical reactivity from our new light-driven proton-pump platform.

Motivated by traditional dye-sensitized solar cells, we bathed photoacid-dye-sensitized cation-exchange membranes in aqueous solutions of varied electrolyte concentration and analyzed their photoelectrochemical behavior. When wetted by aqueous acid on one side and aqueous base on the other side, unsurprisingly, we observed high fluxes for acid and base crossover. To mitigate this effect, we interfaced this cation-exchange membrane with an anion-exchange membrane to form a photoacid-dye-sensitized bipolar membrane. This slowed crossover, but not to a level that enabled reproducible and analytical evaluation of diode performance, using techniques previously developed by the solid-state physics community.

Through a grant from the DOE Office of Science Early Career Research Program, we methodically evaluated means to overcome these limitations. By wetting cation-exchange-membrane–liquid-junction constructs with aqueous moderate acid on one side ($pH \geq 1$) and aqueous weak acid on the other side ($pH \leq 4$), pH differences across the membrane were found to be stable for days. Yet, use of standard reference electrodes resulted in ion leakage that masked important fundamental information. Therefore, we developed a method to characterize these junctions using Ag/AgCl wires. Remarkably, and wholly supported by thermodynamic derivations, this setup (i.e. a cation-exchange membrane with reference electrodes that are sensitive to the Cl^- anion) reported on the difference of contributions due to the chemical potential and Donnan electric potential across the membrane, such that at equilibrium, a non-zero value resulted. This allowed us to accurately measure the magnitude and sign of the net built-in electric potential difference across the membrane, which matched predictions from Donnan membrane theory and semiconductor diode theory. The small pH range applicable to measurements, however, precluded observation of current rectification. Moreover, measured open-circuit photovoltages had signs opposite ("reverse") of that expected based on the sign of the net electric potential. Mechanistic details gleaned using nanosecond transient absorption spectroscopy indicate that our photoacid molecules only photogenerate protons as the mobile charged species. Because our photoacid-dye-sensitized cation-exchange membranes are infiltrated with protons, this means that minority-carrier hydroxides are not able to elicit photovoltaic action by standard minority-carrier-dominated charge separation. Instead, measured photovoltages are consistent with charge separation of a proton from its photoacid conjugate base, driven by intrinsic liquid-junction-forming crossover of acid, which results in bulk membrane polarization and "reverse" photovoltaic action.

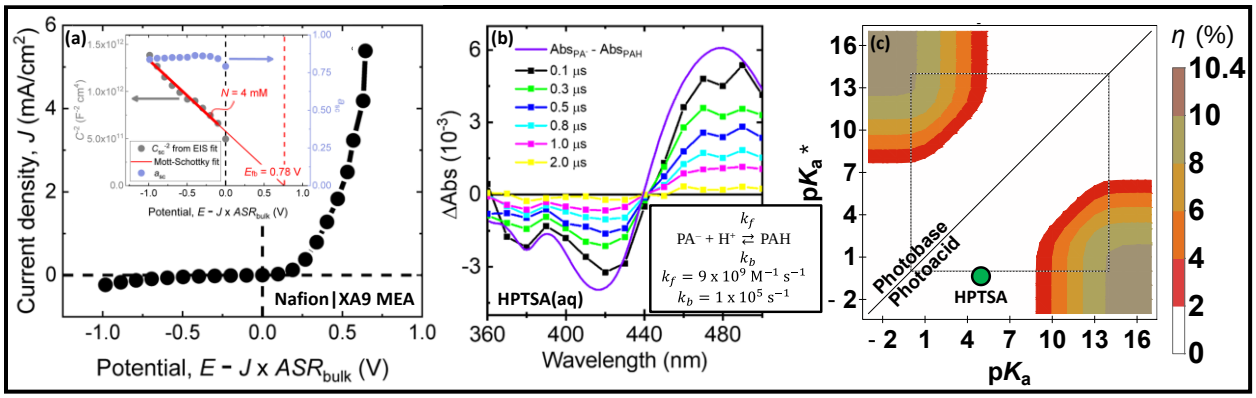

Figure 1. (a) *J–E* data for a Nafion|XA9 bipolar-membrane–electrode assembly (MEA) protonic diode, illustrating net water dissociation (reverse bias) and net water formation (forward bias). Inset: Capacitances (C_{sc}) and ideality factors (a_{sc}) of the space–charge region extracted from best-fits of EIS data to a nonideal Randles equivalent circuit model, and reported as a Mott–Schottky plot with extracted values indicated for the fixed-charge density in the space–charge region (N) and "flatband" potential (E_{fb}), i.e. when $\phi = 0$. **(b)** Transient absorption spectra, after 355 nm pulsed-laser excitation (0.6 mJ/pulse), that resolve the ground-state reprotonation of deprotonated ethylene-diamine-modified 8-hydroxypyrene-1,3,6-trisulfonic acid trisodium salt (HPTSA) photoacid dissolved in aqueous electrolyte at pH ≈ 4. Inset: Dominant reaction and rate constants extracted from best-fits of kinetic data at several pH values in the range (3, 6). **(c)** Ideal detailed-balance sunlight-to-protonic power conversion efficiencies (η), assuming pH = 7, Brønsted proton-transfer theory for a Förster cycle, and a fill factor equal to 0.75, and with properties of HPTSA indicated (green circle).

We also innovated in photoacid-dye-sensitized bipolar membrane measurements by arranging them as membrane–electrode assemblies, analogous to fuel cells, and characterizing them using reversible H_2 redox. Doing this, bipolar membranes exhibited characteristics remnant of a solid-state electronic semiconducting diode. Mott–Schottky analysis proved beneficial to characterize ionic properties and supported that light-driven effects likely result in a decrease in relative permittivity in the space–charge. "Reverse" photovoltaic action was again observed, likely due to dynamic polymer processes initiated by excited-state proton transfer from photoacids.

To better guide our design of dye-sensitized light-driven proton pumps, we developed a methodology to calculate the protonic detailed-balance efficiency limit for generation of H^+ and OH^- from photoacids or photobases in water. Our model includes reversible mass-action kinetics for all photochemical and photophysical processes in the Förster cycle square scheme, including calculation of Einstein coefficients, and proton-transfer rate constants under the assumption of strong electronic coupling. Results indicate that a maximum photovoltage of >300 mV is possible for absorption of sunlight over the width of a space–charge region in typical bipolar membranes, resulting in a ~10% power conversion efficiency. Unexpectedly, decreased dye concentration results in two opposing effects of less sunlight absorption, but improved chemical kinetics, resulting in nearly unchanged predicted photovoltages.

Designs with covalently bonded photoacids or photobases are limited by their experimental $|\Delta pK_a| < 10$, far smaller than the protonic gap of water, i.e. $|\Delta pK_a| = 14$. While development of a new photoacid or photobase motif is tempting, we take an alternative approach by ionically associating photoacids (or photobases) in ion-exchange membranes so they serve as one mobile charge carrier, such that their ground-state pK_a replaces $pK_a = 14$ of water to narrow the protonic gap. Using this, we have shown that conjugate bases of photoacids are mobile within anion-exchange membranes, and that their conjugate acids generate photovoltages. We aim to use this design to generate significant photovoltages, and perform useful work by pressurizing H_2 or driving CO_2 reforming.

DOE Solar Photochemistry Sponsored Publications 2020-2023

1. Schulte, L.; White, W.; Renna, L. A.; Ardo, S.* *Joule*, **2021**, *5(9)*, 2380–2394, DOI: 10.1016/j.joule.2021.06.016. Turning Water into a Protonic Diode and Solar Cell via Doping and Dye Sensitization.

2. Luo, S.; White, W.; Cardon, J. M.; Ardo, S.* *Energy & Environmental Science*, **2021**, *14(9)*, 4961–4978, DOI: 10.1039/D1EE00482D. Clarification of Mechanisms of Protonic Photovoltaic Action Initiated by Photoexcitation of Strong Photoacids Covalently Bound to Hydrated Nafion Cation-Exchange Membranes Wetted by Aqueous Electrolytes. *(Featured in 2020 Energy and Environmental Science HOT articles)*

3. Bhide, R.; Feltenberger, C. N.; Phun, G. S.; Barton, G.; Fishman, D.; Ardo, S.* *Journal of the American Chemical Society*, **2022**, *144(32)*, 14477–14488, DOI: 10.1021/jacs.2c00554. Quantification of Excited-State Brønsted–Lowry Acidity of Weak Photoacids Using Steady-State Photoluminescence Spectroscopy and a Driving-Force-Dependent Kinetic Theory.

4. Phun, G. S.; Bhide, R.; Ardo, S.* (in second round of revision with *Energy & Environmental Science*) Detailed-balance limits for sunlight-to-protonic energy conversion from aqueous photoacids and photobases based on reversible mass-action kinetics.

5. Luo, R. *Ph.D. Dissertation*, **2021**. Elucidation and Impact of Photoacid Proton-Transfer Regeneration Dynamics.

6. Schulte, L. P. *Ph.D. Dissertation*, **2021**. Protonic Diodes and Their Mechanisms of Photovoltaic Action, Current Conduction, and Water Dissociation.

7. Bhide, R. *Ph.D. Dissertation*, **2022**. Understanding Proton-Transfer Dynamics of Reversible Excited-State Photoacids Using Driving-Force-Dependent Kinetic Theories.

Light Harvesting: From the First Step to the Photosystem II Supercomplex Landscape

Q. Li, C. Leonardo, S.-J. Yang, K.B. Whaley and G. R. Fleming
Molecular Biophysics and Integrated Bioimaging Division
Lawrence Berkeley National Laboratory
and
Department of Chemistry, University of California Berkeley
Berkeley CA 94720

Experimental study of natural and synthetic photosynthetic systems involves intense laser pulses. In contrast, sunlight is weak: - a few tens of photons/nm^2/s within the chlorophyll Q band absorption at full sunlight. That photosynthesis can be initiated by absorption of a single photon has often been assumed but not previously demonstrated. Using a quantum light source and correlation measurement we demonstrate that absorption and subsequent emission in the LH2 light harvesting complex comes from single-photon events [15]. This experiment constitutes the first step towards understanding the spatio-temporal nature of the dynamics subsequent to excitation by a weak light source. The design of the photosystem II supercomplex (PSIISC) appears, at first glance, rather enigmatic. It features a remarkably flat energy landscape which seems non-intuitive for a system designed for near unit quantum efficiency at low light. In addition the C_2S_2 PSIISC contains over 200 Chls in 16 subunits with differing ratios of Chla to Chlb as compared to the 98 Chla-containing core antenna/ reaction center (RC) complex of Photosystem I (PSI). However, unlike PSI, PSII must balance efficient light harvesting at low light with photoprotection from the damage of the highly oxidizing reaction center components at excess light levels. By combining the remarkable spectral resolution of 2DEV spectroscopy with quantum dynamical simulations, we show that excitation placed close to the RC initially flows out to the peripheral antennae where quenching sites for excess excitation can be activated [17]. This is the case when excitation is mostly in Chla (figure, left side). In contrast when excitation is mostly in Chlb, energy flows towards the RC (figure, right side). In the former case excitation is close to the RC, while in the Chlb case the excitation is mainly in the periphery. To sum up, the free energy landscape of the PSIISC is determined by entropy not enthalpy as other, funnel-like antenna systems are.

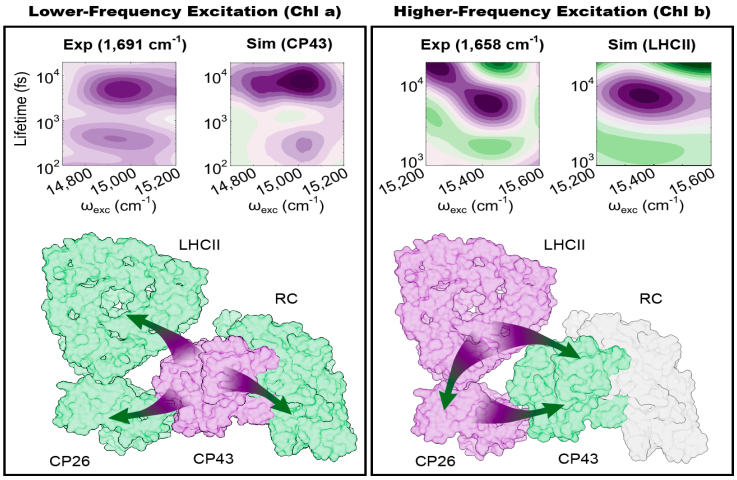

Figure. 2DEV spectroscopic experiments and simulations show that below 20 ps energy flows towards the peripheral antennae for Chla excitation (left) and towards the core for Chlb excitation (right)

DOE Solar Photochemistry Sponsored Publications 2020-2023

1. Vibronic mixing enables ultrafast energy flow in light-harvesting complex II. E.A. Arsenault, Y. Yoneda, M. Iwai, K.K. Niyogi, and G.R. Fleming. Nat Com 11, 1460 (2020). doi.org/10.1038/s41467-020-14970-1
2. Solvent Mediated Excited State Solvent Mediated Excited State Proton Transfer in Indigo Carmine P. P. Roy, J. Shee, E. A. Arsenault, Y. Yoneda, K. Feuling, M. P. Head-Gordon, and G. R. Fleming. J. Phys. Chem. Lett. 11, 4156–4162 (2020) doi.org/10.1021/acs.jpclett.0c00946
3. Electron-nuclear dynamics accompanying proton-coupled electron transfer. Y. Yoneda, S. J. Mora, J. Shee, E. A. Arsenault, B. L. Wadsworth, D. Hait, D. Gust, G. F. Moore, A. Gust, M. Head-Gordon, A.L. Moore, T. Moore, and G.R. Fleming JACS. 143, 3104-3112 (2021)
4. The Role of Resonant Nuclear Modes in Vibrationally Assisted Energy Transport: the LHCII Complex. P. Bhattacharyya and G.R. Fleming. J. Chem. Phys. 153, 044119 (2020) doi: 10.1063/5.0012420
5. The role of mixed vibronic Qy-Qx bands in the light-harvesting dynamics of the major antenna complex, LHCII. E. A. Arsenault, Y. Yoneda, M. Iwai, K. K. Niyogi and G.R. Fleming. Nat Comm. 11, 6011 (2020) https://doi.org/10.1038/s41467-020-19800-y
6. Two-Dimensional Electronic–Vibrational Spectroscopy Reveals Cross-Correlation between Solvation Dynamics and Vibrational Spectral Diffusion. M. Cho and G.R. Fleming. The Journal of Physical Chemistry B 2020 124 (49), 11222-11235. DOI: 10.1021/acs.jpcb.0c08959
7. Insights into photosynthetic energy transfer gained from free-energy structure: Coherent transport, incoherent hopping, and vibrational assistance revisited. A. Ishizaki and G.R. Fleming. J. Phys. Chem. B. 125, 3286-3295 (2021)
8. Two-dimensional electronic-vibrational spectroscopy: Exploring the interplay between electrons and nuclei in excited state dynamics. E. A. Arsenault, P. Bhattacharyya, Y. Yoneda and G. R, Fleming J. Chem Phys Perspective 155, 020901 (2021) https://doi.org/10.1063/5.0053042
9. The initial charge separation step in oxygenic photosynthesis. Y. Yoneda, E. A. Arsenault, K. Orcutt, M. Iwai, and G. R. Fleming. Nature Communications 13, 2275 (2022) https://doi.org/10.1038/s41467-022-29983-1
10. Vibronic coupling and two-dimensional electronic-vibrational spectra. E. A. Arsenault, A. J. Schile, D. T. Limmer and G. R. Fleming J. Chem Phys. 155, 054201 (2021) DOI 10.1063/5.0056477
11. Vibronic coupling in Light Harvesting Complex II revisited. E.A. Arsenault, A. J. Schile, D. T. Limmer and G. R. Fleming J. Chem Phys. 155, 096101 (2021) DOI 10.1063/5.0056478
12. Concerted Electron-Nuclear Motion in Proton-Coupled Electron Transfer-Driven Grotthuss-Type Proton Translocation E. A. Arsenault, W.D. Guerra, J. Shee, E.A. Reyes Cruz, Y. Yoneda, B.L. Wadsworth, E.Odella, M.N. Urrutia, G. Kodis, G.F. Moore, M. Head-Gordon, A.L. Moore, T.A. Moore, and G.R. Fleming J Phys Chem Lett, 13, 4479-4485, (2022) doi.org/10.1021/acs.jpclett.2c00585
13. From Antenna to Reaction Center: Pathways of Ultrafast Energy and Charge Transfer in Photosystem II. S-J Yang, E. A. Arsenault, K. Orcutt, M. Iwai, Y. Yoneda and G. R.

Fleming Proc. Natl. Acad. Sci. 119, e2208033119 (2022), DOI 10.1073/pnas.2208033119
14. Two-Dimensional Electronic Vibrational Spectroscopy of Complex Molecular Systems. E. A. Arsenault and G. R. Fleming Nobel Symposium 173 Exploring complex molecular and condensed phase processes and functions by multidimensional spectroscopy from THz to X-rays. Ed. T. Pullerits et al. p13-16 (2022)
15. Single-photon absorption and emission from a natural photosynthetic complex. Quanwei Li, Kaydren Orcutt, Robert L. Cook, Javier Sabines-Chesterking, Ashley L. Tong, Gabriela S. Schlau-Cohen, Xiang Zhang, Graham R. Fleming & K. Birgitta Whaley. Nature
16. Infrared signatures of phycobilins within the phycocyanin 645 complex. P.P. Roy, C. Leonardo, K. Orcutt, C. Oberg, G.D. Scholes, and G. R. Fleming. J Phys Chem B submitted
17. Bidirectional Energy Flow in the Photosystem II Supercomplex. C. Leonardo, S-J. Yang, K. Orcutt, M. Iwai, E.A. Arsenault, and G. R. Fleming, in Preparation

Ultrafast Functional Structural Dynamics in Solar Energy Conversion

L. X. Chen,[1,3] R. D. Schaller,[2,3] X. Li,[4] F. N. Castellano,[5] A. A. Cordones-Hahn,[6] K. D. Glusac,[1,7] P. Kim,[1,3] M. W. Mara,[1] K. L. Mulfort,[1] G. C. Schatz[3]

[1]Chemical Sciences and Engineering Division, [2]Center for Nanoscale Materials, Argonne National Laboratory, Lemont, IL 60439

[3]Department of Chemistry, Northwestern University, Evanston, IL 60208

[4]Department of Chemistry, University of Washington, Seattle, WA 98195

[5]Department of Chemistry, North Carolina State University, Raleigh, NC 27695

[6]SLAC National Accelerator Laboratory, Stanford University, Menlo Park, CA 94025

[7]Department of Chemistry, University of Illinois at Chicago, Chicago, IL 60607

The goal of our team research is to provide a critical knowledge base for understanding fundamental light—matter interactions that influence solar photochemistry as well as emerging new science in photoredox catalysis. We explore ultrafast functional structural dynamics in photoexcited states with strongly coupled electronic and nuclear motions beyond the Born-Oppenheimer approximation across four tasks, A) identifying key excited-state reaction coordinates of transition metal complexes in photochemical reactions; B) steering photoinduced electron transfer processes towards charge accumulation and photocatalytic bond breaking reactions by chemical modifications and tailored light pulse sequences; C) manipulating coherent vibrational motions for interfacial plasmonic driven charge transfer; and D) tracking functional structural and electronic dynamics along excited-state trajectories by ultrafast elemental specific inner shell spectroscopies and solution scattering at XFEL facilities. Specific topics below are described.

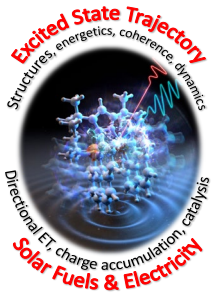

1. *Identifying and steering key reaction coordinates of photoinduced electron transfer (PET) and intersystem crossing (ISC) processes in the metal-metal-to-ligand charge-transfer (MMLCT) state of Pt dimer-NDI systems.* The PET trajectories in the MMLCT state of di-platinum(II) complexes as the electron donor and covalently attached NDIs as electron acceptor (**Fig. 1**) were determined by following their coherent vibrational wavepacket (CVWP) motions of specific vibrational modes, revealing an intermediate state ballistically generated having a distinct spectral feature differing from those of the di-platinum MMLCT and the NDI radical anion states. A sub-20 fs pump pulse launched CVWP motions across several frequencies exhibiingt phase and temporal changes in the NDI radical anion absorption. These distinct CVWP motions indicate that the MMLCT excitation led to the formation of a delocalized CT state between the ligands of the Pt dimer and NDI, which subsequently evolves into the final charge-separated

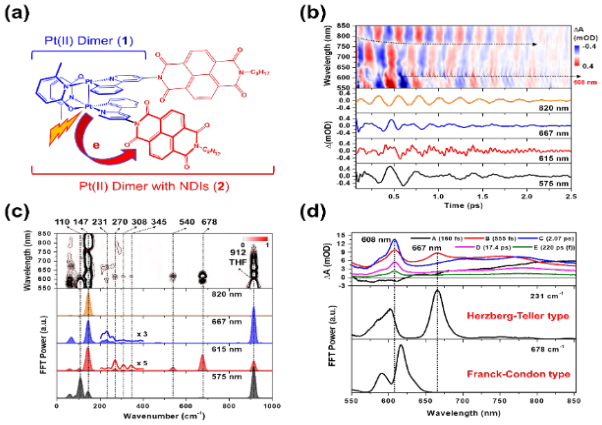

Fig. 1. (a) schematic molecular structure of Pt dimer with two NDIs. (b) 2D-oscillation map and beating signals at specific probe wavelengths. (c) 2D-FFT map and FFT spectra at specific probe wavelengths. (d) (top) evolution associated difference spectra and (middle and bottom) FFT amplitude of 231 and 678 cm^{-1} beatings displayed along probe wavelengths.

state through the collective vibration of the ligands and peripheral NDIs. The key vibrational modes in these di-platinum complexes also strongly influence the dynamics and pathways with spin-vibronic coupling mechansims. The insights gained from this study shed light on how certain key vibrational modes facilitate efficient ISC and PET processes in transition metal complexes and how one can potentially steer reaction direction through modulations these vibrational modes.

2. *Interfacial energy and charge transfer influenced by the plasmonic induced phonon modes in nanoparticles and clusters*. Photoexcitation of plasmonic nanostructures can impulsively generate charge carriers and launch both acoustic and optical (dipolar) vibrations. These nuclear motions may impact energy landscapes at the interface and boost the energies for charges to cross the energy barriers influencing charge transfer efficiencies or energy migration pathways. For sufficiently uniform ensembles, we characterize coherent phonon motions in nanostructured chromophores and their dephasing lifetimes in gold nanoclusters hybridized with nanoparticle TiO_2, (**Fig. 2**) which has yielded emergent mixed states. Calculations on pressure effects were carried out to understand excited state properties in the clusters related to the structural distortion, so that a framework for modeling gold nanocluster excited states and plasmon oscillations in planned experiments.

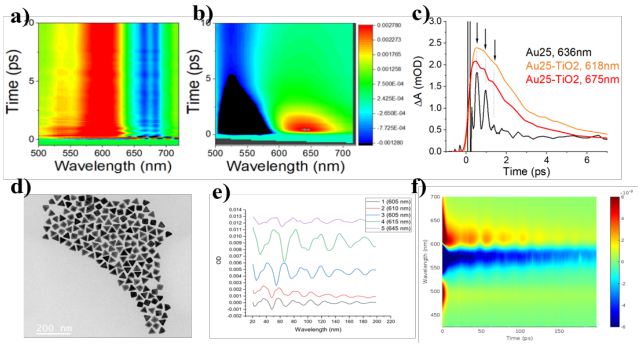

Fig. 2 a) Transient absorption spectra of Au_{25} nanoclusters and b) Au_{25}/TiO2; c) plastic phonon oscillation in the TA signals; d) TEM of Au tetrahedron, e) selected wavelengths of 5 samples with phonon oscillations. f) Transient absorption spectrum of sample 1.

3. *Coupled electron and nuclear motions in excited state and PET processes – Theoretical predications and simulations.* Bimetallic electron donor-acceptor complexes can facilitate electron and energy transfer with excellent structural control through synthetic design. We have carried out ultrafast X-ray spectroscopy and scattering studies on these systems experimentally to capture electronic and nuclear motions in the excited and transient states for catalytic reactions (see poster by Cordones-Hahn et al.). Meanwhile, we have also applied ab initio electron-nuclear dynamics to study the dynamical interplay between two metal-centered charge transfer states in a bimetallic complex. In one example, the photochemical dynamics were initiated by photoexcitation of the Ru-centered metal-to-ligand-charge-transfer (MLCT) state. Electronic dynamics show that although there is a fast partial electron-hole recombination, the Ru-centered MLCT largely remains in its photoexcited state because the Ru-d reorganization prevents it from a complete coherent decay to the ground state (**Fig. 3**). Electron-nuclear excited state dynamics show that the molecular vibrations on the excited state lead to a small rotational motion of the tpphz bridge and closing motion of the mesityl ligands. These vibrational modes are seen to drive the metal-to-metal charge transfer event with both electron and hole populations being transferred with concerted dynamics.

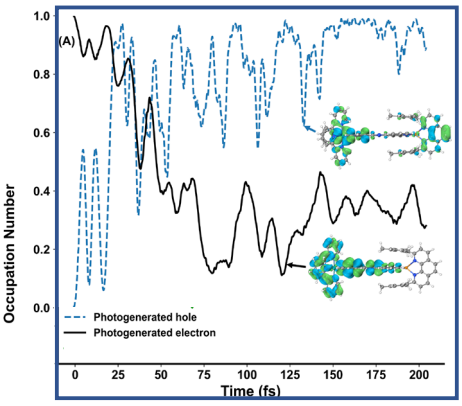

Fig. 3. Time evolution of selected orbital populations of the photoexcited electron (solid line) and hole (dashed line).

DOE Solar Photochemistry Sponsored Publications 2020-2023

1. Spin-vibronic coherence drives singlet-triplet conversion, Shahnawaz Rafiq, Nicholas P. Weingartz, Sarah Kromer, Felix N. Castellano, Lin X. Chen, *Nature*, just accepted (**2023**).
2. Direct observation of the pressure-induced structural variation in gold nanoclusters and the correlated optical response, Qi Li, Charles J. Zeman, IV, Bora Kalkan, Kristin Kirschbaum, Christopher Gianopoulos, Abhinav Parakh, David Doan, Andrew C. Lee, John Kulikowski, George C. Schatz, Guoyin Shen, Martin Kunz, X. Wendy Gu, Nano Lett 23, 132-139 (**2023**).
3. Ligand Structure Dependent Coherent Vibrational Wavepacket Dynamics in Pyrazolate-Bridged Pt(II) Dimers, Kim, Tae Wu, Kim; Pyosang; Mills, Alexis W.; Chakraborty, Arnab; Kromer, Sarah; Valentine, Andrew J. S.; Castellano, Felix N.; Li, Xiaosong; Chen, Lin X., J. Phys. Chem. C 126, 28, 11487–11497 (**2022**)
4. Layered structures of assembled imine-linked macrocycles and two-dimensional covalent organic frameworks give rise to prolonged exciton lifetimes, Helweh, Waleed; Flanders, Nathan C.; Wang, Shiwei; Phelan, Brian T.; Kim, Pyosang; Strauss, Michael J.; Li, Rebecca L.; Kelley, Matthew S.; Kirschner, Matthew S.; Edwards, Dillon O.; Spencer, Austin P.; Schatz, George C.; Schaller, Richard D.; Dichtel, William R.; Chen, Lin X., J. Mat. Chem. C 10, 3015-26 (**2022**).
5. Proton-Coupled Electron Transfer in a Ruthenium(II) Bipyrimidine Complex in Its Ground and Excited Electronic States, M. C. Drummer, R. B. Weerasooriya, N. Gupta, E. J. Askins, X. Liu, A. J. S. Valentine, X. Li, K. D. Glusac, *J. Phys. Chem. A*, 126, 4349–4358 (**2022**)
6. Exploring Potential Energy Surfaces Using Reinforcement Machine Learning, A. W. Mills, J. J. Goings, D. Beck, C. Yang and X. Li, *J. Chem. Info & Modeling*, 62, 3169–3179 (**2022**)
7. Ultrafast branching in intersystem crossing dynamics revealed by coherent vibrational wavepacket motions in a bimetallic Pt(II) complex, Pyosang Kim, Andrew J. S. Valentine, Subhangi Roy, Alexis W. Mills, Felix N. Castellano, Xiaosong Li, Lin X. Chen, *Faraday Discussions,* (**2022**).
8. Relativistic Nonorthogonal Configuration Interaction: Application to L2,3-edge X-ray Spectroscopy, A. Grofe , X. Li, *Phys. Chem. Chem. Phys*., 24, 10745– 10756 (**2022**).
9. Non-fullerene acceptors with direct and indirect hexa-fluorination afford >17% efficiency in polymer solar cells, Guoping Li, Liang-Wen Feng, Subhrangsu Mukherjee, Leighton O. Jones, Robert M. Jacobberger, Wei Huang, Ryan M. Youg, Robert M. Pankow, Weigang Zhu, Norman Lu, Kevin L. Kohlstedt, Vinod K. Sangwan, Michael R. Wasielewski, Mark C. Hersam, George C. Schatz, Dean M. DeLongchamp, Antonio Facchetti, Tobin J. Marks, *Energy & Environmental Science*, 15, 645-659 (**2022**).
10. Unveiling Bridging Ligand Mediated Metal-Metal Interactions in Excited State Bimetallic Complexes, Michael W. Mara, Brian T. Phelan, Zhu-Lin Xie, Tae Wu Kim, Darren J. Hsu, Xiaolin Liu, Andrew J. S. Valentine, Pyosang Kim, Xiaosong Li, Shin-ichi Adachi, Tetsuo Katayama, Karen L. Mulfort, Lin X. Chen, *Chemical Science*, 13, 1715–1724 (**2022**).
11. Intersystem Crossings in Late-Row Elements: A Perspective, A. J. S. Valentine, X. Li, *J.*

Phys. Chem. Lett., 13, 3039–3046 (**2022**).

12. Long-Lived Excited State in a Solubilized Graphene Nanoribbon, M. C. Drummer, R. B. Weerasooriya, N. Gupta, B. T. Phelan, A. J. S. Valentine, A. A. Cordones, X. Li, L. X. Chen and K. D. Glusac, *J. Phys. Chem. C*, 126, 1946–1957 (**2022**).
13. Bimetallic Copper/Ruthenium/Osmium Complexes: Observation of Conformational Differences Between the Solution Phase and Solid State by Atomic Pair Distribution Function Analysis, Z.-L. Xie, X. Liu, A. J. S. Valentine, V. M. Lynch, D. M. Tiede, X. Li, K. L. Mulfort, Angew. Chem. Intl. Ed., 61, e202111764 (**2022**).
14. Excited State Charge Distribution of a Donor-π-Acceptor Zn Porphyrin Probed by N K-Edge Transient Absorption Spectroscopy, Amy A. Cordones, C. Das Pemmaraju, Jae Hyuk Lee, Ioannis Zegkinoglou, Maria-Eleni Ragoussi, Franz J. Himpsel, Gema de la Torre, Robert W. Schoenlein, *J. Phys. Chem. Lett.*, 12, 1182 (**2021**).
15. Revealing the three-dimensional orientation and interplay between plasmons and interband transitions for single gold bipyramids by photoluminescence excitation pattern imaging, Quan Liu, Dandan Ge, Frank Wackenhut, Caitlan D. Coplan, Charles Cherqui, Marc Brecht, Xiao-Min Lin, George C. Schatz, Richard D. Schaller, Pierre-Michel Adam, Renaud, Bachelot, Alfred J. Beixner, *J. Phys. Chem. C*, 125. 26978-85 (**2021**)
16. Source of bright near-infrared luminescence in gold nanoclusters, Qi Li, Charles J. Zeman, George C. Schatz, X. Wendy Gu, ACS Nano, 15, 16095-105 (**2021**).
17. General Design Rules for Bimetallic Platinum(II) Complexes, Alexis W. Mills, Andrew J. S. Valentine, Kevin Hoang, Subhangi Roy, Felix N. Castellano, Lin X. Chen, Xiaosong Li, *J. Phys. Chem*. *A*, 125, 9438−9449 (**2021**)
18. Excited-State Bond Contraction and Charge Migration in a Platinum Dimer Complex Characterized by X-Ray and Optical Transient Absorption Spectroscopy, Nicholas P. Weingartz, Michael W. Mara, Subhangi Roy, Jiyun Hong, Arnab Chakraborty, Samantha E. Brown-Xu, Brian T. Phelan, Felix F. Castellano, Lin X. Chen, *J. Phys. Chem. A*, 125, 8891−8898 (**2021**).
19. Ultrafast Excited-State Dynamics of Photoluminescent Pt(II) Dimers Probed by a Coherent Vibrational Wavepacket, Pyosang Kim, Andrew J. S. Valentine, Subhangi Roy, Alexis W. Mills, Arnab Chakraborty, Felix N. Castellano, Xiaosong Li, and Lin X. Chen, *J. Phys. Chem. Lett.* 12, 29, 6794–6803 **(2021).**
20. Anisotropic Transient Disordering of Colloidal, Two-Dimensional CdSe Nanoplatelets upon Optical Excitation, Alexandra Brumberg, Matthew S. Kirschner, Benjamin T. Diroll, Kali R. Williams, Nathan C. Flanders, Samantha M. Harvey, Ariel A. Leonard, Nicolas E. Watkins, Cunming Liu, Eli D. Kinigstein, Jin Yu, Austin M. Evans, Yuzi Liu, Shelby A. Cuthriell, Shobhana Panuganti, William R. Dichtel, Mercouri G. Kanatzidis, Michael R. Wasielewski, Xiaoyi Zhang, Lin X. Chen, Richard D. Schaller, *Nano Lett*. 21, 1288–1294 (**2021**)
21. Interplays of electron and nuclear motions along CO dissociation trajectory in myoglobin revealed by ultrafast X-rays and quantum dynamics calculations, Megan L. Shelby, Andrew Wildman, Dugan Hayes, Michael W. Mara, Patrick J. Lestrange, Marco Cammarata, Lodovico Balducci, Maxim Artamonov, Kelly A. Fransted, Henrik Lemke, Diling Zhu, Tamar

Seideman, Brian M. Hoffman, Xiaosong Li, Lin X. Chen, *Proc. Natl Acad. Sci. USA* 118, (**2021**).

22. Transient Lattice Response upon Photoexcitation in CuInSe2 Nanocrystals with Organic or Inorganic Surface Passivation, Samantha M. Harvey, Daniel W. Houck, Matthew S. Kirschner, Nathan C. Flanders, Alexandra Brumberg, Ariel A. Leonard, Nicolas E. Watkins, Lin X. Chen, William R. Dichtel, Xiaoyi Zhang, Brian A. Korgel, Michael R. Wasielewski, and Richard D. Schaller, *ACS Nano* 14, 13548 – 13556 (**2020**)
23. Photophysics of graphene quantum dot assemblies with axially coordinated cobaloxime catalysts, Varun Singh, Nikita Gupta, George Hargenrader, Erik Askins, Andrew Valentine, Gaurav Kumar, Michael Mara, Neeraj Agarwal, Xiaosong Li, Lin X. Chen, Amy Cordones, Ksenija Glusac*, J. Chem. Phys*. 153, 124903 (**2020**)
24. Two-photon excited deep-red and near-infrared emissive organic co-crystals, Yu Wang, Huang Wu, Penghao Li, Su Chen, Leighton O. Jones, Martin A. Mosquera, Long Zhang, Kang Cai, Hongliang Chen, Xiao-Yang Chen, Charlotte L. Stern, Michael R. Wasielewski, Mark A. Ratner, George C. Schatz, J. Fraser Stoddart, Nature Comm. 11, 4633 (**2020**).
25. Photophysical implications of ring fusion, linker length, and twisting angle in a series of perylenediimide-thienoacene dimers. Leonard, A. A.; Mosquera, M. A.; Jones, L. O.; Cai, Z.; Fauvell, T. J.; Kirschner, M. S.; Gosztola, D. J.; Schatz, G. C.; Schaller, R. D.; Yu, L.; Chen, L. X., *Chemical Science,*11, 7133-7143 (**2020**).
26. Phase control of coherent acoustic phonons in gold bipyramids for optical memory and manipulating plasmon-exciton coupling. Kirschner, M. S.; Lin, X.-M.; Chen, L. X.; Schaller, R. D., *Applied Physics Letters* 116, 153102 (**2020**).
27. Pressure-induced optical transitions in metal nanoclusters, Qi Li, Martin A. Mosquera, Leighton O. Jones, Abhinay Parakh, Jinson Chai, Rongchao Jin, George C. Schatz, X. Wendy Gu, ACS Nano, 14, 11888-11896 (**2020**)
28. Atom vacancies and electronic transmission Stark effects in boron nanoflake junctions, Leighton O. Jones, Martin A. Mosquera, George C. Schatz, Tobin J. Marks, Mark A. Ratner, J. Mat. Chem. C, 8, 15208-18 (**2020**).
29. Embedding methods for quantum chemistry: applications from materials to life sciences, Leighton O. Jones, Martin A. Mosquera, George C. Schatz, Mark A. Ratner, J. Am. Chem. Soc. 142, 3281-3295 (**2020**).
30. Domain separated density functional theory for reaction energy barriers and optical excitations, Martin A. Mosquera, Leighton O. Jones, Carlos H. Borca, Mark A. Ratner, George C. Schatz, J. Phys. Chem. A, 124, 5954-5962 (**2020**)
31. Orbital control and coherent charge transport in transition metal platinum(II)-Platinum(II) lantern complexes in molecular junctions, Leighton O. Jones, Martin A. Mosquera, Mark A. Ratner, George C. Schatz, J. Phys. Chem. C, 124, 3233-3241 (**2020**).
32. Control of charge carriers and band structure in 2D monolayer molybdenum disulfide via covalent functionalization, Leighton O. Jones, Martin A. Mosquera, Mark A. Ratner, George C. Schatz, Appl. Mat. Interfaces, 12, 4607-15 (**2020**).

33. Ab Initio Methods for L-edge X-ray Absorption Spectroscopy, J. M. Kasper, T. F. Stetina, A. J. Jenkins, X. Li, *Chemical Physics Reviews*, 1, 011304 (**2020**).

34. Real-Time Time-Dependent Electronic Structure Theory, X. Li, N. Govind, C. Isborn, A. E. DePrince and K. Lopata, *Chemical Reviews*, 120, 9951–9993 (**2020**).

35. Natural Transition Orbitals for Complex Two-Component Excited State Calculations, J. M. Kasper and X. Li, *J. Computational Chem*., 41, 1557–1563 (**2020**).

36. Exciton Coherence Length and Dynamics in Graphene Quantum Dot Assemblies, V. Singh, M. R. Zoric, G. N. Hargenrader, A. J. S. Valentine, O. Zivojinovic, D. R. Milic, X. Li, K. D. Glusac, *J. Phys. Chem. Lett*. 11, 210–216 (**2020**).

Theory-Guided Search for a Practical Singlet Fission Material

Eric A. Buchanan, Thomas F. Magnera, Zdenek Havlas, Alexandr Zaykov, Kateřina Fatková, and Josef Michl
Department of Chemistry
University of Colorado
Boulder, Colorado 80309

Among the desirable attributes of a practical singlet fission material, a triplet yield of 200% is the most difficult to meet. Up to now, most theory-based predictions of suitable structures only checked the ratio of S_0-S_1 and S_0-T_1 vertical excitation energies of an isolated molecule. Given the amount of effort usually required to synthesize a newly proposed material and to examine its photophysics properly, rate constants of singlet fission and competing processes need to be predicted, and this has been the focus of our efforts. We have generalized our SIMPLE program from a consideration of a molecular pair at a time to the simultaneous consideration of three molecules and this major effort is now nearly complete. We have used programs developed by N. Marom at Carnegie University to predict crystal structures of new materials, and we have worked with a colleague, Prof. J. Eaves, to develop procedures for estimating the rates of common competing processes. Our efforts were focused on sturdy indigoid materials and we are currently attempting to synthesize dicyanonorcibalackrot (**1** in Figure 1; we have already made **2**), expected to perform singlet fission up to two orders of magnitude faster than the parent cibalackrot, where the formation of charge-separated states and excimers dominates. Figure 2 compares the predicted structures of the critical molecular pairs in cibalackrot and in **1**.

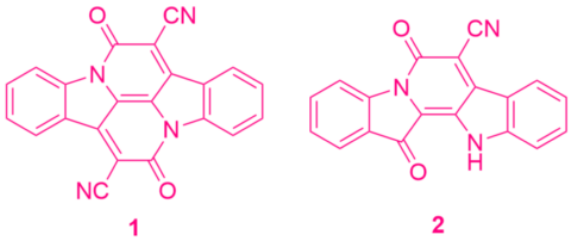

Figure 1. Structures of norcibalackrots

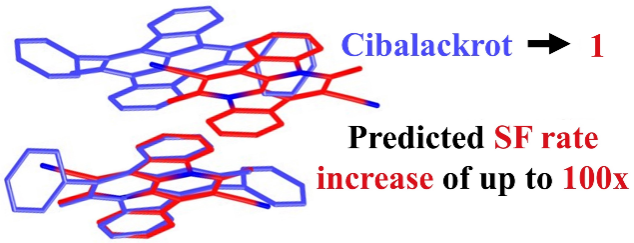

Figure 2. Predicted packing of **1** (red) relative to known packing of cibalckrot (blue).

Triplet Ion Pairs Interrupt Ion Recombination

Matthew J. Bird, Qin Wu and John R. Miller
Chemistry Division and Center for Functional Nanomaterials
Brookhaven National Laboratory
Upton, NY 11973

A principal aim of our research is fundamental understanding of electron transfer reactions for control of light-driven energy storage. Recent emphasis is on the role of electronic couplings and learning how to control those couplings. This poster explores the different but closely related subject of triplet ion pairs in which spin may inhibit exoergic back reactions to enhance energy storage. Ion pairs are produced by pulse radiolysis in o-xylene at Brookhaven's LEAF accelerator. High concentrations of a fluorene oligomer (F_1) rapidly captured holes and high concentrations of TCNE or benzoquinone (BQ) captured electrons. When BQ is the electron acceptor the decay profile in the Figure, starting from ions pairs separated over a range of distances follows transport-limited recombination, decaying as t^{-n}, n=~0.5. This highly non-exponential kinetics was predicted for diffusion-limited recombination in a Coulomb field. Theory predicts n=0.5 in the limit of long times for single ion pairs with a range of initial separation distances. In non-polar alkane liquids experiments of Tagawa confirmed t^{-n} decay, but with n near but not equal to 0.5; van den Ende measured and fit kinetics to find n closer to 0.6.

When TCNE is the electron acceptor the kinetics are dramatically different. Instead of diffusion-limited ion recombination the ion pairs $^3(D^+,A^{\bullet-})$, live much longer, ~1.9 µs.

A fit shown in Figure 1 finds t^{-n} kinetics with n=~0.54 for $F_1^{\bullet+}$ recombining with $BQ^{\bullet-}$. Nearly indistinguishable kinetics are seen for recombination of $F_1^{\bullet+}$ with $F_1^{\bullet-}$ although the anions, $F_1^{\bullet-}$ and $BQ^{\bullet-}$ are chemically very different and have energies different by 2.2 eV based on their reduction potentials (E_{red}= -3.08 for F_1 vs. -0.91 V).

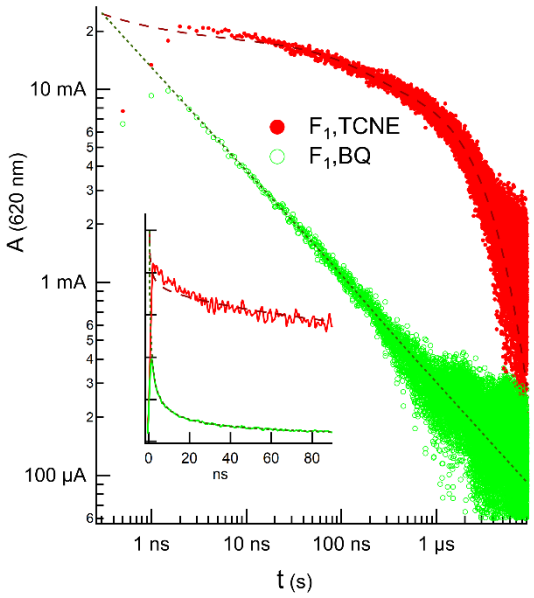

The poster will provide a partial explanation for the dramatic differences between long-lived triplet ion pairs and diffusion limited ion recombination using constrained DFT calculations. The experiments enable estimates of the yields of long-lived pairs yielding a tentative conclusion that spin-sorting may occur during ion recombination. Understanding how to control production of long-lived triplet pairs may open avenues to more efficiently convert light-produced ion pairs to stored energy.

Overall Water Splitting on Single Semiconductor Particles

Gaukhar Askarova,[1] Chengcan Xiao,[2] Mahdi Hesari,[1] Koushik Barman,[1]
Frank E. Osterloh,[2] and Michael V. Mirkin[1]

[1]Department of Chemistry and Biochemistry, Queens College-CUNY, Flushing, NY 11367
[2]Department of Chemistry, University of California Davis, CA 95616

This project is aimed at using nanoelectrochemical techniques in combination with mathematical modeling to measure photocatalytic activity and characterize heterogeneity of single semiconductor microcrystals. We employed photo-scanning electrochemical microscopy (photo-SECM) to quantitatively measure for the first time the kinetics of hydrogen and oxygen evolution reactions (OER and HER) at individual overall water-splitting (OWS) photocatalyst particles. Because the OWS at an unbiased microcrystal produces no net electric current, SECM is the only technique available for probing the intrinsic kinetics of both oxygen and hydrogen evolution reactions. A finite-element model was used to evaluate local O_2 and H_2 fluxes from photocurrent transients and photo-SECM approach curves (Fig. 1) and confirm stoichiometric H_2/O_2 evolution on a single Al-doped $SrTiO_3/Rh_{2-y}Cr_yO_3$ microcrystal with no observable lag during chopped illumination cycles.

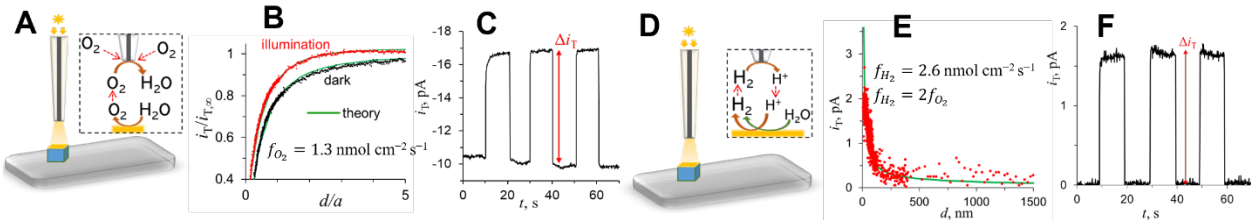

Fig. 1. Probing OWS at a single $Al/SrTiO_3/Rh_{2-y}Cr_yO_3$ microcrystal by photo-SECM. The SECM tip simultaneously served as a light guide to illuminate the photocatalyst particle and as an electrochemical nanoprobe. (A,D) Schematic representation of SECM detection of photogenerated O_2 (A) and H_2 (D). The fluxes of oxygen (B) and hydrogen (E) were evaluated from the fit of the experimental approach curves (symbols) to the theory (green solid curves). Chopped light current transients were used to measure local fluxes of O_2 (C) and H_2 (F) at the particle surface.

Using photo-SECM with a chemically modified nanotip, we visualized for the first time the OWS at a single bipyramidal microcrystal of phosphorus-doped $BiVO_4$. Particulate bismuth vanadate is a promising photoelectrocatalyst for visible-light-driven water oxidation, however, OWS has been difficult to attain because its conduction band is too positive for efficient hydrogen evolution. The obtained current patterns for both O_2 and H_2 agree well with the accumulation of photogenerated holes and electrons on {010} basal and {110} lateral facets, respectively. The developed experimental approach is an important step towards nanoelectrochemical mapping of the activity of photocatalyst particles at the sub-facet level.

In the future, we will carry out experiments with the single microcrystals attached to a conductive support to apply an external bias, measure the potential dependences of HER and OER kinetics independently and investigate the rate limiting step of the water splitting process.

Designing Proton Wires for Artificial Photosynthetic Systems

D. A. Heredia,[1] E. J. Gonzalez,[1] R. E. Dominguez,[1] E. A. Reyes,[1] K. Knappenberger,[1] S. Hammes-Schiffer,[2] G. R. Fleming,[3] G. F. Moore,[1] T. A. Moore,[1] and A. L. Moore[1]

[1] School of Molecular Sciences Arizona State University, Tempe, Arizona 85287-1604
[2] Department of Chemistry, Yale University, New Haven, Connecticut 06520-8107
[3] Department of Chemistry, University of California, Berkeley, California 94720

Inspired by the PCET process in photosystem II involving Tyr_z-His190, a polybenzimidazole phenol system has been used to illustrate an E*n*PT process involving one-electron oxidation of the phenol accompanied by translocation of *n* protons along the attached polybenzimidazole wire. This process is referred to as multi-PCET (MPCET).[1] The construct of Figure 1 illustrates a system that undergoes MPCET as demonstrated by IRSEC (spectroelectrochemistry in the IR). It features a high-potential porphyrin, which initiates the process by photochemically oxidizing the attached phenol linked to the Grotthuss-type proton wire based on three benzimidazole units. In addition to fully characterizing the dynamics of the E3PT process (with G. Fleming), the study of this system and the ones designed to undergo E1PT and E2PT processes[2-3] provide a better understanding of the thermodynamics of the processes, including the large solvent effect. The driving force for the PCET process was increased by ~ 400 mV in a dyad consisting of a porphyrin fluorinated at the *beta*-positions linked to a simple benzimidazole phenol (BIP). With this system, it should be possible to decrease the electronic coupling by including a spacer between the BIP and the *meso* phenyl group of the porphyrin and still observe a high yield of the photoinduced PCET process. We anticipate that the charge-separated species will have a longer lifetime in this new generation of PCET-based artificial photosynthetic reaction centers. Additionally, we are experimenting with PCET in proteins. In preparation for this, constructs consisting of a four-helix bundle enclosing an Mn-porphyrin (Mn(II)-Por) docked to a high potential bacterial reaction center (BRC) are being assembled. Exciting the BRC reversibly oxidizes Mn(II)-Por to Mn(III)-Por, demonstrating electron transfer between the BRC and the porphyrin in the four-helix bundle. This is a promising result for the development of hybrid artificial photosynthetic constructs in which energy-conserving processes could be reengineered and optimized.

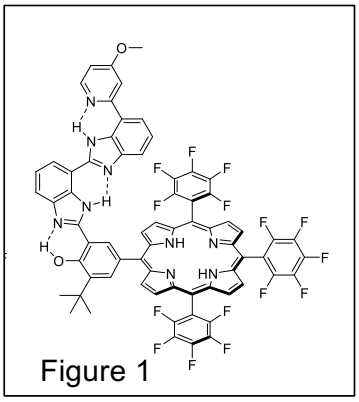
Figure 1

1. Odella, E.; Wadsworth, B. L.; Mora, S. J.; Goings, J. J.; Huynh, M. T.; Gust, D.; Moore, T. A.; Moore, G. F.; Hammes-Schiffer, S.; Moore, A. L., Proton-Coupled Electron Transfer Drives Long-Range Proton Translocation in Bioinspired Systems. *J. Am. Chem. Soc.* **2019,** *141* (36), 14057-14061.
2. Yoneda, Y.; Mora, S. J.; Shee, J.; Wadsworth, B. L.; Arsenault, E. A.; Hait, D.; Kodis, G.; Gust, D.; Moore, G. F.; Moore, A. L.; Head-Gordon, M.; Moore, T. A.; Fleming, G. R., Electron-Nuclear Dynamics Accompanying Proton-Coupled Electron Transfer. *J. Am. Chem. Soc.* **2021,** *143* (8), 3104-3112.
3. Arsenault, E. A.; Guerra, W. D.; Shee, J.; Reyes Cruz, E. A.; Yoneda, Y.; Wadsworth, B. L.; Odella, E.; Urrutia, M. N.; Kodis, G.; Moore, G. F.; Head-Gordon, M.; Moore, A. L.; Moore, T. A.; Fleming, G. R., Concerted Electron-Nuclear Motion in Proton-Coupled Electron Transfer-Driven Grotthuss-Type Proton Translocation. *J. Phys. Chem. Lett.* **2022,** *13* (20), 4479-4485.

Breaking an Iron Law in Electrocatalysis and Shedding More Light on Solar Photoelectrochemistry

D. Nishiori, E. A. Reyes Cruz, N. P. Nguyen, L. K. Hensleigh, and G. F. Moore
School of Molecular Sciences, The Biodesign Institute Center for Applied Structural Discovery
Arizona State University
Tempe, Arizona 85287

Scaling relationships governing tradeoffs between thermodynamic and kinetic metrics of performance can hamper the design of efficient electrocatalysts.[1] In this poster presentation, we showcase evidence for breaking a molecular scaling relationship[2] by using a binuclear iron porphyrin featuring extended electronic conjugation[3] (Fig. 1a). In addition to efforts involving homogeneous catalysis, we also report on heterogenized molecular materials immobilized at light-harvesting surfaces.[4] These assemblies enable studies of the interplay between light absorption, charge separation, and chemical catalysis. In particular, we highlight a formalism relating the turnover frequency (TOF) of immobilized catalysts to the external quantum efficiency (EQE), incident photon flux, electron stoichiometry of the catalyzed reaction (n), the per-geometric area loading of catalyst (Γ_{C_T}), and the Avogadro constant (N_A) (Fig. 1b).

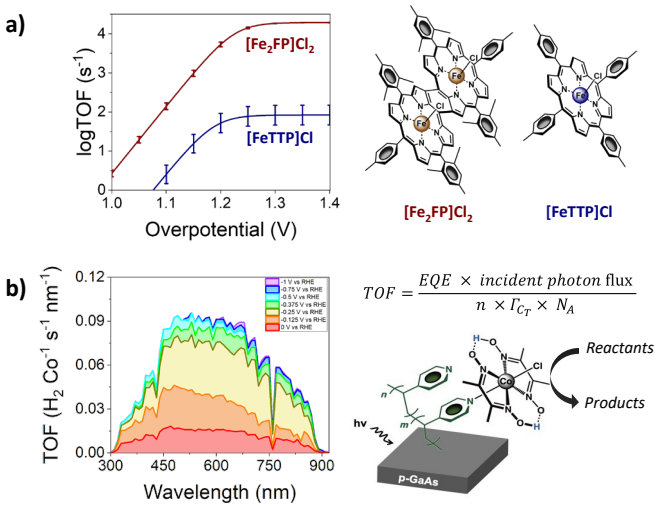

Figure 1. (a) Catalytic Tafel plots recorded using a binuclear fused iron porphyrin ([Fe_2FP]Cl_2, red) or a monomeric iron porphyrin ([FeTTP]Cl, blue) for oxygen reduction catalysis. (b) Spectral-resolved turnover frequencies collected at varying bias potentials using 1-sun illumination and a cobaloxime-polypyridyl-modified GaAs working electrode.

References

1. Reyes Cruz, E. A.; Nishiori, D.; Wadsworth, B. L.; Nguyen, N. P.; Hensleigh, L. K.; Khusnutdinova, D.; Beiler, A. M.; Moore, G. F. **Molecular-Modified Photocathodes for Applications in Artificial Photosynthesis and Solar-to-Fuel Technologies**. *Chem. Rev*. **2022**, *122*, 16051–16109.

2. Nishiori, D.; Reyes Cruz, E. A.; Moore, G. F. **Breaking an Iron Law in Electrocatalysis**. *under review*.

3. Reyes Cruz, E. A.; Nishiori, D.; Wadsworth, B. L.; Khusnutdinova, D.; Karcher, T.; Landrot, G.; Lassalle-Kaiser, B.; Moore, G. F. **Six-Electron Chemistry of a Binuclear Fe(III) Fused Porphyrin**. *ChemElectroChem* **2021**, *8*, 3614–3620.

4. Nguyen, N. P.; Wadsworth, B. L.; Nishiori, D.; Reyes Cruz, E. A.; Moore, G. F. **Understanding and Controlling the Performance-Limiting Steps of Catalysts-Modified Semiconductors**. *J. Phys. Chem. Lett*. **2021**, *12*, 199–203.

Time-resolved Studies of Metal Organic Framework Self-Healing after Photo-Promoted Ligand Dissociation

Qingyu Ye, Daniel Cairnie, and Amanda J. Morris
Department of Chemistry
Virginia Tech
Blacksburg, VA 24060

The observation of structural rearrangement upon charge separation, reduction or oxidation, and catalysis within molecules is well-known. From the classic example of the transition of an iron porphyrin from a puckered to planar arrangement as it is reduced from the Fe(III) to the Fe(II) oxidation state to the photodissociation of metal-halide bonds in rhodium dimers, these events are critical in understanding the mechanism by which those catalysts promote desired chemistry. By exploiting MIL-101(Fe) as a model MOF platform, we have recently unveiled the self-healing photodynamic nature of the MOF structure. The excited state in MIL-101(Fe) was studied via time-resolved infrared (TRIR) spectroscopy. By probing the vibrational fingerprints of the carboxylate bonds upon photoexcitation, a transient change of the carboxylate-Fe bonding configuration was observed, namely, a shift from bidentate bridging coordination to monodentate counterpart. We observed clear ground state bleaches (1400 cm^{-1} and 1590 cm^{-1}), corresponding to the major ground state IR absorption peaks. Meanwhile, excited-state absorption peaks were observed at 1360 cm^{-1} and 1710 cm^{-1}, suggesting the formation of monodentate coordination mode. Over 40 ± 1 μs, the Fe-O bond reforms to regenerate the ground state MOF configuration. Interestingly, the visible time-resolved absorption investigation recorded a broad excited state absorption from 400-700 nm, previously attributed to the transient generation of Fe(II) states, which decayed with a similar lifetime. However, the same broad feature observed for isolated Fe-oxo clusters decayed on the ultrafast time scale. The significantly extended lifetime of the Fe-oxo excited state in MIL-101(Fe) compared to isolated clusters coupled to the similarity in the decay lifetimes of the vibrational and visible transients suggests the LMCT event, where an electron is injected from the carboxylate to the Fe-oxo cluster, results in a bond-breakage event and only upon reformation of that bond can the charge recombine to regenerate the ground state. Compared to the irreversible photo-deligation events in traditional photocatalysis, the observed reversible photodynamic phenomenon could potentially point out a key merit of MOFs and provide new pathways to promote efficient photocatalysis – the generation of charge-separated states with extended lifetimes that resist common degradation pathways and self-heal.

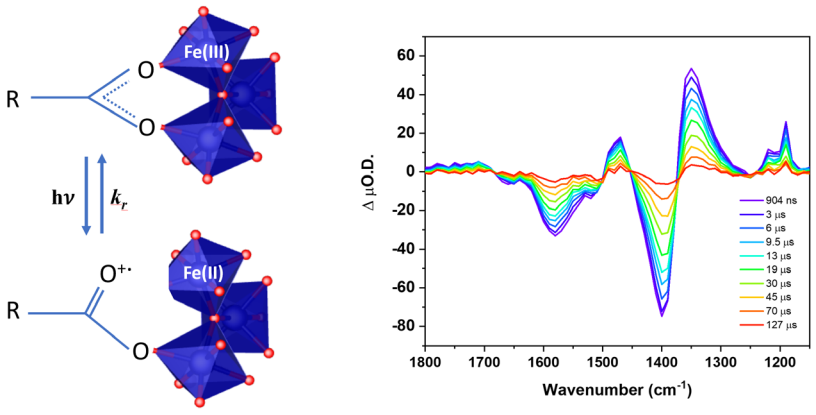

Figure. After photoexcitation, the coordination mode between the carboxylate and Fe-oxo within MIL-101(Fe) switches from bidentate bridging to monodentate configuration as probed by time-resolved infra-red spectroscopy.

Silicon Nanocrystal-Rhenium Complex CO_2 Reduction Photocatalyst Hybrids

Simran S. Saund and Nathan R. Neale
Chemistry and Nanoscience Center
National Renewable Energy Laboratory
Golden, CO 80401

Direct coupling of light-harvesting semiconductors and molecular catalysts is an attractive approach in designing new systems for artificial photosynthesis that could enable cooperativity not possible with either system alone. Toward these ends, we have tethered a Lehn-type rhenium carbonyl coordination complex to dodecyl-terminated silicon nanocrystals (Si NCs) using a two-step surface functionalization process as shown in **Figure 1**. Diffuse reflectance infrared Fourier transform spectroscopy and cyclic voltammetry are used to characterize successful surface attachment and redox properties of the hybrid structure. UV-visible spectroelectrochemical measurements confirm the formation of a Re(0) reduction product in thin films of the hybrid assembly under cathodic potentials. During reduction, only electrochemical and spectroscopic features associated with monomer are observed (**Figure 2**), not the Re–Re dimer, suggesting that the hybrid structure prevents a common deactivation pathway for Lehn-type CO_2 reduction catalysts.

We present initial results of CO_2 photoreduction to CO using the solution-phase Si NC-Re complex hybrid photocatalyst in the presence of a sacrificial electron donor.

Additionally, we use density functional theory (DFT) to show that there is an energetic coupling between the Si NC and the Re complex, consistent with our prior work tuning the photophysics of Si NCs by coupling to covalently bound organic ligands. The DFT model predicts alignment of the Si conduction band above the Re(0) complex LUMO for small Si clusters. When extended to larger diameter (smaller bandgap) Si NCs, photoexcitation into states high in the conduction band likely is required to enable sufficient energy for charge transfer.

Finally, we will describe our early efforts to use boron-doped B:Si NCs in similar photocatalyst hybrid schemes and compare these to those with intrinsic Si NCs.

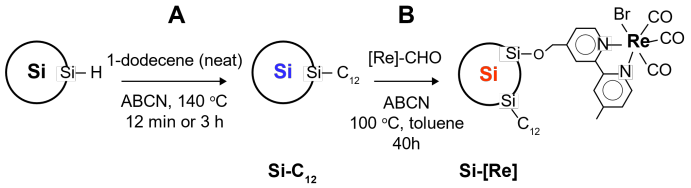

Figure 1. Synthetic scheme for Si-C_{12} (A, 3 h reaction) and Si-[Re] (A, 12 min reaction time, then B, 40 h reaction time).

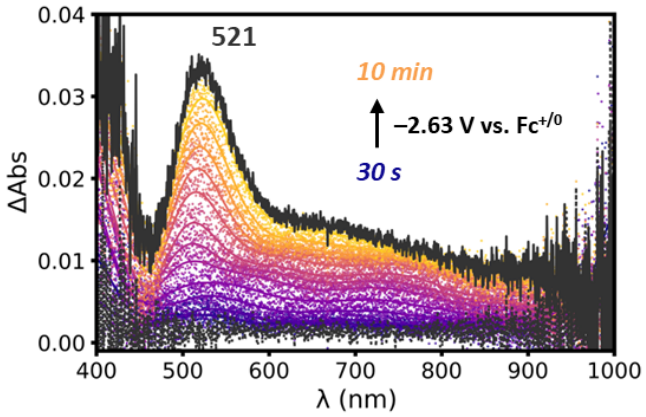

Figure 2. Electronic difference spectra of a Si-[Re] NC film on an ITO-coated glass slide submerged in CH_3CN with 100 mM $TBAPF_6$ as supporting electrolyte taken before (black dotted trace), during (blue to yellow symbols, for clarity Savitzky-Golay smoothed representations of the raw data are included) and after (black solid trace) electrolysis at –2.63 V vs. $Fc^{+/0}$.

Charge Separation and Catalysis Studied with Advanced EPR Spectroscopy

Jens Niklas,[1] Oleg G. Poluektov,[1] Kristy L. Mardis,[2] David M. Tiede,[1] Karen L. Mulfort[1]
[1]Chemical Sciences and Engineering Division, Argonne National Laboratory, Lemont, IL 60439
[2]Department of Chemistry, Physics and Engineering Studies, Chicago State University, Chicago, IL 60628

The goal of our research is to resolve fundamental mechanisms of photochemical energy conversion and to use this information for solar fuels production. We study light-induced charge separation in a variety of organic and inorganic systems, including organic and hybrid organic-inorganic donor-acceptor systems, as well as transition metal solar fuels catalysts.

Electron Paramagnetic Resonance (EPR) is a powerful spectroscopic technique which can provide deep insight into the electronic structure, kinetics, and spin dynamics of systems containing unpaired electrons. Conventional continuous wave X-band EPR spectroscopy is rarely sufficient to fully characterize the system. Hence, we use a multi-frequency approach employing X-band (9 GHz), Q-band (34 GHz), and high-frequency D-band (130 GHz), and combine that with advanced pulse and multi-resonance techniques like Electron-Nuclear-Double-Resonance (ENDOR). This allows us to determine magnetic resonance parameters, but they typically do not provide a clear chemical picture of the system. To resolve geometry and electronic structure we supplement the measurements with computational approaches, *e.g.* DFT calculations. In addition, the comparison of experimentally determined and calculated magnetic resonance parameters can serve as a validation for the computational results.

In organic donor-acceptor systems using semiconducting polymers as donors the application of EPR/ENDOR spectroscopy and DFT has revealed that the positive polaron on the polymer is delocalized, which is an important reason for the efficient charge separation as it minimizes the wasteful process of charge recombination. Furthermore, the combination of pulsed light excitation with time-resolved EPR spectroscopy provided information about charge separation kinetics and spin dynamics of spin-correlated radical pairs in different donor-acceptor systems, and showed that the neutral triplet exciton can be substantially more delocalized than the positive polaron.

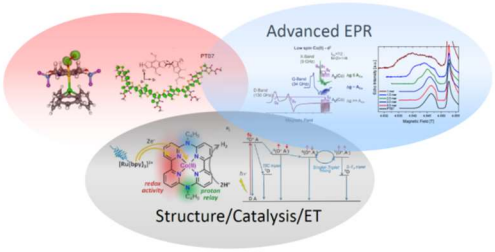

Advanced multi-frequency EPR combined with DFT applied to Charge Separation and Catalysis

We have carried out a systematic study of molecular cobalt catalysts that are active for aqueous H_2 evolution and CO_2 reduction. We expect that the catalyst's microenvironment is very important for efficient catalysis and selectivity, but it is challenging to quantitatively characterize. While direct ligands to the cobalt ion can often be studied by simple EPR techniques, characterizing the environment beyond requires more advanced techniques and can provide valuable information about proton transfer in the second coordination sphere and beyond. ENDOR spectroscopy results will be presented that help us understand the solvation and key intermediates of the Co(II) catalysts, and we will use the knowledge gained to design next generation catalysts with outer coordination sphere components tailored to further understand their impact on catalytic function.

Spin Dynamics in Photochemistry and Catalysis

Oleg G. Poluektov,[1] Jens Niklas,[1] Mandefro Teferi,[1] Ryan G. Hadt,[2] Theodor Agapie,[2] Jacob Olshansky,[3] and Matthew Y. Sfeir[4]

[1]Chemical Sciences and Engineering Division, Argonne National Laboratory, Lemont, IL 60439

[2]Division of Chemistry and Chemical Engineering, California Institute of Technology Pasadena, CA 91125

[3]Department of Chemistry, Amherst College, Amherst, MA 01002

[4]Department of Physics, City University of New York, New York, NY 10016

Most photochemical reactions involve unpaired electron spins and, as a consequence, demonstrate pronounced magnetic field effects. The yield of these photochemical reactions, such as charge separation, charge recombination, intersystem crossing (ISC), singlet fission (SF), and spin catalysis, strongly depends on spin dynamics. The goal of our solar energy conversion research is to resolve fundamental mechanisms for spin dynamics control of photochemistry and catalysis. To achieve this goal, we focus on the two photochemical systems: surface modified inorganic nanoparticles which demonstrate spin-correlated radical pair (SCRP) phenomena and organic molecular constructs with strong SF signature due to spin dynamics within spin-correlated triplet pairs.

While photochemical charge separation in organic donor-acceptor systems leads to the well-known formation of SCRP, much less is known about spin dynamics of RPs in charge separated states for inorganic photocatalytic systems, such as surface-modified nanoclusters composed of transition metals and transition metal oxides. Previously we reported SCRP phenomenon in TiO_2 nanoparticles with dopamine surface modification. Here we focus on ZnO quantum dots connected/doped/linked with organic dye molecules. These two types of nanoparticles, ZnO and TiO_2, are fundamentally important as model systems for photocatalysis. Nontrivial time-resolved EPR spectra observed in ZnO quantum dots systems were explained by complex spin dynamics within SCRP. It was demonstrated that observed SCRP spin dynamics depend upon type of organic dye, size of quantum dots, and length of the connecting bridge.

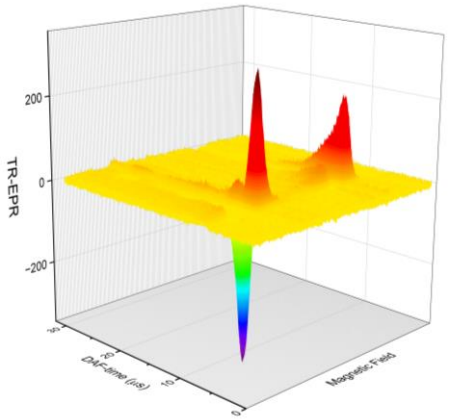

Complex spin dynamic in SCRP of perylene surface-modified 5nm ZnO quantum dots reveals in nontrivial time-resolved EPR 2-D spectra.

Singlet Fission is a photophysical process in which singlet exciton generated by light absorption of a ground state molecule interacts with a neighboring molecule in ground state. This interaction can create a correlated triplet pair in singlet state ^{1}(TT), which is under certain conditions converted by coherent spin-mixing to the quintet state ^{5}(TT), potentially followed by decay to two independent triplets. Generation of two excitons from one photon (multiple exciton generation) allows to substantially increase the efficiency of solar energy conversion. One important question is how the generation of the correlated triplet pair and, therefore, the efficiency of SF can be improved. Here we report on spin dynamics study of three recently developed dipyridyl pyrrole bipentacenes which demonstrate structure dependent efficiency of SF, ISC, and decay of the strongly coupled triplet pair to two weakly coupled triplets.

Controlling Redox Properties of Organic Radical Cations through Combined Effects of Ion Pairing, Hemicolligation and Conjugation.

Dmitry E. Polyansky, Gerald F. Manbeck, Mehmed Z. Ertem
Chemistry Division, Energy & Photon Sciences Directorate
Brookhaven National Laboratory
Upton, NY 11973-5000

The properties of strongly oxidizing radicals in organic media are important for understanding charge transport in organic solar cells, mechanistic studies of electron transfer in solutions, and probing chemical transformations in nuclear fuel processing. However, investigation of such reactive species is challenging due to their transient nature and, in some cases, limited availability of methods for their generation. Conventional electrochemical techniques, such as cyclic or pulsed voltammetry can only yield approximate values of reduction potentials of highly oxidizing radicals due to irreversibility of electron transfer. This irreversibility often arises from a fast chemical reaction which follows the electron transfer.

We have developed a redox equilibrium ladder approach for accurate measurements of reduction potentials of reactive organic radicals generated by pulse radiolysis (PR) in 1,2-dichloroethane (DCE) in a wide potential range. First, we have verified the accuracy of this method using a series of organic compounds which exhibit reversible electrochemical behavior. The values of potentials determined from PR show very good agreement with the values from direct electrochemical measurements spanning the range of about 300 mV and thus demonstrating the validity of chosen approach. Next, we have turned into more systematic analysis of reduction potentials within a homologous series of substituted biphenyl derivatives. The plot of $E_{1/2}$ as a function of Hammett sigma (σ_p) is shown in Figure 1 and surprisingly demonstrates a saturation at high sigma values. Interestingly, inclusion of a chloride anion as an ion pair partner results in a good match between predicted and calculated potentials. We interpret our experimental and theoretical findings in terms of cooperative effects of ion pairing and hemicolligation between biphenyl radical cation and chloride anion with the latter being a product of DCE radiolysis. This reactivity provides new insights into redox properties of strong oxidants in complex ionic environments and can be used for fine-tuning potentials of these oxidants. Our future work is focused on realizing redox ladder approach for other classes of organic radicals and solvent systems as well as using these radicals for studying electron transfer processes.

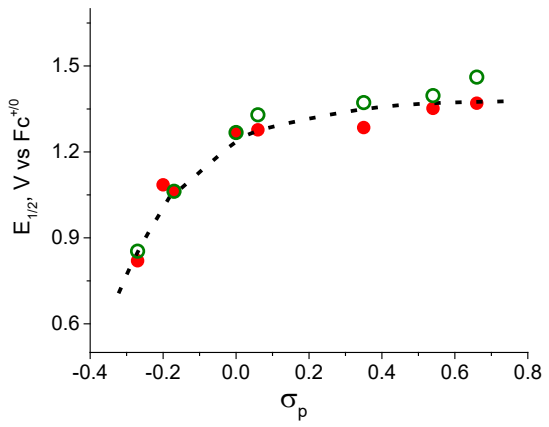

Figure 1. Reduction potentials of 4,4′-substituted biphenyl cations determined by PR (red circles) and potentials of [BP…Cl]• complexes predicted by DFT calculations (green circles) in DCE solvent. Dotted lines are only for visual guidance.

Ab Initio Quantum Dynamics of Charge Carriers in Advanced Solar Materials

Oleg Prezhdo
Department of Chemistry
University of Southern California
Los Angeles, CA 90089

Our group develops methods for modeling excited state dynamics in nanoscale, molecular and condensed phase materials, and applies them to study photoinduced processes in diverse and modern systems for solar energy harvesting, as exemplified in the figures below.

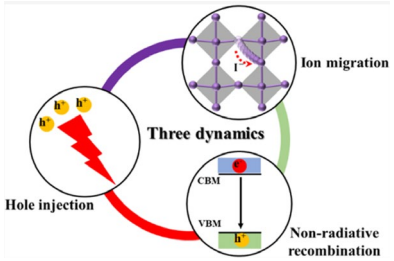

Figure 1. Ion migration, hole trapping, and charge loss are coupled closely in metal halide perovskites. Holes accelerate ion migration by decreasing diffusion barrier. It also promotes charge recombination by increasing electron-phonon interactions. The synergy stems from the soft perovskite lattice. Thus, high concentration of holes should be avoided. [*JACS* **144**, 6604 (2022)].

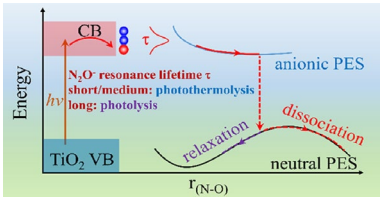

Figure 2. Even a transient injection of photogenerated charges into adsorbed molecules can initiate bond breaking in semiconductor and plasmonic photocatalysis. The chemistry is activated by a combination of excited state evolution and local heating. The contributions of photolysis and photothermolysis, and their efficiencies depend on resonance lifetime and catalytic interfacial interaction. [*JACS* **145**, 476 (2022)].

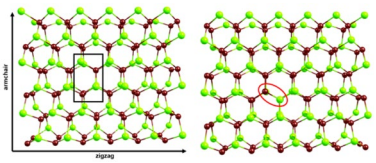

Figure 3. Following a recent synthesis of layered γ-phosphorus carbide, we predict and characterize a stable monolayer. High and anisotropic charge mobility of pristine material can be strongly influenced by common defects. At low concentrations, defects trap charges and inhibit mobility. At high concentrations, defects change carrier effective masses and can both increase and decrease mobility. We predict defect Raman and IR signatures [*JPCL* **14**, 214 (2023)].

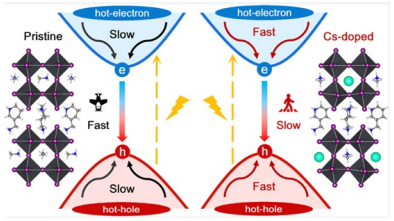

Figure 4. Spontaneous symmetry breaking in organic and mixed organic-inorganic 2D metal halide perovskites drives rapid interlayer charge separation and extends charge carrier lifetime. It occurs due to thermal fluctuations and slight structural inhomogeneity. Doping enhances the effect and provides composition-structure-dynamics-function relationships to tailor optoelectronic properties of layered perovskites [*JACS* **145**, 5297 (2023)].

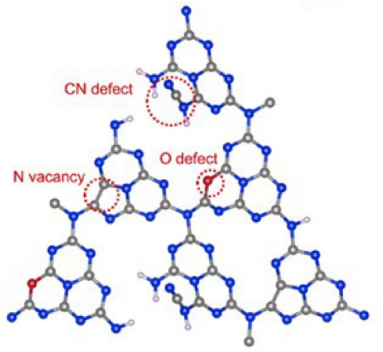

Figure 5. Metal-free graphitic carbon nitride is an excellent and benign photocatalyst for water splitting and many other reactions. We rationalize how defect engineering, realizable experimentally, can improve both oxidation potential and carrier lifetime. [*JPCL*, **13**, 1033 (2022)].

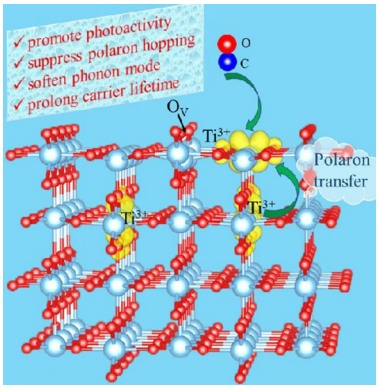

Figure 6. TiO_2 electron polarons enhance CO adsorption, while CO attracts electron polarons to the surface, decoupling them from holes and enhancing charge lifetime. CO adsorbs one atom away from electron polaron. [*JACS Au*, **2**, 234 (2022)].

Photoelectron Spectroscopy of Interfacial Oxides

Xueqiang Zhang[1,2], Bo-An Chen[1,2], Andrew J. E. Rowberg[3], Brandon C. Wood[3], Tuan Anh Pham[3], Tadashi Ogitsu[3], Sylwia Ptasinska[1,4]

[1]Radiation Laboratory, University of Notre Dame, Notre Dame, IN 46556
[2]Department of Chemistry and Biochemistry, University of Notre Dame, Notre Dame, IN 46556
[3]Quantum Simulations Group and Laboratory for Energy Applications for the Future (LEAF), Lawrence Livermore National Laboratory, Livermore, CA 94550
[4]Department of Physics and Astronomy, University of Notre Dame, Notre Dame, IN 46556

There are several key features of interfacial oxides that need to be characterized such as electronic, molecular, and geometric structures, which depend on solvent and electrolyte interacting with a material. Our approach focuses on providing a level of molecular detail on local chemical and electronic structures under the aspect of in situ and operando conditions. Advanced in situ X-ray and UV photoemission spectroscopies (XPS and UPS) at Notre Dame Radiation Laboratory facilities and DOE computing centers (in collaboration with LLNL), offer a symbiotic relationship between experimental photoemission measurements and high-level first principles methods to obtain valuable insights into the kinetics and dynamics of chemical processes at the semiconductor/electrolyte interfaces. The integration of ab initio simulation with XPS was successfully utilized and demonstrated in our previous works in which we provided a description of interfacial processes, particularly oxidation at the interface of III-V semiconductors with water and oxygen molecules. In our recent work, we probed several important chemical motifs formed during oxidation of GaP(111) surfaces and obtained their reaction kinetics [1]. We identified two distinct experimental conditions that correspond to kinetically and thermodynamically controlled oxidation. At low temperature conditions, surface exposure to O_2 produces kinetically facile Ga-O-Ga configurations. Whereas at higher temperatures, we observed thermodynamically driven transformation in which oxygen to insert into Ga-P bonds as part of a thermodynamically driven transformation into a complex, heterogeneous 3D network of surface PO_x ($1 \leq x \leq 4$) groups and Ga_2O_3 species, the latter of which eventually dominates upon depletion of surface phosphorus (Fig. 1).

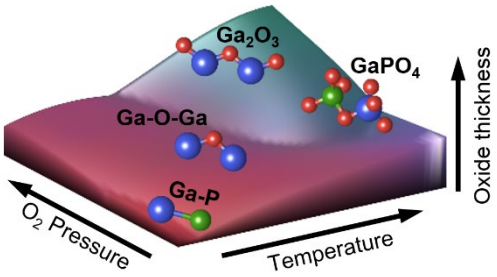

Fig. 1. Schematic illustration of interfacial oxide formation on GaP (111) at different experimental conditions.

Currently, we advanced our experimental and theoretical capabilities to obtain a realistic and reliable description of the chemistry of complex interfaces with a particular focus on 2D materials doped with heteroatoms/molecules or decorated with metallic nanostructures. Some preliminary results on photoelectron spectroscopy of 2D materials will be reported at the meeting.

[1] X. Zhang, B.C. Wood, A.J.E. Rowberg, T.A. Pham, T. Ogitsu, J. Kapaldo, S. Ptasinska, Journal of Power Sources, 560 (2023) 232663.

Energy level alignment and hot-carrier extraction in monolayer MoS_2 photoelectrodes

Rachelle Austin, Michael Van Erdewyk, Justin Toole, Rafael Almaraz, Thomas Sayer, Yusef Farah, Amber Krummel, Andrés Montoya Castillo, Justin B. Sambur*
*Department of Chemistry, Colorado State University, Fort Collins, CO, 80525

Hot carrier-based energy conversion systems could double the efficiency of conventional solar energy technology or drive photochemical reactions that would not be possible using fully thermalized, "cool" carriers, but current strategies require expensive multi-junction architectures. Using an unprecedented combination of photoelectrochemical and in situ transient absorption spectroscopy measurements (Figure 1), our group demonstrated ultrafast (<50 fs) hot exciton and free carrier extraction under applied bias in a proof-of-concept photoelectrochemical solar cell made from earth-abundant and potentially inexpensive monolayer (ML) MoS_2.[1] Our approach facilitates ultrathin 7 Å charge transport distances over 1 cm^2 areas by intimately coupling ML-MoS_2 to an electron-selective solid contact and a hole-selective electrolyte contact. Theoretical investigations of the spatial distribution of exciton states suggest greater electronic coupling between hot exciton states located on peripheral S atoms and neighboring contacts likely facilitates ultrafast charge transfer. Our work delineates future 2D semiconductor design strategies for practical implementation in ultrathin photovoltaic and solar fuels applications.

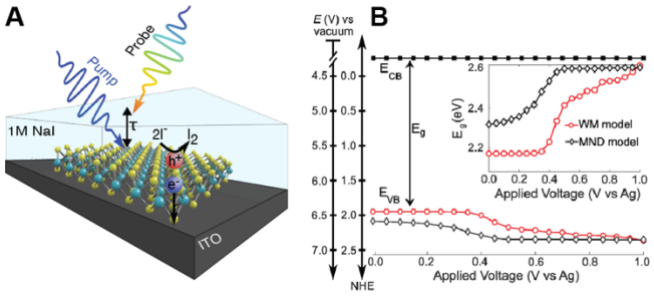

Figure 1. (A) Cartoon illustration of the three-electrode photoelectrochemical cell. **(B)** Band energy diagram of a ML-MoS_2 electrode as a function of applied potential.

Boosting the energy efficiency of hot carrier-based photoelectrochemical cells requires maximizing the hot carrier extraction rate relative to the cooling rate. One could expect to tune the hot carrier extraction rate constant (k_{ET}) via a Marcus-Gerischer relationship, where k_{ET} depends exponentially on $\Delta G^{0'}$ (the standard driving force for interfacial electron transfer). $\Delta G^{0'}$ is defined as the energy level difference between a semiconductor's conduction/valence band (CB/VB) minima/maxima and the redox potential of reactant molecules in solution. A major challenge in the electrochemistry community is that conventional approaches to quantify $\Delta G^{0'}$ for bulk semiconductors (e.g., Mott-Schottky measurements) cannot be directly applied to ultrathin 2D electrodes. The specific problem is that enormous electronic bandgap changes (>0.5 eV) and CB/VB edge movement take place upon illuminating or applying a potential to a 2D semiconductor electrode. We have developed an *in situ* absorbance spectroscopy approach to quantify interfacial energetics of 2D semiconductor/electrolyte interfaces using a minimal many-body model (Figure 1B). Our results show that band edge movement in monolayer MoS_2 is significant (0.2-0.5 eV) over a narrow range of applied potentials (0.2-0.3 V). Such large band edge shifts could change k_{ET} by a factor of 10-100, which has important consequences for practical solar energy conversion applications. We discuss the current experimental and theoretical knowledge gaps that must be addressed to minimize the error in the proposed optical approach.

Reference: (1) Austin, R.; Farah, Y. R.; Sayer, T.; Luther, B. M.; Montoya-Castillo, A.; Krummel, A. T.; Sambur, J. B. Hot Carrier Extraction from 2D Semiconductor Photoelectrodes. *PNAS* **2023**, *120* (15), e2220333120.

Models to Understand Quantum Superpositions of ESIPT Reactions

Alfy Benny and Gregory D. Scholes
Department of Chemistry
Princeton University
Princeton, NJ 08544

In recent work, we have been investigating experiments that show how a molecular exciton state can launch two a superposition of two chemical reactions. Specifically, we studied femtosecond proton transfer in a symmetric molecule with two identical reactant sites that are spatially apart (pigment yellow 101, PY101). PY101 comprises a chromophore pair, where each chromophore can undergo excited state intramolecular proton transfer (ESIPT). For this molecule, only a single ESIPT reaction happens after photo-excitation; the proton is transferred on either the left or the right side of the molecule. With this reaction launched from a superposition of two local basis states, our experimental data suggest that the nuclear wavepackets evolve in lock-step as a superposition of probability amplitudes until decoherence collapses the system to a product. The work indicates that in this, and related, experimental designs, the transition from quantum to classical dynamics can be studied.

A key step to move forward in our understanding is to better elucidate details of the reaction dynamics and mechanism. This will allow us to interpret more clearly the isotope effects, that provide the main evidence for our conclusions. The poster will report advances in our models for coupled ESIPT reactions.

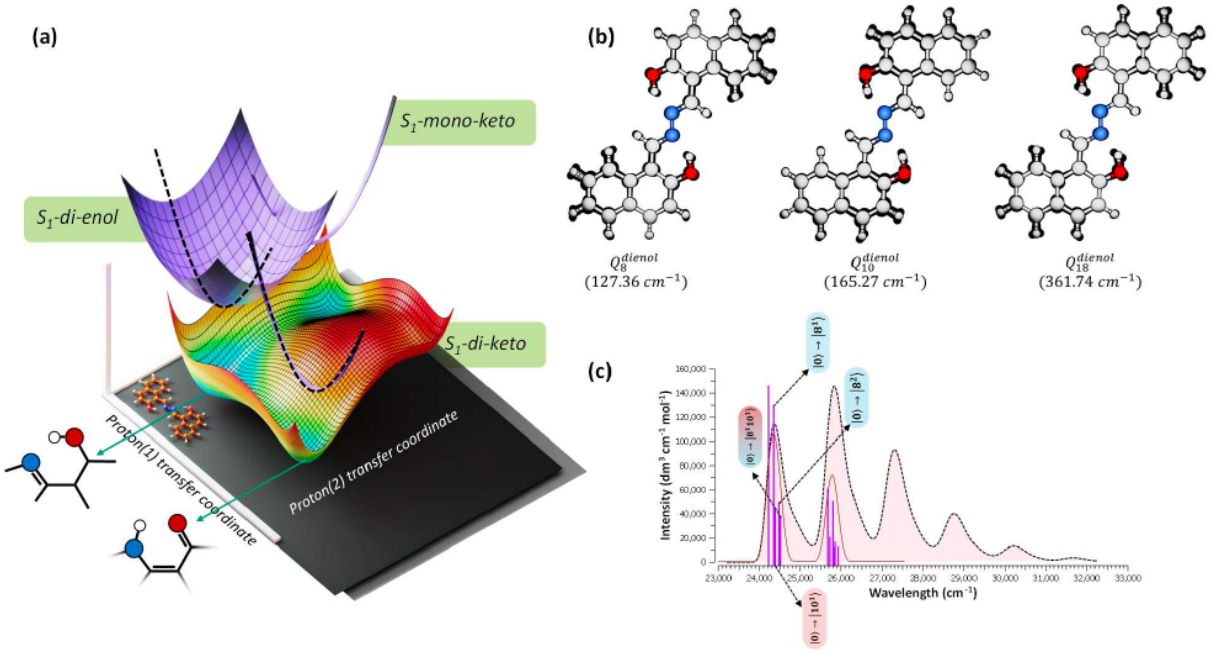

Figure: (a) The calculated S1 potential energy surface of PY101. (b) In-plane vibrational modes in PY101 that involve a change in N-O separation. (c) Computed vibronic absorption spectrum. The pink lines highlight the Franck-Condon active modes.

Modulating Integrated Multielectron Processes with Singlet Fission Chromophores

Matthew Y. Sfeir,[1,2] Luis M. Campos,[3] Kaia Parenti,[3] Guiying He,[1,2] Huaxi Huang,[3] Peter Budden,[1,2] Bernardo Salcido-Santacruz,[2,4] Daniel Malinowski[3]
[1]Department of Physics, Graduate Center, City University of New York, New York, NY 10016
[2]Photonics Initiative, Advanced Science Research Center, City University of New York, New York, NY 10031
[3]Department of Chemistry, Columbia University, New York, New York 10027
[4]Department of Chemistry, Graduate Center, City University of New York, New York, NY 10016

Singlet fission is commonly defined as the generation of two triplet excitons from a single absorbed photon. Singlet fission is frequently depicted as sequential two-step conversion in which a bound biexciton (triplet pair) state dissociates into two "free" triplet excitons. However, this model discounts the potential for direct harvesting from the coupled biexciton state. Here we present recent findings on the design of SF frameworks that promote the direct use of triplet pair states.

The grand goal is to develop next-generation systems that activate *multielectron chemical transformations near the multiexciton generation site*, avoiding loss-prone transport processes. This approach is only possible using a strategy that integrates SF chromophores with *active chemical bridges*. The bridge serves a dual role in mediating the electronic and spin coupling between SF chromophores to optimize multiexcitons for energy harvesting or as a substrate to turn triplet pairs into chemical potential. We will introduce current results supporting the hypothesis of the project. We have found how quantum interference principles control the nature and lifetime of triplet pair states. Additionally, we demonstrate how individual triplet excitons can be extracted directly from a bound biexciton pair prior to triplet pair dissociation. We are now merging these concepts to understand the design principles for development of photochemically active chemical bridges.

Key collaborators: Alex Miller (UNC); Oleg Poluektov, Jens Niklas (ANL); Ming Lee Tang (Utah); Renee Frontiera (UMN)

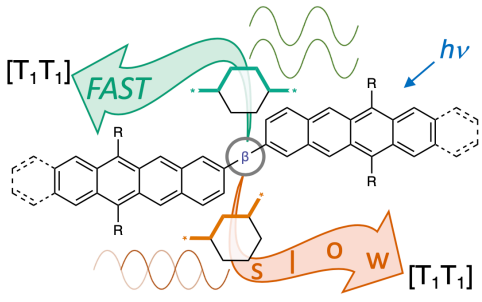

Figure 1. Molecular design to modulate integrated multielectron processes.

Optical Generation and Manipulation of Spin Qubits

Martin L. Kirk,[1] David A. Shultz,[2] Patrick Hewitt,[2] Anil Reddy Marri, [2] Vivek Mishra,[2] Shiyue Gao,[1] Ranjana Dangi,[1] Ju Chen,[1] and Art van der Est[3]
[1]Department of Chemistry and Chemical Biology, University of New Mexico, MSC03 2060, 1 University of New Mexico, Albuquerque, NM 87131
[2]Department of Chemistry, North Carolina State University, P.O. Box 8204, Raleigh, NC 27695
[3]Department of Chemistry, Brock University, 1812 Sir Isaac Brock Way, St. Catharines, ON, Canada L2S 3A1

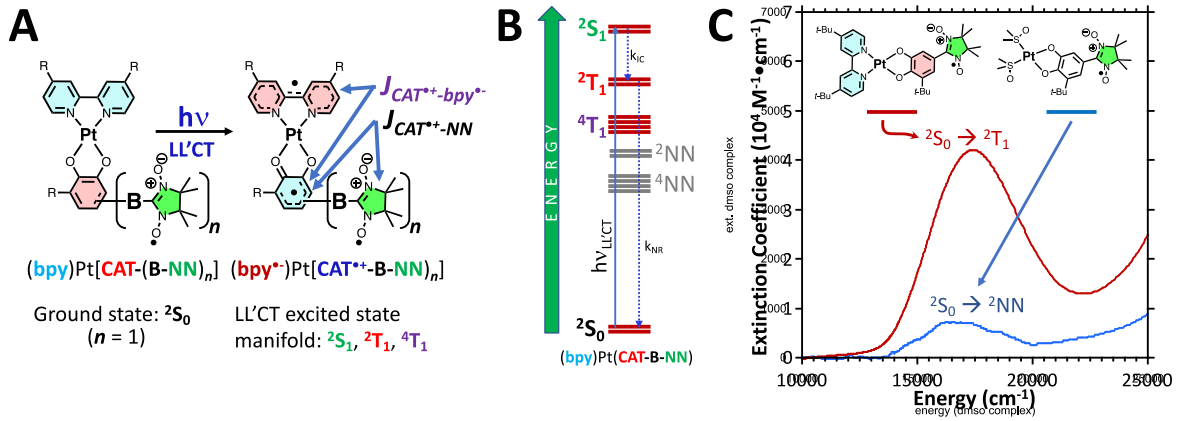

Figure 1. **A:** Structure of radical-appended LL'CT complexes. **B:** Jablonski diagram including ground-state, 3-spin LL'CT excited state, and radical-localized manifolds. **C:** Absorption spectra of a radical-substituted-LL'CT- and control complexes. The latter contains an NN radical, but lacks the LL'CT chromophore (no acceptor).

This project (DE-SC0020199, "Optical Generation and Manipulation of Spin Qubits") focuses on light initiation and control of molecular electron spin polarization (ESP). The research advances our understanding of how photogenerated quantum (spin) bits (qubits) develop large ground-state ESPs on an ultrafast timescale that persists into the ms regime. We observe ESP in numerous radical-elaborated systems that can be understood using our *modified reversed quartet mechanism*. This highlights structure-property relationships and excited state contributions to control the sign and magnitude of ESP.[1-7] New plans include understanding D-A biradical spin coherence, the field dependence of T_1 and T_2, multi-spin ESP, and the generation of ESP using alternative radicals.

Selected References

1. Kirk, M. L.; Shultz, D. A.; Marri, A. R.; Hewitt, P.; van der Est, A., Single-Photon-Induced Electron Spin Polarization of Two Exchange-Coupled Stable Radicals. *J. Am. Chem. Soc.* **2022,** *144*, 21005.
2. Kirk, M. L.; Shultz, D. A.; Hewitt, P.; van der Est, A., Excited State Magneto-Structural Correlations Related to Photoinduced Electron Spin Polarization. *J. Am. Chem. Soc.* **2022,** *144*, 12781.
3. Kirk, M. L.; Shultz, D. A.; Hewitt, P.; van der Est, A., Excited State Exchange Control of Photoinduced Electron Spin Polarization in Electronic Ground States. *J. Phys. Chem. Lett.* **2022,** *13* (3), 872.
4. Kirk, M. L.; Shultz, D. A.; Hewitt, P.; Stasiw, D. E.; Chen, J.; van der Est, A., Chromophore-Radical Excited State Antiferromagnetic Exchange Controls the Sign of Photoinduced Ground State Spin Polarization. *Chem. Sci.* **2021,** *12*, 13704.
5. Kirk, M. L.; Shultz, D. A.; Chen, J.; Hewitt, P.; Daley, D.; Paudel, S.; van Der Est, A., Metal Ion Control of Photoinduced Electron Spin Polarization in Electronic Ground States. *J. Am. Chem. Soc.* **2021,** *143* (28), 10519.
6. Shultz, D. A.; Stephenson, R.; Kirk, M. L., Dinuclear Ligand-to-Ligand Charge Transfer Complexes. *Dalton Trans.* **2023,** *52*, 1970.
7. Chen, J.; Yang, J.; Yadav, M.; Shultz, D. A.; Kirk, M. L., Origin of Ferromagnetic Exchange Coupling in Donor–Acceptor Biradical Analogues of Charge-Separated Excited States. *Inorg. Chem* **2023,** *62* (2), 739.

Fluence Dependent Charge Carrier Dynamics in Polymer-Wrapped Semiconducting Single-Walled Carbon Nanotubes

Zachary X. W. Widel, James J. Alatis, Yusong Bai, Francesco Mastrocinque, George E. Bullard, Jean-Hubert Olivier, and Michael J. Therien
Department of Chemistry
Duke University,
Durham, North Carolina, 27708

Due to the spatial extent of the single-walled carbon nanotube (SWNT) exciton (~2 nm), multiple excitons can coexist in a single tube. Multi-body interactions therefore can play key roles in the relaxation processes of electronically excited SWNTs depending on the excitation fluence conditions. Analyses of fast and ultrafast SWNT excited-state dynamical data must therefore consider how excited state relaxation mechanisms involving exciton-exciton annihilation, multiple exciton generation, the formation of biexcitons, and trion generation complicate analyses of photoinduced charge separation (CS) and thermal charge recombination (CR) dynamics in SWNT systems. Utilizing a hybrid R-PBN(b)-Ph_6PDI-[(6,5)SWNT] superstructure, we describe how the ultrafast CS and CR dynamics that are triggered upon SWNT E_{00}→E_{11} excitation are affected by excitation fluence. We determine two distinct pathways for decay of the CS state: classical thermal recombination between geminate charge carriers (**Fig. 1A**) and a pathway mediated by multi-body interactions derived from an excess population of excitons (**Fig. 1B**).

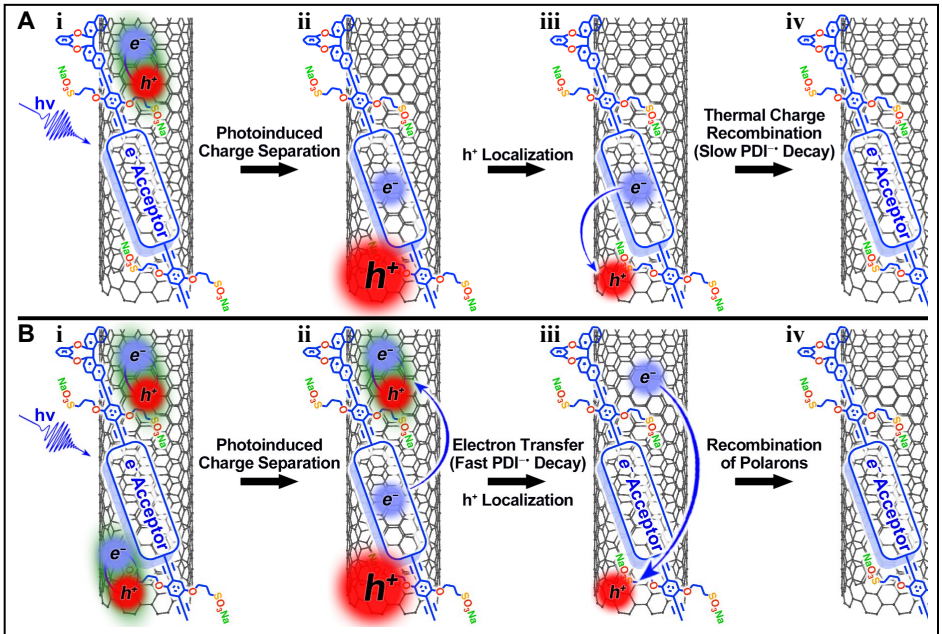

Figure 1: Schematic illustration of light-triggered charge separation and subsequent dynamical processes in R-PBN(b)-Ph_6-PDI-[(6,5)SWNT] superstructures, highlighting the two dominant pathways for $PDI^{-\bullet}$ decay. (A) At low optical excitation fluences classical thermal charge recombination dominates, where: (i) upon E_{00} → E_{11} optical excitation a limited population of excitons is formed within the SWNT which undergo ultrafast CS, forming (ii) a PDI radical anion ($PDI^{-\bullet}$) and a SWNT hole polaron ($SWNT^{\bullet+}$), which subsequently undergo thermal CR. (B) As excitation fluence increases, so too does the amplitude of decay by a second charge recombination pathway. (i) With increasing excitation fluence, an increasing exciton population is manifest following the ultrafast CS reaction that produces the $PDI^{-\bullet}/SWNT^{\bullet+}$ charge separated state. Increasing exciton density increases the amplitude of a second decay pathway for the $PDI^{-\bullet}/SWNT^{\bullet+}$ charge separated state (iii) in which excitons interact with the $PDI^{-\bullet}$ resulting in the formation of a SWNT electron polaron ($SWNT^{-\bullet}$) in a process faster than thermal CR time scale. (iv) These SWNT electron and hole polarons ($SWNT^{-\bullet}$ and $SWNT^{\bullet+}$) recombine to return the polymer-wrapped SWNT superstructure to its ground state.

X-ray Scattering Approaches for Tracking In-situ and Photoelectrochemical Operando Structures of Amorphous and Molecular Transition Metal Oxide Water-Splitting Catalysts

Justin M. Hoffman[1], Niklas B. Thompson[1], Mark Muir[2], Alex B. F. Martinson[2], Karen L. Mulfort[1], Lin X. Chen[1], and David M. Tiede,[1]
[1]Chemical Sciences and Engineering and [2]Materials Sciences Divisions
Argonne National Laboratory
Lemont, Illinois 60439

Cobalt-oxo phosphate (CoPi) is an amorphous oxyhydroxide electrocatalyst that is of interest as a model for water splitting catalysis because of its reactivity and self-repair, analogous to the oxygen-evolving complex of Photosystem II. CoPi films show UV-Vis absorptions with oxo-ligand-to-metal (LMCT), metal-to-metal (MMCT) charge transfer and metal d-d transitions similar to those seen more generally in transition metal oxides and related molecular catalysts. As part of our program that investigates photochemistry associated with catalysts for solar fuels chemistry, we are developing operando and time-resolved high energy X-ray scattering (HEXS) and atomic pair distribution function (PDF) approaches for tracking the structures of amorphous, electrode-supported thin film and solution-phase molecular transition metal oxide catalysts. HEXS-PDF offers unique opportunities to resolve structure features across inner and outer coordination shells (0.1 to 1 nm) and intermediate length (1 nm to 50 nm) ranges. These measurements are particularly relevant for probing reaction mechanisms requiring atomic reorganization in the outer coordination sphere.

Capabilities for tracking atomic structure within ultrathin films have been enhanced by the development of beamlines with micro-focused high energy X-rays, allowing PDF analyses from grazing incidence scattering (GI-PDF). Particularly for functional thin films at liquid-solid interfaces, GI-PDF offers opportunities for selectively enhancing detection of scatting from interfacial catalyst films. Here, we investigate the use of GI-PDF for characterization of electrode-supported thin film solar fuels catalysts using CoPi as a model. For relatively thick, >100 nm films, the structure of surface-supported CoPi is found to correspond closely to that measured for ex-situ powder samples. With progressively thinner films new PDF peaks are seen, suggestive of having resolved nucleating CoPi clusters and their associations with the IZO support. These nucleating structures provide a new avenue for investigating interfacial charge transfer processes.

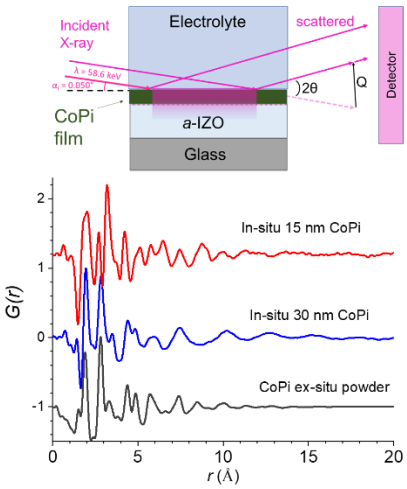

Further, we have been extending PDF analysis to molecular catalysts using the $[Co_4O_4](OAc)_4(py)_4$ cubane as a catalyst model. Solution PDF measurements are found to provide information on the outer coordination sphere ligand and solvation layer structures. Modeling of the measured broadening of the outer sphere PDF peaks associated with the pyridine and acetate ligands suggests dynamical picture of the cubane atomic structure, which is supported by molecular dynamics simulations that also reveal the presence of persistent H-bonded H_2O molecules to the Co-oxo core in aqueous solution.

Theory of (Photo)Electrocatalytic Reactions on 2D Transition Metal Dichalcogenides

Taylor Aubry,[1] Elisa Miller-Link,[2] Derek Vigil-Fowler,[1] Jao van de Lagemaat[2]
[1]Computational Sciences Center, [2]Chemistry And Nanoscience Center,
National Renewable Energy Laboratory
Golden, Colorado, 80401

Layered, two-dimensional transition-metal chalcogenide semiconductors such as MoS_2 VS_2, TiS_2, and WSe_2 are known (photo)electrocatalysts for the electrochemical splitting of water to form hydrogen and oxygen, CO_2 to form C1 and higher products, N_2 to form NH_3, and other reactions that will form the basis of a future zero-carbon economy. These reactions have complex, multiple step reaction kinetics and are catalyzed by defects or step edges. They involve multiple coupled electron and proton transfer events. In previous work,[1] we showed that electrochemical conditions strongly modify the electronic properties by electrochemical doping, state filling, bandgap renormalization, and phase transitions. This complexity makes it hard to make predictions about the electrocatalytic behavior of these materials if electrochemical conditions are not accurately treated.

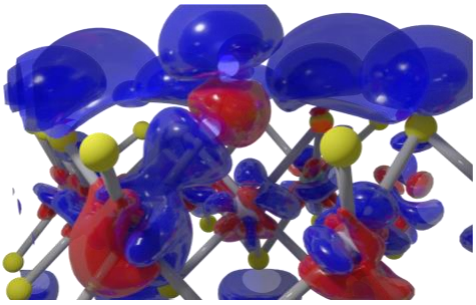

Fig 1. Charge density difference(blue negative, red positive) for a 0.1 V negative potential step for N_2 (light blue) bound to a Mo atom at a sulfur vacancy site showing bond weakening and polarization of the N_2 molecule.

In this contribution, we theoretically investigate the nitrogen reduction reaction on 2-D MoS_2 nanosheets using a Grand Canonical Ensemble approach implemented in JDFTx.[2] This approach can accurately address electrochemical conditions such as applied potential, solvent polarization, pH, ionic strength, etc. We study the reaction pathways, intermediate energies and the electronic properties of the intermediate complexes to gain a better understanding of the electrochemical reduction reactions in realistic microenvironments. We find that the electrochemical conditions modify the electrocatalytic pathways in a non-trivial manner and that the local structure of the 2-D catalyst changes considerably during the reaction sequence causing a strong potential dependency of reaction steps that are not normally considered to be potential dependent. Electronic effects such as π-back bonding from the transition metal sites to antibonding orbitals on the N_2 molecule and local relaxation of the microenvironment affect the reaction pathway and the dependence of the reaction on electrochemical bias. We find that calculating intermediate energies in vacuum can lead to the wrong step to be identified as rate limiting. We extend these results to other catalytic substrates (e.g. H and CO) and identify future experiments.

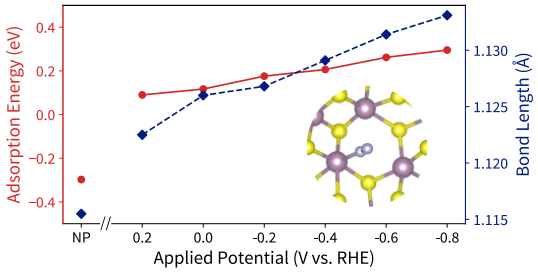

Fig. 2 Adsorption energy for N_2 on a Mo atom in the sulfur vacancy and N_2 bond length as a function of applied potential. While the adsorption energy changes over 0.2 eV, the N_2 bond length increases, indicating an activation of the N_2 triple bond.

[1] Ref: https://pubs.rsc.org/en/content/articlehtml/2019/ee/c9ee00513g
[2] https://www.sciencedirect.com/science/article/pii/S2352711017300559

Strategies for Water Oxidation with Abundant Metals: Catalyst Design, Immobilization on Conducting Substrates, and Sensitizer Integration

Gibson Kirui, Krista Kulesa, Carlos Lucecki, Emerson Perry, Cláudio Verani*
Department of Chemistry
Wayne State University
Detroit, MI, 48202

In this poster, the PI Verani will present current progress on the understanding of Earth-abundant molecular catalysts for water oxidation covering the **three proposed objectives** of grant DE-SC0022114, namely, (i) catalyst design ad mechanisms, (ii) immobilization of catalysts on conducting substrates, and (iii) integration of catalyst/sensitizer systems.

For the **first objective**, we aim to interrogate the mechanisms of water oxidation in new molecular manganese, iron and cobalt catalysts with redox-active ligands. We will present two Co catalysts capable of water oxidation and reduction; Kulesa using imidazole-based (**A**) and Lucecki using quinoline-based catalysts (**B**). Then we will discuss metal cooperativity contrasting mono and bimetallic Co/Co_2 amido systems (**C**, **D)**) developed by Lucecki and Perry, which preclude ligand oxidation and mitigate the need for metal-centered high oxidation states. We will also discuss initial progress on similar Fe/Fe_2 and Mn/Mn_2 systems developed by Perry. The next steps involve understanding the electronic structure of high-oxidation products from reactions $[M^{n+}(L)] - e^- \rightarrow [M^{(n-1)+}(L)]$ *vs.* $[M^{n+}(L)] - e^- \rightarrow [M^{n+}(L^{\bullet+})]$. We will use spectro-electrochemistry and electrolysis to isolate these species by EPR, in collaboration with Oleg Poluektov at ANL. Progress in the **second objective** entails a collaboration with Javier Concepcion at BNL to build modular and hierarchical Ru-Co structures on ITO surfaces to enhance the stability of catalysts by immobilization. Thus far, Kirui made progress on assembling the Ru module (**E**) on ITO and developed two Co surfactants (**F**). For the next cycle we plan to use Perry's Fe/Fe_2 and Mn/Mn_2 systems for immobilization on carbon black and comparison of the catalytic activity between in solution and immobilized species. The **third objective** entails the design of integrated heterometallic photosensitizer/catalyst systems for photoinduced water oxidation. Lucecki has made initial progress on a system that incorporates phenanthroline to the amido-rich systems described above, using aromatic bridges of different lengths (**G**) to favor electron transfer and prevent recombination between catalyst and sensitizer.

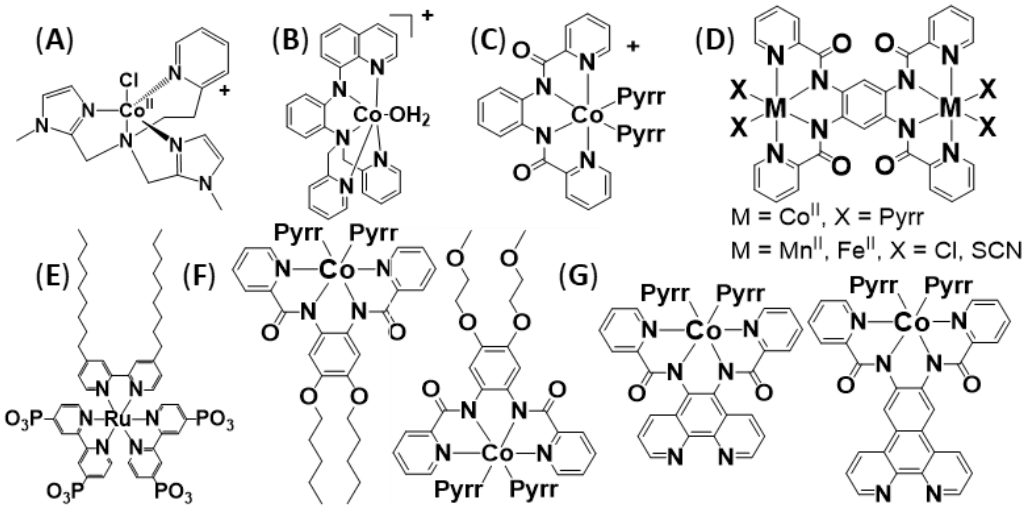

From UV to XUV: Revealing interfacial charge dynamics in semiconductor heterostructures

Josh Vura-Weis
Department of Chemistry
University of Illinois at Urbana-Champaign
Urbana, IL 61801

Charge separation and diffusion at interfaces is a crucial step in semiconductor photochemistry, and is often a major factor that limits their efficiency. In systems as diverse as dye-sensitized solar cells, quantum dot heterostructures, and organic photovoltaics, charge transfer across an interface first creates a bound state before full charge separation yields free carriers. There are several potential sources of this bound state even in high-dielectric materials, including intrinsic surface states, charge localization on defects, and band bending. In this work, we use a combination of femtosecond transient visible and ultraviolet spectroscopy to study the charge injection from CdSe quantum dots into ZnO nanowires. The visible probe selectively probes the CdSe band-edge bleach and reveals both the initial exciton formation and the subsequent injection of a photoexcited electron. The UV probe selectively probes the appearance of free carriers in ZnO. A delay is observed between the CdSe injection signal and the ZnO free-carrier signal, a phenomenon that has been previously attributed to a surface Charge Transfer State (CTS). However, our analysis of a range of QD sizes reveals two surprising results. First, each size of QD shows both a slow and a fast injection time, which is likely due to ZnO facet-dependent coupling. Second, the trend in charge injection times from small to large quantum dots (i.e. large to small ΔG for charge separation) is incompatible with the CTS model. We show that a band-bending model incorporating two populations of QDs matches well to the experimental result.

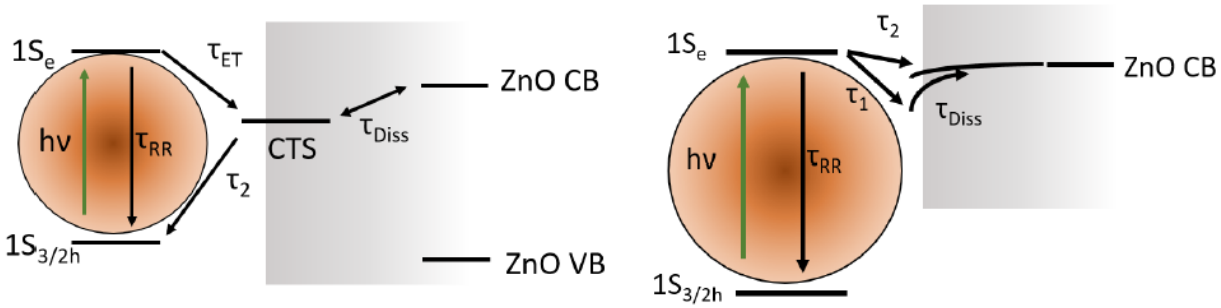

We will also preview the development of a tabletop femtosecond soft X-ray transient absorption instrument that will provide a new tool for the photochemistry community. This system uses high-harmonic generation to produce a broadband continuum from 100-300 eV, a range that is resonant with the core-to-valence transitions of elements such as B, C, P, S, and most lanthanides. Initial experiments will focus on mapping the element-specific charge distribution of organic photovoltaic heterostructuctures from the initial exciton, to the charge transfer state, and finally to free charges.

Translating Homogeneous Hydrogenation Activity to Electrochemical Reduction

Xinran S. Wang & Jenny Y. Yang
Department of Chemistry
University of California, Irvine
Irvine, California 92617

Scheme 1

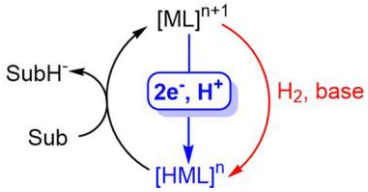

The reduction of CO_2, either through hydrogenation or electrochemical pathways, is an attractive route to non-fossil carbon products. Hydrogenation catalysts typically generate a metal hydride intermediate from hydrogen and a base (**Scheme 1**, red). The parallel electrochemical 'hydrogenation' route uses two electrons from the electrode and a proton from solution to generate equivalent metal hydrides (**Scheme 1**, blue).

Extensive work has been performed on the development of both molecular CO_2 hydrogenation catalysts and electrocatalysts. However, there are few examples of translating reactivity between these two reduction mechanisms. To further our understanding, we investigated the aqueous CO_2 hydrogenation catalyst $[Co(dmpe)_2(H)]^{2+}$ (**2**) (dmpe = 1,2-*bis*(dimethylphosphino)ethane) for electrocatalytic reduction. **2** exhibits one of highest activities for a first-row transition metal catalyst in water. The proposed hydrogenation mechanism is depicted in red in **Scheme 2**. To obtain the electrochemical potential and pH requirements to generate the metal hydride intermediate, we measured the pK_a (12.9(5)) and reduction potential (-1.5 V vs SCE) shown in blue in **Scheme 2**.

Scheme 2

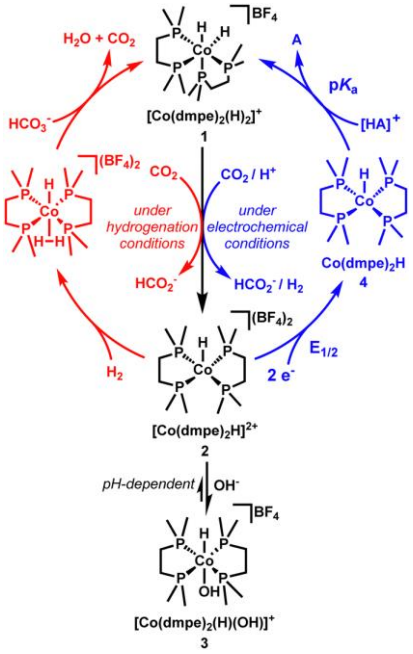

Controlled potential electrolysis (CPE) experiments were performed with **3** at –1.50 V vs. SCE using a 0.2 M sodium carbonate solution saturated with CO_2 to the appropriate pH value. Results from these experiments are summarized in **Table 2**. Under electrolytic conditions, the Faradaic yield for formate is optimized at pH 7.8. At other pH conditions, the Faradaic efficiency for H_2 is higher than that of formate.

Table 1. Summary of CPE data with $[Co(dmpe)_2(OH)H]^+$ (**3**).

	Faradaic yield (% H_2)	Faradaic yield (% HCO_2^-)
pH 7.2	52 ± 6	40 ± 7
pH 7.8	47 ± 5	54 ± 4
pH 8.1	57 ± 3	37 ± 2
pH 8.7	62 ± 2	22 ± 5

A complicating factor in electrochemical reduction that does not exist in hydrogenation is the direct reduction of protons to hydrogen. Despite the challenges in favoring CO_2 reduction versus H_2 evolution in aqueous solvents, selective homogenous CO_2 reduction catalysts have been reported. success in selective aqueous CO_2 reduction electrocatalysts have relied on favoring the kinetic reactivity of CO_2. Catalyst designs that can kinetically inhibit the hydrogen evolution reaction may be particularly valuable for aqueous catalysts.

Spin Selective Charge Dynamics in Molecules and at Interfaces

Xiaoyang Zhu and Colin Nuckolls
Department of Chemistry
Columbia University
New York, NY 10027

This research program aims to explore molecular strategies for spin-selective tuning of excited states and spin-selective charge transfer. During the current funding period, the PIs have accomplished the following: 1) turning-on of singlet fission by contortion; 2) demonstration of spin-selective interfacial charge transfer; 3) exploration of controlled molecular chirality for spin-selective chemistry. This abstract focuses on 2) and 3).

Spin selective dynamics is key to important interfacial charge transfer reactions, such as those involving molecular oxygen, which in the ground state is a spin triplet and its reactions often involve the conversion between singlet and triplet molecular species. The fundamental requirement of angular momentum conservation thus may serve as a reaction barrier or mechanism of control. The PIs have embarked on a new approach to systematically probe spin selectivity in interfacial charge transfer reactions. The PIs are exploring the use of a novel source for highly spin-polarized electrons from photo-excited transition metal dichalcogenide (TMD) monolayers or heterobilayers with unique spin-valley locking. Initial experiments have successfully demonstrated the spin-selective interfacial charge separation at room temperature in TMD heterobilayers. Promising results are also coming out on spin selective charge injection from TMDs to molecular films.

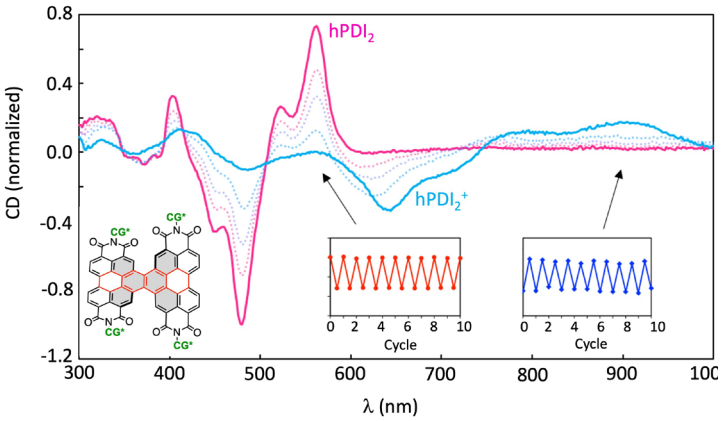

Fig. 1. ON and OFF chirality in thin films of chiral PDI dimer from charge transfer. The different curves show CD spectra as the molecule is oxidized from the neutral to the cationic state. The process is reversible, as shown at two wavelengths.

Complimenting the approach based on two-dimensional materials, the PIs are exploring molecular systems for spin polarization based on the chiral-induced spin selectivity (CISS) effect, an intriguing mechanism under debate. The PIs discovered that π-conjugated perylene diimide (PDI)-based twistacenes, known as the helical perylene diimide (shown for the dimer in the inset, with chiral side groups), possess the highest known circular dichroism (CD) activity. Interestingly, the PIs discovered that the CD response can be electrochemically tuned, Fig. 1. Experiments are underway to establish the connection between CD activity and spin selectivity in interfacial electron transfer.

How General Are Changes in Excited State Surface Chemistry of Colloidal Quantum Dots?

McKenna N. Grega, Jianing Gan, and John B. Asbury
Department of Chemistry
The Pennsylvania State University
University Park, PA 16802

The ligand-nanocrystal boundaries of colloidal quantum dots (QDs) mediate the primary energy and electron transfer processes that underpin photochemical and photocatalytic transformations at their surfaces. The ligand-nanocrystal boundary also serves critical functions of protecting nanocrystal surfaces from photochemical degradation and maintaining colloidal stability. In recent work, we demonstrated using time-resolved infrared (TRIR) spectroscopy that certain types ligand-nanocrystal interactions exhibit marked reduction in surface bonding strength in the excited states of the nanocrystals. Ligands with other types of surface anchoring groups did not exhibit such changes in excited state surface bonding. These findings suggested that it may be possible to design ligand-nanocrystal interactions to control when ligands exhibit weaker bonding to nanocrystal surfaces such that they can facilitate photocatalytic reactions.

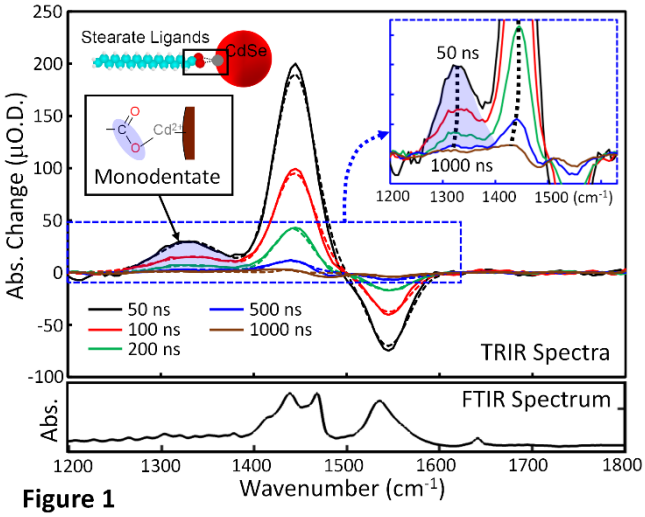

Figure 1

An important step toward designing ligand-nanocrystal interactions for enhanced activity and durability of QD photocatalysts is to identify the generality of the phenomenon among various types of ligand structures and nanocrystal compositions. Toward this end, we examined changes in the excited state surface chemistry of CdSe QDs passivated with stearic acid ligands. Transient absorption and photoluminescence spectroscopies were used to characterize the vibrational spectra of the ligands in the excited states of the QDs and to compare their time-dependence to the dynamics of the electronics states. The transient vibrational spectra of the symmetric and antisymmetric stretch modes of the carboxylate anchoring groups of stearate ligands on CdSe QDs depicted in the TRIR spectra in **Figure 1** indicate a net reduction of their higher frequency antisymmetric stretch and an enhancement of the lower frequency symmetric stretch modes. These changes are consistent with the influence that image dipoles created by the polarizable excited excitonic states of the QDs have on the transition dipole moments of the carboxylate anchoring groups. Importantly, a lower frequency transient vibrational feature around 1330 cm^{-1} appears in the TRIR spectra that was not present in the ground state infrared absorption (FTIR) spectrum of the QDs. This feature corresponds to the C–O single bond of more weakly bonded carboxylate groups in the monodentate bonding geometry. The inset in the upper right of **Figure 1** indicates a slow relaxation process through time-dependent changes of the transient vibrational features. This observation indicates restoration of the original ligand bonding to the nanocrystal surfaces on the microsecond time scale. These findings suggest that changes in excited state surface chemistry may be general to metal chalcogenide QDs and motivates continued work to elucidate the origins and means to control the phenomenon.

Controlling opto-electronic properties of QD arrays through beneficial ligand/QD interactions

Marissa S. Martinez, Zhiyuan Huang, Michelle Nolen, Nicholas Pompetti, Carrie Farberow, Justin C. Johnson, and Matthew C. Beard
Materials, Chemical, and Computational Sciences
National Renewable Energy Laboratory
Golden, CO 80401

Hybrid QD organic/inorganic hybrid systems, where the organic component is chemically bound to the inorganic nanocrystal surface and can electronically interact with the core-QD electronic states, are interesting for controlling energy flow solar energy conversion strategies. For example, we have demonstrated that the inorganic core can photosensitize surface bound SF molecules when light is absorbed within the QD and energy is transferred to singlet (S1) states of the surface-attached SF molecules. The reverse can also be used to enhance or sensitize MEG that occurs in the QDs if light is first absorbed into surface attached molecules and the energy is subsequently transferred to the QDs. Here we are motivated to understand and control the fundamental interactions between derivatized tetracene ligands on PbS QD surfaces as thin QD films. In this study, we functionalized PbS QDs with a dicarboxylic acid tetracene derivative, Tc(Ac-COOH)$_2$. The acetylene spacer group between the acene core and the carboxylic acid anchors as well as the overall rigidity of the molecule predispose it to form π-stacked and hydrogen-bonded aggregates in solution. We find that there are three primary QD/diacid structures, each with a unique binding mode and dictated by the QD-ligand and ligand-ligand intermolecular and steric interactions and they can be accessed nearly independently from one another. They are: (1) low concentrations produces mixed oleate/tetracene ligand structures where the tetracene carboxylates tilt and interact with QD surfaces; (2)intermediate concentrations produces mixed oleate/tetracene ligand structures with ligand-ligand interactions through intramolecular hydrogen bonding with the ligands perpendicular to the QD surface and weaker QD/ligand electronic interactions; and (3) at high concentrations, the full ligand exchange has occurred and the ligands tilt towards the surface while the QD film compacts. When the tetracene ligands lie flat the benzene ring pi-system interacts strongly with the p-orbitals at the PbS surface and produces strong QD-ligand interactions evidenced through QD/ligand state mixing, with a coupling energy of ~ 700 meV.

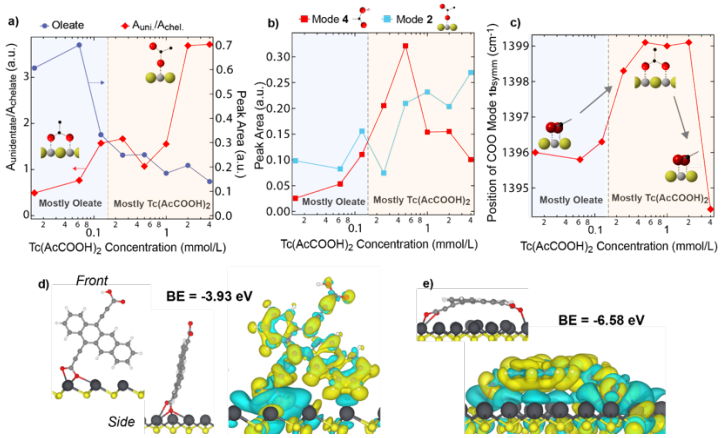

Fig. (a-c) FTIR analysis of surface bound ligands, (d-e) DFT simulations of interacting ligands

Light Harvesting in Semiconductor Quantum Dots

Warren F. Beck,[1] Benjamin G. Levine,[2] P. Gregory Van Patten,[3] Mengliang Zhang[3]

[1]Department of Chemistry, Michigan State University, East Lansing, Michigan 48824
[2]Department of Chemistry and Institute for Advanced Computational Science, Stony Brook University, New York 11794
[3]Department of Chemistry, Middle Tennessee State University, Murfreesboro, Tennessee 37132

We are probing the dynamics of semiconductor quantum dots (QDs) using broadband multidimensional electronic spectroscopy (2DES/3DES) and electronic structure calculations. Our results indicate a many-electron, molecular theory for the electronic structure of QDs, where the vibrations of organic surface-capping ligands serve as branching modes in a coherent nonadiabatic mechanism for nonradiative decay. In planned work, we will investigate how the photoinduced charge-transfer and triplet–triplet excitation energy transfer properties of QDs depend on the extent of quantum coherent mixing of the core electronic and ligand vibrational states.

The Beck group has characterized vibronic coherences that accompany hot-carrier cooling (X3→X1) and photoluminescence in QDs with hexadecylamine[1] or oleate ligands. Global modeling of the 2DES spectra from the oleate QDs suggests that the exciton transitions dynamically localize on surface sites during nonradiative relaxation. Oscillation maps show that photoinduced charge transfer to methyl viologen dication acceptors involves vibronic coherence in a bridging charge-transfer state with mixed QD and acceptor character.

Analysis by the Levine group of conical intersection structures connecting the excited states of amine- and carboxylate-passivated QDs indicates that coupling between core electronic excitations and ligand vibrations occurs through two distinct mechanisms. Lower frequency ligand modes (<400 cm^{-1}) couple directly to core vibrations, which are driven by core electronic excitations. However, higher frequency vibrations tend to be local to the ligand and are driven directly by the delocalization of core electronic excitations on the ligands.

The Van Patten and Zhang group have developed a novel and reliable thermal desorption DART-MS method to identify organic ligands and possible residues on QDs.[2] We are currently extending our methods to prepare soluble CdSe QDs capped exclusively by a thiol-containing, electronically-active ligand with a distinct vibrational spectrum (2-phenylethane thiol). We are also developing strategies to quantify precisely the ligands on QD surfaces.

(1) Tilluck, R. W.; Mohan T M, N.; Hetherington, C. V.; Leslie, C. H.; Sil, S.; Frazier, J.; Zhang, M.; Levine, B. G.; Van Patten, P. G.; Beck, W. F. Vibronic Excitons and Conical Intersections in Semiconductor Quantum Dots. *J. Phys. Chem. Lett.* **2021**, *12*, 9677–9683, DOI: 10.1021/acs.jpclett.1c02630.
(2) Frazier, J.; Cavey, K.; Coil, S.; Hamo, H.; Zhang, M.; Van Patten, P. G. Rapid and Sensitive Identification and Discrimination of Bound/Unbound Ligands on Colloidal Nanocrystals via Direct Analysis in Real-Time Mass Spectrometry. *Langmuir* **2021**, *37*, 14703–14712, DOI: 10.1021/acs.langmuir.1c02548.

Tuning Counterion Chemistry to Reduce Carrier Localization in Doped Pi-conjugated Semiconductors

Jeffrey L. Blackburn, Tucker Murrey, Alejandra Hermosilla-Palacios, Justin Earley, Obadiah Reid, Andrew J. Ferguson, Garry Rumbles
Collaborators – Alexander Spokoyny, Benjamin Schwartz (U. California, Los Angeles), Klaus Eckstein, Tobiash Hertel (Julius-Maximilian University Würzburg)
Materials, Chemistry, and Computational Science Center
National Renewable Energy Laboratory, Golden, CO 80401

A fundamental challenge for incorporating pi-conjugated semiconductors into opto-electronic applications is exerting fine control over charge carrier densities *via* electronic doping, while ensuring these charge carriers are not localized due to the inherently low Coulomb screening. Since conventional wisdom holds that such charge carriers are strongly localized by Coulomb attraction of the associated counterion, fundamental mechanisms giving rise to free carriers that contribute to dark- and/or photo-current in organic semiconductors are still unclear. Semiconducting single-walled carbon nanotubes (s-SWCNTs) have demonstrated promising performance for several energy harvesting devices and serve as an illustrative model system for mechanistic understanding of pi-conjugated semiconductors.

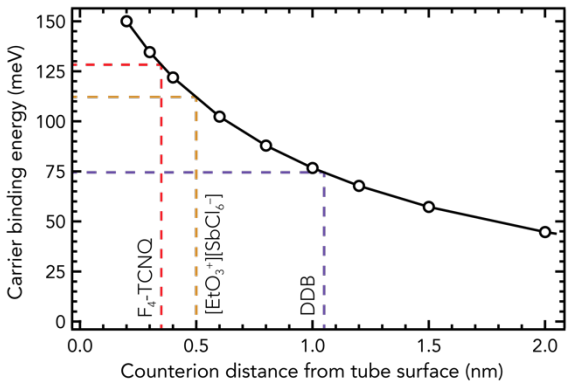

Figure 1. Displacing the counterion from injected holes in DDB-doped s-SWCNTs reduces the electrostatic attraction, enhancing hole delocalization and conductivity.

Here, we compare a series of molecular charge-transfer dopants based on functionalized dodecaborane (DDB) clusters to explore the impact of the dopant's chemical and electronic structure on the doping efficacy and charge carrier transport in s-SWCNT networks. The inherent structure of these molecules provides electron delocalization over the interior DDB core, which sits ~1 nm from the hole injected into the s-SWCNT due to the sterically bulky functional groups. Analysis of charge transport across a series of dopants indicates that this large separation between charges reduces the coulomb attraction and carrier binding energy (Fig. 1), thereby increasing the charge carrier mobility. This fundamental understanding of a strategy that enhances carrier delocalization ultimately allows for an increase in the electrical conductivity of s-SWCNT networks at lower charge carrier densities.

To probe the free carrier generation process in even finer detail, we further simplified the system by probing charge carriers in *isolated doped s-SWCNTs in a low dielectric solvent (toluene)*. We use solution-phase microwave conductivity to simultaneously measure the collective dielectric constant (ε_r) and electrical conductivity (σ) of redox-doped s-SWCNTs. We find that carrier injection by redox dopants increases the local dielectric constant, which reduces the Coulomb attraction between the injected carriers and counterions and enhances carrier delocalization. This result questions the typical assumption of a static low-dielectric environment for charge carriers in doped pi-conjugated semiconductors and provides a fundamental insight into how appreciable densities of mobile charge carriers and high conductivities can be achieved.

Understanding and Controlling Charge-Carrier Selectivity at Nanoscale Catalyst/Semiconductor Photochemical Interfaces

Shannon W. Boettcher, Aaron Kaufmann, Meikun Shen, Kaden Wheeler
Department of Chemistry and the Oregon Center for Electrochemistry
University of Oregon
Eugene, Oregon, 97403

Controlling charge transfer rates, through mechanistic understanding and design, at electrocatalyst/semiconductor interfaces is required to for building efficient semiconductor photoelectrochemical systems. Conventional electrocatalyst nanoparticles such as Pt (for H_2 evolution) or CoO_x (O_2 evolution) are often deposited onto semiconductor light absorbers to enhance the overall water-splitting efficiency of photocatalyst particles. Ideally, the electrocatalyst nanoparticles each selectively collect only one of the photogenerated charge carriers and drive fuel-forming reactions at low overpotential (e.g., H_2 and O_2). Due to the complexity of the nanoscale catalyst-semiconductor interface, the photochemical properties of these nanocontacts are difficult to characterize, especially during the photocatalytic reactions and often have different mechanisms operative than macroscopic-thin films. We report new measurement techniques and used them to study catalyst nanocontacts on well-defined metal-oxide semiconductor photocatalysts including $BiVO_4$ and $SrTiO_3$. We use new approaches to characterize charge-carrier selectivity combining different spectroscopy methods, including XPS, with directly nanoscale photovoltage measurements. This work underpins rational control over properties of particulate "overall-water-splitting" photocatalyst systems.

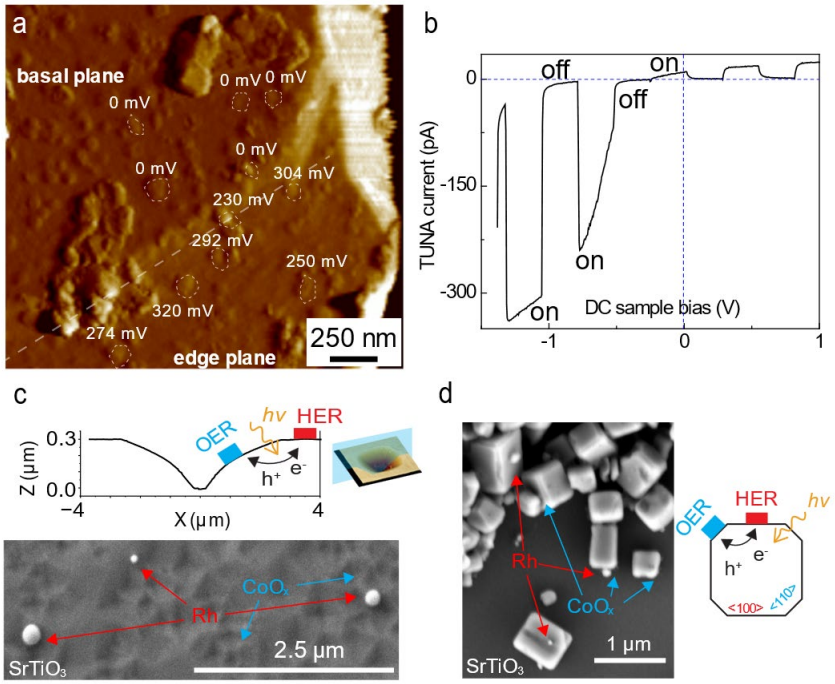

Sensitizers for Solar Fuels Production: (carbene)M(amide) Complexes (M = Cu, Ag, Au)

Stephen Bradforth[1], Mark Thompson[1], Collin Muniz[1], Austin Mencke[1], Michael Kellogg[1], Fabiola Cardoso-Delgado[1], Thabassum A. N. Kallungal[1], Nina Baluyot-Reyes[1], Matthew Bird[2]

1. Department of Chemistry, University of Southern California, Los Angeles, CA 90089
2. Chemistry Department, Brookhaven National Laboratory, Upton, NY 11973

Generating a sustainable fuel from sunlight plays an important role in meeting the energy demands of the modern age. In our poster we will discuss our work with two-coordinate carbene-metal-amide (cMa, M = Cu(I) and Au(I)) complexes, exploring them as sensitizers for driving electrocatalytic reactions, such as the hydrogen evolving reaction (HER), enabling light driven reduction of water to hydrogen. The cMa complexes studied here absorb visible photons ($\varepsilon_{vis} > 10^3$ $M^{-1}cm^{-1}$), maintain long excited state lifetimes ($\tau \sim 0.2$-1 μs) and are predicted to have high excited state reducing potential.

A series of steady state and time-resolved spectroscopies were performed on several carbene-metal-amide (cMa) complexes, where M = Cu and Au. Using ps-to-ns and ns-to-ms transient absorption spectroscopies (psTA and nsTA, respectively), the excited state kinetics from light absorption, intersystem crossing, and eventually intermolecular charge transfer were thoroughly characterized. Ultrafast intersystem crossing (ISC) rates for the Cu-based cMa complexes were obtained from time correlated single photon counting (TCSPC) experiments utilizing a thermally activated delayed fluorescence (TADF) model, leading to rate constants of 3×10^9-20×10^9 s^{-1} for ISC in their excited states ($S_1 \rightarrow T_1$). These rates were corroborated with psTA. The ISC rates for Au-based complexes are instrument limited by TCSPC, but psTA allows us to measure their ISC rate constants as 80×10^9-130×10^9 s^{-1}. The psTA additionally revealed an early time ($\sim0.5\times10^{12}$ s^{-1}) relaxation rate attributed to solvent relaxation and vibrational cooling. The nsTA experiments for a gold-based cMa complex demonstrated efficient intermolecular charge transfer from the excited cMa to either an electron acceptor or donor (N-methyl-phthalimide and 1,3-dimethyl-2-phenyl-2,3-dihydro-1H-benzo[d]imidazole, BIH, respectively). Spectroelectrochemical experiments allow us to identify products observed in the nsTA as the formation of the oxidized and reduced forms of the cMa sensitizer, respectively. These measurements set the stage for us to be able to use these cMa complexes as excited state reductants for producing hydrogen from water.

With this data in hand, we turned to study a set of cMa complexes as photoreductants to drive HER. The first step was to verify the excited state oxidation potentials of the complexes. This was accomplished using a Rehm-Weller analysis of quenching data and we found that Cu and Au-based cMa complexes have $E^{+/*}$ of -2.33 V vs. $Fc^{+/0}$. Next, we paired two different cMa complexes (Au_{BCz}^{MAC} and Cu_{PhC}^{MAC}) with a cobalt-glyoxime electrocatalyst and BIH sacrificial reductant to photo-catalytically generate hydrogen. Up to 40 equivalents of hydrogen (relative to cMa) are generated over 20 hours of irradiation. We also find that both Au_{BCz}^{MAC} and Cu_{PhCz}^{MAC} carry out photo-driven hydrogen production from water without the addition of the cobalt-glyoxime electrocatalyst. In this "catalyst free" system the cMa sensitizer partially decomposes to give metal nanoparticles that catalyze water reduction, producing up to 70 equivalents of hydrogen on extended irradiation.

BODIPY and Dipyrrin as Unexpected Robust Anchoring Groups on TiO_2 Nanoparticles

Josephine A. Jayworth, Matt D. Capobianco, Han-Yu Liu, Cristina Decavoli, Jan Paul Menzel, Jessica G. Freeze, Jana Jelušić, Spencer Adler, Hailiang Wang, Victor S. Batista, Robert H. Crabtree, and Gary W. Brudvig
Department of Chemistry and Energy Sciences Institute
Yale University
New Haven, CT 06520-8107

Devising cost effective methods for efficiently capturing and storing solar energy is among the grand challenges of science. We are using insights from studies of natural photosynthetic systems to develop bioinspired materials for photo-electrochemical water oxidation and solar fuel production by using molecular catalysts and dyes attached to mesoporous metal oxide photoanodes. Covalent attachment of molecules to metal oxide surfaces typically demands the presence of an anchoring group that in turn requires synthetic steps to introduce. BODIPY (4,4-difluoro-4-bora-3a,4a-diaza-*s*-indacene) chromophores (Figure 1) have long been used in dye-sensitized solar cells, but carboxylic acid or pyridyl groups typically had to be installed to act as surface anchors. We now find that even without the introduction of such anchors, the BODIPY derivative **2** can bind to TiO_2 surfaces via its BF_2 group through boron–oxygen surface bonds (Figure 2), as shown by X-ray photoelectron spectroscopy (XPS) and density functional theory (DFT) calculations. Dipyrrin, the parent molecule of BODIPY, is also capable of binding directly to TiO_2 surfaces, likely through its chelating nitrogen atoms. These binding modes prove to be even more robust than that of an installed carboxylate and offer a new way to attach molecular complexes to surfaces for (photo)electrocatalytic applications since, once bound, we show that surface bound BODIPY and dipyrrin derivatives exhibit ultrafast photoinjection of electrons into the conduction band of TiO_2, as predicted by quantum dynamics simulations.

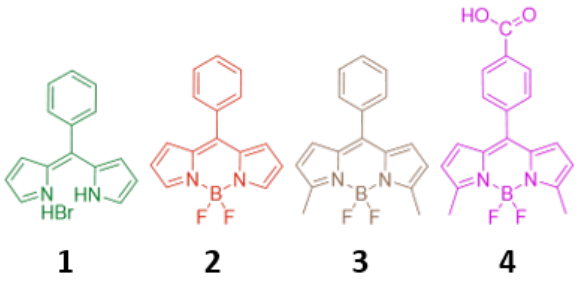

Figure 1. Structures of compounds used for our investigations.

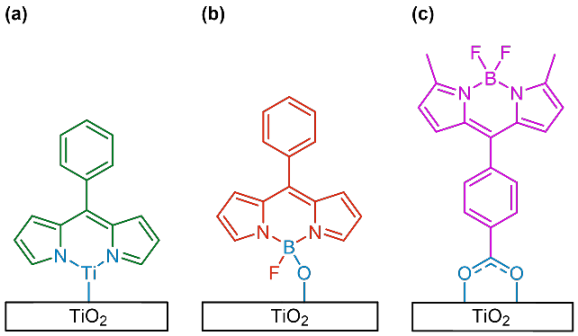

Figure 2. Hypothesized binding modes for **1**/TiO_2, **2**/TiO_2 and **4**/TiO_2.

J.A. Jayworth, M.D. Capobianco, H.-Y. Liu, C. Decavoli, R.H. Crabtree and G.W. Brudvig, *Dalton Trans.* (2022) **51**, 14260.

Photoelectrochemical Properties of n-Type and p-Type $BiFeO_3$ Photoelectrodes

Daye Seo, Andjela Radmilovic, Sophya F. Alamudun, Xin Yuan, and Kyoung-Shin Choi
Department of Chemistry
University of Wisconsin-Madison
Madison, Wisconsin, 53706

The overall objective of our project is to develop and investigate potentially promising ternary oxide-based semiconductor photoelectrodes for use in solar hydrogen production. For each system we investigate, we elucidate composition-morphology-property relationships, accurately assess advantages and limitations, and develop effective strategies to address the limitations and enhance desired photoelectrochemical properties and stabilities.

In this presentation, we will discuss our recent efforts in developing $BiFeO_3$ photoelectrodes. $BiFeO_3$ is a semiconductor with a relatively narrow bandgap of ~2.2 eV. Its conduction band minimum (CBM) and valence band maximum (VBM) positions straddle the water reduction and oxidation potentials. These features make $BiFeO_3$ a promising material for use in a photoelectrochemical cell (PEC) for water splitting. However, previous experimental and theoretical studies on $BiFeO_3$ mainly focused on its ferroelectric properties, and the photoelectrochemical properties of $BiFeO_3$ have not yet been thoroughly investigated.

We will first discuss the synthesis and properties of n-type $BiFeO_3$ that can serve as a photoanode (**Fig 1a**). We show that we can intentionally generate more oxygen vacancies in the pristine n-type $BiFeO_3$ via annealing with N_2, which increases the majority carrier density. We will discuss how this change affects the bandgap, flatband potential, photocurrent generation, and photoelectrochemical stability of $BiFeO_3$ photoanodes. Next, we will discuss how we can modify our synthesis to produce p-type $BiFeO_3$ that can serve as a photocathode (**Fig 1b**). In our method, we substitutionally dope Na^+ at the Bi^{3+} site, which generates shallow acceptor states. We will show the photoelectrochemical performances of the resulting Na-doped $BiFeO_3$ photocathodes and compare the differences and similarities between $BiFeO_3$ photoanodes and photocathodes. The understanding gained from this study will be used to produce and investigate various Bi-based photocathodes.

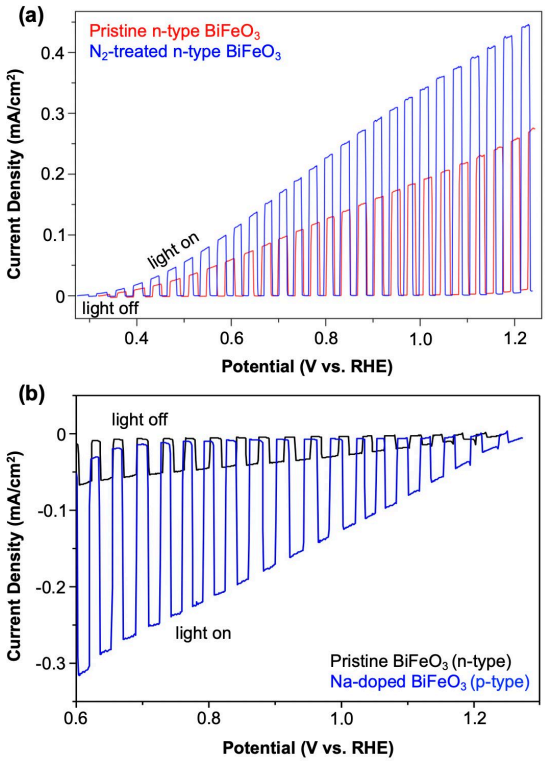

Fig. 1. (a) J-V plots of pristine n-type $BiFeO_3$ (red) and N_2-treated n-type $BiFeO_3$ (blue) for sulfite oxidation in pH 9.2 borate buffer. (b) J-V plots of pristine n-type $BiFeO_3$ (black) and p-type Na-doped $BiFeO_3$ (blue) for O_2 reduction in pH 13 KOH. (All measurements were performed under AM 1.5G illumination).

CO insertion into a Ru-H bond: the role of formyl intermediates in the interconversion between isomers

Sai Desai, Andressa Muller, Chiara Cappuccino, Mehmed Z. Ertem, Javier J. Concepcion
Chemistry Division
Brookhaven National Laboratory
Upton, NY 11973

Metal hydrides play a pivotal role in mediating key elementary steps leading to the formation of CO_2 reduction products. A detailed understanding of the hydride transfer step may enable efficient conversion of CO_2 to formic acid, methanol, and other value-added chemicals. The change in Gibbs free energy for the hydride transfer (thermodynamic hydricity) between donor (e.g., a metal-hydride) and acceptor (e.g., CO_2) determines if the hydride transfer is viable or not. A series of Ru hydride isomers with N-heterocyclic carbene (NHC) ligands will be presented in this poster. Three main aspects will be discussed for this series: a) interconversion between the three isomers; b) thermodynamic hydricity; and c) kinetic hydricity. In topic a) the interconversion between isomers through formyl intermediates generated by insertion of CO into a Ru-H bond will be discussed. To our knowledge, this is the first experimental demonstration of this process. Understanding the reactivity of metal formyl intermediates might enable the identification of homogeneous catalysts that operate at lower temperatures, pressures, and/or overpotentials than currently known catalysts for CO_2 hydrogenation and electrochemical/photochemical CO_2 reduction. In topic b) the thermodynamic hydricity within this series will be discussed. The difference in thermodynamic hydricity changes by ~10 kcal/mol within the series. Such a change is difficult to achieve with the introduction of electron-donating and/or electron-withdrawing groups. Topic c) will address the kinetics for the reaction of the different isomers with CO_2 in acetonitrile to generate formate using a combination of ^{1}H-NMR and stopped-flow IR. The reaction of the Ru-NHC hydrides in this series with CO_2 is significantly faster than for other Ru hydrides with similar or even lower hydricities. This is a clear demonstration of the *trans* effect of the carbene ligand on the rate of hydride transfer (kinetic hydricity).

Preliminary experiments with Fe and Co analogues using the same ligand environment will also be presented. The changes in stability, isomerization rates and thermodynamic and kinetic hydricities on going from Ru to Fe and Co analogues will be discussed.

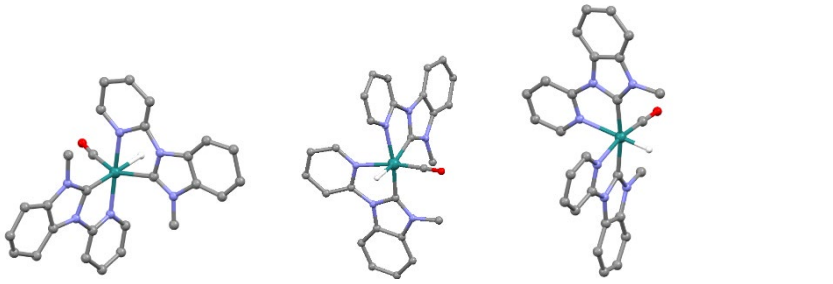

C-*trans*_H, C-t*rans*_CO C-*trans*_H, N-t*rans*_CO N-*trans*_H, N-t*rans*_CO

Figure 1. X-ray structures of the isomeric Ru-NHC hydrides.

Directional Excited State Charge Transfer for Solar Energy Conversion Tracked with Element Specificity

Amy Cordones-Hahn,[1] Michael Mara,[2] Xiaosong Li,[3] Karen Mulfort,[2] Ksenija Glusac,[4] Lin Chen[2,5]

[1]Stanford PULSE Institute, SLAC National Accelerator Laboratory, Menlo Park, CA 94025
[2]Chemical Sciences and Engineering, Argonne National Laboratory, Lemont, IL 60439
[3]Department of Chemistry, University of Washington, Seattle, WA 98195
[4]Department of Chemistry, University of Illinois, Chicago, Chicago, IL 60607
[5]Department of Chemistry, Northwestern University, Evanston, IL 60208

Solar energy conversion to fuels and electricity requires multi-step photo-redox and photo-chemical processes. Following light absorption, the direction of electron density migration and nuclear motions resulting from photon energy dissipation are governed by the interplay between electrons and nuclei in excited states. Thus, a detailed understanding of the light-driven electronic and nuclear response of energy conversion materials is needed to optimize photochemical reaction outcomes, minimize energy losses, and increase light energy conversion efficiency. The continued development of novel ultrafast x-ray methods provides unprecedented opportunities for tracking electronic/nuclear motions in real time along excited state trajectories.

We are applying ultrafast x-ray absorption spectroscopy (XAS) to directly detect how electronic/nuclear reorganization in the excited and intermediate states facilitate directional charge transfer towards catalytic reaction sites. Our focus is on heterobimetallic donor-bridge-acceptor motifs that combine light absorber and catalytic sub-units. By using the elemental specificity of XAS, we track the real-time excited-state charge distribution at specific metal, ligand, and bridge atoms and can fully resolve and distinguish intra- and inter-molecular electron transfer pathways. Using metal atom XAS, we probed metal-metal coupling in the excited states of tetrapyridophenazine (tpphz) bridged Cu-Ru and Cu-Os complexes. We observed efficient metal-to-metal electron transfer in the former, but not the later complex (Figure 1, lower panels), and now aim to understand how tuning metal and bridge composition influences the excited state coupling. Metal atom XAS was also used to investigate tpphz-bridged Ru-Pt and Ru-Rh complexes (with S. Rau and B. Dietzek), thought to drive reductive photochemistry at the Pt and Rh moieties. Our initial investigations of these systems show that excited state metal-to-metal charge transfer is not a dominant process in either system, contrasting previous conclusions from optical spectroscopy. Finally, to investigate the intra-ligand electron transfer processes that may instead dominate in these systems, we have demonstrated that N atom XAS can spectrally distinguish unique ligand and bridge N sites in tpphz-bridged dimers. We applied this method in the ultrafast time domain to track ligand-to-bridge electron transfer in real-time.

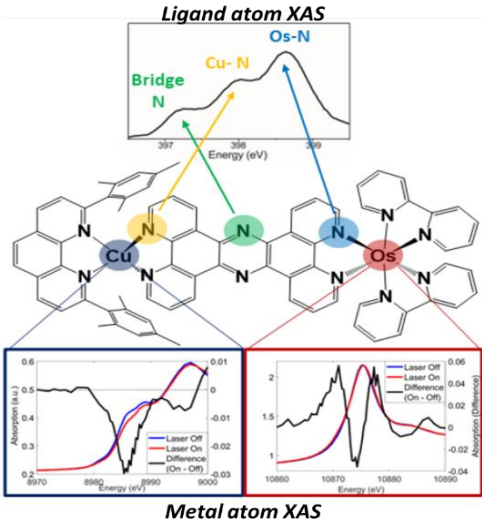

Figure 1. The combination of metal and ligand atom XAS provides an unprecedented view of excited state electron transfer processes in donor-acceptor dyads.

Designing Disordered Photocathodes for Solar-Driven Glycerol-to-H2 Photoelectrochemistry

Hamed Mehrabi, Zebulon Schichtl, Samuel Conlin, Blake Stirling, and Robert H. Coridan
Department of Chemistry and Biochemistry
University of Arkansas
Fayetteville, AR 72701

The overall goal of this research project is to design disordered colloidal composites to increase light absorption in thin film-based photoelectrodes. Recently we have focused on the potential for pairing $CuBi_2O_4$ photocathodes and glycerol-assisted dark electrolysis as a route to photoelectrochemical (PEC) hydrogen generation. $CuBi_2O_4$ can achieve relatively positive photocurrent onset potentials for hydrogen evolution (> 1V vs. RHE), though the incident photon-to-current collection efficiency is limited by the material's short minority carrier diffusion length (~ 50 nm).[1] Coupling this material with favorable hierarchical structure can form the basis for a simple, passive light concentrating strategy. This tailors the behavior of thin layers of $CuBi_2O_4$ to absorb significant fractions of incident light in layers that are thin enough to induce high carrier collection yields. Here we highlight recent progress in our research program towards those goals. We use finite-element, time-domain (FDTD) simulations to design the hierarchically structured colloidal composite scaffold on which a thin film $CuBi_2O_4$ photocathode can be structures. The simulations allow us to identify the optimal ensemble design of a composite that colocalizes the light absorbing semiconductor and emergent light concentration in the composite. This work includes the development of a machine learning-based emulation technique to act as a sparse approximation of larger design parameter spaces. We have also developed a chemical approach to the synthesis of colloidal "atoms", or sacrificial colloids functionalized with Cu and Cu/Bi metal layers to simultaneously form the light concentrating pore and functionalize it with a light-absorbing semiconducting oxide layer. Finally, we will discuss the effect of using a bipolar membrane for separating the anode and cathode compartments of an integrated PEC system to improve the generalizability of the glycerol electrooxidation reaction.[2] In future work, we aim to combine these three ideas to fabricate a scalable demonstration of a high-rate solar-to-H_2 integrated PEC device.

1. Cooper JK, Zhang Z, Roychoudhury S, Jiang C-M, Gul S, Liu Y-S, Dhall R, Ceballos A, Yano J, Prendergast D, Reyes-Lillo SE (2021) CuBi2O4: Electronic Structure, Optical Properties, and Photoelectrochemical Performance Limitations of the Photocathode. *Chemistry of Materials*, 33(3):934–945. https://doi.org/10.1021/acs.chemmater.0c03930

2. Schichtl ZG, Conlin SK, Mehrabi H, Nielander AC, Coridan RH (2022) Characterizing Sustained Solar-to-Hydrogen Electrocatalysis at Low Cell Potentials Enabled by Crude Glycerol Oxidation. *ACS Applied Energy Materials*, 5(3):3863–3875. https://doi.org/10.1021/acsaem.2c00377

Identifying and Circumventing Kinetic Barriers to Metal Hydride Complex Formation in Fuel-forming Catalysis

Jillian L. Dempsey, Jaruwan Amtawong, Zoe Claytor, Annie McCullough, Charlotte Montgomery
Department of Chemistry
University of North Carolina at Chapel Hill
Chapel Hill, NC 27599-3290

Proton-coupled electron transfer (PCET) processes underpin the catalytic transformations that take energy-poor substrates to energy-rich fuels. Many of these catalytic transformations proceed through metal hydride intermediates. Intriguingly, mechanistic studies undertaken by our lab reveal the PCET reactions that form metal hydride intermediates almost exclusively follow a stepwise electron transfer–proton transfer pathways. Moreover, in several examples, ligands are initially protonated, followed by a tautomerization to yield the stable metal hydride product. The preference for a stepwise reaction over a concerted proton-coupled electron transfer (CPET) route that circumvents the high energy, charged intermediates associated with stepwise pathways, as well as a kinetic preference for protonating the ligand over direct metal protonation, suggests multiple factors dictate the PCET reactions that form metal hydride species. Projects in our lab aim to understand the factors underpinning reaction pathways that yield metal hydride complexes.

We hypothesized that an intrinsic barrier to metal protonation both inhibits access to the CPET pathway and kinetically favors ligand protonation over metal protonation. High inner-sphere reorganization energies arising from the geometric changes that occur upon metal protonation are suspected to give rise to this barrier. In support of this hypothesis, we show a strong correlation between the isolated proton transfer reaction and associated reorganization energy. This trend holds for a range of metal and ligand architectures. Our ongoing work is focused on examining the mechanisms by which PCET reactions proceed to test the hypothesis that a CPET process is accessible for coordination complexes that have low reorganization energies for proton transfer.

In parallel, we are examining how ligand acid-base functionality can be leveraged for kinetically accessible protonation sites. Using the model complex $[Co^{III}Cp(P_2{}^RN_2{}^{R'})(CH_3CN)]^+$, which reacts to form a cobalt hydride species, we are examining the thermodynamic and kinetic factors that dictate ligand-based vs. metal-based PCET reactivity. Combining electrochemistry and spectroscopy, we are mapping the PCET pathways by which the cobalt hydride species forms. Our data show that acid strength, acid concentration, pendant amine basicity, and timescale between electron transfer steps dictate the mechanism of hydride formation. Ongoing work is focused on establishing structure–reactivity relationships for the $P_2{}^RN_2{}^{R'}$ class of ligands.

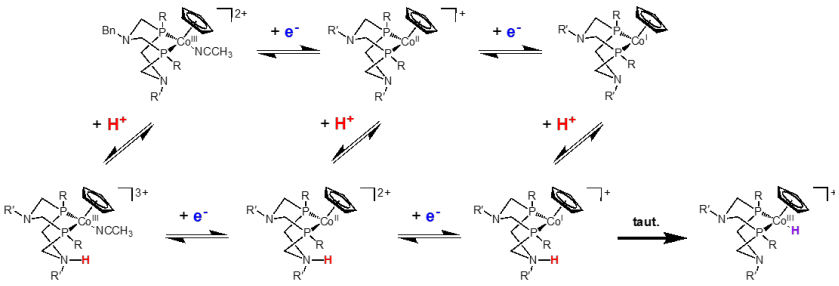

Figure 1. PCET pathways for ligand-based metal hydride formation for $[Co^{III}Cp(P_2{}^RN_2{}^{R'})(CH_3CN]^+$ complexes

Gating of Spin-based Quantum States for QISE

Subrata Ghosh, Anitha Alanthadka, Devon Adecer, Harini Wimalasekera, Mitra Rooien, Sergey Varganov, and Natia L. Frank*
Department of Chemistry
University of Nevada
Reno, NV 89557

The optical manipulation of spin quantum states provides an important strategy for quantum control with both temporal and spatial resolution for quantum computing, sensing and communications. While significant progress has been made in the discovery of molecular spin-based qubits with long decoherence times, current challenges are focused on molecular quantum sensors that have long decoherence times, (achieved by isolation from the bath) and strong coupling to the environment (achieved by strong coupling to the bath) required for sensing of external field or analytes. We report here a strategy for coupling molecular spin-based qubits to the bath without sacrifice of decoherence times. Photochromic ligands that undergo isomerization in response to changes in solvation, electric field, temperature, or light can be used to modulate electron transfer-coupled spin transition processes, spin-orbit coupling, and ligand-metal electronic coupling in bound transition and lanthanide metal ions. Visible light irradiation (λ_{exc} = 550-600 nm) of a spirooxazine cobalt−dioxolene complex induces photoisomerization of the ligand that in turn triggers a reversible intramolecular charge-transfer coupled spin- transition process at the cobalt center between a low-spin Co(III)−semiquinone doublet and a high-spin Co(II)−bis-semiquinone sextet state. Determination of the spin relaxation and decoherence times of the low-spin Co(III)−semiquinone doublet state reveal slow spin dynamics and decoherence, and a change in the population of the SQ state (m_s ± 1/2) qubit state with light modulation. Extension of this strategy to low-spin transition metal (S = 1/2) and lanthanide complexes leads to reversible changes in spin relaxation rate, decoherence time, and g-value with changes in photochromic ligand state, providing a robust strategy for quantum sensing in molecular spin-based qubits. We report here a Cu(II) (N4) photochrome complex (S=1/2) that exhibits a shift in g-value at room temperature upon photoisomerization with a metastable state lifetime of 25-85 min at room temperature. Pulsed EPR measurements reveal an significant change in decoherence rates with isomerization, and Rabi oscillations with a spin-flip rate of 56 ns. Theory and pulsed EPR spectroscopy provides effective modeling of the phenomenon and long-term strategies to further modulate spin-based molecular systems for quantum sensing at the single molecule level.

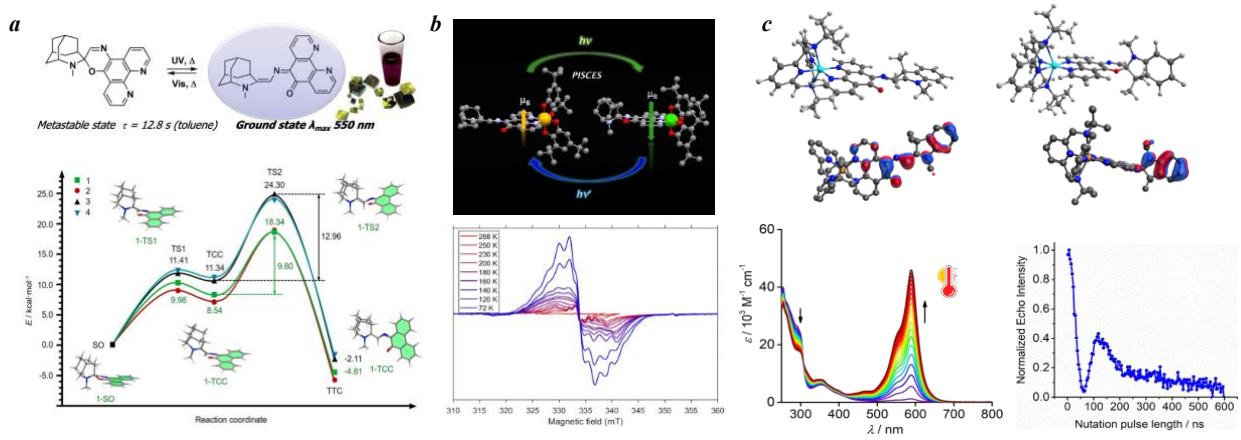

Identification of Nuclear Coordinates Driving Solar Energy Conversion Processes Using Ultrafast Raman Techniques

Christopher Rich, Margaret Clapham, Polly Lynch, Shahzad Alam, Renee R. Frontiera
Department of Chemistry
University of Minnesota
Minneapolis, MN 55104

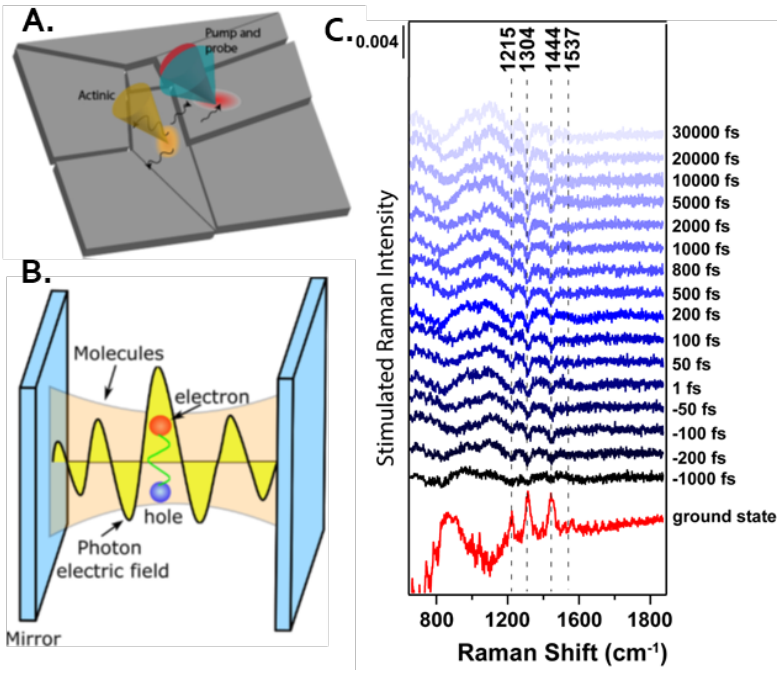

Figure 1. A. Depiction of spatially-offset femtosecond stimulated Raman spectroscopy. B. Raman probing of excitonic polaritons. C. Preliminary FSRS results of rubrene polariton dynamics.

The goal of our DOE-sponsored research is to use advanced Raman spectroscopies to provide synthetic insight on molecular-based solar energy conversion systems. Specifically, we aim to identify certain nuclear coordinates and vibrational coherences which can be rationally modified in order to improve function. We make use of femtosecond stimulated Raman spectroscopy (FSRS), which monitors multidimensional structural changes on an ultrafast timescale. Our group has made a number of technical advancements to the FSRS technique, including incorporation of an optical microscope, development of spatially-offset FSRS, coherent control methods to identify driving from spectator modes, and development of methods to discriminate electronic from vibrational signatures. We now make use of these technical advancements to provide definitive scientific insight into the optimal design of molecular systems for solar energy conversion and capture, including fundamentals of how to control electron transfer and transport. Our work towards this goal contains three independent but interrelated aims, all of which experimentally map multiple dimensions of highly reactive potential energy landscapes in complex environments. First, we use spatially-offset FSRS to identify specific nuclear coordinates promoting electron and exciton transport (Figure A), focusing on both inter- and intra-molecular motions. Second, we are using advanced Raman techniques to map out potential energy landscapes of polaritonic systems (Figure B), including preliminary FSRS results on structural changes occurring during rubrene singlet fission (Figure C). Finally, we are integrating electrochemical capabilities into our ultrafast Raman system, in order to determine how applied bias can impact specific nuclear coordinates driving photoelectrochemistry.

Functionally Active Linker Design for Photoactive Molecules at Semiconductor Interfaces

Elena Galoppini, Yang Zhang, Katherine Lloyd
Chemistry Department, Rutgers University, Newark, NJ 07102

Robert A. Bartynski, Sylvie Rangan, Jonathan Viereck
Department of Physics and Astronomy, Rutgers University, Piscataway, NJ 08854

For the design of new photocatalysis and solar devices, and a better understanding of relevant photophysical processes, it is necessary to achieve molecular-level control over specific interfaces. This remains a significant and evolving challenge because of the heterogeneity and complexities associated with surfaces of nanostructured materials and electrodes. The poster will illustrate our results and future plans toward advanced linker-anchor designs to tune charge separation between organic/redox active groups and semiconductors. Originally developed for applications in dye-sensitized solar cells, molecular-based approaches with tunable linker-anchor moieties have since become relevant to solar fuels production, solar energy capture and conversion at interfaces.

Recent Results: Our approaches have demonstrated that it is possible to predictably shift the energy alignment at the chromophore (ZnTPP or C60/TiO_2 or /ZnO interfaces using helical peptide linkers with a large (18.6 D) and highly oriented molecular dipole. In this funding cycle we demonstrated two synthetically versatile approaches that lead to shifts up to 600 meV (**Fig. 1a**). These results point to the use of molecular dipole monolayers for controlling energy level alignment at organic/inorganic interfaces.

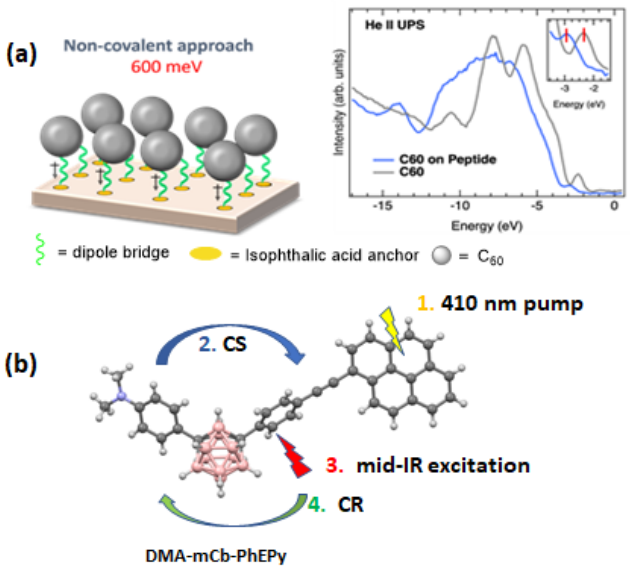

Figure 1. (a) schematic representation of the non-covalent dipole approach and UPS spectra showing 600 meV HOMO shift. (b) Charge transfer experiment with Donor-Acceptor system with IR-active linker. (CS= charge separation, CR= charge recombination

We will discuss our progress and future plans in controlling charge transfer rates, especially recombination, and tuning electronic coupling on TiO_2 and ITO by (1) conformational effects of one of the linkers and their substitution position (ortho or peri position in perylenes, for instance); (2) use of novel anchor groups 2-hydroxyisophthalic acid and pyridine-2,6-dicarboxylic acid.

Finally, we developed IR-active linkers, where charge transfer can be promoted by excitation with infrared radiation. The first model system (Pyrene-m-carborane-*N,N*-dimethylaniline) is currently being studied by the Rubtsov group at Tulane. Probing in the visible (400 nm pump) shows spectral changes which are consistent with IR-induced charge recombination. (**Fig. 1b**). Our future plans include synthetic modifications to enhance both this effect and substitutions to allow surface attachment.

From Captured CO_2 to Value-added Chemicals: A Photochemical Approach

Lin Chen,[†] Amy Cordones-Hahn,[‡] Ksenija D. Glusac,[†] David Kaphan,[†] Alex Martinson,[†] Karen Mulfort,[†] David Tiede,[†] Peter Zapol[†]

[†]Chemical Sciences and Engineering Division, Argonne National Laboratory, Lemont, Illinois 60439

[‡]Stanford PULSE Institute, SLAC National Accelerator Laboratory, Menlo Park, California 94025

We investigate *photoreductive CO_2 capture,* an approach that combines the direct-air capture of CO_2 with its conversion into value-added chemicals, such as formate ion, using visible light as an energy input. We investigate light-responsive MOFs as scaffolds for photochemical upgrading of CO_2, transition metal complexes with pendant groups for direct-air CO_2 capture and metal-oxide nanoclusters for desired chemical transformations.

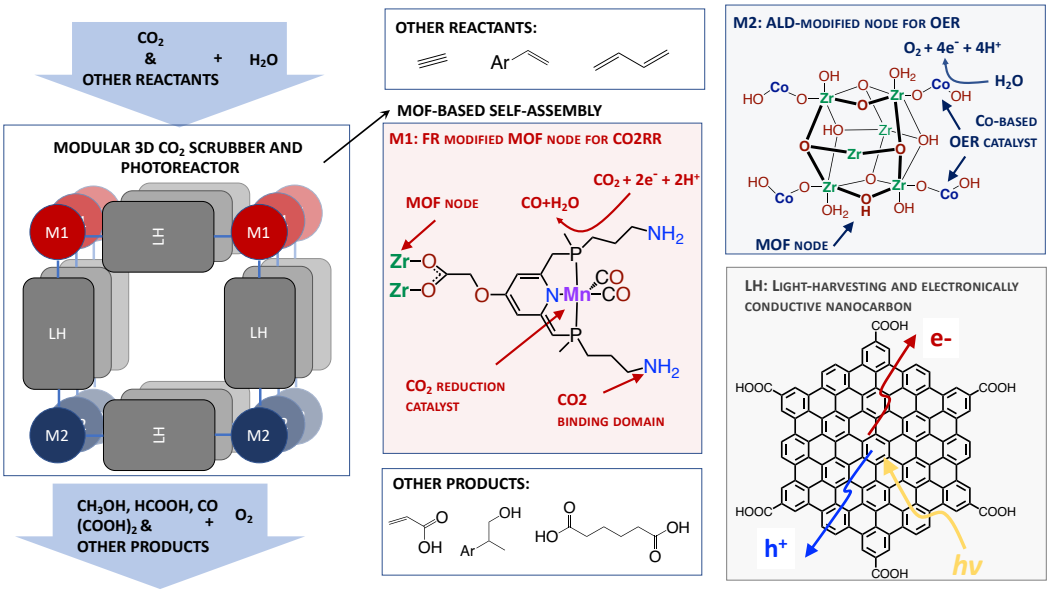

Here, we report our recent findings on photo-reductive CO_2 capture that include: (i) the discovery of light-responsive nanographene MOFs whose bandgaps can be tuned throughout UV/Vis/near-IR ranges using a simple post-synthetic oxidation reaction; (ii) the exploration of photo-reductive CO_2 capture using Zr-bicarbonate intermediates on MOF nodes; (iii) development of an atomic layer deposition method for the preparation of well-defined In-oxide nanoclusters in polymer matrix and these materials were explored for CO_2 capture; (iv) a study of reactive CO_2 capture via the insertion of CO_2 into metal-hydride bonds to generate metal-formate adducts; (v) study of secondary coordination sphere effects in electrocatalytic CO_2 reduction via novel Co-based complexes with pendant N-containing moieties; (vi) study of CO_2 capture by Rh-based catalysts with pendant alcohol groups. These studies have provided us with novel chemical approaches that combine capture and conversion of CO_2. In our future work, we plan to explore the factors that control the CO_2 capture selectivity in the presence of other air constituents (molecular oxygen and water), as well as factors that lead to the loses in photochemical activation of our porous materials.

Tuning Photoelectrochemical Thermodynamics and Kinetics via Semiconductor Strain and Elevated Pressure

Ann L. Greenaway, Zebulon Schichtl
Materials, Chemistry, and Computational Science
National Renewable Energy Laboratory
Golden, CO 80401

Harnessing charge transfer across a semiconductor-electrolyte interface requires detailed control over the surface density of states (DOS). Surface strain is well-recognized as a tool to modify structure/property relationships, and as photoelectrochemical fuel-forming reactions continue to gain interest, strain presents an underutilized route to understanding and controlling reactivity. We are interested in the effect of surface strain in two areas: (1) limiting undesirable degradation reactions and (2) understanding semiconductor-electrolyte interactions and reaction rates for multi-step product formation. Semiconductor corrosion in aqueous environments remains a critical issue across photoelectrochemical fuel-forming reactions despite extensive study, and increasing interest in complex product formation (*e.g.* C_{2+} products in CO_2R) will require fine control over reactivity which may be accessible via strain. We are developing platforms to investigate the influence of strain on both semiconductor degradation and complex product formation, as fine control over surface strain is difficult to achieve. NREL has previously demonstrated that *dynamic* strain, directly imparted by use of a superelastic alloy substrate, can reversibly modify the activity of TiO_2 for both HER and OER. We plan to expand on previous work on dynamic strain by investigating strain effects on competing reactions (CO_2R and HER), and directly using X-ray photoelectron spectroscopy to investigate reactant binding with strained semiconductor surfaces in an ambient pressure system. Because *static* strain can also be imparted into many semiconductors through substrate choice, we will similarly investigate reactant binding to statically strained surfaces (*e.g.* GaInP).

We are also developing a platform to investigate pressure as a tool to tune reaction dynamics. Fuel-forming reactions (CO_2R and N_2R) require a H^+ source, which has led to work in aqueous (photo)electrochemical environments where reaction rates are limited by reactant gas solubility and fuel formation inevitably competes with HER. Translation to high-pressure, non-aqueous (organic) environments could improve understanding of reaction fundamentals, by removing substrate starvation, addressing elementary reaction steps without competing processes, and limiting aqueous corrosion. We are currently awaiting delivery of a high-pressure reactor which will enable investigation of CO_2RR up to supercritical pressures (83 bar at 31 ºC). This pilot reactor will be used to establish electrochemical baselines for CO_2RR on metallic surfaces with controlled H^+ concentrations, with future work focused on investigating elemental reactions under illumination in a next-gen reactor with integrated windows.

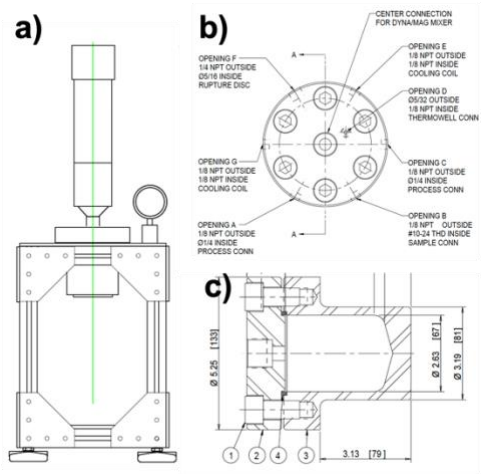

Figure 1: Schematics of a) the overall CO_2RR reactor, b) top view and c) side view of cell.

Steric Versus Lewis Basicity Influence of the Second Coordination Sphere on Electrocatalytic CO_2 Reduction by Manganese Bipyridyl Complexes

David C. Grills and Mehmed Z. Ertem
Chemistry Division
Brookhaven National Laboratory
Upton, NY 11973-5000

In this study,[1] our goal was to obtain a greater insight into the balance between steric and Lewis basic influence on the efficiency of CO_2 reduction mechanisms with $[Mn^I(R_2\text{-bpy})(CO)_3(CH_3CN)]^+$ pre-catalysts, and on their respective transition state geometries/energies for the rate-determining C–OH bond cleavage step that leads to CO evolution.

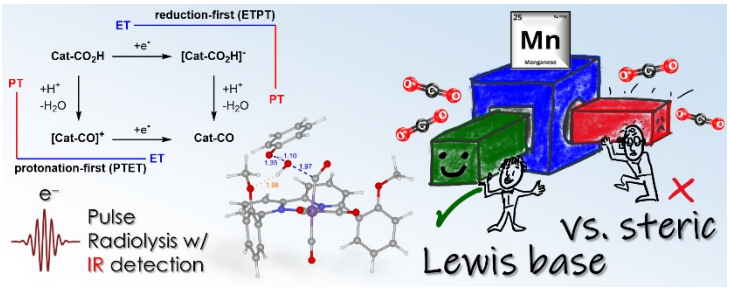

We focused on the second coordination sphere (SCS), creating a series of catalysts with varying amounts of steric bulk and Lewis basicity in the functional groups at the 6,6'-positions of the bipyridyl (bpy) ligand. A common pathway seen in CO_2 reduction with this family of catalysts is dimerization, creating a Mn–Mn bonded dimeric intermediate that needs to be further reduced (at a significant energy cost), in order to produce the catalytically active intermediate. Dimerization can be prevented by introducing steric bulk into the SCS. However, this tends to waste energy by increasing the activation barrier for the critical rate-determining C–OH bond cleavage step. The introduction of Lewis basic groups into the SCS of a bulky catalyst can offset this energy wastage and provide a lower-energy pathway via hydrogen bonding interactions with Brønsted acids that are typically added to the reaction mixture, albeit often with slower reaction kinetics.

In this work, we have shown that there is a fine balance between the steric bulk and the Lewis basicity of the SCS when optimizing the thermodynamic and kinetic parameters of a catalytic CO_2 reduction process. For example, we show that the diphenyl-substituted bpy ligand is just bulky enough to sufficiently hinder dimerization in the presence of CO_2 (yet not fully prevent it in the absence of CO_2), while it is not too bulky so that the activation barrier for C–OH bond cleavage remains low. Thioethers in the SCS are worse hydrogen-bond acceptors than ethers, resulting in poorer CO_2 reduction performance. The knowledge gained from this work will aid the development of new and improved CO_2 reduction catalysts with fully optimized SCS's to minimize overpotentials and maximize rates of catalysis.

1. Blasczak, V.; McKinnon, M.; Suntrup, L.; Aminudin, N. A.; Reed, B.; Groysman, S.; Ertem, M. Z.; Grills, D. C.; Rochford, J. *Inorg. Chem.* **2022**, *61*, 15784-15800.

Acknowledgments: We thank our collaborator, Prof. Jonathan Rochford (U. Mass, Boston), for the synthesis of the Mn complexes and their complete electrochemical analysis.

Improving and measuring water oxidation catalyst viability

Colton Breyer, Miguel Ibanez, Jake Kerkhof, Mustafa Yildirim, Luka Pochkua, Nilay Kanova, Carlamarina Osuna Alvarez, Diane Smith*, Douglas Grotjahn
Department of Chemistry and Biochemistry
San Diego State University
San Diego, CA 92182-1030

* deceased 24 October 2022; this presentation is in her memory

Our overall goals are to (1) slow the rate of water oxidation electrocatalyst (WOEC) degradation, (2) enable molecular WOEC activity in acid, and (3) create and refine new methods for characterizing WOEC stability. We have made progress in all three areas.

Our labs published a paper in early 2021 disclosing the profound benefits of including a sulfonate functional group in the active site of a water oxidation catalyst (**1a**), improving initial rates in Ce(IV)-driven reactions by 300x, and in electrocatalytic reactions in 0.1 M nitric acid by >40x. Key questions about what are the roles of the sulfonate are being investigated through analog synthesis: for **1b**, initial rates in Ce(IV)-driven reactions increase by 30x, and in electrocatalytic reactions in pH 7 phosphate buffer by 3x relative to those for **1a**; for **2**, electrochemical studies are in progress. In collaboration with Jamal Musaev a computational and experimental study of the mechanism of **1a**, **1b** and **2** is underway, with the goal to predict further improvements and then test them experimentally.

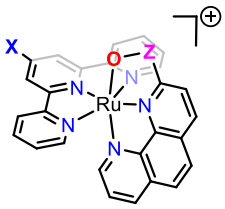

Z = SO_2
1a X = H (published 2021)
1b X = OEt
2 X = H, Z = P(O)(OR)

We have further investigated the effects of a sulfonate group in the active site of WOEC by comparing **4** from the Sun group with mono-sulfonate analogs **5**: turnover number with Ce(IV) is increased 1.4x with **5b-1** and observed catalytic current in pH 7 phosphate buffer increased 6x with 100% faradaic efficiency for **5a-1**. Notably, **4** become heterogeneous after 15 h of bulk electrolysis at pH 7, whereas **5a-1** remains homogeneous, Catalyst **5a-1** also gave strong electrocatalytic currents at pH values as low as 2.5. Current computational studies are underway to determine the mechanistic improvements produced by the sulfonate group.

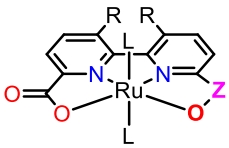

4 Z = CO, R + R = HCCH
L = picoline
5 Z = SO_2
a R + R = HCCH
b R = H
-1 L = picoline
-2 L = isoquinoline

It is possible that sulfonate anions exert an electrostatic effect on redox (cf Yang group) and also catalysis. We have several ideas to explore electrostatic effects including NHC complexes **3** with varying numbers of R^{1-4} being SO_3 and the remaining R being H. Progress in synthesis and characterization will be reported, with significant progress on the tetrasulfonate.

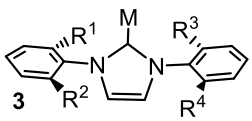

3

We have also developed a method to estimate kinetic parameters for WOEC using cyclic voltammetry for data suffering from a non-purely kinetic regime, which is very common for WOEC. By statistically extracting a catalytic potential through the optimization of fits and intercepts, our method provides a way to treat non-ideal electrochemical data to fairly compare catalytic performance. Data for several catalysts will be shown.

New photoelectrodes, water oxidation catalyst dynamics, and mechanistic studies

Craig L. Hill, Tianquan Lian, and Djamaladdin G. Musaev
Department of Chemistry
Emory University
Atlanta, GA 30322

I. Roles of 3d-metals (TM), adjacent to the active site metal, on stability and reactivity of M-$Co_2TM_2P_2$ polyoxometalate (POM) water oxidation catalysts (WOCs). We have now prepared several POM WOCs that contain the same catalytic 3d metal on the outside of the structure (usually Co; blue balls in Fig. 1) and two internal 3d-metal ions (**TM**) on the inside. Both the catalytic activity and stability vary with **TM**. Fig. 1 shows the first two isostructural POM WOCs we prepared, characterized and compared: $[Co_4(H_2O)_2(PW_9O_{34})_2]^{10-}$ **Co_4P_2** and $[Co_2Ni_2(PW_9O_{34})_2]^{10-}$, **$Co_2Ni_2P_2$.** Several more have now been made and assessed. The electronic and geometry structures of the **$Co_2Ni_2P_2$** and **$Co_2Fe_2P_2$**, as well as the mechanism of water oxidation by these complexes were investigated at the DFT level.

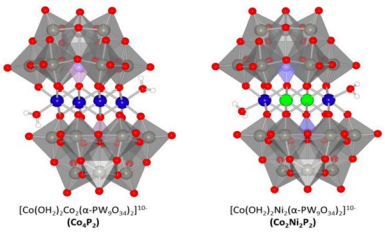

Fig. 1. Co_4P_2 (left) and **$Co_2Ni_2P_2$** (right) water oxidation catalysts. Co: blue; Ni: green; WO_6, gray octahedra.

II. Functionalization of amorphous TiO_2 with an acid-compatible POM for photoelectrochemical water oxidation. We have prepared nanoporous n-type TiO_2 photoelectrodes functionalized with $K_{16}[Co_9(H_2O)_6(OH)_3(HPO_4)_2(PW_9O_{34})_3]$ (**Co_9POM**) by the 3-aminopropyltrimethoxysilane (APS) ligand, and studied the effect of **Co_9POM** on TiO_2 for photoelectrochemical water oxidation in sulfate buffer solution (pH = 2) under UV light. The current-potential curves in Fig. 2 (a) show that **Co_9POM** greatly enhances the water oxidation current, which remains steady during the bulk electrolysis. X-ray photoelectron spectroscopy confirms the stability of **Co_9POM** by exhibiting no change of the cobalt chemical environment after bulk electrolysis.

III. Developing *in-situ* Raman spectroscopy tools for studying water oxidation mechanisms at photoelectrode/liquid interfaces. We have successfully characterized the Raman spectra of WOC-catalyst-modified photoanodes. Fig. 2 (b) are the Raman spectra displaying the characteristic Raman features of amorphous TiO_2 (purple), TiO_2 functionalized with **Co_9POM** (orange), and **Co_9POM** in solid form (green). Observation of characteristic features of WOCs on functionalized TiO_2 provides evidence of the modified semiconductor/liquid interface. Future *in-situ* Raman spectroscopy of functionalized photoanodes will provide more insight into catalyst function and the mechanism of catalytic OER catalytic by the novel hybrid photoanode.

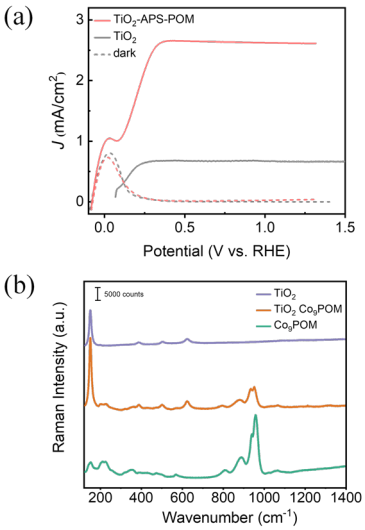

Fig. 2. (a) Current density of unmodified TiO_2 photoanode (black) and functionalized TiO_2 photoanode (red) under 365 nm illumination (solid) and in the dark (dash) (b) Raman spectroscopy of TiO_2 (purple), functionalized TiO_2 (orange) and Co_9POM (green)

Fundamental Studies of the Vibrational, Electronic, and Photophysical Properties of Tetrapyrrolic Architectures

David F. Bocian,[1] Dewey Holten,[2] Christine Kirmaier,[2] and Jonathan S. Lindsey[3]

[1]Department of Chemistry, University of California Riverside, Riverside, CA 92521
[2]Department of Chemistry, Washington University, St. Louis, MO 63130
[3]Department of Chemistry, North Carolina State University, Raleigh, NC 27695

A long-term objective of our program is to design, synthesize, and characterize tetrapyrrole-based molecular architectures that absorb sunlight across the visible and near-infrared spectrum, funnel energy, and separate charge (hole, electron) with high efficiency and in a manner compatible with current and future solar-energy conversion schemes. Here, progress in two areas of our recent work is described.

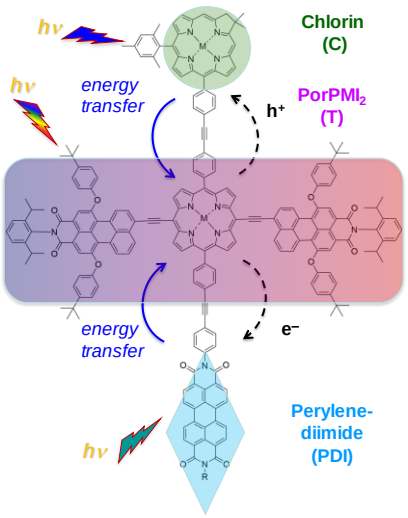

We have developed panchromatic absorbers – based upon a tetrapyrrole strongly coupled to a perylene dye – that afford strong and relatively uniform absorption across the violet to red spectral regions along with robust singlet excited state properties. A panchromatic bis(perylene-monoimide)-porphyrin triad has been incorporated into various pentads to afford long-lived charge separation. The electron acceptor is a peryelene-diimide and the electron donor (hole acceptor) is a chlorin or bacteriochlorin. The pentad in which the central porphyrin is a free base and the chlorin is the zinc chelate, affords a long-lived (microseconds) charge separation across the dyad. The pentad in which the hole acceptor is a bacteriochlorin attached to the core via a phenylethyne linker gives little charge separation despite improved energetics for the hole/electron-shift reaction, likely due to facile charge-recombination. The studies highlight design criteria for balancing panchromatic absorption and long-lived charge separation in molecular architectures for solar-energy conversion.

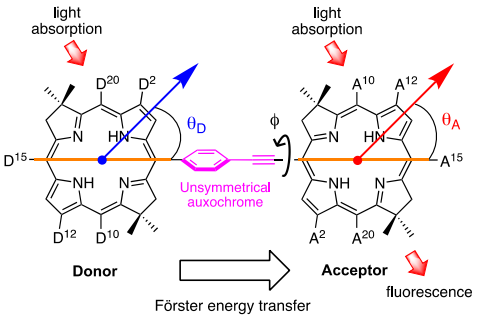

To probe energy-transfer processes akin to those in photosynthetic systems, nine synthetic bacteriochlorin–bacteriochlorin dyads have been prepared wherein the constituents are joined by a phenylethyne linker. The design-predicted donor–acceptor excited-state energy gaps in the dyads agree well with those obtained from time dependent density functional theory calculations and with the measured range of 197 – 1089 cm^{-1}. Similar trends with donor–acceptor excited-state energy gaps are found for (1) the measured ultrafast energy-transfer rates of $(0.3\ ps)^{-1}$ – $(1.7\ ps)^{-1}$, (2) the spectral overlap integral (J) in Förster energy-transfer theory, and (3) donor–acceptor electronic mixing manifested in the natural transition orbitals for the $S_0 \rightarrow S_1$ transition. The collective insights are valuable for studies relevant to artificial photosynthesis and other processes requiring ultrafast energy transfer.

The native efficiency of photo-driven water oxidation: comparing molecular and semiconductor catalysis

Frances A. Houle, Thomas Cheshire, Gabriel Benitez, Ramzi Massad and Chenqi Fan
Chemical Sciences Division and Molecular Biophysics and Integrated Bioimaging Division
Lawrence Berkeley National Laboratory
Berkeley, CA 94720

The electrochemical oxygen evolution reaction (OER) is well known to require a high overpotential, limiting its efficiency. Because the availability of charge carriers and water are essentially unlimited, the origin of the high overpotential is chemical. Photodriven OER is also relatively inefficient, however the flux of photogenerated charge carriers is limited by the solar resource and the photophysics of the dye or semiconductor as well as the chemistry. The interdependence of reactions and excitations is the focus of the present work, where we use stochastic chemical kinetics simulations to examine two very different ways of making O_2, dyes coupled to molecular catalysts, and photocatalytic semiconductors.

Continuous photoexcitation of Ru-BPY dyes by sunlight leads to charge injection into a substrate followed by electron transfer from molecular Ru catalyst to reduce the dye to its ground state. The full photophysical kinetics for charge injection have been determined by quantitative modeling of transient absorption measurements for these dyes, with an injection rate coefficient estimated to be around 10^{11}-10^{12} s^{-1} from all excited states.[1] The upper limit to the overall solar driven injection frequency is about 60 s^{-1}, which limits the accessible OER rate to about 15 s^{-1}. Simulations of a Ru molecular catalyst - dye complex reveals that the overall OER rate is many orders of magnitude slower for that system, however.[2] The calculations show that charge carrier losses are negligible: the reaction rate is controlled by formation of intermediates that are not charge-carrier activated and that react slowly at ambient temperature. This points to opportunities for new catalyst designs to improve efficiency. For comparison, we consider OER on UV-excited TiO_2 as a model system because of the extensive experimental and theoretical data on it. Charge carriers are stored in traps near the O-containing reaction centers. We are examining the kinetics reported in several experimental and theoretical studies for the hole-driven reactions that differ in their interpretation of how the final O-O bond is formed and how holes participate. Hole availability has been proposed to be a key kinetic bottleneck,[3] in contrast to what we have found for fully molecular systems. We will describe simulations of mechanisms built from theoretical data to evaluate this interpretation and compare their predictions to experimental observations.

1. Cheshire, T.P., Boodry, J., Kober, E.A., Brennaman, M.K., Giokas, P.G., Zigler, D.F., Moran, A.M., Papanikolas, J.M., Meyer, G.J., Meyer, T.J., and Houle, F.A. (2022). A Quantitative Model of Charge Injection by Ruthenium Chromophores Connecting Femtosecond to Continuous Irradiance Conditions. J Chem Phys. 10.1063/5.0127852.
2. Massad, R.N., Cheshire, T.P., Fan, C.Q., and Houle, F.A. (2023). Water oxidation by a dye-catalyst diad in natural sunlight: timing and coordination of excitations and reactions across timescales of picoseconds to hours. Chem Sci *14*, 1997-2008. 10.1039/d2sc06966k.
3. Kafizas, A., Ma, Y.M., Pastor, E., Pendlebury, S.R., Mesa, C., Francas, L., Le Formal, F., Noor, N., Ling, M., Sotelo-Vazquez, C., et al. (2017). Water Oxidation Kinetics of Accumulated Holes on the Surface of aTiO2 Photoanode: A Rate Law Analysis. Acs Catal *7*, 4896-4903. 10.1021/acscatal.7b01150.

Understanding Hole Potentials Under Multiple Concurring Redox Processes at Semiconductor Photocatalysts

Shu Hu
Department of Chemical and Environmental Engineering
Yale University, New Haven, CT 06510

Particulate photocatalysts, usually in a powder suspension or panel form, coevolve reductive and oxidative reactions in nanoscale proximity. Photocatalysis involves light absorption, charge separation, charge transfer, surface catalysis, and chemical transport across multiple scales. The local charge separation and local coevolution have unique advantages such as operation in neutral pH water or water vapor instead of strong acid or base, promising scale-up solar-to-chemical conversion. Despite the near-unity quantum efficiency achieved for $SrTiO_3$ particles, the timescale mismatch between light absorption and surface catalysis poses a grand challenge in understanding how efficient charge separation can be achieved. We design photocatalyst-electrodes for probing photocatalysts under operating conditions. The H_2/O_2 gas compositions are varied, and the charge separation efficiencies are measured using carrier-selective back contacts. Notably, we probe the hole quasi-Fermi levels during operation. Local potential and kinetics measurements in a photoelectrochemical cell are combined with semiconductor physics and micro-kinetic modeling, to elucidate the roles of nanoparticle co-catalysts, molecular co-catalysts, and corrosion pinholes in local charge separation. We design the charge separation to achieve multi-electron charge accumulation, selective-area polymerization, and lateral electric field control.

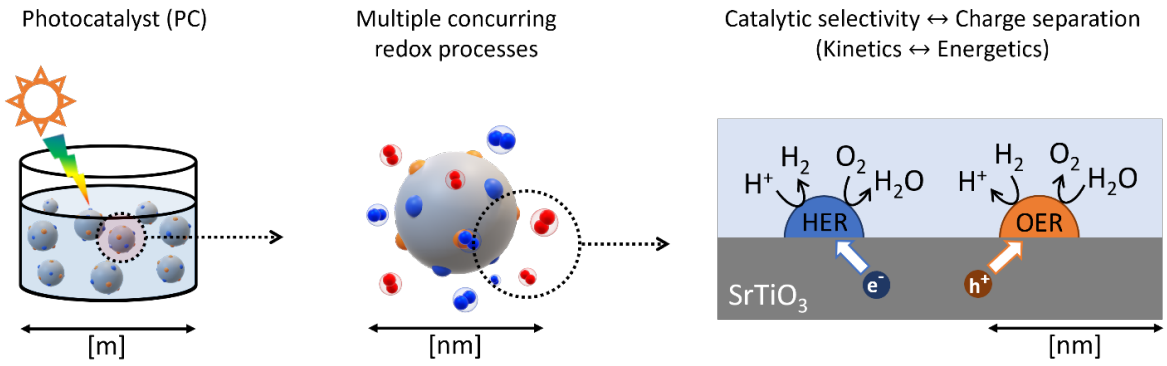

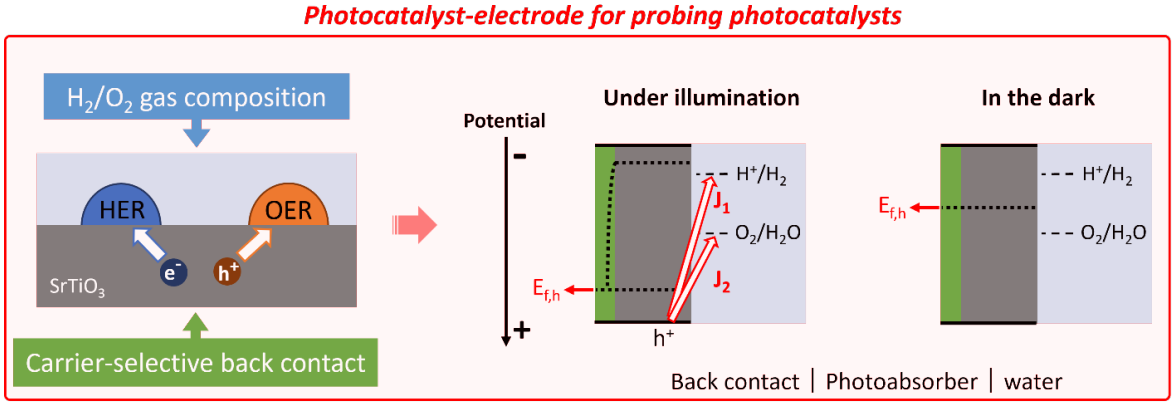

Structural, Photophysical, and Photocatalytic Properties of Covalent Organic Frameworks

Daniel Streater,[1] and Jier Huang*[1,2]

[1]Department of Chemistry, Marquette University, Milwaukee, WI 53233
[2]Department of Chemistry, Boston College, Chestnut Hill, MA 02467

Covalent organic frameworks (COFs) are a promising class of polymeric materials with future uses across a wide range of applications such as gas storage, drug delivery, catalysis, and light emitting devices (LED). Their versatility is the result of ordered structures that form into predictable, porous topologies defined by the shape and size of their monomeric units. To achieve and maintain their ordered structures, COF monomers are typically rigid, aromatic molecules with a high degree of non-covalent ππ interactions that favor the formation of layered two-dimensional or interpenetrated three-dimensional structures. These aromatic monomers also impart promising photosensitizing characteristics for light-driven catalytic reactions and emitting devices. Yet, while many monomers have intrinsically varied donor-acceptor (D-A) characteristics little is known about how they affect the photophysical properties of the aggregate COFs. Furthermore, a widespread class of COFs are formed via Schiff base condensation, but little is known about the resultant imine bond and its relation to monomer selection. Thus, the relationship between imine COF D-A architecture and photophysical properties is of the utmost importance. In this poster, I will share some of our latest findings on two COF projects:

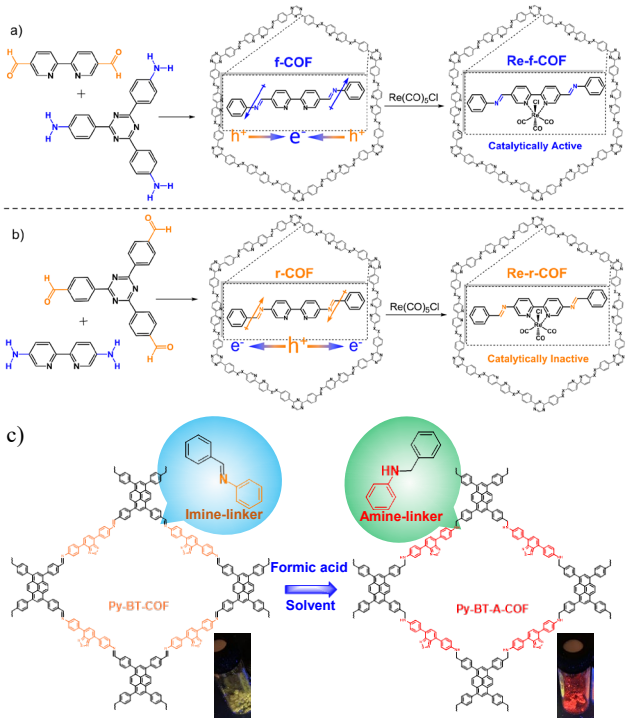

Figure 1. Illustration of synthetic scheme of Re-COF from monomers having amine and aldehyde functional groups switched yielding a reversed imine linker. (a) Re-f-COF (b) Re-r-COF. (c) The illustration of reduction of imine to amine linker in Py-BT-COF leads to enhanced photoluminescence.

1) The impact of COF monomer structure and imine directionality on light absorption, charge separation (CS), and photocatalytic performance for CO_2 reduction. We found monomer structure has moderate impact but imine direction has outsized impact on CS and photocatalytic performance of COFs (Figure 1a and 1b).

2) The impact of linkage electronic property on photoluminescence properties. We found that the reduction of imine to amine linker in Py-BT-COF (Figure 1c) leads to significantly enhanced emission quantum yield and white light emission.

Fundamental Studies of Molecular Frameworks for Solar Energy Conversion

Boris Kramar, Alice Li, Subhadip Goswami, Jiaxin Duan, Anna S. Bondarenko, Aaron E. B. Stone, Emily Weiss, Roel Templaar, Richard Schaller, Lin X. Chen, Joseph T. Hupp

Department of Chemistry
Northwestern University
Evanston, IL 60093

This poster will present results relevant to light-to-electrical and light-to-chemical energy conversion as enabled by crystallographically well-defined, porous molecular frameworks – both metal-organic frameworks (MOFs) and hydrogen-bonded organic frameworks (HOFs). Precise knowledge of local and long-range structure provides bases for connecting structure to activity and for gaining maximum benefit from corresponding computational studies. With chromophoric MOFs as light absorbers we are able to observe fast energy transport and antenna behavior involving as many as 300 aligned chromophores, culminating in exciton splitting and delivery of charges to framework-appended redox species, including species that are catalytic for hydrogen evolution or CO_2 reduction. Notably, the size of the antenna is strongly dependent on framework topology, while the mechanism of exciton propagation appears to involve an unusual, pH-tunable, linker-to-node hole-transfer scheme not previously encountered in MOF chemistry. When combined with anisotropic charge-transport, these frameworks display many of the features required for efficient light-to-chemical energy conversion. Interestingly, we are finding that the design rules for MOF-enabled photocatalysis are, in key ways, the opposite of the rules we and others have intuited for effective electrocatalysis.

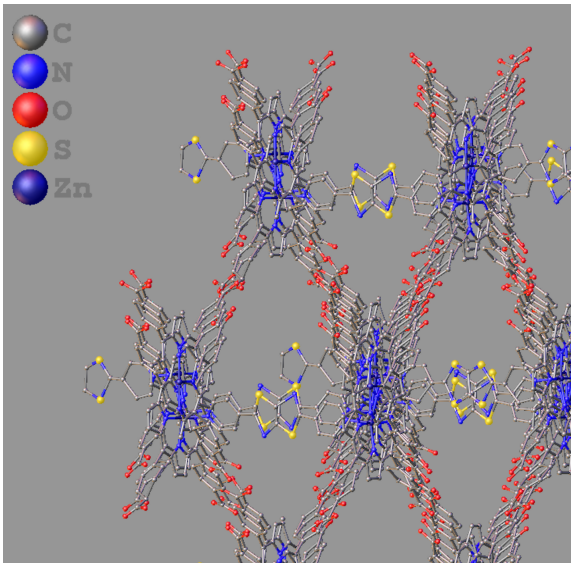

Single-crystal X-ray diffraction (SCXRD) derived representation of structure of new two-component HOF comprising hydrogen-bonded & π-stacked tetra-benzoic-acid-functionalized Zn-porphyrins (red absorbers) together with cross-connecting dipyridyl thiazolothiazole units (blue-emitting annihilators). This assembly displays optical upconversion based on triplet-triplet annihilation.

Shown in the figure is a representation of a new porous HOF that displays optical upconversion via triplet-triplet annihilation (TTA-UC). Upconversion, of course, offers a means of converting low-energy photons of perhaps marginal value for catalysis into higher energy photons, better able to drive catalytic reactions. Our broader motivations in developing porous, light-absorbing HOFs include: a) expanding antenna sizes beyond the range achievable thus far with MOFs, b) engendering much more rapid charge-transport than observed thus far with low-density MOFs, and c) imparting much greater energy-transport anisotropy. Depending on the approaches targeted for light-to-electrical and light-to-chemical energy conversion, realization of any or all of these objectives could translate to more effective conversion.

Controlling Intermolecular Coupling in Triplet-Forming Aggregates at Interfaces

Nicholas Pompetti, Benjamin Feingold, Marissa Martinez, Matt Beard, Justin C. Johnson
Chemistry and Nanoscience Center
National Renewable Energy Laboratory
Golden, CO 80401

Processes involving triplet states that interact amongst multiple chromophores depend critically on the relative intermolecular dispositions within the molecular architectures. Singlet fission, triplet-triplet annihilation based upconversion (TTA-UC), and some forms of photochemical transformations rely on two or more molecules serving to harbor and guide triplets toward productive pathways for improved solar photoconversion. Whereas rigid covalent dimers and crystals can have well-defined interchromophore geometries, molecular arrangement at interfaces with charge or energy acceptors/donors can be more difficult to study and engineer. Simultaneous strong surface binding and appropriate intermolecular juxtapositions can be challenging to achieve but are nonetheless crucial to properly direct the excited state energy flow.

Here, we have employed tetracene mono- and di-carboxylic acid compounds toward creating tailored aggregates that have distinct photophysics. Monoacids in solution resist aggregation in better solvents until high concentration (> 1 M), whereupon they exhibit spectral broadening and red-shifting in absorption spectra, commonly observed in other aggregate systems, e.g. perylenes. NMR and dynamic light scattering studies suggest that aggregate size is directly influenced by the solvent. Differences in excited state dynamics between the aggregate types are apparent, and both excimer-forming and triplet-forming regimes can be accessed. Diacids show distinct behavior, with a stark transition between isolated monomer and dimer behavior around 0.1 mM in DMF solvent, Figure 1. The concentration dependence of absorption and fluorescence both show evidence for a species that lies between the monomer and the stable dimer, suggesting an intermediate with a distinct bonding structure from that of the others. The excited state outcomes include excimer and charge-transfer (CT) pathways. Theoretical calculations are underway to reveal the optimized geometries that are likely responsible for this behavior. Attachment to both TiO_2 and quantum dots is being performed in the different concentration regimes, where low, medium, and high concentrations lead to distinct photophysical behavior.

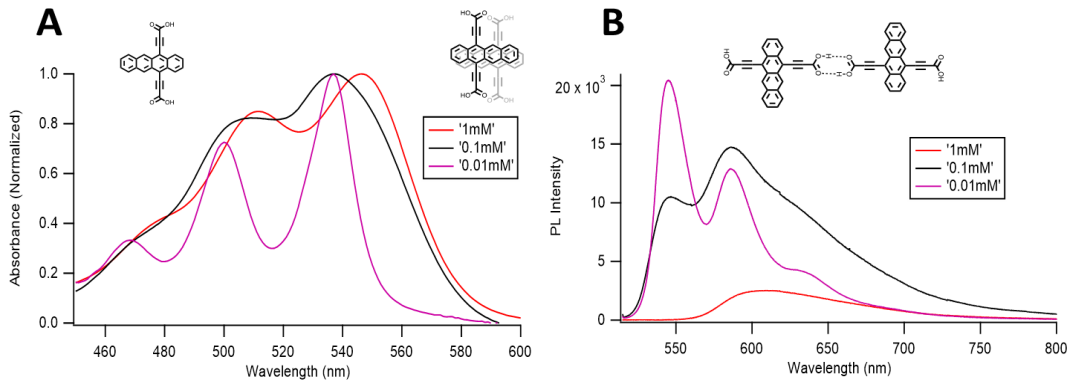

Figure 1. A) Absorbance and B) fluorescence spectra of tetracene di-acid in DMF. Structures at top show monomer and potential aggregate geometries.

Mechanism of Photochemical N_2 Reduction

David W. Mulder[1], Lauren M. Pellows[2], Mark Willis[3], Andrew Clinger[4], Zhi-Yong Yang[4], Gordana Dukovic[2], Lance C. Seefeldt[4], John W. Peters[3], Paul W. King[1]
[1]Biosciences Center, NREL, Golden, CO 80401; [2]Dept. of Chemistry, University of Colorado, Boulder, CO 84322; [3]Dept. of Chemistry and Biochemistry, Oklahoma University, Norman, OK 73019; [4]Dept. of Chemistry and Biochemistry, Utah State University, Logan, UT 84322

This research program focuses on understanding the basic principles for coupling nanocrystals to biological nitrogenases for the photocatalytic reduction of N_2 to ammonia (NH_3, Figure 1). Nitrogenases are two-component enzyme systems composed of Fe protein and MoFe protein. The Fe protein functions in ATP-dependent electron delivery to MoFe protein, an obligatory step in the catalytic reduction of N_2 to NH_3. We demonstrated that nanocrystalline materials can replace Fe protein to deliver photoexcited electrons to MoFe protein for catalytic NH_3 production. Recent progress has focused on creating a systematic understanding of the properties controlling assembly, electron transfer and product formation rates in nanocrystal-MoFe protein complexes. The foundation is producing insights on the MoFe protein catalytic mechanism and properties of nanocrystals that control of electron delivery.

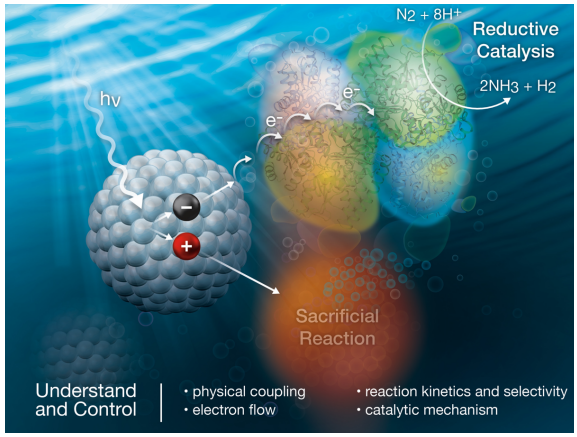

Figure 1. CdS quantum dot (sphere) nitrogenase MoFe protein (blue-green) complex. Photon absorption by QD generates a photoexcited electron-hole pair, electron transfer to MoFe protein catalyzes reduction of N_2 to NH_3 and H_2.

Recent work investigating the properties of CdS quantum dots (QDs) and nanorods are pointing to the importance of nanocrystal synthesis in tuning photochemistry for electron delivery to MoFe protein. In addition, to understand QD-MoFe protein assembly, which is essential to continuous delivery of photoexcited electrons, microscale thermophoresis was developed to interrogate binding interactions. The results on binding thermodynamics are helping to guide nanocrystal synthesis and to establish fundamental correlations between binding and electron delivery. The efforts in these areas are informing on conditions for cryo-illumination, which coupled to electron paramagnetic resonance spectroscopy, is being used to trap intermediates of the N_2 reduction reaction. Collectively, the progress is addressing knowledge gaps in understanding the first principles that govern the productive coupling of nanocrystals to enzymes for catalysis.

References

1. B. Chica, et. al. **2022**. "Dissecting Nitrogenase MoFe Protein P-cluster P^{2+} to P^{+} Conversion in CdS Nanocrystal–MoFe Protein Complexes". *J. Am. Chem. Soc.* **144**:5708-5712.
2. J.L. Ruzicka, et. al. "The Kinetics of Electron Transfer from CdS Nanorods to MoFe Protein of Nitrogenase". **2022**. *J. Chem. Phys.* **126**:8425–8435.
3. G.E. Vansuch, et. al. **2023**. "Elucidating mechanistic intermediates in CdS quantum dot-nitrogenase MoFe protein complexes during photochemical N_2 reduction to ammonia". *JACS. In review.*

Spin-Exchange Carrier Multiplication in Engineered Quantum Dots Enabled by Magnetic Dopants

Victor I. Klimov
Nanotechnology and Advanced Spectroscopy Team, C-PCS, Chemistry Division
Los Alamos National Laboratory
Los Alamos, New Mexico 87545

Carrier multiplication (CM) is a process whereby a kinetic energy of a hot carrier (E_{kin}) relaxes via generation of additional electron-hole pairs (excitons). This effect has been extensively studied in the context of advanced photoconversion as it could boost the yield of photogenerated excitons.[1,2] The key limitation in CM arises from phonon-assisted energy losses whereby E_{kin} quickly dissipates as heat before conducting 'useful work'. In particular, for direct, spin-independent Coulombic interactions, the *energy-loss rate* due to phonons (r_{loss}) is a factor of >3 higher than the *energy-gain rate* due to Coulomb collisions (r_{gain}). As a result, conventional materials show only moderate CM yields in the range of photon energies relevant to solar energy.

Our recent studies show that this problem can be tackled by exploiting not direct but *spin-exchange (SE) Coulomb interactions* mediated by manganese impurities (Mn^{2+}) incorporated into colloidal quantum dots (QDs).[3,4] In particular, using properly engineered Mn:CdSe QDs, we achieved ultrafast up-hill SE transitions that occurred with unprecedented energy gain rates of ~10 eV ps^{-1}. As a result, the energy gain/loss ratio is increased to ~10, suggesting that the SE scheme can, in principle, lead to dramatic improvements in CM.

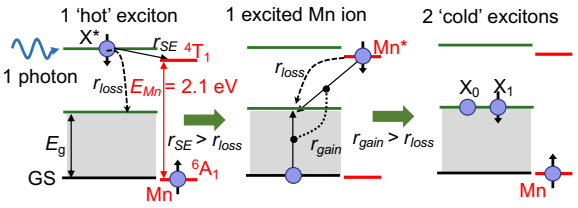

Figure 1. Spin-exchange carrier multiplication (SE-CM) occurs via two steps: (1) hot-exciton (X*) transfer to Mn (rate r_{SE}) to create Mn*; (2) spin-flip relaxation of Mn* to generate two band-edge excitons (rate r_{gain}) with spins 0 and 1 for spin conservation. Both steps benefit from very fast SE rates that exceed r_{loss}.

Recently, we realized high-yield spin-exchange CM (SE-CM) with Mn-doped PbSe/CdSe QDs.[5] In these QDs, CM occurs via two SE steps (Fig. 1). First, an exciton generated in a CdSe shell is rapidly transferred to a Mn dopant. Then, the excited Mn ion (Mn*) undergoes spin-flip relaxation which creates two excitons in a PbSe core. The observed CM benefits from very short timescales of SE interactions (~100 fs) and favorable energy gradients that promote generation of biexcitons and hinder competing relaxation pathways. The developed QDs demonstrate an almost 3-fold enhancement of the CM yield versus undoped QDs and a considerable reduction in the electron-hole pair creation energy, pointing towards a significant potential of SE-CM in advanced photoconversion.

1 Nozik, A. J. Quantum dot solar cells. *Physica E* **14**, 115-120 (2002).
2 Schaller, R. D. & Klimov, V. I. High efficiency carrier multiplication in PbSe nanocrystals: Implications for solar-energy conversion. *Phys. Rev. Lett.* **92**, 186601 (2004).
3 Singh, R., Liu, W., Lim, J., Robel, I. & Klimov, V. I. Hot-Electron Dynamics in Quantum Dots Manipulated by Spin-Exchange Auger Interactions *Nat. Nanotech.* **14**, 1035-1041 (2019).
4 Livache, C., Jin, H., Kozlov, O. V., Fedin, I. & Klimov, V. I. High-efficiency photoemission from magnetically-doped quantum dots driven by multi-step, spin-exchange Auger ionization. *Nat. Photonics* **16**, 443-440 (2022).
5 Jin, H., Livache, C., Kim, W. D. & Klimov, V. I. Spin-Exchange Carrier Multiplication in Manganese-Doped Colloidal Quantum Dots. *Nat. Mater. in press* (2023).

Modular Nanoscale and Biomimetic Assemblies for Photocatalytic Hydrogen Generation

Kara L. Bren, Todd D. Krauss, Ellen M. Matson
Department of Chemistry
University of Rochester
Rochester, NY and 14627

Our goal is to understand and optimize photochemical production of H_2 by nanocrystalline quantum dots (QDs) in systems incorporating molecular and bio-inspired catalysts and compounds. The development and study of these catalytic systems yields new insights into the surface chemical and charge transfer properties of QDs, which remain poorly characterized.

We have been keenly interested in improving proton reduction yields by accelerating hole transfer from QDs, which is a major fundamental obstacle. Recently, we discovered that incorporation of oxygen-vacancies in polyoxovanadate-alkoxide clusters quenches the photoluminescence (PL) of the QDs at near-unity efficiency. We also found that these oxygen-deficient clusters irreversibly form a complex with phosphonate-capped QDs, suggesting an explanation for why PL quenching is so efficient (Fig. 1). To determine whether the observed PL quenching is from electron or hole transfer, we studied the dynamics of the QD excited state with transient absorption (TA) spectroscopy. The lack of an appreciable decay in the TA dynamics (which are sensitive only to electron transfer) confirms that hole transfer is primarily responsible for the observed PL quenching behavior. Future experiments will determine the kinetics of hole-transfer from the QDs to the polyoxovanadate clusters, which we expect to be exceptionally fast due to the strong QD-hole acceptor association.

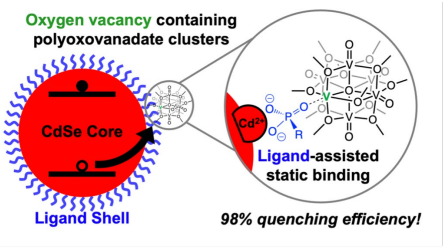

Figure 1: Schematic of interaction between phosphonate-capped QDs and POV cluster with oxygen vacancy.

In studies of the biomolecular cocatalyst component of these systems, we have deepened our understanding of the relationship between the properties of proton donors and catalytic mechanism. Previous work showed that the pK_a and sterics of buffer acids in solution impact the mechanisms of electrocatalytic H_2 production by biocatalysts. To apply these concepts to a more complex reaction, we have now shown that the pK_a of proton donors as well as the applied potential impacts the selectivity for CO_2 vs. proton reduction in two different biocatalysts, with more anodic potentials and less acidic proton donors favoring CO_2 reduction. In other work, these biocatalysts have been paired with both molecular and QD photosensitizers in multicomponent systems for photochemical H_2 production. We have demonstrated remarkable longevity (>100 hr) for photochemical H_2 production by a system consisting of a synthetic biocatalyst and an organic dye (Fig. 2). Furthermore, we have demonstrated that this same synthetic biocatalyst yields greater H_2 evolution enhancement with CdSe QDs when compared to molecular cocatalysts. Ongoing studies are addressing the mechanistic basis for this enhancement.

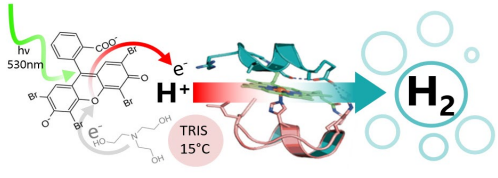

Figure 2: Heavy metal-free system for robust (> 100 hr) photochemical H_2 production

Fundamental Investigations of Processes that Limit the Durability of III-V Photoelectrodes for Solar Fuels Production

Jake M. Evans, Alexandre Z. Ye, Weilai Yu, Azhar I. Carim, Nathan S. Lewis
Division of Chemistry and Chemical Engineering
California Institute of Technology
Pasadena, CA 91125

Photoelectrochemical (PEC) water-splitting using inorganic semiconductor photoelectrodes enables one-step generation of H_2 (g) with water and sunlight as the only inputs. Stability is the most persistent challenge impeding the continued development of solar-driven water-splitting devices. Group III-V semiconductors are attractive candidates for use such systems due to the potential for high efficiency. However, maximizing the efficiency of a water splitting cell requires the use of highly acidic or alkaline electrolytes, so photoelectrode materials must be durable in such electrochemical environments under operating conditions. Consequently, we have systematically investigated the chemical and physical factors that limit the durability of GaAs, InP, and GaInP photocathodes, with and without decoration with hydrogen-evolution electrocatalyst materials, for solar-driven hydrogen generation in both acidic and alkaline electrolytes. From this analysis, we identified cathodic plating of In^0 and formation of As^0 as the primary chemical failure modes. Mitigation of these failure modes provides enhanced durability along with high efficiency. However, miscut defects act as structural failure modes for pn^+-GaInP photocathode stacks, and thus further enhancements in durability will require mitigation of these structure-related failure processes. For photoanodes, corrosion resistance can be imparted to semiconductor photoanodes via coating the surface with thin, transparent amorphous TiO_2 (*a*-TiO_2) films. Recent work utilizing *a*-TiO_2 coated GaAs microislands and planar electrodes indicates that both intrinsic and extrinsic defects limit the durability of these photoelectrodes under operating conditions. Extrinsic defects have been linked to atmospheric particulates that occlude the surface, leading to exposed GaAs. Intrinsic defects represent electrochemically active defect sites in *a*-TiO_2, with future work on localized electrochemistry of *a*-TiO_2 coated electrodes aimed at identifying and characterizing these sites.

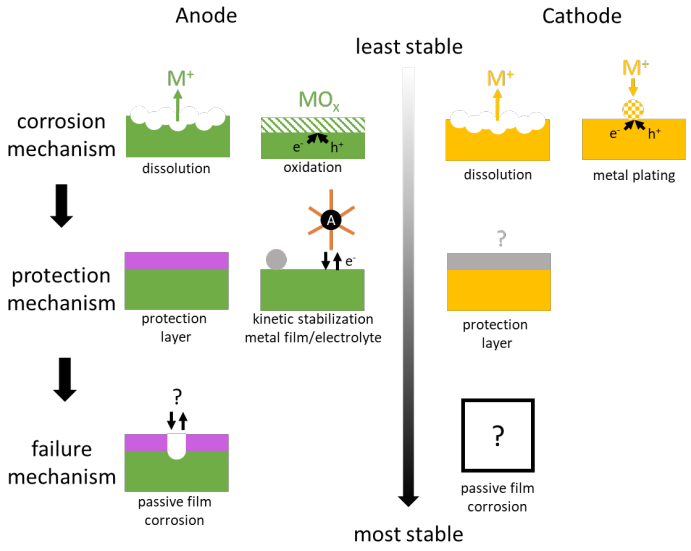

Figure 1. Schematic of the approach and discoveries in protected photoelectrodes under recent DOE support. Photoanodes are known to corrode via dissolution or oxidative passivation and protection mechanisms such as kinetic stabilization or protective film deposition have shown significant advancements in stability. Further work on understanding failure mechanisms in protective films is expected to yield similar increases in stability. Corrosion mechanisms in photocathodes have been recently described, and future work on protection layer development is expected to greatly enhance device lifetime.

Atomistic Characterization of Physical and Chemical Characteristics of Metal/Semiconductor Interfaces on Functioning Photocatalysts

John R. Hemmerling, Aarti Mathur, Ahmet Sert and Suljo Linic
Department of Chemical Engineering
University of Michigan
Ann Arbor, MI 48109

Materials that have received increasing attention in photocatalysis (including solar water splitting) contain a semiconductor (SC) light absorber and attached metal electrocatalysts (EC). In these photoelectrochemical systems, the SC serves to provide an electromotive force (voltage) that is used by the ECs to drive (electro)chemical reactions. In general, our understanding of the photocatalytic function of these SC/EC photoelectrocatalysts is based on simple models that often assume that: (i) the interface is static, and that it does not evolve under the reactions conditions, (ii) electrocatalytic reactions take place on the electrocatalyst surface and sites at the SC/EC interface are not catalytically different than those at the surface, and (iii) the fluxes of charge carriers between the SC and EC, which regulate the photovoltage generated under light illumination, are controlled by the inherent, as-fabricated barrier heights (i.e., the Schottky model or models involving Fermi level pinning). It has been recognized over recent years that these simple models cannot fully capture the behavior of SC/EC photoelectrocatalysts, particularly under reaction conditions. The overarching objective of this project is to study how the atomistic complexities associated with the functioning semiconductor/metal-electrocatalyst (SC/EC) interfaces impact their performance. We mainly focused on the water oxidation (i.e., OER) half-reaction, which takes place under highly oxidizing and corrosive conditions that often induce oxidative changes to the SC/EC interface.

We investigated the role of oxidized interfaced in the studies of planar SC/EC photoelectrocatalysts. In these planar systems, SC/EC interface was controlled by careful fabrication of insulating oxide layer between the SC and EC. The studies showed that the thickness of the insulating oxide layer is a critical factor governing the photo-voltage generated by these SC/EC systems (Figure 1). We also investigated EC metal nanoparticles deposited on SC, where the SC and the SC/EC interface directly interacts with the OER environment. We specifically focused on describing the interface of a functioning semiconductor (Si) and nanoparticle electrocatalysts (Ni) in photoelectrochemical water oxidation. We showed that under oxidizing conditions the interface is completely oxidized. We found that the interface plays a critical role in (1) affecting the fluxes of energetic electrons and holes between SC and EC and therefore modulating the electron/hole recombination rates, (2) changing the barrier height of the junction by affecting the effective work functions of the SC and EC, and (3) introducing nonidealities which detrimentally impact the performance. [1–2–3]

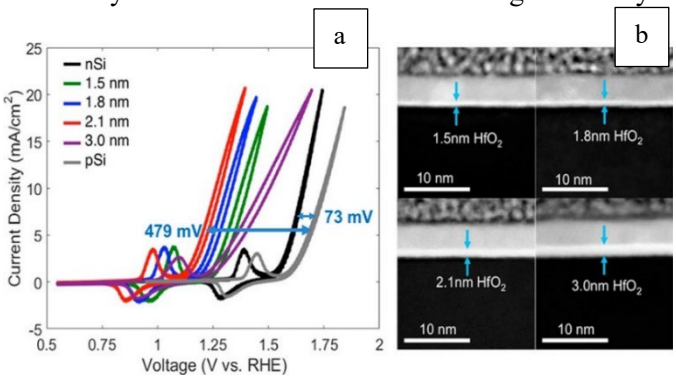

Figure 1: a) Performance (photovoltage) measured under 1 Sun illumination in a three-electrode setup for p-Si/HfO2/Ni planar photoelectrocatalysts for different thicknesses of the HfO2 insulator film. n-Si/Ni system was used as a control in dark electrochemical measurements. b) Characterization of n-Si/HfO_2/Ni samples. Cross-sectional STEM images for different thicknesses of the HfO2 insulator.

References:
1. Hemmerling, J., Quinn, J. & Linic, S. *Advanced Energy Materials* **10**, 1903354 (2020).
2. Hemmerling, J. R., Mathur, A. & Linic, S. *Acc. Chem. Res.* **54**, 1992–2002 (2021).
3. Hemmerling, J. R., Mathur, A. & Linic, S. *Advanced Energy Materials* **12**, 2103798 (2022).

New Architectures for Probing the Water Dissociation Mechanism in Bipolar Membranes

Tianyue Gao, Amy Metlay, Wenxiao Deng, Leanna Schulte, Yein Yoon, and Thomas Mallouk
Department of Chemistry
University of Pennsylvania
Philadelphia, PA 19104

Bipolar membranes (BPMs) manage proton transport and inhibit product crossover in photoelectrochemical cells for CO_2 reduction and water splitting, and they are also interesting as components of fuel cells, electrolyzers, acid-base redox flow batteries, and electrochemical cells for ocean capture of CO_2. The key reactions that occur at the interface between the cation- and anion-exchange layers of BPMs are water autodissociation (in reverse bias) and acid-base neutralization (in forward bias). Catalysis of both reactions is essential to the efficient operation of BPM-based cells and is traditionally understood in terms of a buffer mechanism. However, the best catalysts differ for forward and reverse bias reactions, and the effects of catalyst conductivity, local electric fields, and bipolar junction structure are not yet fully understood.

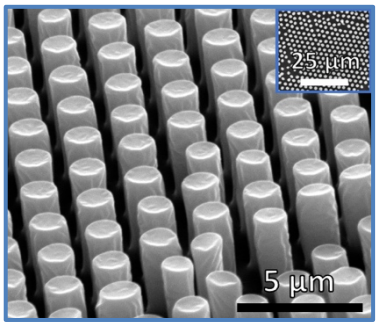

Earlier experiments with 3D bipolar junctions made by electrospinning of anion- and cation-exchange polymers have resulted in high performance BPMs, but it has been difficult to probe and model the local pH and electric field in these complex architectures. We have used a nanosphere lithography method to pattern the anion exchange layer as an array of high aspect ratio cylindrical pillars (shown in the image at the right), which are then filled with a conformal graphite oxide or TiO_2 catalyst layer and the cation exchange polymer. Finite element modeling of the membrane junction shows that the local electric field, which strongly affects the reaction rate under reverse bias, is very sensitive to the abruptness of the polyanion-polycation junction. We are now adapting a ratiometric dye method that we developed for measurements of local pH at the BPM-catalyst interface (Z. Yan et al., *Nat. Chem.* **13**, 33-40 (2021)) to operando measurements of the pH profile in these structurally well-defined 3D junctions.

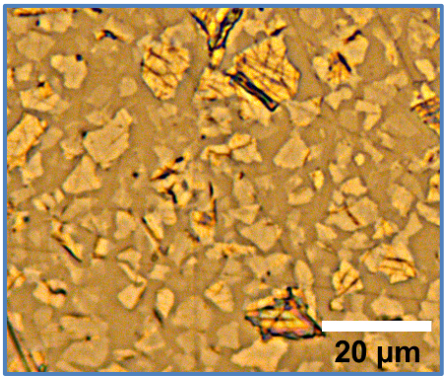

Graphite oxide (GO), grown as a monolayer or a few-layer film, is a good catalyst for water autodissociation in BPM junctions. SS-NMR and titration data suggest that hydroxyl groups on the GO basal plane surface are the catalytic sites. When GO is made by oxidative exfoliation of natural graphite crystals, the monolayer sheets are ~0.5 nm thick and several microns in their lateral dimensions. This enables us to image them directly in a light or Raman microscope, as shown at the left. By using Langmuir-Blodgett deposition, we can control the lateral packing density of these sheets on the anion-exchange membrane surface and in the resulting BPM junction. Interestingly, full 2D tiling or multilayer coverage of the junction results in poorer performance than partial tiling, suggesting that transport of ions through the gaps between the sheets competes with H^+/OH^- recombination at the basal plane surface. Experiments are underway to directly image lateral pH gradients in these junctions under reverse and forward bias.

Bridge Torsional Angle Acceleration of Intramolecular PCET from Aggregated Donor States

Gerald F. Manbeck, Dmitry E. Polyansky, Mehmed Z. Ertem, and Javier Concepcion
Chemistry Division, Energy & Photon Sciences Directorate
Brookhaven National Laboratory
Upton, NY 11973-5000

The rate of charge transfer between discrete donor-acceptor (D/A) pairs is well-modeled by semi-classical electron transfer theory. In contrast, cases involving electronic delocalization among multiple donors or acceptors are less straightforward to model. Generalized Marcus theory (gMT) has been proposed to account for inter-donor or inter-acceptor delocalization in aggregated states and significant effects on rates were predicted to occur by supertransfer or nuclear factor tuning. (*Chem. Sci.* **2018**, 9, 2942-2951) Our previous work tested predictions of gMT using a series of $[Ru(L)_n(OH)_{3-n}]^{2+}$ donor-acceptor complexes containing 1, 2, or 3 identical, covalently bound, and geometrically-fixed phenolic electron donors linked to Ru through phenanthroline-benzimidazole bridges (OH = 2,4-di-tert-butyl-6-(1-methyl-1H-imidazo[4,5-f][1,10]phenanthrolin-2-yl)phenol), Figure 1. Upon flash photolysis and oxidative quenching by methyl viologen, the transient Ru(III) oxidizes an appended phenol. While formally a proton-coupled electron transfer reaction, our data suggest a stepwise, electron transfer-first mechanism. The intramolecular charge transfer rate is accelerated by 3.2-fold and 6-fold as the number of donors is sequentially increased from 1 to 2 and 3, respectively. This acceleration occurred without a change in driving force and is attributed to the effects of gMT: larger electronic coupling (H_{DA}) and decreased reorganization energy (λ_{DA}) which lowers the activation barrier.

This poster presents the next iteration of this work in which the *N*-methyl benzimidazole bridge is varied to the *N*-H benzimidazole to change the thermodynamics. This small change results in increased planarity of the N—H—OPh hydrogen bonding geometry, which affects the redox potential, D-A coupling, and rates of the photoinduced intramolecular PCET reaction. The effects on coupling and reorganization are probed by temperature-dependent flash photolysis. In addition, mixed donor systems comprised both N-methyl and N-H bridges are investigated. The practical aspects of our results, e.g. accelerated differential charge separation vs recombination are highlighted by equal rates of recombination independent of the number of phenol groups.

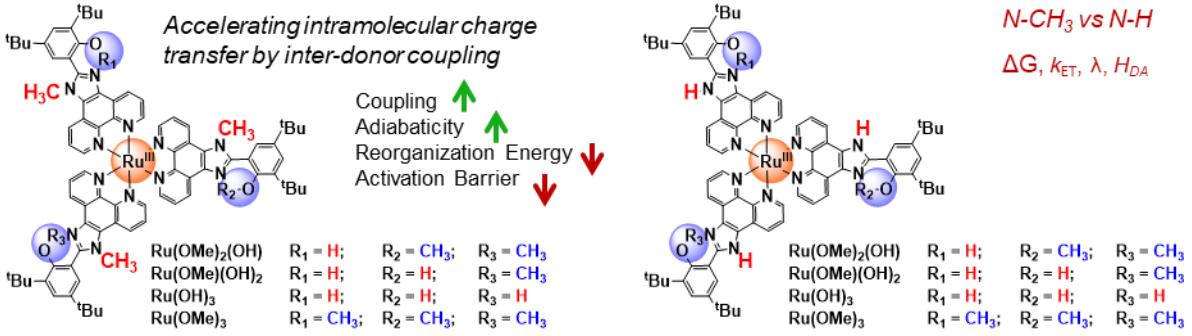

Figure 1.

Total X-ray Scattering for Interfacial Atomic Structure Analysis of Solar Fuels Catalysis

Alex B. F. Martinson, Justin M. Hoffman, Mark W. Muir, Niklas B. Thompson, Sam Amsterdam, Karen L. Mulfort, David M. Tiede
Chemical Sciences and Engineering and Materials Science Divisions
Argonne National Laboratory
Lemont, IL 60439

Amorphous thin film materials and heterogenized molecular catalysts supported on electrode and other functional interfaces are of central importance to solar and electrochemical fuels catalysis. However, the amorphous character and complexity of the interfacial architectures pose challenges for probing mechanisms of multi-step catalysis. A fundamental understanding of the mechanisms for interfacial electro-catalysis requires resolving atomic structures of active sites along the sequence of proton-coupled redox steps, a task made more difficult by the background of electrode and semiconductor support structures. We identify and develop platforms for atomic structure analyses of thin-film oxides and molecular catalysts at functional interfaces by utilizing high-energy (>50 keV) X-ray scattering and atomic pair distribution function (PDF) analysis.

Amorphous conductive oxides offer an ideal platform for PDF analysis of supported thin films by minimizing overwhelming background Bragg diffraction and Ohmic voltage loss, while maximizing electrode stability. We explore atomic layer deposition (ALD) of indium zinc oxide (IZO), in which the zinc disrupts the crystallinity of In_2O_3. ALD enables conformal coating of high surface area substrates that maximize visible light absorption and X-ray interaction. We readily vary the composition of IZO thin films through alternation of In- and Zn-based cycles, **Figure 1**.

We further investigate grazing-incidence total X-ray scattering (GITXS) for PDF analysis using synchrotron light sources. Compared to the commonly used grazing-incidence wide-angle X-ray scattering (GIWAXS), which has been applied to highly ordered layered or crystalline materials, GITXS/PDF expands such analysis to short range ordered materials and can be used to examine the atomic pair correlations dependent on the direction relative to the surface. We perform an orientation analysis of four conductive indium oxide thin films prepared using different synthesis techniques. The indium oxide films are found to differ markedly in orientation with respect to the planar support and degree of order, and hence, the terminal surface chemistries, **Figure 1**. We anticipate that orientational analysis of GITXS/PDF data will offer many opportunities to extend structural analyses of interfaces and interfacial films by providing a means to determine bonding anisotropy within disordered and non-crystalline interfacial films.

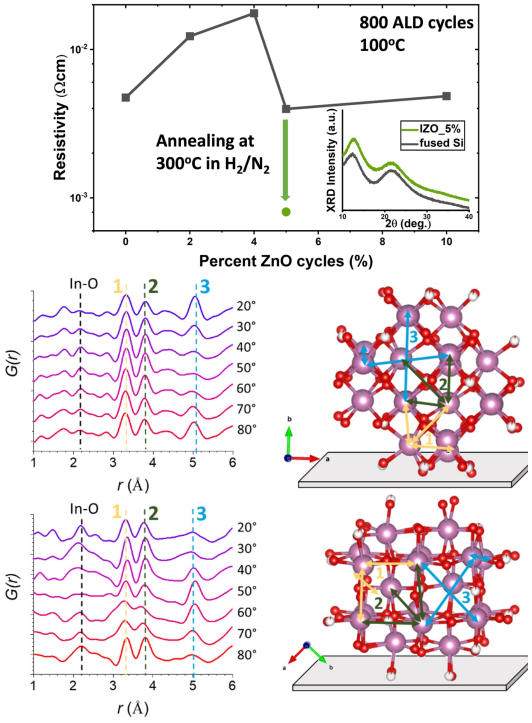

Figure 1. Conductive and amorphous IZO grown by ALD. G(r) for (upper) commercial and (lower) ALD ITO film shown for each of the integrated slices. Proposed orientation with atomic pair correlations labelled.

Understanding the Effects of Charge Delocalization, Electronic Coupling, and Intramolecular Electrostatics on Electrocatalysis in Multimetallic Systems

Jukai Zhou, MD. Waseem Hussain, Weixuan Nie, Drew E. Tarnopol, Charles C. L. McCrory

Department of Chemistry and Macromolecular Science & Engineering Program
University of Michigan
Ann Arbor, MI, 48109

Molecular catalysts show promise for the electrochemical CO_2 reduction (CO_2R) reaction due to their single-product selectivity and functional tunability through structure modification. However, incorporating molecular catalysts into practical, heterogeneous, multimetallic structures remains an outstanding challenge. This project focuses on determining how the interrelated effects of charge delocalization, electronic coupling, and intramolecular electrostatics influence catalytic activity and selectivity in extended multidimensional catalyst architectures. We do this using a bottom-up approach to study these effects as we build in structural complexity from simple molecular systems towards extended multidimensional structures.

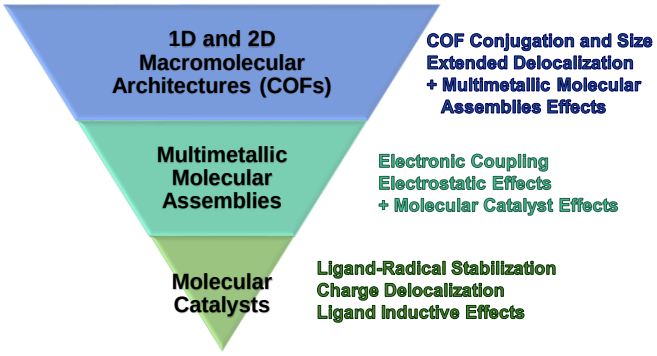

Bottom-up approach for designing new macromolecular catalysts for CO_2 reduction.

Previously, we explored how charge delocalization and intramolecular electrostatics influence CO_2R activity and reaction selectivity by molecular catalysts.[1,2] We have expanded our work to explore the role of all three effects on CO_2R activity in multimetallic assemblies. For example, by systematically modifying the structure of multimetallic assemblies, we have demonstrated that electrostatic effects are the most influential intramolecular interactions on per-site activity in multimetallic systems.[3] We also successfully incorporated similar Co-based molecular building units in larger 2D coordination polymers. Preliminary studies suggest a shift in CO_2R product distribution from CO in the parent complexes to methanol in the 2D structures. Future work will focus on developing a mechanistic understanding for the shift in product distribution through a combination of systematic structure modifications and spectroelectrochemical studies.

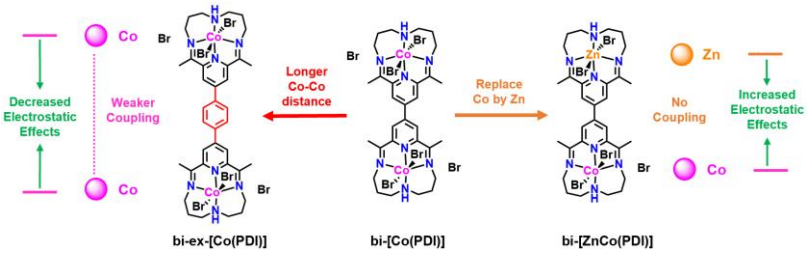

Tuning linker structure in multimetallic molecular assemblies influences parameters that control catalytic activity.[3]

(1) Nie, W-X.; Tarnopol, D. E.; McCrory, C. C. L. *J. Am. Chem. Soc.*, **2021**, *143*, 3764-3778.

(2) Nie, W-X.; McCrory, C. C. L. *Dalton Trans.*, **2022**, *51*, 6993-7010.

(3) Zhou, J.; Nie, W-X.; Jana, G.; Rodriguez, A.; Tarnopol, D. E.; Mendoza-Cortes, J. L.; McCrory, C. C. L. *submitted*

The Impact of Electric Fields on Electron Transfer at Metal Oxide-Electrolyte Interfaces

Quentin Loague, Matthew Goodwin, and Gerald J. Meyer
Department of Chemistry
University of North Carolina at Chapel Hill
Chapel Hill, NC 27599

Dye-sensitized solar cells have received considerable attention since the advent of mesoporous metal oxide thin films that were first described by Grätzel and O'Regan [1]. Fundamental interest in light driven interfacial electron transfer in these materials is motivated by applications in electrical power generation and in solar fuels production. Our present DOE-funded research is focused on the role electric fields play in dye-sensitized electron transfer. Molecular dyes based on $(d\pi)^6$ transition metal complexes and organic pigments report on the field magnitude and direction at dye-TiO_2 interfaces. An electroabsorption apparatus was recently constructed that provides routine experimental determination of the change in dipole moment $\overrightarrow{\Delta\mu}$ that accompanies light absorption, a value needed to extract $\overrightarrow{E}$ from electroabsorption data measured at metal oxides interfaces [2]. As is shown schematically, the direction of the spectral shift reports on whether $\overrightarrow{E}$ is parallel or antiparallel to the sensitizer $\overrightarrow{\Delta\mu}$. Provided that the angle between these vectors is known, the magnitude of $\overrightarrow{E}$ can be extracted from the magnitude of the spectral shift. In ongoing research, we have used this electroabsorption feature to quantify the electric field magnitude reported by Galoppini's rigid-rod sensitizers set at controlled distances from TiO_2 [3] and by a sensitizer linked to core-shell nanocrystals with controlled shell thicknesses [4].

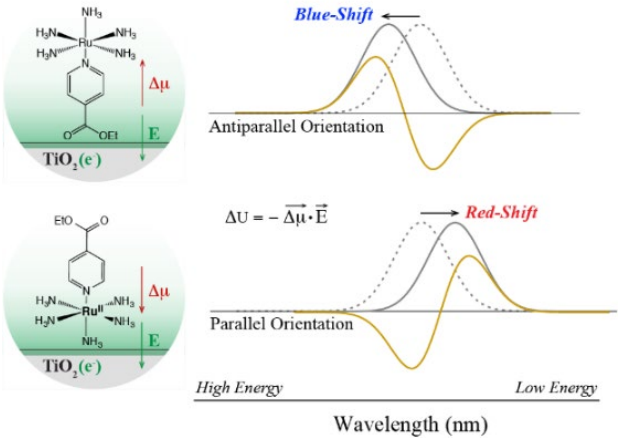

These recent experimental findings will be discussed with implications for solar energy conversion [3,4]. The poster will also present ongoing research to realize electric field reporters that are insensitive to the angle between $\overrightarrow{E}$ and $\overrightarrow{\Delta\mu}$ and are instead impacted by the polarizability tensor.

References:

[1] *"A Low-Cost, High Efficiency Solar Cell Based on the Dye- Sensitized Colloidal TiO_2 Films"* O'Regan, B.; Grätzel, M. *Nature* **1991**, *353*, 737.

[2] "*Stark Spectroscopic Evidence that a Spin Change Accompanies Light Absorption in Transition Metal Polypyridyl Complexes"* Maurer, A.B.; Meyer, G.J. *J. Am. Chem. Soc.* **2020**, *142*, 6847.

[3] "*Reorganization Energies for Interfacial Electron Transfer Across Phenylene Ethynylene Rigid-rod Bridges*" Heidari, M.; Loague, Q.; Bangle, R.E.; Galoppini, E.; Meyer, G.J. *ACS Appl. Mater. Interfaces* **2022**, *14*, 35205.

[4] "*Sensitizer Electroabsorption as a Probe of Electrons Injected into Nanocrystalline SnO_2/TiO_2 Core/Shell Thin Films*" James, E.M.; Bennett, M.T.; Meyer, G.J. *J. Phys. Chem. C* **2023**, *127*, 5904.

PARTICIPANT LIST for the 44th DOE SOLAR PHOTOCHEMISTRY P.I. MEETING

Shane Ardo	University of California, Irvine
Polly Arnold (virtual registrant)	Lawrence Berkeley National Laboratory
John Asbury	Pennsylvania State University
Robert Bartynski	Rutgers University
Victor Batista	Yale University
Matthew Beard	National Renewable Energy Laboratory
Warren Beck	Michigan State University
David Beratan	Duke University
Louise Berben	University of California, Davis
Matthew Bird	Brookhaven National Laboratory
Jeffrey Blackburn	National Renewable Energy Laboratory
Shannon Boettcher	University of Oregon
Stephen Bradforth	University of Southern California
Gary Brudvig	Yale University
Luis Campos	Columbia University
Ian Carmichael	Notre Dame Radiation Laboratory
Felix Castellano	North Carolina State University
Lin Chen	Argonne National Laboratory
Kyoung-Shin Choi	University of Wisconsin
Javier Concepcion	Brookhaven National Laboratory
Amy Cordones-Hahn	SLAC National Accelerator Laboratory
Robert Coridan	University of Arkansas
Stephen Cronin	University of Southern California
Jillian Dempsey	University of North Carolina, Chapel Hill
Mehmed Zahid Ertem	Brookhaven National Laboratory
Christopher Fecko	DOE Office of Basic Energy Sciences
Graham Fleming (virtual registrant)	Lawrence Berkeley National Laboratory
Natia Frank	University of Nevada, Reno
Renee Frontiera	University of Minnesota
Elena Galoppini	Rutgers University
Ksenija Glusac	Argonne National Laboratory
John Gordon	Brookhaven National Laboratory
Ann Greenaway	National Renewable Energy Laboratory
John Gregoire	California Institute of Technology
David Grills	Brookhaven National Laboratory
Doughlas Grotjahn	San Diego State University
Thomas Hamann	Michigan State University
Alexander Harris (virtual registrant)	Brookhaven National Laboratory
Dugan Hayes	Rhode Island University
Craig Hill	Emory University
Dewey Holten	Washington University
Frances Houle	Lawrence Berkeley National Laboratory
Shu Hu	Yale University
Jier Huang	Boston College
Libai Huang	Purdue University
Joseph Hupp	Northwestern University
Kevin John (virtual registrant)	Los Alamos National Laboratory
Justin Johnson	National Renewable Energy Laboratory
Prashant Kamat	Notre Dame Rational Laboratory

Paul King	National Renewable Energy Laboratory
Adam Kinney	DOE Office of Basic Energy Sciences
Martin Kirk	University of New Mexico
Christine Kirmaier	Washington University
Victor Klimov	Los Alamos National Laboratory
Todd Krauss	University of Rochester
Benjamin Levine	Stony Brook University
Nathan Lewis	California Institute of Technology
Xiaosong Li	University of Washington
Tianquan Lian	Emory University
Jonathan Lindsey	North Carolina State University
Suljo Linic	University of Michigan
Stephen Maldonado	University of Michigan
Thomas Mallouk	Pennsylvania State University
Jerry Manbeck	Brookhaven National Laboratory
Alex Martinson	Argonne National Laboratory
Ellen Matson	University of Rochester
Charles McCrory	University of Michigan
James McCusker	Michigan State University
Gail McLean	DOE Office of Basic Energy Sciences
Gerald Meyer	University of North Carolina, Chapel Hill
Josef Michl	University of Colorado
John Miller	Brookhaven National Laboratory
Alexander Miller	University of North Carolina, Chapel Hill
Elisa Miller-Link	National Renewable Energy Laboratory
Michael Mirkin	City University of New York
Ana Moore	Arizona State University
Gary Moore	Arizona State University
Thomas Moore (virtual registrant)	Arizona State University
Amanda Morris	Virginia Polytechnic Institute and State University
Karen Mulfort	Argonne National Laboratory
Djamaladdin Musaev	Emory University
Nathan Neale	National Renewable Energy Laboratory
Jens Niklas	Argonne National Laboratory
Daniel Nocera	Harvard University
Colin Nuckolls	Columbia University
Lisa Olshansky	University of Illinois Urbana-Champaign
Frank Osterloh	University of California, Davis
John Peters	Washington State University
Oleg Poluektov	Argonne National Laboratory
Dmitry Polyansky	Brookhaven National Laboratory
Stephen Pratt	Argonne National Laboratory
Oleg Prezhdo	University of Southern California
Sylwia Ptasinska	Notre Dame Radiation Laboratory
Erin Ratcliff	University of Arizona
Jennifer Roizen	DOE Office of Basic Energy Sciences
Mike Rose	University of Texas, Austin
Garry Rumbles	National Renewable Energy Laboratory
Justin Sambur	Colorado State University
Richard Schaller	Argonne National Laboratory
Greg Scholes	Princeton University

Viviane Schwartz	DOE Office of Basic Energy Sciences
Matt Sfeir	City University of New York
David Shultz	North Carolina State University
Mark Spitler	University of North Carolina, Chapel Hill
Ming Lee Tang	University of Utah
Michael Therien	Duke University
David Tiede	Argonne National Laboratory
William Tumas	National Renewable Energy Laboratory
Claudia Turro	The Ohio State University
Jao van de Lagemaat	National Renewable Energy Laboratory
Claudio Verani	Wayne State University
Dunwei Wang	Boston College
Hailiang Wang	Yale University
Michael Wasielewski	Northwestern University
Philip Wilk	DOE Office of Basic Energy Sciences
Jenny Yang	University of California, Irvine
Xiaoyang Zhu	Columbia University